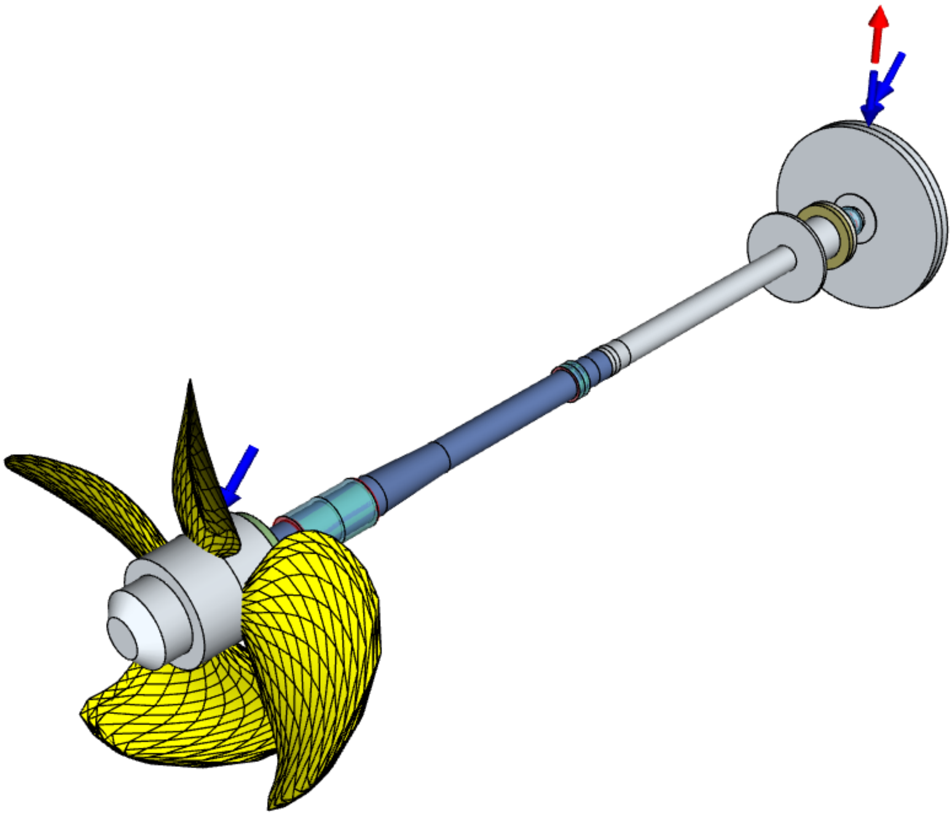

Dimensioning of marine propulsion shafts

Whirling and torsional vibrations

Master's thesis in the international master's programme Naval Architecture and Ocean Engineering

GUÐNI PÁLL GUNNARSSON
SINDRI PÁLL SIGURÐSSON

DEPARTMENT OF MECHANICS AND MARITIME SCIENCES
CHALMERS UNIVERSITY OF TECHNOLOGY
Gothenburg, Sweden 2021
www.chalmers.se

MASTER'S THESIS 2021

Dimensioning of marine propulsion shafts

Investigation on marine propulsions shaft diameter, from classification societies. To see if the diameter can be decreased, compared with current calculation methods.

GUNNARSSON & SIGURÐSSON

Department of Mechanics and Maritime Sciences
Division of Marine Technology
CHALMERS UNIVERSITY OF TECHNOLOGY
Gothenburg, Sweden 2021

Master's Thesis 2021:29
Investigation on marine propulsions shaft diameter, from different classification society. To see if the diameter can be decreased, compared with current calculation methods.
GUÐNI PÁLL GUNNARSSON
SINDRI PÁLL SIGURÐSSON

Supervisor: Tobias Huuva, Berg Propulsion Production AB
Examiner: Per Hogström, Mechanics and Maritime Sciences

Master's Thesis 2021
Department of Mechanics and Maritime Sciences
Division of Marine Technology
Chalmers University of Technology
SE-412 96 Gothenburg
Telephone +46 31 772 1000

Cover figure:
Shaft line setup based on one of the case study shaft line of the report, simulated in Nauticus Machinery Shaft alignment from DNV.

Typeset in LaTeX
Printed by Chalmers Reproservice
Gothenburg, Sweden 2021

Dimensioning of marine propulsion shafts
Investigation on marine propulsions shaft diameter, from different classification societies. To see if the diameter can be decreased, compared with current calculation methods.
GUÐNI PÁLL GUNNARSSON & SINDIR PÁLL SIGURÐSSON
Department of Mechanics and Maritime Sciences
Chalmers University of Technology

Abstract

Dimensioning of marine propulsion shafts for new builds is done early in the design phase of a vessel. Thus, often the designer only has the main particulars of the vessel including the general size and power requirements, as well as the intended purpose of the vessel. With the limited information, a shaft line needs to be dimensioned which is fit for purpose, fulfils class requirements as well as showing good vibrational behavior. Until now this has been done safely and successfully using old principles and fundamentally relying on a single formula that is recognized by all the major classification societies for giving a safe design. This method has been shown to give very reliable designs but is however believed to result in overly dimensioned components. By utilizing expertise, access to good data, and a systematic approach in behavior analysis, it is believed to be possible to step away from current methods and provide slimmer and more power-dense shaft lines.
This thesis describes the underlying theory of rotating machinery often summarized as rotor dynamics. A comprehensive study of classification rules and requirements governing the design of marine propulsion shafts. Case studies of typical shaft lines for different types of vessels, for those a software tool from DNV-GL is used to simulate the shaft behavior. The simulation software Nauticus Machinery available from DNV-GL is a specialized marine shaft line analysing software, containing few different tools. The tools used during this thesis work are Nauticus Shaft Alignment, Nauticus Torsional Vibration, and approved formulas and equations from classification societies. Using this combination of software and formulas the writers evaluate an improved method to define the minimum shaft diameter.

Keywords: propulsion shaft, whirling, torsional vibration, shaft alignment, shaft dimensioning, classification societies.

Acknowledgements

This thesis constitutes part of the requirements for the master's degree in Naval Architecture and Ocean Engineering at Chalmers University of Technology, Gothenburg, and has been carried out with Berg Propulsion Production AB, Öckerö, between January and June of 2021.
We would like to express our gratitude to our supervisor Tobias Huuva, Ph.D., and Samuel Ottosson for all their support and guidance throughout the project. We would like to thank our examiner Per Mottram Hogström, Director of the Master program in Naval Architecture and Ocean Engineering, for his guidance and motivating enthusiasm. Special thanks go to Deniz Yagiz and Nancy Phang for their expert support and feedback on the details of rotor dynamics analysis.

Many thanks to all the people at Berg Propulsion for a warm welcome and for showing interest in our project.

Guðni Gunnarsson & Sindri Sigurðsson, Gothenburg, May 2021

Contents

List of Figures

List of Tables

Abbreviations

ABS	American Bureau of Shipping
CAT	Caterpillar Inc
COO	Chief operating officer
CPP(CP)	Controllable pitch propeller
Ch	Chapter
DNV(DNVGL)	Det Norske Veritas
DV	Dang Van
Est	Estimated
FEM	Finite Element Method
FPP(FP)	Fixed Pitch Propeller
GB	Gear box
HCF	High cycle fatigue
HSS	High Speed Shaft
IACS	International Association of Classification Societies
ICE	Ice-classification
KR	Korean Register of Shipping
LCF	Low cycle fatigue
LSS	Low Speed Shaft
MCR	Maximum Continuous Rating
ME	Main engine
MTA	Marine Thruster Azimuth
PRS	Polish Register of Shipping
Pt	Part (as in: section)
RS	Russian Maritime Register of Shipping
RoPax	Roll-on and roll-off Passenger vessel
PTO	Power take off (connection on gearbox)
RPM (rpm)	Round per minute
SCF	Stress consentration factor
SN(-diagram)	Plot of stress (S) against the number of cycles (N)
TVC(TVA)	Torsional vibration calculations (- analysis)

1 Introduction

Marine propulsion systems are designed in accordance with industry standards from classification societies [3], which in turn are developed by modeling and experience from the field. Increasing accuracy in numerical models allow for more detailed studies on the phenomena of the operation of propulsion systems and, in turn, optimization of the design.

1.1 Background

Berg Propulsion is one of the world's leading designer and manufacturer of Controllable Pitch Propulsion systems, Azimuthing Thrusters, and Transverse Thrusters. It is a Swedish company with main office and manufacturing on the Swedish west coast as well as sales and service offices located in Shanghai, Dubai and Singapore. The company was founded in 1912 and started to build propellers in 1929. In 2013, Johan Walter Berg AB and the brand name Berg Propulsion was acquired by Caterpillar Inc, also known as CAT. Caterpillar is one of the worlds largest manufacturer of heavy equipment and machinery. For the marine industry Caterpillar is a supplier of both generators and main engines under the brands, Caterpillar and MaK. With the acquisition, Berg Propulsion became part of Caterpillar Marine under the brand of CAT Propulsion Systems. With this Caterpillar was now able to offer complete power and propulsion package. June 30th 2020, the Berg Propulsion brand is brought back to the scene when Swedish investors with Stefan Sedersten, former COO of Berg Propulsion, bought back the company from Caterpillar. [6] [7] [30] [29]

The main propulsion systems usually consist of blades, hub, shafting, control system, and some integration components based upon customer need. Analyses of the behaviour of the propulsion shaft lines are carried out in an increasingly systematic way giving a good insight in vibration behaviours and resonances. Having access to good data and experties at the company Berg Propulsion, gives the potential of developing new procedures for dimensioning of shaftlines.

1.2 Aim

The project aim is to develop current calculation methods that Berg Propulsion uses to calculate the shaft diameter for low-speed shaft. The current method of calculating the low-speed shaft at Berg Propulsion is to use the DNV version of the IACS (International Association of Classification Societies)formula. That is a conservative old, simple formula that describes the minimum allowed diameter and maximum hollow bore. Though the formula states that the equation defines the minimum diameter, there are some rumors in the industry that you can have the diameter lower and still get it approved by the classification society. By having the shaft diameter smaller, not only are savings on expenses on material weight, but also savings on the mechanical equipment on the shaft. Smaller flanges, smaller bearing, and so on

- The aim is to look into the the basics and background of classification rules with the intention of establishing a refined calculation method for the dimensioning of shaft lines.

1.3 Research question

Can you make shaft diameter smaller than current calculations methods and get approval from the classification society ?

- How much room is there for weight/design optimisation in the propulsion shaft line ?
- How much cost reduction is within reasonable reach by optimising the shaft line ?
- Can the new improved approach be used for preliminary design, or is it too extensive ?

The thesis goes over the path and the surrounding environment that was undergone, in the development of the new improved minimum shaft diameter method.

1.4 Limitations

- Definition of a success in the project is to decrease the diameter of the propulsion shaft and get it approved by the classification society.
- Calculation/simulation results are limited to classification society approval.
- The project is only focusing on the shaft itself (only low speed shaft), though other components do influence the behaviour of the shaft. Foremost components like the propeller, engine, and bearings.
- Rules and regulations in respect of the scope of the project. That is, low-speed shaft, ductile material, and maximum ultimate strength of the material(some equations are only applicable for a certain range of ultimate strength).
- Software license limitation. Because of license limitations, simulation of a 2-stroke engine TVC could not be performed.

2

Theory

This chapter provides the theoretical basis for the thesis work. It starts by describing different mechanical components of a shaft line. Following is an introduction of the theory behind the statical and the dynamic loads that are present during an operation. Important dynamic design phenomena theories, the vibrational behaviour, and fatigue. Lastly, the foremost rules and classifications that were used from IACS and DNV societies.

2.1 Shaft line

A shaft line is the collection of machinery components needed to propel a ship, more specifically the components that serve the purpose of transmitting the power from the prime mover to the propeller. The propulsion shafting is the main concern of this project but it is crucial to recognise the different components making up a complete shaft line. The purpose of the propulsion shaft is to transmit torque from the engine or motor for rotating the propeller. In the case of a typical propeller shaft, the shaft is also a structural member that supports all the weight and forces from the propeller. This is described as a low-speed shaft below. In the case of high-speed shafts, the shaft is more similar to a driveshaft in a heavy-duty truck. Its only purpose is to transfer the mechanical power or torque from the engine to the propeller [16].

2.1.1 Low-speed shaft

Low-speed shaft - LSS, like the name implies, is a shaft that rotates at a low rotational speed. But without any reference, a low speed does not mean anything. For a shaft line setup, the low speed would be the rotational speed of the propeller. The engines and electric motors often operate at higher rotational speed than the designed speed of the propeller. In this case reduction gears are required [16], and are typically positioned right by the engine. Connected to the output of the reduction gear is the shaft which the propeller is then attached to.

The speed range for a propeller in a commercial vessel could be from 70 to 250 revolutions per minute. The limit has been getting lower with an increased size of propellers on the very large cargo vessels at the same time as the low-speed two-stroke propulsion engines have gotten larger, more powerful and more fuel-efficient. Low speed 2 stroke engines operate at the same speed as the propeller and are thus directly connected, as seen in figure 2.1, where the engine crankshaft is considered an indirect continuum of the propulsion shafting. Looking at the large MAN B&W engines they operate at 70 - 80 rpm [24] and similar to the WinGD 2 stroke diesel engines. WinGD building on the tradition of Sulzer diesel engines and Wärtsilä two-stroke [35]. One example, the record setting WinGD 12X92DF engine delivering power output rated at 63,840 kW at 80 rpm and its performance measures a thermal efficiency of 51-53% [36].

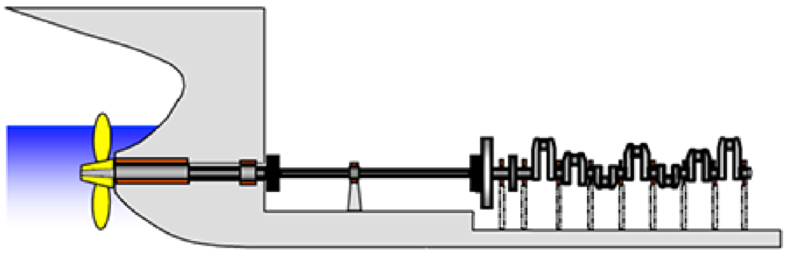

Figure 2.1: *The figure describes the setup of a low speed shaft line, directly coupled to a low speed engine. In a shaft alignment calculation the crankshaft in this case is modeled with the propulsion shafting*

In figure 2.2 an LSS shaft line is demonstrated, incorporating a reduction gear, controllable pitch propeller, CPP, and typically a medium-speed engine. In comparison with the directly coupled shaft, this setup is more common in ferries, fishing vessels and different types of specialised service and research type vessels. The setup gives more flexible operation and quicker response. The control mechanics for rotating the blades on a CPP propeller are often located on the reduction gearbox and the mechanical actuation is done by hydraulics or shaft running through the middle of the propeller shaft. By having the possibility to rotate the blades, effectively changing the pitch of the propeller, changing from forward to reverse thrust can be done seamlessly as well as controlling the load on the engine according to operation modes.

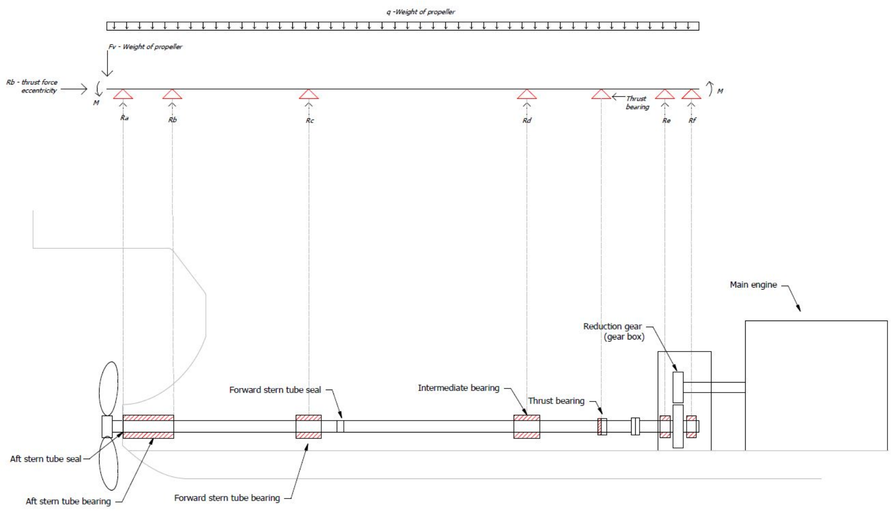

Figure 2.2: *The figure descripes the setup of a low speed shaft line with reduction gear. Simplified beam schema is presented above. In a shaft alignment calculation the output shaft and gear of the reduction gear is included*

2.1.2 High-speed shaft

In contrast to the earlier discussion about LSS, high-speed shafts are usually directly coupled to medium or high-speed diesel engines, hence the high speed notation, they operate at the speeds of the propulsion engine. High-speed shafts, HSS, are combined with azimuth thrusters the reason being that the reduction gearing is located in the angle drives of the thrusters. In the thruster housing, there are two ring and pinion drives that transfer the mechanical power through a 90-degree turn, hence the nickname Z-drives. Having a ring gear that usually has more teeth than the pinion gear means a reduction in rotational speeds, to suit the propeller and engine combination [16].
(**Note:** HSS are not considered in this thesis investigation).

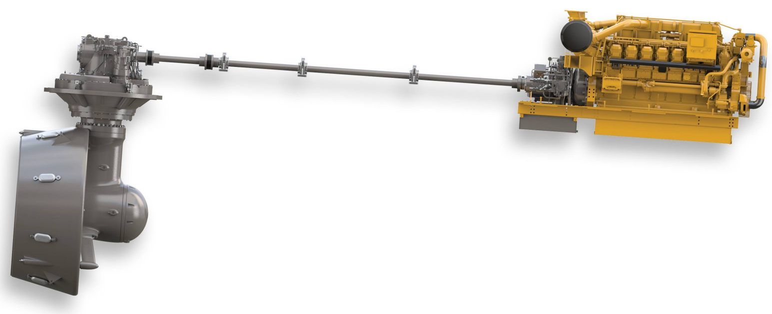

Figure 2.3: *Typical high speed shaft line, directly coupled to a high speed diesel engine. MTA thruster unit coupled to a CAT 3516 engine with an engine mounted clutch. Gears located in the top housing of the thruster unit by the input shaft and also in the leg of the thruster by the propeller shaft. Curtesy of Berg Propulsion Production AB.*

2.1.3 Engine

In the case of Berg Propulsion, most commonly propulsion power comes from medium or high-speed marine diesel engines. Reciprocating internal combustion engines will always cause some torsional vibrations, especially if the engine suffers from misfiring. Another way of delivering the propulsion power needed is to have diesel engines connected to generators. The generating set, engine and generator, then delivers just electric power. Electric motors are used to turn the propeller, giving in many cases more flexibility in operation and fewer vibrations.
In the book Ship Knowledge, the range of marine engine speeds is categorised in the following manner. [16]:

- **High-speed** four-stroke engines, RPMs above 960.
- **Medium-speed** four-stroke engines, RPMs ranging from 240-960.
- **Low-speed** two-stroke engines, RPMs below 240.

The large slow 2 stroke engines are efficient but very tall and heavy, usually accompanied with fixed pitch propeller, FPP, and not flexible in manoeuvring. The shaft line shown in figure 2.1 is a typical setup using a directly coupled low-speed engine with an FPP propeller. Having an FPP propeller and direct connection to the engine, doing a reverse manoeuvre, requires that a 2 stroke engine will be stopped and then started again, turning in the opposite direction to reverse the rotation of the propeller. This is typical for dry bulk, tanker and container vessels. The two-stroke engines are typically in-line engines with 5 to 9 cylinders in a row, the slow running, long stroke and huge torque from each cylinder makes torsional vibrations critical in the shaft. The firing pulses from the engine along with fluctuating moment from the propeller can match natural twisting and bending modes of the shaft. The most critical phenomena being the engine's main excitation order coinciding with the first torsional natural frequency of the shafting system [10]. This phenomenon is due to the fact that the crankshaft of the engine and the propeller shaft are rotating at the same speed and the torque input is pulsating very much. The power of each cylinder can easily be 3500 kW at 80 - 200 rpm. This results in much higher torque values per cylinder at the same time the strokes per minutes are fewer [24].
Compared for example V12 and V16 engines as common examples of medium and high-speed engines and more importantly the power output of each cylinder of about 1000 kW at 500 rpm giving much lower torque values per power stroke. This can be demonstrated by a simple example, power is in essence the ability to do certain amount of work within a time frame. It does not really matter how the work is proceeded (ideal simplification), it can be demonstrated by cycling up a steep hill within 5 minutes. The task requires the same amount of work whether one has the cycle in high gear or low gear. How ever it is much harder to step the pedals and turn the crank in high gear, this results in slow rotation but high torque on the crank, the other way is to be in lower gear, much easier to step the pedals but it needs many more revolutions. Hence, low torque but high rpm's on the crank, delivering the same amount of work. It is torque that snaps a shaft not power, then fatigue complicates things further [16][17][28].

2.1.4 Sterntube & Propeller shaft

From the Wärtsilä encyclopedia of marine technology we get the description as following:

> *Stern tube:* The watertight tube enclosing and supporting the propeller shaft. It consists of a cast-iron or casted steel cylinder fitted with a bearing surface within which the propeller shaft, enclosed in a sleeve, rotates. The stern tube is installed from aft and bolted to the stern frame boss. It can be press-fitted or installed with epoxy resin [32].

For a typical single propeller merchant or fishing vessel, the stern tube is a tubular section running through the aft structure of a ship, below the waterline. In essence, it is an open-ended tube between typically the machinery room and the open water. The stern tube makes a way for the propeller shaft to run through the hull, mechanically connecting the propeller to the propulsion engine or motor, as well as supporting the propeller. For this purpose, the stern tube is fitted with bearing surfaces and seals on the aft and forward end [16].
The bearings are usually of white metal and lubricated with oil. To prevent the surrounding water to enter the stern tube and most importantly not flood the machine room there are circular lip seals on the aft end of the stern tube that seal against the propeller shaft.

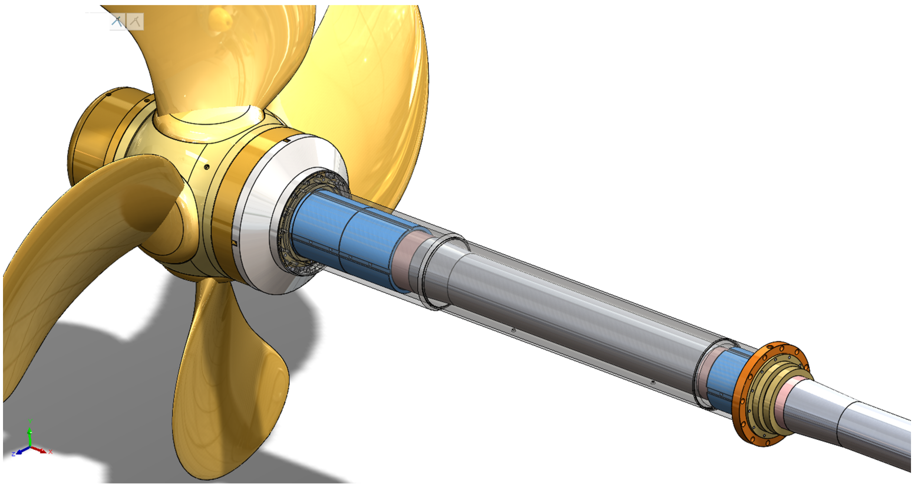

Figure 2.4: *3D rendered image of a propeller shaft and a stern tube. The stern tube is somewhat transparent. Stern tube bearings highlighted blue.* Courtesy of Berg Propulsion AB.

There are different types of setups, with single, two or more stern tube bearings, oil lubricated or seawater lubricated bearings. Here we will describe the setup of the 3 examples studied.

- Typical RoPax setup with twin screws having very long stern tubes extended outside the hull on either side supported by struts. The length demands a mid bearing resulting in a stern tube having aft, mid and forward bearing. Oil lubricated white metal bearings with seals at aft and forward end.

- Typical single screw tanker vessel having stern tube straight through the middle of the stern, aft bearing and forward bearing, aft and forward seals.

- Twin screw dredger vessel with ducted propellers having stern tubes running through fins or narrow skegs on either side. Forward and aft bearings with seals on forward and aft end.

The propeller shaft is the part of shafting the propeller is attached to. The shaft extends outside of the hull such that it acts as a counter lever, supporting the weight of the propeller, therefore there acts a large moment on the propeller shaft which is supported by the aft and forward stern tube bearings. The shaft forward of the stern tube is not affected much by this moment.

> *Propeller shaft or tail shaft:* The aftermost section of the propulsion shafting in the stern tube in single screw ships and in the struts of multiple screw ships to which the propeller is fitted [33].

2.1.5 Intermediate shaft

The intermediate shaft is an extension of the propeller shaft for applications where the shafting between propeller and gearbox or engine is long. Typical for ferries, Ro-Pax vessels, offshore service vessels for example. Those types of vessels have in common twin-screw arrangements where the machinery space is rather far forward from the propellers, thus requiring longer shafting than for example single screw tanker where the engine would be located just forward of the stern structure. The intermediate shafts are often forged as one piece having flanges on both ends. The intermediate shafts transmit the torque from the engine but they do not support any weight but their own. Therefore much smaller moment acts on them than the propeller shaft. See pair of a typical intermediate shaft in figure 2.5 [11].

> *Intermediate shafting* The lengths of shafting between the propeller shaft and the engine or the gearbox [34].

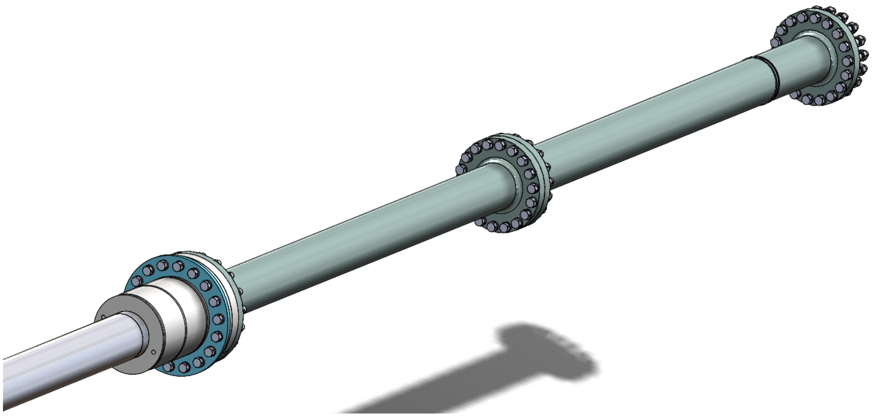

Figure 2.5: *3D rendered image of two intermediate shafts (gray-green).* Courtesy of Berg Propulsion AB.

2.1.6 Propeller

The propeller has the purpose of converting the mechanical torque into thrust to propel the ship. In the context of this thesis, the important factors are the weight of the propeller and forces acting on the propeller shaft when in operation. It is typical for a controllable pitch propeller to have 4 or 5 blades. “The number of blades affects the vibration excitation or "beats" caused by the propeller as it operates in a non-uniform wake field” [28, page 228].

2.1.7 Bearings

The bearings are carefully placed along the shaft according to shaft alignment. Both as standard beam support, but also dynamic support for lateral vibrations. Thus the number and location of bearings have to be calculated to fulfil the standards of the classification [11]. Typically two or more bearings are placed in the stern tube to support the bending moment from the propeller. After that, it depends on the length and circumstances of the intermediate if bearings are needed there. Berg does not produce their bearings, but they buy them from a third partner.
There is also a thrust bearing. The thrust bearing purpose is to fix the axial movement of the thrust from the propeller pushing the ship and axial vibrations [11]. This bearing is either placed as a separate bearing at the shaft or inside the gearbox. See example of stern tube bearings in figure 2.4.

2.2 Static-loads

By looking into the usual stresses that a propeller shaft is exposed to, it can be listed out as the torsional shear stress from the torque applied to the shaft, Normal stress from the axial load, normal- and shear stress from the transverse bending loads [5]. When multiple loads are applied to the body, see image 3.1.

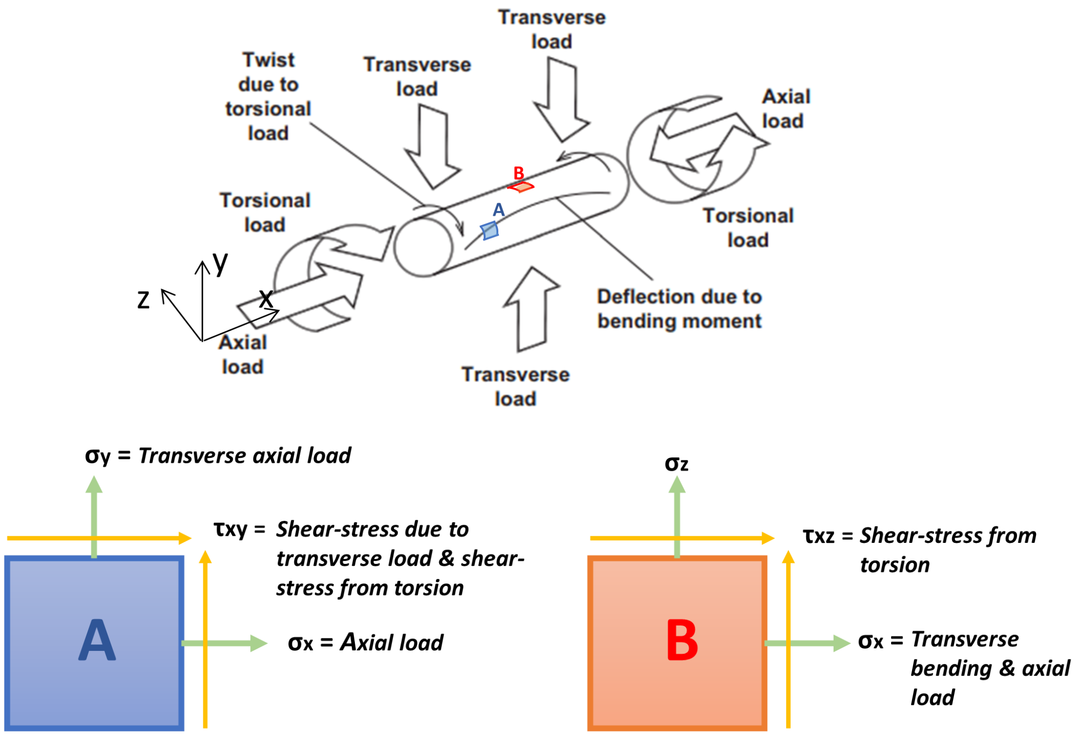

Figure 2.6: *A common combination of load cases on a circular body, With on-plane distortion theory [5]. Figure edited with image from [2],*

Because the shearing stress due to transverse load is maximum at the centre of the shaft, decreasing moving to the outer body of the shaft (the first moment of the portion of the area Q is equal to zero) and the opposite is applied for the bending moment from the transverse load and the torsion, where the maximum load is at the outer part of the shaft. Because of that (also the vertical shear load relative to other loads is minor) the shearing stress due to transverse load is neglected. According to that statement area marked by "B" in image 3.1, is considered the critical design criteria. With that definition and based on distortion energy theory and Von Mises criterion the maximum allowed stress for the (ductile) shaft can be estimated in the statical environment. The Von Mises criterion is defined like so, see equation 2.1[5].

$$\sigma' = \frac{1}{\sqrt{2}}\sqrt{(\sigma_x-\sigma_y)^2+(\sigma_y-\sigma_z)^2+(\sigma_z-\sigma_x)^2+6(\tau_{xy}^2+\tau_{yz}^2+\tau_{zx}^2)} \tag{2.1}$$

But in a simpler approach as it has been defined here above, the equation for on-plane stress can be calculated with formula 2.2[5].

$$\sigma' = \sqrt{\sigma_x^2-\sigma_x\sigma_y+\sigma_y^2+3\tau_{xy}^2} \tag{2.2}$$

and with final simplification, as it can be assured that the critical design criterion when the shaft is under unidirectional transverse load (often gravity), axial load, and torsional load the maximum allowed stress can be estimated with formula 2.3. (for more information see section 5-5 in Shigley's[5]).

$$\sigma' = \sqrt{\sigma_x^2 + 3\tau_{zx}^2} \tag{2.3}$$

Though this design model is simple, the fact in reality, it is not. There the shaft is under more load phenomena, oscillations in the dynamic spectrum, other unpredictable loads (new load vectors) like irregularities from the propeller in water, manoeuvring, and ice. The Classification societies present methods and simple formulas that can be trusted for the shaft design [21] [10] [11].

2.2.1 Breakdown of the IACS M68.4 formula

The IACS M68.4 formula is the method that Berg Propulsion uses to define their shaft diameters, which is further discussed in chapter 2.4.1. By looking into the formula and trying to solve and understand from what it is defined. From the start, it can be assumed that the formula is based on empirical data. The two factors 'K' and 'F' are both multipliers to influence the data result, but also to adjust the unit dimensions. Within the cubed square root it can be seen how the formula is divided into these three sections, where we have (in this order) the load, the inertia, and the material [21]. (as it has been said, the IACS formula is further discussed in chapter 2.4.1. For the convenience of side by side comparison, the ICAS M68.4 formula for minimum shaft diameter can be seen here in equation 2.4.

$$d_{min} = F * k \sqrt[3]{\frac{p}{n_0} * \frac{1}{1 - \frac{d_i^4}{d_0^4}} * \frac{560}{\sigma_B + 160}} \tag{2.4}$$

To conclude where it might originate from few different solutions were set up, with one standing out. By setting up a statical torsional load case for a hollow cylindrical section and solve it for the diameter [5], the equation looks fairly similar to the IACS M68.4. See equation solution here below (equation 2.5).

$$\begin{gathered} \tau = \frac{T \cdot D}{2 \cdot J} \rightarrow \tau = \frac{60P \cdot D \cdot 32}{2\pi n \cdot 2 \cdot \pi(D^4 - d^4)} \rightarrow \\ \textit{skipping few steps (full step by step in appendix B section B.1)} \\ \rightarrow D^3 = \frac{P}{n} \cdot \frac{1}{1 - \frac{d^4}{D^4}} \cdot \frac{480}{\tau\pi^2} \rightarrow D = \sqrt[3]{= \frac{P}{n} \cdot \frac{1}{1 - \frac{d^4}{D^4}} \cdot \frac{480}{\tau\pi^2}} \end{gathered} \tag{2.5}$$

As it can be seen, in the final solution when the diameter has been isolated from the statical torsional load of the shaft, the equation resembles the IACS M68.4. The only difference is the material element of each equation and, as previously mentioned, the multiplier factors (which influence the result based on the empirical study of the formula)

Typically in a statical approach for ductile materials, the yield strength is regarded as the point of failure [5], however, it can be seen in the IACS M68.4 formula the material factor is in respect of the ultimate strength. It is rather reasonable that the critical design criteria of a propulsion shaft are based on fatigue and the endurance

limit for the dynamic load of the system [5] [17]. Therefore the material part of the IACS M68.4 formula is limited to the fatigue strength of the design. The fatigue investigation of the formula is done in the dynamic chapter of the report, see section 3.1.2.
In addition, since the IACS M68.4 formula is based on an empirical study from IACS, so deviation is expected.

2.2.2 Stress concentration

A critical design factor for a mechanical component such as the shaft is the stress concentration factors. The stress concentration factor is a result influence of different components on the mechanical structure, or irregularity and defect. In the shaft case, components like change in diameter, shrink-fit coupling, flanges, notches, keyways, and more. It is critical to consider these factors when designing the shaft [10] [11].
The simple definition is that when the geometry is subjected to stress, and typically the stress is considered uniform throughout the cross-section of the geometry under the load. When the loading is uniform and the geometry as well, the stress distribution can be assumed to be homogeneous as well. But when the load or the geometry is not uniform the stress distribution varies along the part. The peak maximum stress occurs at these specific locations, as here previously mentioned [5].
The stress concentration factor (K_t and K_{ts} for shear load) is the ratio between the peak maximum stress and the average mean stress (the regular stress, for instance for normal stress $\sigma = F/A$), see equation 2.6 [5].

$$\frac{\sigma_{max}}{\sigma_{avrage}} = K_t \Longrightarrow \sigma_{max} = K_t * \sigma \tag{2.6}$$

Though the stress consideration factor is typically focused on a cross-section that is smaller in the area (material loss due to notches, keyways, shrinkage of diameter) the factor is not a function of the size, but rather the shape or the specific part. Flange fillet for example, the factor mainly based on the fillet radius, meaning if the radius is small the stress concentration is high [5].
To calculate the factor, one can simply use charts of Theoretical Stress-Concentration factors, which can be found in mechanical engineering books, or simply on the internet.
Have in mind that these Theoretical Stress-Concentration factors are only applicable for static loading. In the case of a ship's propulsion shaft, failure due to fatigue is the critical design criterion [17] [5]. Though these factors are not valid in the dynamic environment, a specific factor is used for the fatigue stress concentration which is derived from the Stress-Concentration factor K_t. Called the Fatigue Stress-Concentration Factor K_f, which is a reduced factor of K_t with a scale relation called notch sensitivity q. Similar to the other maximum stress, see equation 2.7 [17] [5].

$$\frac{\sigma_{max}}{\sigma_{avrage}} = K_f \Longrightarrow \sigma_{max} = K_f * \sigma \tag{2.7}$$

The reason for the maximum dynamic stress affecting the fatigue life is not the same maximum stress at the notch (K_t for irregularities in the material), but it is the mean stress over the volume around the maximum stress area. More on this will be addressed in the fatigue section of the thesis, see section 2.3.4.1 [5].

2.3 Dynamic-Loads

The dynamic loads on a propulsion shaft in operation are mainly divided into three cases. The lateral vibrations, torsional vibration, and axial vibration. These dynamic loads (mainly lateral- and torsional vibrations [10] [11]) are critical to know when designing a shaft and its fatigue limit.

2.3.1 Lateral vibrations - Whirling

Rotor dynamics describes the dynamic lateral vibration behaviour of rotating machinery. Especially flexural vibrations that can occur at the so called critical speed. For establishing the theory describing rotor dynamics, the most basic setup of rotating machinery is considered, see figure 2.7. There is a shaft of some length supported by two bearings, the shaft holds a disk that has a mass m [22].

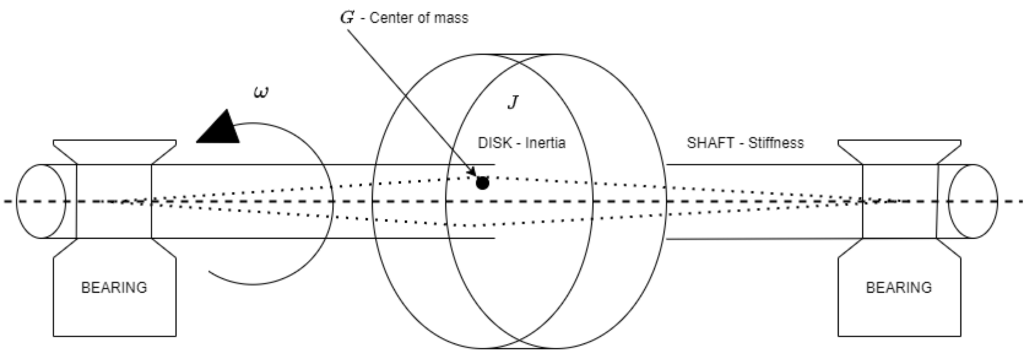

Figure 2.7: *Geometry of rotating disk on a shaft, supported by bearings. The angular velocity of the shaft is ω, the center of mass G is outside of the neutral axis. The thin dotted lines denote the deflection of the shaft, during whirling vibration* [22, p. 405]. Drawing inspired by graphics in Inman (2001).

This disk in the simple model can represent a stator in an electric motor or fan blades in a gas turbine. Because of manufacturing precision less than perfect, and possible residual mass like paint or some kind of dirt, the disk's centre of mass is not perfectly centred at the longitudinal neutral axis of the shaft [22].

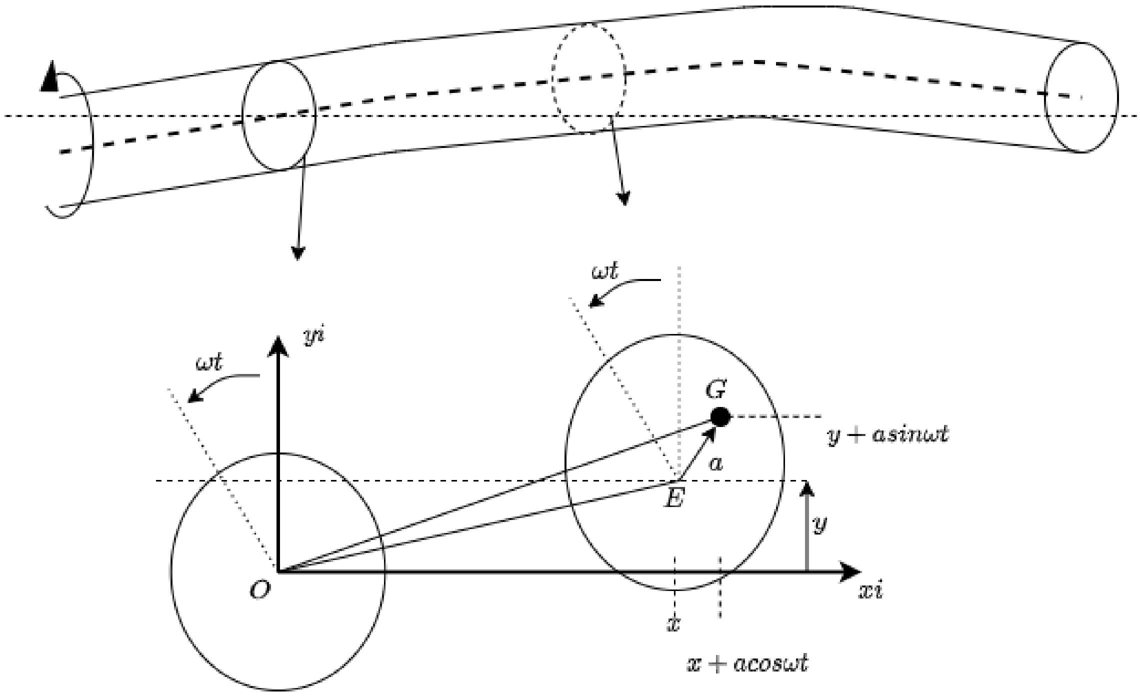

Figure 2.8: *Notation for whirling calculations.* [22, p. 405] Drawing inspired by graphics in Inman (2001).

The dynamic force balance of the rotating shaft and disk system is described in vector form by equation 2.8,

$$m\ddot{\mathbf{r}} = -kx\hat{\mathbf{i}} - ky\hat{\mathbf{j}} - c\dot{x}\hat{\mathbf{i}} - c\dot{y}\hat{\mathbf{j}} \tag{2.8}$$

where, the inertial force is at the left side and at the right side the stiffness and damping components. Here, m is the mass of the disk, $\ddot{\mathbf{r}}$ is the second derivative of the position vector $\mathbf{r}$ giving the acceleration of the mass center. The stiffness coefficient k is related to the displacements x and y, similarly the damping coefficient c is related to the velocities $\dot{x}$ and $\dot{y}$ [22].
From the geometry we get equation 2.9 for the transverse position of the center of mass from the neutral axis, $\mathbf{r}$.

$$\mathbf{r} = (x + a\cos\omega t)\hat{\mathbf{i}} + (y + a\sin\omega t)\hat{\mathbf{j}} \tag{2.9}$$

Here, the angular velocity of the shaft is given by ω. The angular velocity has the units of radians per second, $\frac{rad}{s}$, as can be seen on figure 2.8 the rotation of the shaft is defined as $\omega \cdot t$ resulting in the angular displacement in radians. Worth noting is that usual practice is to give engine speeds in rotations per minutes, *rpm*, then normally noted with n_0 [31]. Figure 2.8 describes also the geometry of the whirling motion and relates that to equation 2.9 and 2.10 [22].

$$\ddot{\mathbf{r}} = (\ddot{x} - a\omega^2\cos\omega t)\hat{\mathbf{i}} + (\ddot{y} - a\omega^2\sin\omega t)\hat{\mathbf{j}} \tag{2.10}$$

$$(m\ddot{x} - ma\omega^2\cos\omega t + c\dot{x} + kx)\hat{\mathbf{i}} + (m\ddot{y} - ma\omega^2\sin\omega t + c\dot{y} + ky)\hat{\mathbf{j}} = \mathbf{0} \tag{2.11}$$

$$m\ddot{x} + c\dot{x} + kx = ma\omega^2 \cos\omega t \tag{2.12}$$

$$m\ddot{y} + c\dot{y} + ky = ma\omega^2 \sin\omega t \tag{2.13}$$

Steady state solution of equation 2.12

$$x(t) = \frac{ar^2}{\sqrt{(1-r^2)^2 + (2r\zeta)^2}} \cos\left(\omega t - \arctan\frac{2r\zeta}{1-r^2}\right) \tag{2.14}$$

similarly for equation 2.13

$$y(t) = \frac{ar^2}{\sqrt{(1-r^2)^2 + (2r\zeta)^2}} \sin\left(\omega t - \arctan\frac{2r\zeta}{1-r^2}\right) \tag{2.15}$$

where, $r = \frac{\omega}{\sqrt{k/m}}$ and $\zeta = c/(2m\omega_n)$. The phase angle, ϕ, describing the angular shift between the rotation of the shaft about its neutral axis and the rotation of the disk about the shaft, is given by $\phi = \arctan\frac{2r\zeta}{1-r^2}$ [22].

$$\tan\theta = \frac{y}{x} = \frac{\sin(\omega t - \phi)}{\cos(\omega t - \phi)} = \tan(\omega t - \phi) \tag{2.16}$$

This gives the relationship $\theta = \omega t - \phi$ which differentiated in respect to t gives the velocity of whirling $\dot{\theta} = \omega$. It is called syncronous whirling when the speed of whirling is the same as the angular velocity. Whirling is the rotation of the disk around the nautral axis of the shaft. The amount of deflection is described by $\mathbf{r}$ the radius from the nautral axis to the circular path the shaft follows when whirling about the nautral axis [22].

$$\mathbf{r} = x\hat{\mathbf{i}} + y\hat{\mathbf{j}} \tag{2.17}$$

$$|\mathbf{r}(t)| = \sqrt{x^2 + y^2} = X\sqrt{\sin^2(\omega t - \phi) + \cos^2 \omega t - \phi} = X \tag{2.18}$$

$$X = \frac{ar^2}{\sqrt{(1-r^2)^2 + (2r\zeta)^2}} \tag{2.19}$$

When $r \cong 1$, the system hits a resonance and the diflections of the shaft-disk system or rotor, can start to experience very large amplitudes. At $r = 1$ the angular velocity of the disk equals the natural bending frequency of the shaft, $\omega_r = \sqrt{k/m}$, this is called the critical speed of the rotor [10][22]. Since the marine shafting systems have many vibration modes, each having a natural frequency, the propulsion shaft will have whirling speeds for each mode of vibration. Those are the critical operating speeds later estimated by shaft alignment procedures.

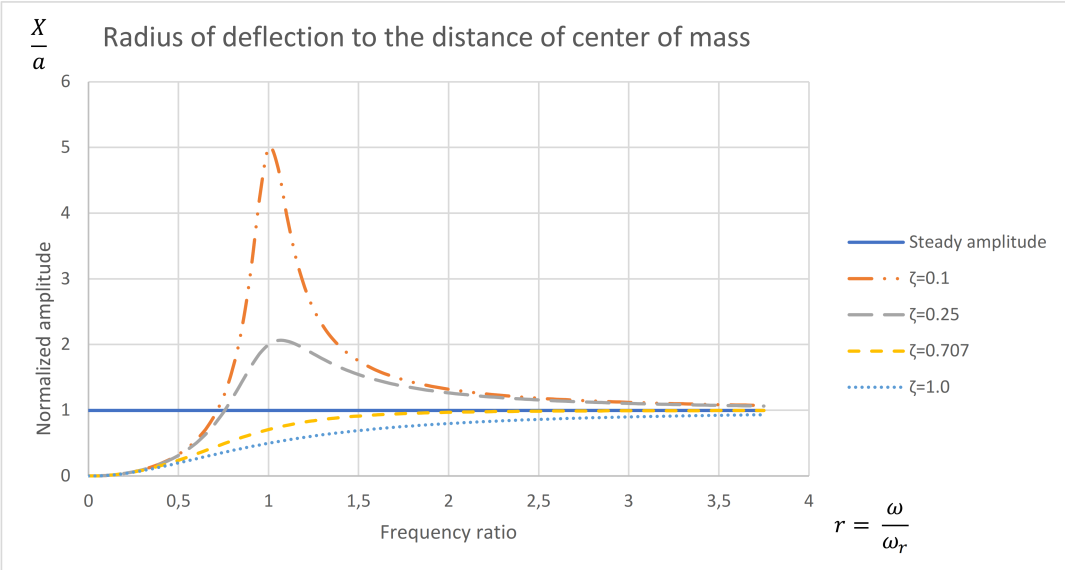

Figure 2.9: *Normalized deflection amplitude versus frequency ratio for different amount of damping. The resonance behaviour is clearly demonstrated close to frequency ratio of one. The steady state amplitude becomes equal to the offset of the center of mass* [22, p.407].

For further reading about marine shafting lateral and axial vibration theory, the interested reader can access the open access article, *Vibration Characteristics and Power Flow Analysis of a Ship Propulsion Shafting System with General Support and Thrust Loading* by Deshui Xu, Jingtao Du, and Chuan Tian at the College of Power and Energy Engineering, Harbin Engineering University, Harbin 150001, China. Published 13 June 2020, *Hindawi - Shock and Vibration.*

2.3.2 Torsional vibrations

Torsional vibration calculation - TVC is an important step in the design of a propulsion system for ships. It is essential to carry out these calculations early in the design phase when the shafting diameters have been selected [31]. Typically the propulsion shafting is dimensioned according to the classification requirements very early on in the design phase, with minimal amount of inputs using the simple IACS M68.4 rules, then when preliminary shaft arrangement has been drawn the shaft design is checked for torsional vibrations problems in a TVC analysis. Usually this would be done at the same time as first shaft alignment and whirling analysis are made. There are different stakeholders in a ship building project that could do a TVC analysis, the engine or gearbox manufacturer, supplier of flexible couplings as well as the propeller and shafting manufacturer.
The reason for doing those calculations early in the design process of a ship is to locate possible problems before the actual physical ship building is underway. It is much easier and less expensive to do modifications, move or add support bearings, change shaft dimensions while still in the design phase rather than needing to scrap or change something already built and manufactured, like stern tube and bossing or large propeller shafts [31]. According to rotor dynamics experts at Berg Propulsion,

the experience is that most often only small adjustments are needed and those can be done by choosing the correct flexible coupling, tuned according to TVC analysis, that dampens out unwanted harmonics [19].
Torsional vibration is a vibration phenomena related to a unsteady torque applied to a shaft. *The vibration occurs in an angular direction around the center axis of the shaft in a plane perpendicular to the cross section of the shaft.* [22, page 452] The rotation of the shaft fluctuates, hence, it is time dependent. It is also dependent on position along the shaft because the shaft is twisted by the torque it is transmitting. Hence, the rotation is given by $\theta(x,t)$, where x is the position along the length of the shaft and t denotes time.
To establish the general equation of motion for a shaft transmitting torque, a short section of a shaft is considered which has a moment force and reaction at each end [22].

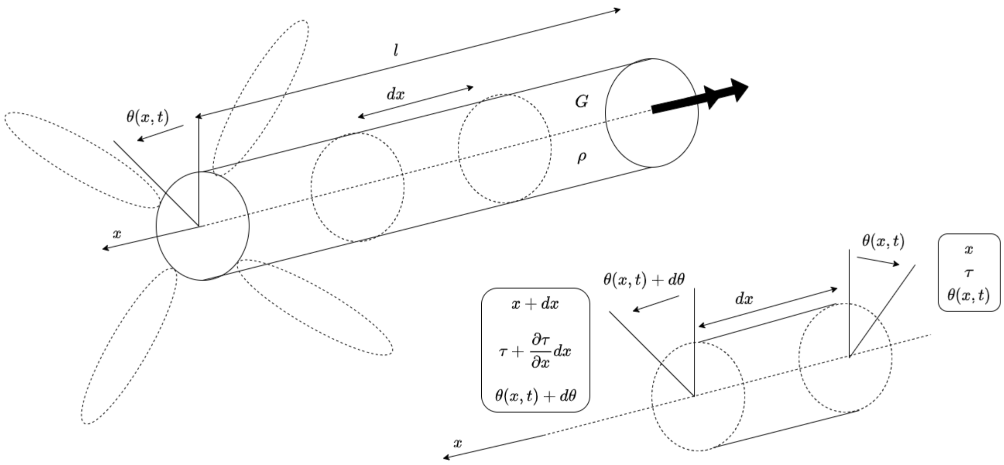

Figure 2.10: *The figure describes the twist of a shaft transmitting torque and relation between, torque, twist angle and position* [22, p. 452]. Drawing inspired by graphics in Inman (2001).

$$\tau = GJ\frac{\partial \theta(x,t)}{\partial x} \tag{2.20}$$

$$\tau + \frac{\partial \tau}{\partial x}dx - \tau = J_0\frac{\partial^2 \theta}{\partial t^2}dx \tag{2.21}$$

$$\frac{\partial}{\partial x}\left(GJ\frac{\partial \theta}{\partial x}\right) = \rho J\frac{\partial^2 \theta}{\partial t^2} \tag{2.22}$$

When the stiffness of the shaft GJ can be regarded as constant, the result is equation 2.23, describing twisting vibration of a shaft.

$$\frac{\partial^2 \theta(x,t)}{\partial t^2} = \left(\frac{G}{\rho}\right)\frac{\partial^2 \theta(x,t)}{\partial x^2} \tag{2.23}$$

Table 2.1: *Notation for TVC formulation.*

τ	: Torque
$\theta(x,t)$	: Rotation
G	: Shear modulus
J	: Polar moment of area
GJ	: Torsional stiffness

2.3.2.1 Damping in TVC

Damping is not as clearly defined as the inertia and stiffness properties of shafts and engine components. The inertia of a shaft or a wheel can be calculated directly from its geometry and density, similarly, the stiffness is a property of the geometry and material properties.

> The calculation results depend upon inertial moments of actual masses, stiffness of shafting components, as well as the excitation forces and moments exerted by the propulsion engine(s) and the propeller. Inertial moments and stiffness can be determined with no ambiguities. However, this is not the case with either the damping or the engine excitation. Actually, during validation onboard the calculation supposed damping is the main influential factor to be verified. [31, p. S-156]

Propeller damping factors used to define the propeller absolute damping b_{Ap}, are the Frahm number D_F, see equation 2.25 and Archer number D_A, see equation 2.26. The relationship between those two factors can be demonstrated by [31, p. S-168]:

$$D_A = D_F \cdot \frac{30}{\pi} \tag{2.24}$$

The application of the Frahm number:

$$b_{Ap} = D_F \cdot \frac{30}{\pi} \cdot \frac{T_p}{n_p} = D_F \cdot \left(\frac{30}{\pi}\right)^2 \cdot \frac{P_0}{n_{p0}^3} \cdot n_p = D_F \cdot \left(\frac{30}{\pi}\right)^3 \cdot \frac{P_0}{n_{p0}^3} \cdot \omega_p \tag{2.25}$$

The application of the Archer number:

$$b_{Ap} = D_A \cdot \frac{T_p}{n_p} = D_A \cdot \left(\frac{30}{\pi}\right) \cdot \frac{P_0}{n_{p0}^3} \cdot n_p = D_A \cdot \left(\frac{30}{\pi}\right)^2 \cdot \frac{P_0}{n_{p0}^3} \cdot \omega_p \tag{2.26}$$

The practical values of the damping factors are for Frahm, between 2.9 to 3.7 and for Archer, 25 to 35 [31].

In Nauticus Machinery TVC where the propeller properties are defined, a typical value for Frahm is suggested as 2.8. For the Archer number, the lowest value possible is 20, the range of typical values is stated 25-35 [13]. A good rule-of-thumb value according to Berg rotor dynamic experts is Archer number equal to 27.

Another model for calculating the propeller damping is the Schwaneke damping. With this model the damping is calculated through elaborate formulation using a collection of factors, all describing the geometrical properties of the propeller [13].

The propeller damping C is given by [13, p. 41]:

$$C = f \cdot \left(\frac{D_B}{D}\right) \cdot D^5 \cdot \left(\frac{H}{D}\right)^2 \cdot \frac{A_E}{A_o} \cdot n \tag{2.27}$$

$$f \cdot \left(\frac{D_B}{D}\right) = 4.271 \cdot \left[\frac{\sqrt{\frac{D}{D_B} - 1}}{8 \cdot \frac{D}{D_B}} + \frac{\sqrt{\frac{D}{D_B} - 1}}{12 \cdot \left(\frac{D}{D_B}\right)^2} - \frac{\sqrt{\frac{D}{D_B} - 1}}{3 \cdot \left(\frac{D}{D_B}\right)^3} + \frac{\arctan\sqrt{\frac{D}{D_B} - 1}}{8}\right] \tag{2.28}$$

Table 2.2 summarises notation and definitions used in propulsion system calculations [31, pp. S-168 - S-169].

Table 2.2: *Notation and definitions for propulsion system calculations.*

P_0	: Engine nominal rating power, MCR $[kW]$
n_0	: Engine nominal speed at MCR $[rpm]$
i	: Gearbox transmission ratio
$n_{p0} = \frac{n_0}{i}$	: Propeller nominal speed $[rpm]$
$\omega_p = \frac{\pi \cdot n_p}{30}$	: Propeller angular velocity $[rad/s]$
n_p	: Propeller speed $[rpm]$
$T_0 = \frac{30}{\pi} \cdot \frac{P_0}{n_0}$	: Engine nominal torque $[kNm]$
$T_{p0} = i \cdot T_0$	: Propeller nominal torque $[kNm]$
$P = P_0 \cdot \left(\frac{n_p}{n_{p0}}\right)^3$	: Propeller power curve $[kW]$
$T_p = T_0 \cdot \left(\frac{n_p}{n_{p0}}\right)^2$	: Propeller torque curve $[kNm]$

2.3.2.2 Application factor KA

In calculations of the dynamic torsional load (simply torsional vibration) on a shaft the application factor KA is used. The application factor is the factor that describes the range between the nominal torsional load and the amplitude of the torsional vibration, that is the increase in rated torque affected by superimposed dynamic or impact loads. For each different load case, a separate application factor is used. These application factors can either be acquired with Torsional Vibration Analysis (also called TVC) or in cases of lack of data they can be estimated from provided tables [10] [11].

For the continuous normal operations of the ship the factor KA_{norm} is utilized (it is a KA factor, but labeled KA_{norm} to identify what amplitude is for normal operating conditions). The KA_{norm} is a key design criterion in the dynamic response since it is the factors that have an important influence on the high cycle fatigue assessment of the shafts. The KA_{norm} can be defined like previously said with TVC or estimated from a table like DNV provides, where the given KA is based on different system types [10] [11], see table 2.3.

Table 2.3: *DNV definition for estimated application factor for different system setup[11]*

System type KA_{norm}	**KA**
Turbines and electric drives	1.1
Diesel engine drive system with fluid clutch between engine and gears	1.1
Diesel engine systems with highly flexible coupling between engine and gears	1.3
Diesel engine system with no flexible coupling between engine and gears	1.5
Generator drives	1.5

A more precise approach is to define the KA based on simulated TVC data. The KA is calculated by certain formula, see equation 2.29 (only applicable for geared plants). Where τ_v is the torsional amplitude and τ_0 the nomial torsional load [10] [11].

$$K_A = 1 + \frac{T_v}{T_0} = 1 + \frac{\tau_v}{\tau_0} \tag{2.29}$$

KAP defines the amplitude of the highest torsional loads, which define the lowest accumulative fatigue criteria (lowest of the low-cycle fatigue). That is frequent loads like extreme maneuvering, clutching in shock load, and if the vessel is ice-class grated the torsional load from ice shock [11]. The KAP is calculated with the given formula, see equation 2.30 (only applicable for geared plants)[10] [11].

$$KAP = \frac{T_{peak}}{T_0} = \frac{\tau_{peak}}{\tau_0} \tag{2.30}$$

δKA is the factor for the torque range for reversible torsion, that is the torsional range is applied in both directions (minus and positive loads). This is applicable for reversing plants. The load case is regarded as low cycle stress and can simply be defined as the KA amplitude times two. But with more precision and if one has the data the ΔKA can be calculated as so, see equation 2.31 (only applicable for geared plants)[10] [11].

$$\Delta KA = \frac{\tau_0 KAP + |\tau_{max_{reversed}}|}{\tau_0} \quad or \rightarrow \Delta KA = 2KAP \quad or \quad KA_{ice} + K_{AP} \tag{2.31}$$

The application factor is important in this study and is used in the calculations of the minimum allowed shaft diameter, in this project [10] [11].

An example how the application factor is displayd can be seen on figure 2.11 (figure is presented in DNVGL-CG-0038 [10] for their definition of the application factor)

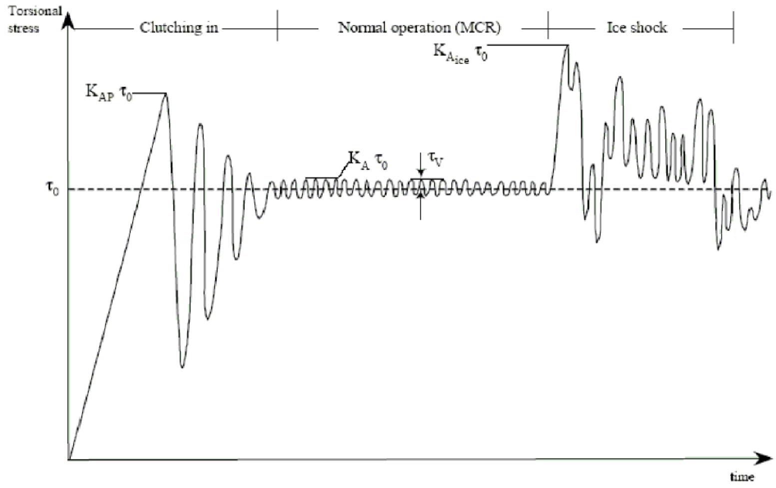

Figure 2.11: *Torsional vibratory stress for different load scenario and its relation with mean stress tau_0 and KA, in time domain. Based on direct coupled plant. Image gotten from DNVGL-CG-0038 [10]*

2.3.2.3 Estimating the application factor

If the application factor is needed for a shaft or other propulsion calculations, and a TVC analysis has not been done for that specific propulsion system, an estimated application factor can be acquired.
The application factor for a normal operating condition (KA_{norm} or simply KA (sometimes K_A) has been mentioned here in the previous section and can be obtained from table 2.3.
A low cycle application factor KAP (Application factor, temporary occasional peak torques, can simply be estimated as 1.4 [12]

The ice-class application factor is more difficult to estimate than the other two factors here previously. The torque is based on peak torque when the propeller hits the ice. An empirical method to estimate the factor is described in DNVGL-RU-SHIP Pt.6 Ch.6. Part 15.5.3. An extensive step-by-step solution will be found in Appendix B sectionB.3. The calculation output will provide the peak torque, which can then be used with equation 2.30. The estimation is based on few variables, that is if the propeller is in a duct, the different ice-class, the mass moment of inertia ratio between the propulsion side and engine side, the pitch ratio at radius 0.7, and others. Note the ice-class should not be less than the KAP, and if that happens, the calculations will always depend on the critical amplitude, which would then be KAP [12].

2.3.3 Axial vibration

Acts in the axial direction, along the shaft, resulting in alternating compression and tension.
The axial vibration is not considered in this thesis study, since it is a minor dynamic load and does not affect the fatigue-life or vibrations of a marine shaft. As it is stated

in DNV CG 0038 [10, p. 6], "stresses are considered negligible for marine shafting systems as they are dominated by torsional- and bending stresses", and in terms of fatigue strength "the combined vibratory torsional and rotating bending stresses (axial stresses disregarded) relative to the respective component fatigue strengths." [10].

2.3.4 Fatiuge

When a part is subjected to its critical yield strength the material enters the permanent deformation, and in many mechanical design cases that is considered a failure [5]. The ultimate strength, or the tensile strength of the material, is the maximum stress the material can be subjected to before a complete failure of the part. The observation of this kind of failure is in the respect of stress/strain. In the Berg Propulsion case for a shaft line, the most common material chose for the shafts is EN 1.1170 (28Mn6) steel, which has requirement standards: tensile strength of $\sigma_B = 600N/mm^2$, and yield strength: $\sigma_y = 350N/mm^2$. Fatigue failure due to stress/cycle is another design criterion important in dynamic load cases such as the rotating shaft of a vessel. That is the breakdown of the mechanical component fails way below the ultimate strength of the material due to accumulative repeated cycle load on the part. Fatigue failure predicts the number of cycles a component can withstand before a failure, by comparing the operation of the part to experimental empirical data or do a real-life experiment on the design.
A brief explanation of fatigue strength is that the estimation for the life for the part or the design criteria for the part can be explained and plotted up in an SN-graph (or Wöhler curve) [17] [5]. The y-axis is the fatigue strength or the stress range and the x-axis the number of cycles, see an example of the graph in figure 2.12.

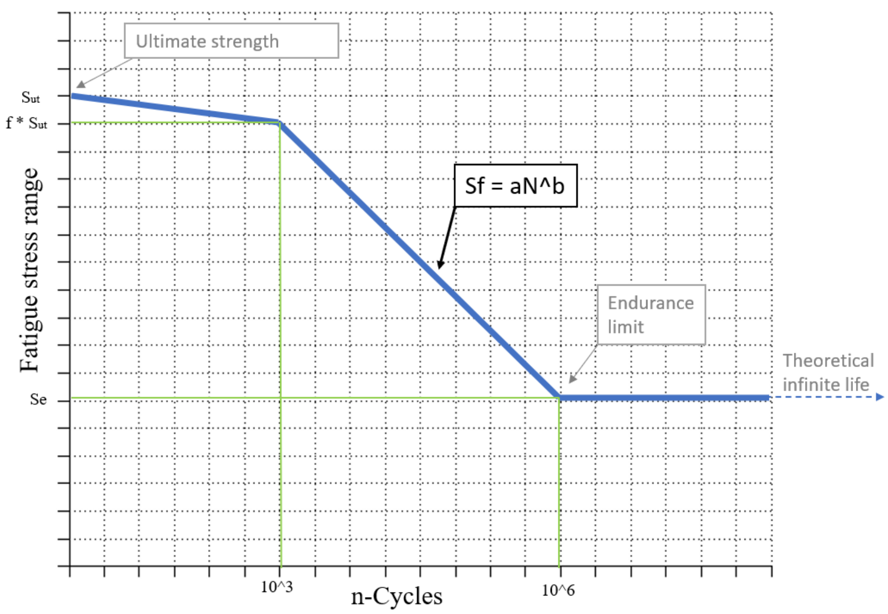

Figure 2.12: *Example SN- diagram for a steel material with LCF range up to* 10^3 *and enurance limit at* 10^6*. The x-axis is number of cycles in log scale and y-axis is the fatigue stress range [17] [5].*

Where each point on the graph describes the number of cycles the material can withstand with the given stress. Depending on the material, the shape, type of load, surface finish, and more the curve changes. It can be expensive and time-consuming to perform real-life tests for particular designs, so a conservative SN curve can be plotted for different cases. Note that typical SN diagrams are only applicable for completely reverse loading [17] [5].
The SN diagram is divided into two cases, the low cycle fatigue and the high cycle fatigue. The low cycle is typically rated for cycles up to 10^3 or 10^4 number of cycles (note that DNV rates LCF for up to 10^4, this is all based on experimental data). Low cycle fatigue are high stresses that can only accumulate few cycles before failing, they are accounted for stresses that can both be plastic deformation and elastic-. The high cycle fatigue accounts for more than the given number of cycles for LCF and up [10] [11].
An explanation along with figure 2.12, the diagram on the figure represents a conservative SN diagram with steel material and LCF at 10^3. The diagram is divided into three slopes, begins at the ultimate tensile strength, and with a fixed slope (in log scale) it reaches the HCF zone. The slope is defined by the constant f at the 10^3 cycle, the Fatigue Strength Factor, which is a conservative factor based on the material ultimate strength. From this point is another fixed slope (in log scale) to the endurance limit, Se at 10^6. The endurance stress limit is defined like so, see equation 2.32 [5].

$$S_e = k_a k_b k_c k_d k_e k_f * S'_e \tag{2.32}$$

Where the Se' strength is conservatively $0.5S_{ut}$ (if the $S_{ut} <$ 1400MPa) , but can also be acquired from an experimental data graph, where the ratio between Se' and S_{ut} ranges from 0.4 to 0.6. The k factors account for different set-ups, surface condition, size factor, load factor, temperature-, reliability-, miscellaneous effect- and more. The slope between $f * S_{ut}$ and Se can be described as $Sf = aN^b$, where the a and b factors can be solved for, see equation 2.33

$$\begin{gathered} f * S_{ut} = a(10^3)^b \qquad \& \qquad S_e = a(10^6)^b \longrightarrow \quad ... \\ ... \quad a = (f * S_{ut})^2/S_e \qquad \& \qquad b = -[log(f * S_{ut}/S_e)]/3 \end{gathered} \tag{2.33}$$

From the endurance limit (below it) the part should be able to withstand an infinite amount of cycles without failure [5].(remember this statement, because that will be the main design criteria when trying to unravel the IACS M68 formula (mimic it))

This explanation of the fatigue life of a designed component is simplified and in real life there are other input variables to account for, and based on the mechanical component different approaches to the SN-diagram are supported by empirical data. For instance, when looking at the behaviour of the stress cycle, see image 2.13.

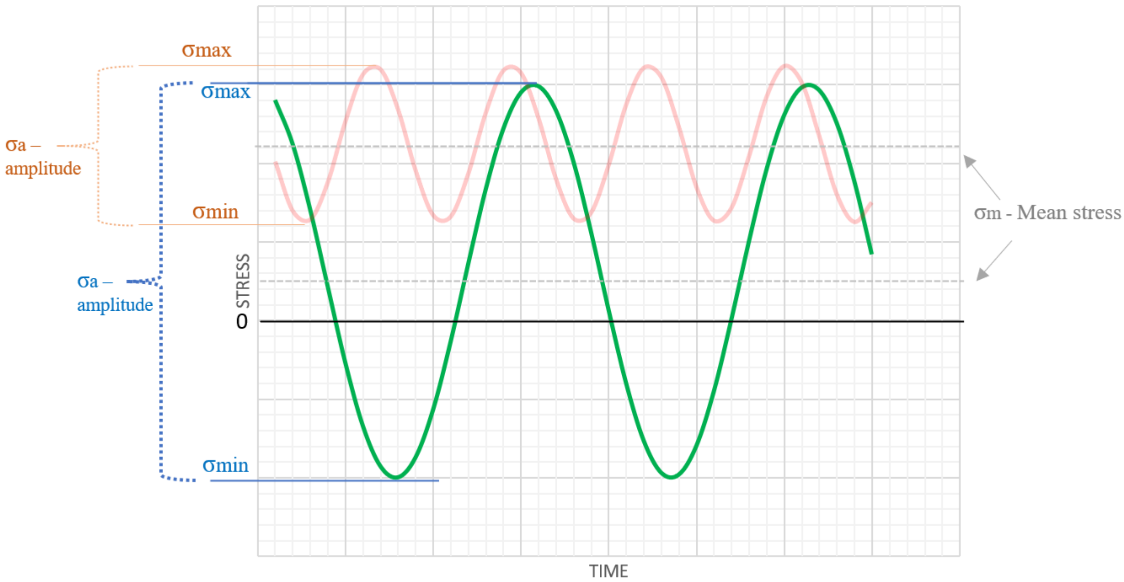

Figure 2.13: *Simplified stress amplitude for two different loadcases*

For the SN diagram (figure 2.12) to be valid the load must be complete reverse stress amplitude, that is when the mean stress is equal 0 ($\sigma_{max} = |\sigma_{min}|$). In the case of a vessels shaft in operation, the torque load is constant with addition to vibrations, Meaning that the mean torque (called Nominal torsional stress at maximum continuous power τ_0) is not zero, and the shaft operation condition is more like the orange line in the graph(figure 2.13), having the mean stress under tension will affect the fatigue life of the component. To address this, either the SN graph for the specific mean value must be acquired, or use methods to check the criteria of failure, approaches like the Soderberg, Goodman, Gerber, Dang Van and more [18] [17] [5].
In addition to this complication, in real-life cases like the ship shaft, will not be submitted to simple dynamic load cases as has been visualized here. Instead, many different factors influence the operating condition of the environment. In statistical calculations, the Rainflow Counting Method can be used to "count" the peaks and divide the stress cycles into separate simpler constant stress amplitude. Each separate cycle can be accumulated with The Palmers-Miner Cycle Ratio Summation Rule, or simply the Miners rule, to examine if the component will reach fatigue failure [9] [18] [5], see the Miner rule in equation 2.34.

$$D = \sum \frac{n_i}{N_i} \tag{2.34}$$

If the component is under different loads, bending-, axial and/or torsional stress, combining them with von-Mieses is an acceptable way to acquire the stress amplitude (σ_a) and mean stress (σ_m) [5] (see section 6-14 in Shigley's)

DNV Classification society uses the torsional load amplitude (according to the theory here previously) to estimate the fatigue life of the shaft. To estimate the load cycle amplitude a factor is used that represents the ratio between the mean torsional load and the maximum load for each loading scenario (load scenario meaning, normal operating conditions, an encounter with ice-, barred speed range, and so on). The factor is called application factor K_A, has been further explained in section 2.3.2.2.

2.3.4.1 Fatigue Stress Concentration Factor

Critical design criteria for a mechanical component like the shaft is the Fatigue Stress Concentration Factor (K_f and K_{fs} for torsion). The Fatigue Stress Concentration Factor is a reduced value of the Stress Concentration factor (previously talked about in section 2.2.2), defined by the notch sensitivity q, see equation 2.35.

$$q = \frac{K_f - 1}{K_t} \qquad or \qquad q = \frac{K_{fs} - 1}{K_{ts}} \tag{2.35}$$

The notch sensitivity can either be acquired from notch sensitivity charts or by using *Neuber equation* [5] (see section 6-10 in Shigley's).

2.4 Classification rules & guidelines

Classification society provides rules and regulations that apply under their flag state, for the ships registered under that specific country. In this chapter the relevant rules and regulations that are applied in this study is presented. *All the classification rules from each society are freely available on their websites.*

2.4.1 IACS

Looking into a few of the major classification society rules, it can be seen how each standard defines the minimum allowed diameter of the propulsion shafting. By looking into the foundation of the rules, the International Association of Classification Societies (or IACS), which is a non-governmental organization that consists of the twelve major classification societies. 90% of shipping tonnage in the world market falls under the IACS classification, so it is safe to say that the standard is respected in the world of shipping [3]. The minimum allowed propulsion shaft diameter is defined in the IACS classification rules (rather a conservative one), which provides the 12 member societies a foundation for their shaft rules and guidelines. By looking into some of the member societies it can be seen that every member defines their minimum allowed shaft diameter with formulas that resemble the IACS formula. Either by just having it completely the same, maybe small changes, or simply just the same but they break it apart into separate equations and also change the letters of the variables. This conservative formula from IACS is defined in their M68 document [21]. The classifications from IACS that are relevant for this thesis study can be obtained from that specific document. Formulas, definitions, and other rules such as material limitations for the calculations, Permissible torsional vibration stresses (used to find barred speed range), influence from different shaft design features, and more [21].

The minimum allowed diameter formula that has been referred to here and will be referred to as the IACS M68.4 formula is defined like so, see equation 2.36 [21].

$$d_{min} = F * k \sqrt[3]{\frac{p}{n_0} * \frac{1}{1 - \frac{d_i^4}{d_0^4}} * \frac{560}{\sigma_B + 160}} \tag{2.36}$$

Not many input values are needed to perform the calculation since the method is considered simple and conservative. Though the classification societies display this method of designing the propulsion shaft(section 2.4 in PRS [26], 5.2 in RS [27], Pt 5, Ch 3 section 203 in KR [23] and many more) some also provide a more complex alternative way of defining the shaft and still be approved by the class [10].
Limitations are defined so the calculation method for the M68.4 formula (applies to all equations and requirements in the m.68 document). Where the selected material is required to be:

- For carbon and carbon manganese steels, a minimum specified tensile strength not exceeding 600 N/mm2 for use in M68.5 and not exceeding 760 N/mm2 in M68.4.
- For alloy steels, a minimum specified tensile strength not exceeding 800 N/mm2.
- For propeller shafts in general a minimum specified tensile strength not exceeding 600 N/mm2 (for carbon, carbon manganese and alloy steels).

Other requirements must also oblige and are listed in the document (one can look it up in m.68 document [21].) and since they do not fall under the study case, it is unnecessary to define them here [21].

The IACS UR M68.5 formula for allowed torsional vibration based on defined material thickness for continuous operation. Torsional vibration analysis of a given shaft with a scenario when one cylinder is misfiring is performed to compare with the Permissible torsional vibration stresses M68.5. This calculation can be used both for coupled and geared plants. The output result is the allowed vibrational range, from no rotation up to the full speed of the shaft. The results can give the barred speed range, that is the shaft rotational speed range where the torsional vibration stress for the given speed exceeds the allowed torsional vibrational stress [21]. See equations 2.37 and 2.38.

$$\pm \tau_C = \frac{\sigma_B + 160}{18} * C_K * C_D * (3 - 2 * \lambda^2) \qquad for : \lambda < 0.9 \tag{2.37}$$

$$\pm \tau_C = \frac{\sigma_B + 160}{18} * C_K * C_D * 1.38 \qquad for : 0.9 < \lambda < 1.05 \tag{2.38}$$

As it has been mentioned, the M68.4 formula is simple and conservative and thus there should be room for improvement. Hence defined by some of the IACS members are more complex and detailed methods for calculating the minimum shaft diameter. IACS classification does mention this, therefore the alternative methods are approved. One method strikes out and was the main method used in the thesis study, it is considered a guideline rule from DNV. The reason for the thesis study to be so dependant on DNV is because of their influence and relevancy in the industry, at least here in northern Europe. The method is defined in a document called DNVGL-CG-0038, see later in section 2.4.2.2.

2.4.2 DNV

The document DNVGL-RU-SHIP Pt.4 Ch.4 goes over the rule requirements, and the calculation methods for the propulsion shaft, hence the name of the document "Rotating machinery – power transmission"[11].
DNV has few variable ways to calculate the critical diameter for the shaft from the classification rules. The first design formula is the IACS M68.4 formula (previously revived in chapter 2.4.1). Were the minimum allowed diameter is defined with the pre-defined formula 2.36 (see page 26). The minimum diameter formula (IACS M68.4) is rather conservative, arguably too safe, and the one that Berg Propulsion uses today to calculate its shaft diameter. Equation can be found on page.18 in DNVGL-RU-SHIP Pt.4 Ch.4. named "2.2.7.2 IACS UR M68.4 Shaft diameter" [11].
In addition, the shaft design should be checked with torsional vibrations, if the shaft can withstand the torsional vibration stresses, see equations 2.37 and 2.38 on page 26. It is under the assumption that the barred speed range is passed rapidly both upwards and downwards with acceptance of 5 seconds, and can not be within 20% of the MCR ($\lambda < 0.8$) [11].

Then DNV provides another method is described in the document, which DNV calles a 'simplified method' , yet it´s more complex than the IACS M68.4 formula. DNV tries to keep it simple and accessible to use, the formula is aimed at geared plants with low torsional vibrations, with shaft material as steel. For the formula to be relevant few different criteria have to be met (same goes for stainless steel shafts):

σ_y limited to 0.7 σ_B (for calculation purpose only)
Application factors $K_{AP} \leq 1.4$
Vibratory torque $T_v \leq 0.35\ T_0$ in all driving conditions
Application factor, torque range $KA \leq 2.7$
Inner diameters $d_i \leq 0.5\ d_0$ except for the oil distribution shaft with longitudinal slot where $d_i \leq 0.77 \leq d_0$
Protection against corrosion (through oil, oil based coating,material selection or dry atmosphere).

It is distinguished into two separate calculations, either for low cycle fatigue (LCF) and high cycle fatigue (HCF). Where the low cycle is defined as the shaft subjected to a specific load case accumulation of not more than 10^4 loads. The case consists of loads on the shaft such as a stop to full operational speed and high repetitive yield in compression followed tension (relevant in both directions), for example, a reverse plant, referred as "crash stop". The High cycle fatigue has its scope on normal operation conditions, and accumulates to more than $3 * 10^6$ and typically up to 10^9 and 10^{10}. Typical high cycle fatigue loads can be forces from each firing pulse of the engine and different loads from the propeller. The minimum diameter from low cycle criteria as it is defined by DNV. See equation 2.39, and page 15 in DNVGL-RU-SHIP Pt.4 Ch.4 [11], and for parameter for different variables.

$$d_{min} = 28 * k_1 * \sqrt[3]{\frac{T_0}{\sigma_y}} \tag{2.39}$$

The minimum diameter from high cycle fatiguesee. See equation 2.40, and page 15 in DNVGL-RU-SHIP Pt.4 Ch.4 [11], and for parameter for different variables.

$$d_{min} = 17.5 * k_2 * \sqrt[3]{\frac{T_0}{0.32 * \sigma_y + 70}} \left(1 + k_3 \left(\frac{M_b}{T_0}\right)^2\right)^{\frac{1}{6}} \tag{2.40}$$

These formulas are recommended by DNV for the diameter of the shaft, the two formulas can only be applied for steel shafts, not stainless steel shafts. Separate equation, with the same shaft requirements as the steel shafts (the list in the same paragraph, above). Required values and further explanation can be acquired from DNVGL-RU-SHIP Pt.4 Ch.4 page 17 [11].

The class offers these 'simplified calculations' for the minimum diameter of the propulsion shaft. For a more detailed method, DNV offers a class guideline document on how to assess the safety factor for LCF and HCF for a shaft setup, the document is called DNVGL-CG-0038. To acquire more detail and push the design to the limit the detailed DNV method can be used, which was done in this thesis study. In the next section(2.4.2.2), a summary of the theory and output of the document is done.

2.4.2.1 ICE-class application

If the vessel under consideration has ice-class the propulsion system must fulfil specific ice-class standardisation. The criteria taken under consideration in this project, the first one is the application factor $KAice$ (previously talked about in section 2.3.2.3). The other one is that the propulsion shaft should be able to withstand the blade failure load. If the propeller hits an ice block with too much force, the propeller should fail before the shaft. This criterion is concerned for ice crashes but is also applied for the failure of the propeller when it grounds [12]. The calculation method and formula can be seen in appendix B.4 (based on DNVGL-RU-SHIP Pt.6 Ch.6 12.5.2 [12])

2.4.2.2 DNVGL-CG-0038

The document DNVGL-CG-0038 from the DNV classification society describes their method how to calculate the approved minimum diameter of a propulsion shaft, including the influence factor from the dimensions of the mechanical components on the shaft. The method takes into consideration the plants set up, if it is geared, or directly coupled, and others. The calculation method is vast and it can change a lot based on small changes (many different paths). The fatigue case is the same as described in the section above (2.4.2), that is low cycle fatigue and high cycle fatigue. If the shaft properties do not fulfil the requirements criteria for IACS M68.4

or the 'simplified method' (mentioned in section 2.4.2) DNVGL-CG-0038 calculation method can be used, it has a slightly larger property requirements margin [10].

Material of forged or hot rolled steels with minimum tensile strength of 400 MPa.
Material tensile strength, σ_B up to 950 MPa and yield strength (0.2% proof stress), σ_y up to 700 MPa.
No surface hardening.
No chrome plating, metal spraying, welds etc. (which will require special considerations).
Protection against corrosion (through oil, oil based coating, paint, material selection or dry atmosphere).

The calculations are divided into two separate fatigue criteria, one where low cycle fatigue is considered (LCF) and the other when the high cycle fatigue (HCF). The LCF load case is the same as described in the section above (2.4.2), that is loads on the shaft that accumulates less than 10^4 cycles. Loads like, from start to full load, from start to peak loads (like ice shock or clutch-ins) [10].

$$\tau_{max} \leq \frac{\sigma_y}{2SK_L} \tag{2.41}$$

The main equation for the LCF, see equation 2.41. Where the τ_{max} is the peak nominal torsional stress. That is the τ_0, the nominal torsional stress at a selected speed, or in this case the maximum since it is the most critical. To get the most probable highest torsional stress, additional loads, such as clutch-in and ice shocks have to be taken into consideration. For geared plants, the τ_{max} (peak nominal torsional stress) is computed using a KA factor (see equation 2.42), the appropriate factor is selected based on the shaft design criteria (like ice class). In figure 2.11 (see again on page 21) the maximum torsional stress is visually described with the combination of the KA factor and τ_0 [10].

$$\tau_{max} = \tau_0 * K_A \tag{2.42}$$

The process of acquiring the peak nominal torsional stress for direct-coupled plants is a little bit different. The equation is like so, $\tau_{max} = \tau(n) * \tau_v(n)$. The torsional vibration, τ_v has to be acquired with TVC analysis. The highest nominal torsional stress is then based on a specific speed [10], see image 2.14.

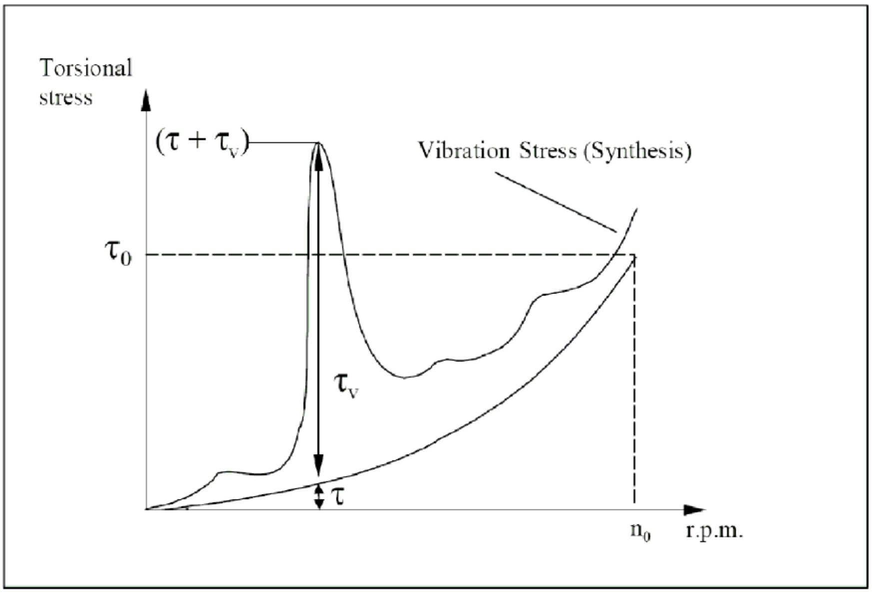

Figure 2.14: *Torsional stress based on torsional vibration (τ_v) and the torsional stress at specific speed (τ).Image was taken from DNVGL-CG-0038 [10]*

In general, the whole calculation method for LCF is based on equation (2.41). Where the diameter of the shaft, the engine load is addressed in the τ_{max}. The component influence factor K_L considers the shaft component and the surface finish [10]. The Safety for LCF can not be lower than 1.25 for LCF calculations[11].
The HCF load case is the same as described in the section above (2.4.2). The load conditions will accumulate not less than $3 * 10^6$ and typically up to 10^9 and 10^10. It includes loads in normal operating conditions, like pulses from the engine and loads from gears, based on formula, see equation 2.43.

$$\frac{1}{s^2} \geq \left(\frac{\tau_v}{\tau_f}\right)^2 + \left(\frac{\sigma_b}{\sigma_f}\right)^2 \tag{2.43}$$

Similar to the calculation method for LCF, each variable in the equation addresses different factors. The τ_v, the nominal torsional vibratory stress for continuous operation. That is based on τ_0 and the KA for normal operating conditions. The nominal reversed bending stress amplitude σ_b. Based on the diameter of the shaft and the rotating bending moment, M_b. According to DNV the rotating bending moment can either be calculated from the shaft alignment or simply be approximated as 40% of the torque at maximum continuous power [10]. T_0. The other two variables in the HCF equation (eq.2.43) is the τ_f high cycle fatigue strength and the σ_f high cycle bending fatigue strength. the determination of those two values can be vast and more complicated, they represent the component influence factors $K_{H\tau}$ and $K_{H\sigma}$. As the name suggests they take into consideration the mechanical component on the shaft and its dimensions in the relation to the material properties and the vibrating stresses [10]. With the dimension of the shaft and the components defined, as well as the material, the safety factor can be determined. Where the minimum safety factor for HCF according to DNV is 1.6 [11].

To see the whole calculation process for both LCF and HCF of the calculation method, including reverse calculation method and direct coupled plant in HCF analysis, one can look up the document DNVGL-CG-0038 or a flowchart created by the writers, based of the document, see in the appendix A.1.

2.4.3 Classification rule requirements for shafting alignment.

The rules specifically for alignment approval from a few different societies. Note, that the rules and instructions are taken straight from each classification document. The exact wording is vital for the definition of the regulations not to be altered. *All the classification rules from each society are freely available on their websites.*

2.4.3.1 DNV - Det Norske Veritas

"For geared plants, the alignment calculations are only applicable for the low speed part of the shaft line, including the output gear shaft with radial bearings. Vertical shaft alignment is always applicable, while horizontal alignment is applicable upon request. The rule requirements applies to fully submerged propellers. [14, p. 32]"
DNVGL-RU-SHIP Pt.4 Ch.2 Rotating machinery, general, Section 4, 1.1.1 Ed.2020-07 Revised.
Criteria for systems requiring shaft alignment calculation or only requiring shaft alignment specification. Shaft alignment calculation report shall be submitted for approval for propulsion plants with one out of the following criteria:

- Minimum shaft diameters (low speed side) of 400 mm or greater for single screw and 300 mm for twin screw
- Gear transmissions with more than one pinion driving the output gear wheel, even if there is only one single input shaft as for dual split paths
- Shaft generator or electrical motor as an integral part of the low speed shaft in diesel engine propulsion
- Single stern tube bearing arrangement.

DNVGL-RU-SHIP Pt.4 Ch.2 Rotating machinery, general, Section 4, 1.3.2 Ed.2020-07 Revised
For all propulsion plants other than those listed above, a shaft alignment specification shall be submitted for information. The shaft alignment specification shall include the following items:

- Bearing offsets from the defined reference line
- Bearing slope relative to the defined reference line if different from zero
- Installation procedure and verification data with tolerances e.g. gap and sag and jacking loads (including jack correction factors and jack positions) and verification conditions (cold or hot, propeller submersion, etc.).

DNVGL-RU-SHIP Pt.4 Ch.2 Rotating machinery, general, Section 4, 1.3.3 Ed.2020-07 Revised
In addition to the requirements listed above
Aft most bearing acceptance criteria and modelling of aft most bearing are dependent of risk:

— White metal lined aft stern tube bearing which is either double sloped, or has a journal diameter 500 mm or greater, criteria is not considered in this study
— Stern tube arrangements incorporating a single stern tube bearing only, are not considered in this study.
— Other propulsion plants where alignment calculation is required shall fulfil requirements in the acceptance criteria listed below.
Guidance note:
Aft most bearing is in most cases to be understood as aft stern tube bearing, but can also be other designs e.g. strut mounted bearings which are common in twin screw designs without skegs. DNVGL-RU-SHIP Pt.4 Ch.2 Rotating machinery, general, Section 4, 1.1.3 Ed.2020-07 Revised

Survey Installation of propulsion plants requiring a shaft alignment calculation shall be verified by a surveyor DNVGL-RU-SHIP Pt.4 Ch.2 Rotating machinery, general, Section 4, 1.1.4 Ed.2020-07 Revised

Acceptance criteria:
The shaft alignment shall fulfil the following acceptance criteria for all relevant operating conditions.

- Acceptance criteria defined by manufacturer of the prime mover, e.g. limits for bearing loads, bending moment and shear force at flange
- Acceptance criteria defined by the manufacturer of the reduction gear, e.g. limits for output shaft bearing loads and load distribution between bearings
- Bearing load limits as defined by bearing manufacturer and Ch.4 Sec.1
- Zero or very low bearing loads are only acceptable if these have no adverse influence on whirling vibration Tolerances for gap and sag less than 5/100 mm are not accepted. Acceptance criteria for aft most tail shaft bearing:
- In hot static and hot running conditions the relative nominal slope between shaft and aft most propeller shaft bearing should not exceed 3 · 10-4 rad (0.3 mm/m) and 50% of minimum diametrical bearing clearance divided by the bearing length, whichever is less. For definition of relative nominal slope, see

Operating conditions:
The shaft alignment calculations shall include the following conditions:
— Alignment condition (during erection of shafting)
— Cold, static, afloat, fully submerged propeller
— Hot, static, afloat, fully submerged propeller
— Hot, running with hydrodynamic propeller loads.
For geared shafting systems:
— Running conditions as required to verify gear acceptance criteria
— All relevant combinations of prime mover operation
— Horizontal alignment is upon request.

2.4.3.2 LR - Lloyd's Register

Few appropriate shaft alignment requirements from Lloyds Register

- Relative slope between the propeller shaft and the aftermost sterntube bearing is, in general, not to exceed 3 × 10-4 rad.

- Intermediate shaft bearings' loads are not to exceed 80 per cent of the bearing manufacturer's allowable maximum load

- Flexible couplings can not exceed the radial, axial and angular alignment requirement from the manufacturer.

- he main gear load is to be within the gearbox maker limit.

Part 13 Shaft Vibration and Alignment - Chapter 4 Shaft Vibration and Alignment - Section 1 Shaft alignment Ed.2020 July

2.4.3.3 BV - Bureau Veritas

Some relevant requirements from Bureau Veritas.

- Aft most stern tube bearing must not have higher slope than 0.3mm/m.
- All bearing must remain loaded.
- Intermediate shaft bearings must not exceed 80% of the provided maximum load from the bearing manufacturer.
- Minimum stern tube bearing length must be not less than two times the diameter of the shaft. But it may be less if the bearing pressure is less than $0.7 N/mm^2$, then the minimum length of the bearing is to be 1..5 times the diameter.

Steelships,Pt C, Ch 1, Sec 7 3.4.2 Ed.2020.Jan

2.4.3.4 ABS - American Bureau of Shipping

From ABS guidance notes on propulsion shafting alignment In general for all ships, shaft alignment calculations and a shaft alignment procedure should be submitted to ABS for reference [1, p. 7]. However, for propulsion shafting of diameters equal to or larger than 300 mm, and propulsion shafting with no forward stern tube bearing, they are to be submitted for review by ABS for compliance with ABS Rule requirements.

The alignment calculations should include bearing loads and bearing reactions, shear forces and bending moments along the shafting, slope boring details as applicable, and a detailed description of the alignment procedure.

The alignment calculations are carried out for theoretically aligned cold and hot conditions of the shafting and for the maximum allowable alignment tolerances. They are to show that:

- Bearing loads under all operating conditions are within the acceptable limits specified by the bearing manufacturer.
- Bearing reactions are always positive (i.e., supporting the shaft), except as determined acceptable in accordance with current ABS Rule requirements.
- Shear forces and bending moments at the crankshaft flange are in accordance with the engine manufacturer's limits.

- The designed relative misalignment slope between the shaft and the aft stern tube bearing is to be positive and not exceeding $0.3 * 10^3 \quad [rad]$.

ABS Guidance notes on - Propulsion shafting alignment, September 2019. American Bureau of Shipping, New York. 2019

3
Methods

The work process during the thesis work is to study the classification rules and utilize the calculation methods stated in those for dimensioning the shaft and checking safety factors. Those are sets of simple calculations where one chooses the correct method for the specific type of application. The DNV class guidelines for the calculation of shafts in marine applications are summarized in an interactive Excel sheet where the designer is guided through the different steps of the calculations. Further detailed analyses are done using the software package Nauticus Machinery from DNV. The goal is to show that it is possible to decrease the dimensions of the shaft and still achieve a safe design with good vibration behaviour.

3.1 Study on the IACS M68 formula

With the definitions made in the theory chapter, an analysis of the IACS M68.4 formula was done. With a statical approach, then implemented with a fatigue endurance limit. The goal is to try and mimic the IACS m68.4 equation from scratch and come up with similar results.

An interesting factor of the IACS M68.4 formula is the stress concentration factor. An investigation of this factor (KA) was done to understand how it is applied in the initial formula. As well as to get a better instinct when emulating the approach for the mimic equation.

3.1.1 Static calculation comparison

Based on the static torsional approach (equation 2.5), where the diameter is solved out for hollow cylinder to compare it to the IACS formula, the marginal difference can be better visualized. A pre-designed RoPax ferry (currently in operation) was used for this comparison case, where the main input values can be seen in table 3.1. According to the parameters for that vessel, the minimum allowed outer diameter based on the ICAS M68.4 formula is $396mm$. From the static torsional approach $286mm$, giving that the maximum shear stress(τ) in the formula (equation 2.5, page 11) is the maximum allowed yield shear stress for the material. According to Maximum shear stress theory, $0.5 * \sigma_y$ (Tresca [5]). Note no safety is applied to the 286mm shaft, meaning it is the critical diameter, see side by side comparison in table 3.2. It is safe to say that the margin between each method is large. Note that the diameter is in relation to area, so the ratio between them has to be taken squared,

$396^2/286^2 = 92\%$, meaning the IACS formula for minimum diameter provides 92% larger shaft than the statical approach. Results can be seen in table 3.2.
Note, defining the shaft diameter based on statical load case is though inaccurate and should not be considered, since the correct design should be based on the dynamic perspective and the fatigue limit of the design. This statical analysis is solely to just examine how the statical loading is comparing with the IACS M68.4 equation.

Table 3.1: *Input parameters used for the calculation comparison. Operating RoPax ferry, from a finished order from BERG database*

The loadcase (RoPax ferry)

D	410	*mm*	*Designed outer diameter*
d	80	*mm*	*Designed inner diameter*
P	12600	*kW*	*Power*
n	150	*rpm*	*Speed*
σ_y	350	*Mpa*	*Yield strength of the material*
σ_B	600	*Mpa*	*Ultimate strength of the material*

Table 3.2: *Calculation results from the IACS M68.4 formula, the statical torsion approach. Response statical stress from torsion and bending on the shaft, based on Von Mises and FEM method*

Approach	Min allowed Diameter [mm]	Maximum stress [Mpa]
IACS M68.4	396	-
Static Torsion	286	-
Von Mieses	*Based on 410mm*	113
FEM		107

In addition, a statical safety analysis was done on the shaft with the given load case. Where Von Mieses calculations were done on the shaft and a computerised method of finite element analysis or simply FEM. According to DNV a conservative method to estimate the bending loads on a propulsion shaft is to take 40% of the torque load [11] and apply it as transverse bending on the shaft, which was done in this case. Since FEM is based on the same theory as Von Mises, the same result was expected, as it did. The FEM result can be seen in figure 3.1. The stress result for both approaches is listed in the same table as the minimum allowed diameters were, in table 3.2.

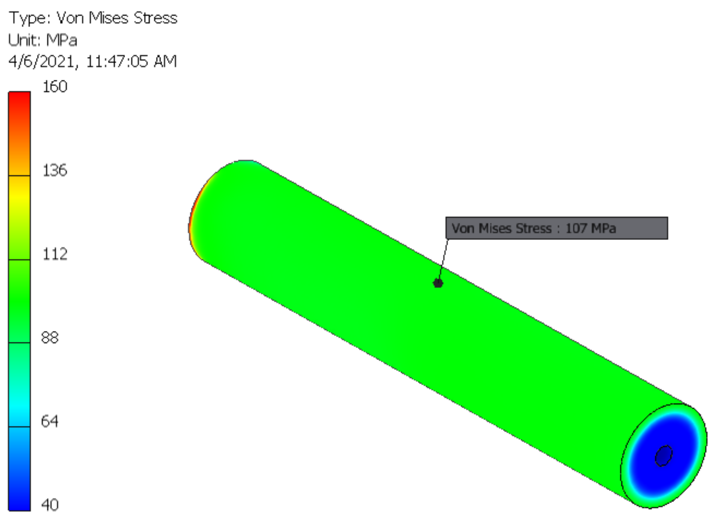

Figure 3.1: *Von Mises FEM analysis of the RoPax vessel.*

This shows, though there is a resemblance between IACS M68.4 and the statical torsional approach equation (equation 2.5), the result is not the same.

3.1.2 Fatigue approach on IACS M68

A dynamic, vibrating rotating shaft has to be designed in terms of fatigue limit. The statical approach has been defined in section 2.2.1 described with equation 2.5. But the torsional load variable in that formula has to be interpreted for a fatigue limit (endurance limit) of a given shaft design, material, and load case. It is not known what fatigue criterion was used by the people who developed the ICAS M68.4. In this study, the fatigue limit method that was used was the Dang van criterion. Using reduction factors for the fatigue limit (S_e) from mechanical coursebook [5].
Note, in this investigation, considering the IACS M68.4 formula, specifies that $\sigma_B < 600Mpa$ [21], and Berg Propulsion default shaft material selection is 600Mpa ultimate strength, thus this investigation will use $\sigma_B = 600Mpa$.
Calculation steps and values can be found in the appendix B section B.2.
The Dang van criterion is a fairly new criterion that was issued in 1971. It gained popularity since it addresses rotating principal stresses and is a multi-axial fatigue analysis. By using this criterion for such a general application, shaft designs, load- and material design, assumptions had to be made to perform the approach. The equations that were used to define the endurance limit for high cycle/finite life, see equation 3.1 (*See page 28 Anders Ekberg, Multiaxial Fatigue [18]*)

$$\sigma_{eq,dv} = \frac{\sigma_1 - \sigma_3}{2} + C_{dv}\frac{\sigma_1 + \sigma_2 + \sigma_3}{3} \longrightarrow \sigma_{edv} = \frac{\sigma_{fl}}{2} + C_{dv} * \frac{\sigma_{fl}}{3} \tag{3.1}$$

Where C_{dv} is a material parameter defined with equation 3.2
This might look familiar, since it is similar to how in regular (not fatigue) failure theory where the tri-axial stress is computed as $TriAxial\ stress = Deviatoric\ stress + Hydrostatic\ stress$.

$$C_{dv} = \frac{3}{2} * \frac{\sigma_{fl} - \sigma_{flp}}{2\sigma_{flp} - \sigma_{fl}} \tag{3.2}$$

Where the σ_{fl} is the fluctuating loading and σ_{flp} is the pulsation loading. According to Anders Ekberg [18] for a general estimation, the definition of these two loads can be presumed the fatigue limit in uniaxial pulsating loading is 80% of that in alternating loading. Meaning to estimate the critical fatigue limit for this case σ_{fl} is defined as the reduced fatigue limit. From the previous definition the σ_{flp} would be 80% off that. [18]

Reducing the endurance limit (S_e) in respect of:

- Actual test data for endurance limit based on tensile strength. Estimated as 50% of ultimate tensile strength.
- Surface finish, machined ≈ 83%
- Torsional load case, 0.59%
- Stress concentration factor (SCF). It states in the IACS formula that their equation is based on a SCF of 1.45. Therefore use the same concentration in this approach.

Results and comparison on the mimic equation and the IACS M68.4 formula are done in the Results chapter.

3.1.3 IACS M68.4 Concentration factor

A question emerged from curiosity, why IACS has defined the k in the M68.4 equation 2.36 and the C_k in the allowed torsional vibration formula M68.5 2.37, the way they have done. Where do these multipliers come from. See each factors´ value for different locations and components in the table on figure 3.3. Both equations have an initial condition for the stress concentration factor (SCF) as a shaft component with a step up with a radius fillet of 0.08d, resulting in a SCF=1.45 [21].

Applying a different designed component to the formula (for instance, keyway or shrink fitted) the multiplying factor K and C_k maintains the required change for different stress concentrations. The IACS formulas are developed and defined with a radius fillet component as the default state of the equation(with a filler radius of 0.08d). In the case of a different stress concentration component, the K and C_k factors are in fact just ratios between the default stress concentration factor and the current stress concentration, see figure 3.2. To get a better perception of how the factors affect the result and where they come from, a brief investigation was done on these factors.

M68.6 Table of k and c_k factors for different design features (see M68.7.2)

Intermediate shafts with						thrust shafts external to engines		propeller shafts		
integral coupling flange [1] and straight sections	shrink fit coupling [2]	Keyway, tapered connection [3,4]	Keyway, cylindrical connection [3,4]	radial hole [5]	longitudinal slot [6]	on both sides of thrust collar [1]	in way of bearing when a roller bearing is used	Flange mounted or keyless taper fitted propellers [8]	Key fitted propellers [8]	Between forward end of aft most bearing and forward stern tube seal
k=1.0	1.0	1.10	1.10	1.10	1.20	1.10	1.10	1.22	1.26	1.15
c_K=1.0	1.0	0.60	0.45	0.50	0.30[7]	0.85	0.85	0.55	0.55	0.80

Figure 3.2: *Table of k and C_k factors from IACSM68 document [21]*

By selecting the factors for flange mount, for the intermediate shaft, and also for the propeller shaft, $K_{int} = 1.00$ and $K_{prop} = 1.22$. Note that the factor for intermediate is just 1 since the default stage of the formula is based on the stress concentration of a fillet radius [21].
Stress concentration factor as previously went over in section 2.2.2, is multiplied by the load or the strength of the material.
It can be assumed that the only significant load case for the intermediate shaft is torsional load, and for the propeller shaft it undergoes torsional load and bending as well . According to IACS the smallest fillet radius allowed is a radius of 0.08d, which was then the critical design form in this investigation. Critical stress concentration factor under torsional load and a bending load was acquired using charts for theoretical stress concentration factors. The K factor provided by IACS (figure 3.2) can be compared with the acquired stress concentration factors, see equation 3.3.

$$K = \frac{SCF}{1.45} \tag{3.3}$$

But since there are two different loads on the propeller shafts, it can be too simple to expect that the stress concentration factor for the propeller shaft is only based on bending load. So three methods were tested to compare the calculated K factor to the IACS provided factor. One method (labeled approach A) where the calculated K factor for propeller shaft is only based on bending SCF. For the next method, since DNV reports a conservative way to define the bending moment, as 0.4 of the torsional load. For example, for every ten units of torsion, we have four units of bending, indicating for every 14 units of load 2/7 (4/14) is bending, and 5/7 (10/14) is torsion. By that means the second method (labeled approach B) was by defining the SCF as this ratio from each load case. And the third one (labeled approach C) was defined the same way but according to Von Mises, where torsional shear-load and normal-load from bending do not result in the same failure criteria [5], see equations on image 3.3.

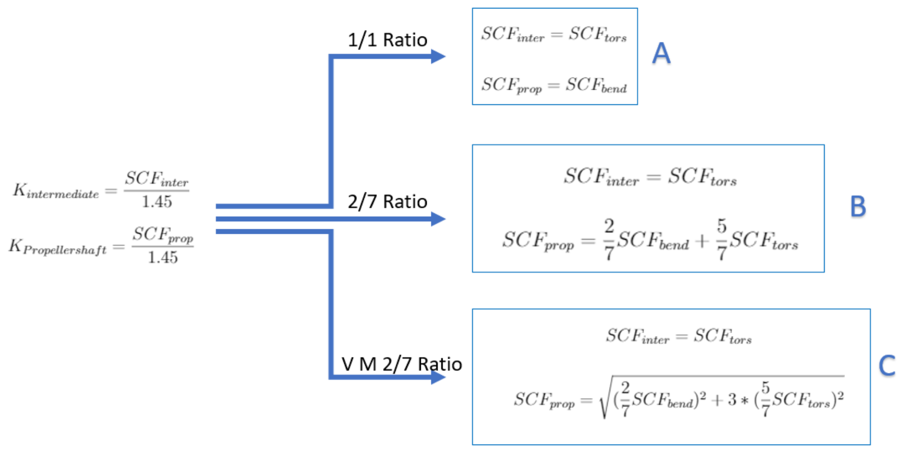

Figure 3.3: *The three SCF approaches done in this study*

With these three approaches, the resulted factor for the stress concentration K can be compared with the provided one from the table. A visual comparison can be seen in figure 3.4. It can be seen on the figure that the blue axis represents the provided value of K from the IACS table (on image 3.2). Meaning that everything below the x-line and left of the y-line is within the design criteria(or over designed) defined by IACS.

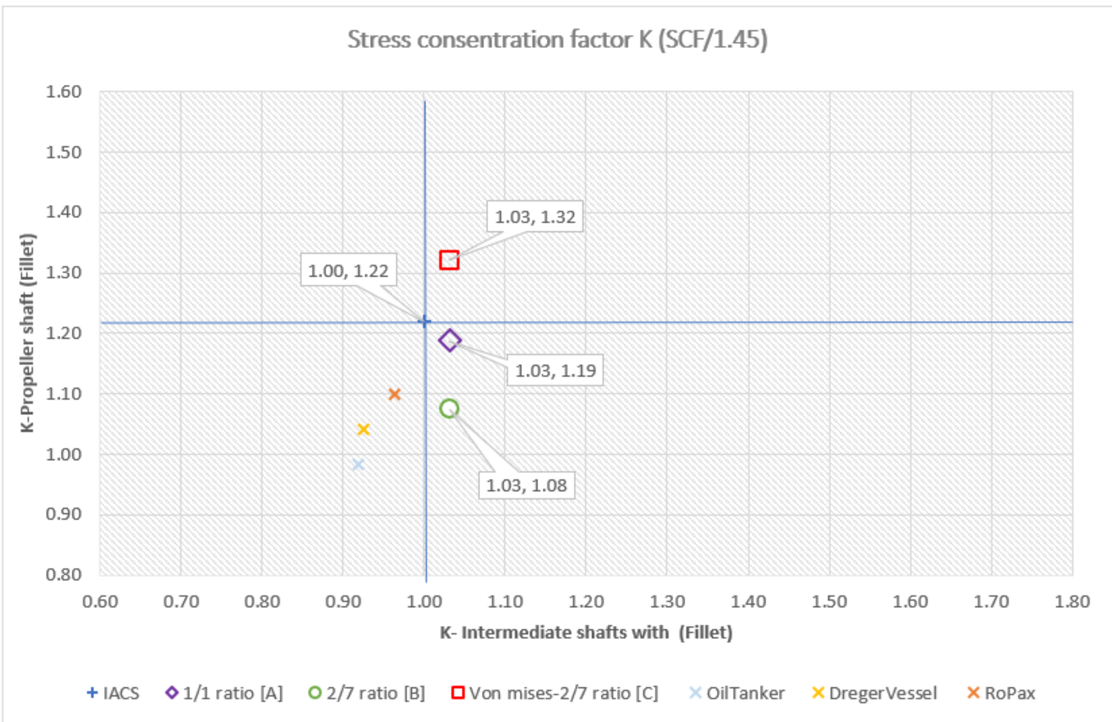

Figure 3.4: *Visual comparison of each calculated K (SCF/1.45), both as the critical factor using the three approaches previously described. And the Berg (finished orders) vessels.*

From the plot (figure 3.4), it can be seen that the three methods are all above (left of the y-axis) the K for intermediate-shaft by a small margin. The three methods are all based on the same formula for this K intermediate, that is why they do all stay on the same horizontal line. One could argue that a 0.03 difference is neglectable. For the propeller shaft K-factors, the three methods line up at different positions. A and B are below the IACS K-factor, and method C is above. It is difficult to justify one method from another, but if one would stick to method C, that would mean that the IACS K factor for the propeller shaft is under-designed (which is hard to believe, coming from such an institution). It is arguably too innocent to estimate that the SCF for the propeller shaft is only based on bending. But out of these three approaches, method-A is the closest one to the provided K-values. It is convincing that IACS had possibly added some extra safety how they approach and defined their provided stress concentration factor K, or done the interpolation of bending SCF and torsion SCF differently than these three approaches done here. Based on the closest approach (method A, propeller shaft SCF only based on bending load) three operating ship shaft designs were put under the test to see where their SCF is on the IACS K scale. On these three ships, a fillet and its parameters were used to define an SCF and based (like before) on equation 3.3 the K was calculated and compared. See again the plot on figure 3.4. They all show a positive result, since the IACS formula should be the critical benchmark for the STC, and they all result in a lower one.

C_k is defined the same way as K. But since it is used in a different formula, M68.5 Permissible torsional vibration stresses there the material factor (ultimate tensile strength) is inverted and thus is C_k defined the same way as K, but inverted, $C_k = 1.45/SCF$ [21].

3.2 Simulation analysis

Nauticus Machinery is one of many software packages DNV Digital Solutions offers, the program is specialised in marine propulsion design and analysis. The main program provides the working environment, file manager and license server. Then there are 8 different calculation tools all related to the rotating propulsion machinery. To be able to do any kind of calculation with the program one needs to open a calculation tool, each of them has a separate license such that one needs to choose which calculations are needed and buy the appropriate license.
To make this thesis project possible, an academic software license was established from DNV through a license server at the Chalmers University of Technology. The license gives access to all of the calculation tools.

Table 3.3: *Summary of Nauticus Machinery calculation packages*

DNV Nauticus Machinery		
Calculation Tool	Background	Used
Shaft Alignment	Continuum Mechanics	X
Torsional Vibrations	Continuum Mechanics	X
Shaft Fatigue	Rule Based	
Propeller Blade	Rule Based	
Gear Rating	Rule Based	
Gear Faceload	Rule Based	
Crankshaft Fatigue	Rule Based	
Controllable Pitch Mechanism	Rule Based	

However the tools were limited to some extent, at first, the Shaft Alignment tool was limited to eight bearing elements, this was later updated and caused no limitation. One important limitation remained for the Torsional Vibration tool, which was to calculate excitation's resulting from a 2 stroke engine.
This capability would have been preferred for comparison reasons. Of the different types of propulsion system arrangements possible for a ship, the direct-coupled low-speed shaft lines propelled by 2 stroke diesel engines are the most susceptible to torsional vibration problems [25][28]. As discussed on page 6 "The engine's main excitation order coincides with the first torsional natural frequency of the shafting system" [10, page 7].

Looking at Berg Propulsion portfolio to find suitable shaft line setups for simulation analysis, the limitation of not being able to simulate 2 stroke propulsion is seen to be of no real concern. The power plants are rarely of a 2 stroke type. The fact is that BERG Propulsion specialises in designing and producing CP propellers which most often are connected to a medium or high-speed diesel engine through a reduction gear. The benefit with having a CP propeller is that it is easier to accelerate fast through any barred speed ranges utilising the adjustable pitch ratio, compared to a fixed-pitch propeller, "running through the barred speed range with zero or low pitch" [10, p. 7]. Even better in regards to torsional vibration problems, electric motors are getting more common for primary propulsion.
A typical application for BERG products are vessels that need to have flexible operation profiles and good manoeuvrability, this could be ferries, fishing vessels, offshore service vessels and tug boats.
With this reasoning, it is suggested that the classification shaft dimensioning methods are overly conservative for many Berg shaft line applications. To be able to analyse the effect of decreased diameters of existing shaft designs, examples of reference shaft lines were simulated in Nauticus Machinery. Analysis and calculations were proceeded according to class requirements. In the process of setting up the simulation models for the three reference shaft lines authors had access to a large collection of specifications and drawings. Those drawings and technical specifications can not be included in this report.

3.2.1 Nauticus Shaft Alignment

The shaft alignment tool provides a way to proceed with the lateral shaft analysis, lateral covering the vertical deflection, and whirling vibration calculations. Deflection analysis in the horizontal plain are also possible but usually only needed if high moments in the horizontal plain are realised. The tool provides detailed class required bearing lubrication analysis.

Description of the tool from a DNV Nauticus Machinery brouchure:

> Nauticus Machinery - Shaft Alignment provides efficient methods to build a shaft model and analyze bearing loads, bending moments, deflections and more. It also provides customised verification results such as hydraulic jacking curves and gap/sag values in flanged connections. Whirling and axial vibration analysis also covered. It provides the after-stern tube bearing lubrication analysis from two aspects: calculating the required minimum shaft rotational speed to ensure sufficient lubrication; calculating the oil film pressure and thickness distribution inside the after stern tube bearing to find the maximum pressure and minimum thickness. [15, p. 2]

3.2.1.1 Building the shaftline model

When beginning building a model in the Shaft Alignment tool detailed drawings and specifications of the whole low speed part is needed. For direct coupled 2-stroke propulsion the the model includes the propeller, propulsion shafting and the engine crankshaft. For a geared propulsion system the model includes the propeller, propulsion shafting towards the reduction gear and the output shaft of the reduction gear including the main gear wheel. Properties of the propeller, location and properties of all bearings and all relevant loads for different operation conditions need to be defined. For a full analysis extra conditions on top of the operation conditions need to be added, those are GAP-SAG conditions for alignment procedures purposes.
The first step in shaft alignment analysis is to recreate the shaft elements as accurately as possible using detailed dimensions from the Shaft Arrangement drawing as well as extra specifications for couplings, bearings and gearbox. The shafting is modelled with shaft elements, a shaft element can be cylinder or a cone, with outer diameter, length and hollow bore. The shaft elements have weight, stiffness and more settings. There are few more specific model elements, those are; flange, spacer ring, shrink fit, bearing, propeller and joint. The main objective of the shaft alignment analysis is to check how well the propulsion shafting is aligned with the supporting bearings. The bearings need to be adjusted by offsetting them in a way for the shaft to be supported evenly and the lubrication pressure to be within a safe range. This is done to stay safe against abnormal or excessive wear on the shaft and bearings. The model gives also the ability to check the natural frequencies in lateral and analyse the mode shapes. This is called whirling vibration analysis, axial vibrations are generally thought to give much lower stress values, therefore the axial analysis is skipped, see section 2.3.3.

Table 3.4: *The table summarises drawings and specifications needed for building the shaft analysis model in lateral.*

	Information needed for shaft alignment
1	Shaft arrangement drawing
	- *Detailed dimensions of all shafts and different components*
2	Sterntube bearing drawing
	- *Length of bearings and bearing clearance*
3	Intermediate bearing drawing
	- *Length of bearings and bearing clearance*
4	Couplings drawing
	- *Length, diameter, flange or not*
5	GB / ME drawing and alignment criteria
	- *Gearbox or Main Engine, bearing clearings and loads*
6	Propeller data
	- *Weight, Inertia, Thrust eccentricity*

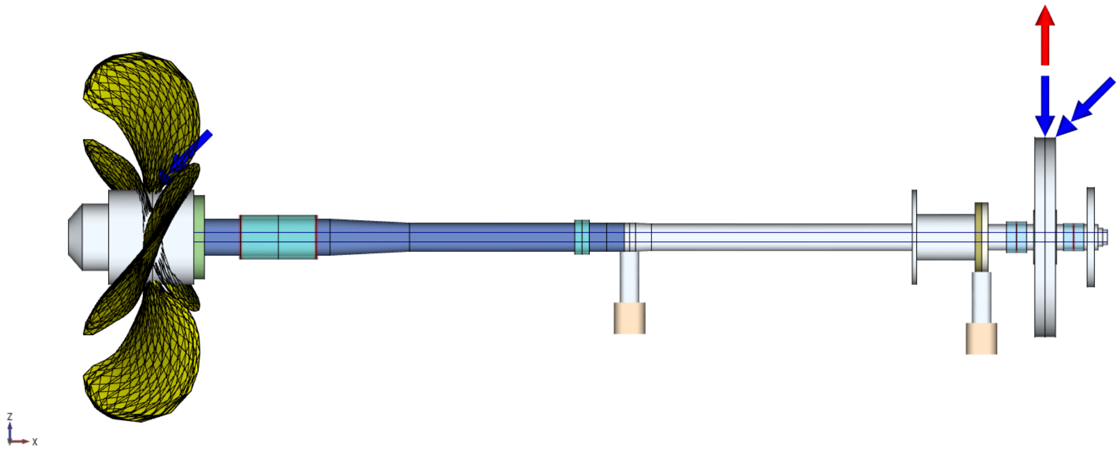

Figure 3.5: *Model of the shaft arrangement in the Nauticus - Shaft Alignment tool. The model represents the shaftline for the bunker tanker.*

In figures 3.5 and 3.6 the shaft elements, modeling the actual shaft, can be seen as light green, blue and gray. The green color represents submersion in water, the blue represent submersion in oil and the gray elements are in air. This definition is done to account for buoyancy effects. From left there the propeller hub is gray, modeled as in air, and actually the weight is also modified such that the specific weight is 1 $\frac{kg}{m^3}$, this is done so that the calculated weight is essentially nil. This is done because the load from the propeller, hub and blades, are defined specifically for different operation modes. The arrow on top of the middle of the hub denotes this load definition. The green shaft section is the propeller flange at the end of the propeller shaft, where the propeller is attached using bolts. The propeller flange is outside the hull submerged in water, just forward of the hub is the bossing and aft stern tube seal, not shown. The blue colored part indicates the part inside the stern tube, the cyan colored elements are the bearings. The aft stern tube seal keeps the lubricating oil inside the stern tube and water outside. The first blue shaft element is the surface where the seal is located, next is the aft stern tube bearing. Rule-of-thumb value for the aft stern tube bearing length ranging from $1.5D$ *to* $2D$ depending on application and needs to be verified during the analysis. Forward stern tube bearing is much smaller than the aft stern tube bearing, reason being the large loads on the aft bearing, both have two contact points defined at either end, noted with a red line. The stern tube bearings are fixed solid and usually have zero slope, in some cases the aft bearing is manufactured with small positive slope, fraction of a millimeter, to account for relative slope difference between the shaft and bearing. Positive slope being the bearing is higher at forward end.

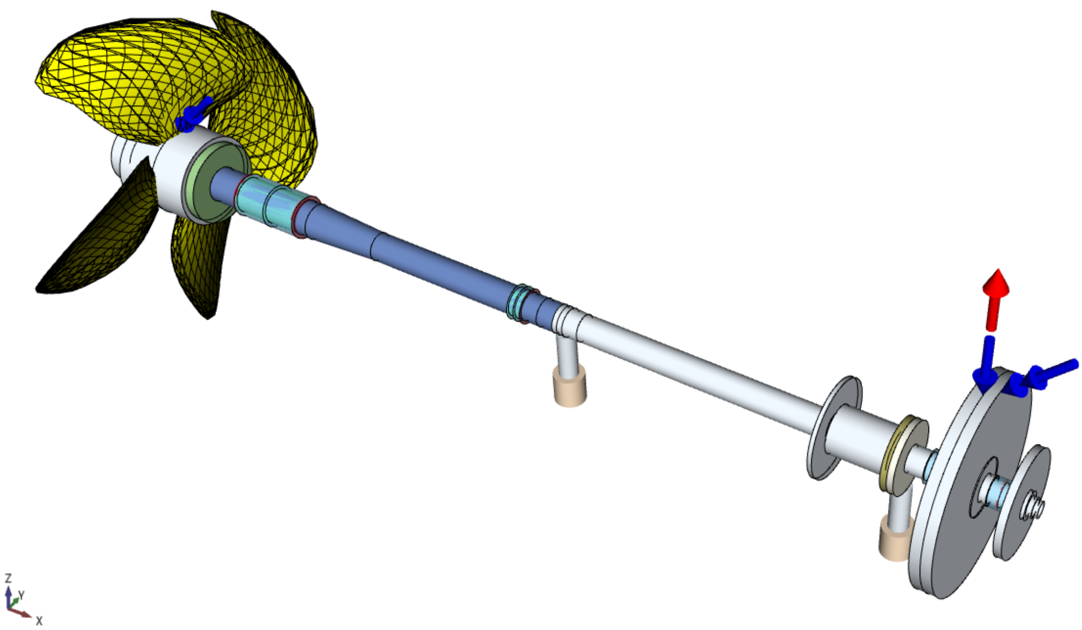

Figure 3.6: *Model of the shaft arrangement in the Nauticus - Shaft Alignment tool, 3D view. The model represents the shaftline for the bunker tanker.*

Where the blue color stops and gray takes over the forward stern tube seal is positioned and keeps the lubricating oil inside the tube. The gray part of the shaft is inside the engine room. Following the shaft to the right we have a thin section with a large diameter, this is a brake disk for being able to stop the shaft, the brake disk is bolted to a shrink fit flange coupling. The flange is in brown color and bolts to the gearbox flange in yellow color. The large wheel is the main gear output wheel supported by the output shaft and journal bearings on either side. The arrows represent the forces acting on the wheel when the pinion wheel transfers torque from the propulsion engine/motor. Furthest to the right is a thin wheel, this is a thrust-bearing that supports the axial force from the propeller.
In shaft alignment the shaft is really acting like a beam, which is rotating resulting in possible whirling vibrations. The fact that the shaft needs to be able to rotate means it is supported by bearings, typically white metal bearings with lubrication. Water lubricated composite stern tube bearings are also available. The principle

is the same, the lubrication needs to be able to form a thin film supporting the shaft without the surface scraping. To align the bearings in such a way that the lubricating pressure in the bearings stays within suitable range , is one of the main objectives of the shaft alignment task. The fact that the shaft has just certain amount of stiffness and is actually curved can make this challenging. This means the shaft supports can not be aligned in a straight line, rather they need to have a vertical offset. To complicate this further the shaft alignment analysis is done for different conditions, with the shafting components cold and static, static meaning the shaft not turning. Another warm static check with the shafting component at running temperatures but stopped, not turning. Two running conditions are checked also, the MCR condition and 0 pitch condition, for CPP propellers.

3.2.2 Nauticus Torsional Vibration

Nauticus - Torsional Vibration tool is a highly specialised tool for calculations of vibratory excitation's and responses in marine type of rotating machinery. The tool includes different types of prime movers, specific shafting coupling connection elements, damper and gear elements found in marine propulsion shafting as well as the propeller definition. The tool has been found to offer a broad range of predefined plotting and result printout definitions which facilitate standard reporting for marine application but could as well be used for analysing rotating shaft systems in general. The calculation are made in the frequency domain, excitations and reactions related to engine speed, all but the ice loads calculations. The ice loads calculations are specific for ice classification and simulate load amplitudes in time domain resulting from the propeller blades milling through ice [15].

3.2.2.1 Inertia and stiffness

The building blocks of the torsional vibration mass elastic model are nodes that define the inertia masses and shaft stiffness elements which connect the inertia nodes. The inertia, noted with two green circles connected vertically by narrow line. A stiffness is an arrow connecting two inertia's, the arrow points in the direction of power, from a power source to a power user. On figure 3.7 the nodes no. 1 and 5 are electric motors, a power source. The power sink, the user in this system is the propeller, inertia element no. 14. The electric motors and the propeller are inertia elements with specific extra features defining the physical properties of those components, the rest of the inertias in this system are regular lump-mass elements. The list of inertia and stiffness elements can be seen in table 3.5 [13].

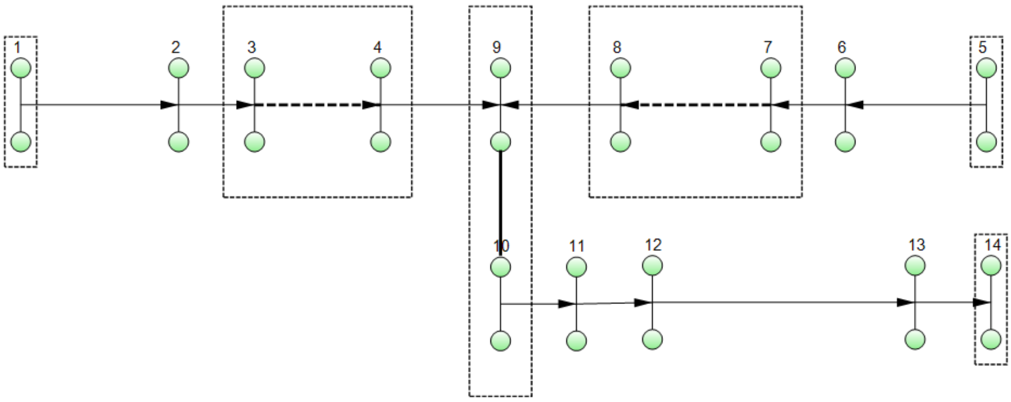

Figure 3.7: *Simple view of Nauticus torsional vibration model. The mass elastic model of the Tanker.*

Different compination of inertia and stiffness elements can then be grouped in specific groups to form a higher level machinery component. The dotted boxes in figure 3.7 can be seen representing elastic coupling, see lump mass nodes 3 and 4 connected by a coupling stiffness, similar with notes 7 and 8.
Notes 9 and 10 are regular lump masses connected by mess stiffness, when adding the gear group joining those, creates a reduction gear that can have a gearing ratio and more properties. The electric motors and propelle are just a single inertia objects. However looking at inerta no.2 and the stiffness connecting no. 1 and 2, those represent the inertia and the stiffness of the output shaft of the electric motor.

Table 3.5: *List of the basic modeling elements availible in the DNV Nauticus Machinery - Torsional Vibration tool.* [13, p. 16]

Modeling elements	
Inertia	Stiffness
Lump mass	Shaft stiffness
Cylinder	Crank throw stiffness
Electric motor	Coupling stiffness
Gas turbine	Mesh stiffness
Steam turbine	Damper stiffness
Propeller	
Generator	

More detailed view of the Tanker model is presented in figure 3.8, where the stiffness is represented by spring connections and damping by damper icons. The inertia values can be seen in black straight above the lump mass elements, moment of inertia given in $kg * m^2$. The stiffness values can be seen in purple above the shaft stiffness connections, represented in the units of $N * m/rad$. The damping is given by red values below the stiffness connections, here they are represented as damping magnifier values.

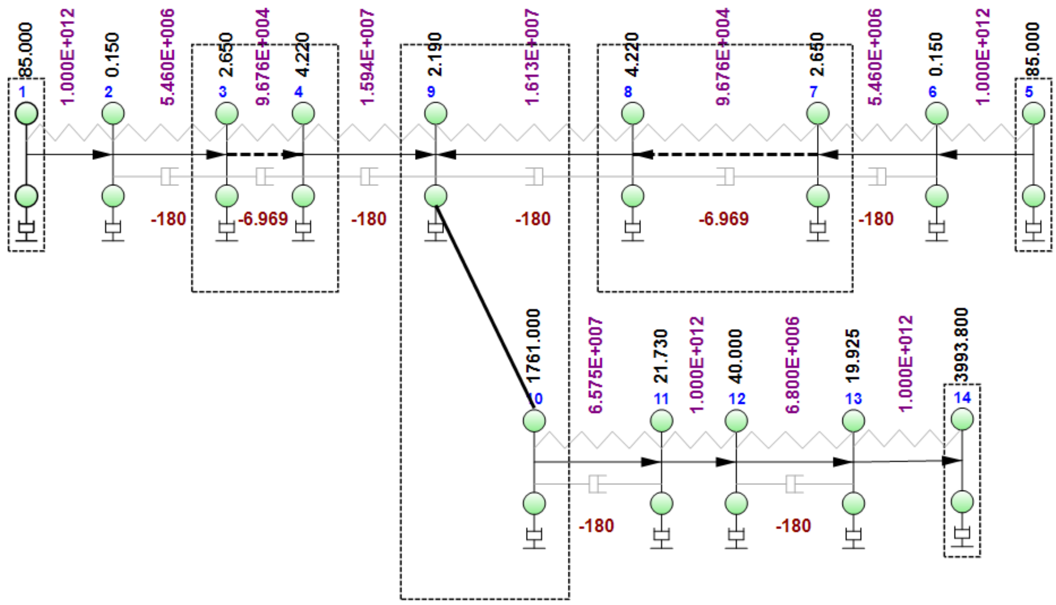

Figure 3.8: *Detailed view of Nauticus torsional vibration model. Showing the different modeling elements along with values for inerta, stiffness and damping.*

3.2.2.2 Damping

Damping for a multi-dimensional systems can be very difficult to determine. This is different from stiffness and inertia. Therefor when the physical propulsion system has been installed in a vessel the vibration behaviour needs to be measured to check if estimated damping values have been acceptable [31]. For this reason the damping values used are often general values that have been shown to fit the application. For the torsional vibration models damping magnifiers were used. The values $M = 180$ for steel shafts and $M = 100$ for gear meshing are rule-of-thumb values that rotor dynamics experts have seen to give good results when using Nauticus Machinery. The damping magnifiers for flexible couplings were computed from damping specification values, for a typical flexible coupling it is good to have a value of about $M = 7$. Similar rule-of-thumb estimates for damping values can be seen in [31, p. S-167] for the TVC analysis program SimulationX.

Table 3.6: *Comparison of how damping values and coefficients are defined for the programs Nauticus Machinery and Shaft Designer [13] [4].*

Damping values

Nauticus Machinery		Shaft Designer	
k	Linear viscous damping $[Nm * s/rad]$	C	Linear viscous damping $[Nm * s/rad]$
κ	Undimensioned damping factor	κ	Undimensioned damping factor
ψ	Ratio of damping energy	ψ	Ratio of damping energy
M	(Dynamic) Magnifier	Q	Vibration magnifier
-	Not defined	ϵ	Percent of critical damping [%]
-	Not defined	M	Dynamic magnifier
ω	Phase velocity of vibration $[rad/s]$	ω	Phase velocity of vibration $[rad/s]$
C	Dynamic stiffness $[Nm/rad]$	K	Stiffness [Nm/rad]

The undimensioned damping factor κ has also be seen with the notation μ. The damping for flexible couplings is often given by this undimensioned factor. Very important to notice is the difference between the damping magnifier values used by Nauticus and Shaft Designer. Since the project work was done using Nauticus Machinery, *M* will represent the damping magnifier used by Nauticus Machinery, also called *dynamic magnifier*. When setting up the torsional vibration analysis models it gave best results to convert the damping values stated for couplings and more to this damping magnifier *M*. Doing this conversion was also really good for a verification check to see if one is using the correct values. It was for example in some cases confusing if specifications were stating damping as *undimensional damping factor* κ or *ratio of damping energy* ψ. But by checking the *dynamic magnifier* it quickly reveals if the specifications have been misinterpreted.

Table 3.7: *Conversion table for different damping values, relevant for Nauticus Machinery [13].The damping magnifier M as used by Nauticus is more often presented as Q. More comprehensive conversion tables available in the Nauticus and ShaftDesigner documentation.*

Damping conversion table

	ψ	κ or μ	k
$M =$	$\frac{\sqrt{4 \cdot \pi^2 + \psi^2}}{\psi}$	$\frac{\sqrt{1+\kappa^2}}{\kappa}$	$\frac{\sqrt{C^2+k^2+\omega^2}}{k \cdot \omega}$

The damping of the propeller is defined with the Frahm's propeller damping factor D_F or Archer's propeller factor D_A, discussed in theory chapter 2.3.2.1. Other ways of defining the propeller damping are available also. If propeller damping is not given on specifications. Typical, rule-of-thumb value for the propeller damping used is *Archer number = 27*.

Table 3.8: *The different possibilities for defining the propeller damping.*

Damping Model	Input
Manual	Dynamic magnifier or dynamic magnifier percent
Schwaneke	Propeller geometric properties
Archer	Typical range 25-30
Frahm	Typical value 2.8
Variable	Knuckle-Point of propeller variable damping curve

3.2.2.3 Propeller

The propeller is the power sink in the system and needs considerable amounts of inputs, depending on if it is a FPP or CPP, ICE classed or not.
The program computes theoretical propeller curve as default, this defines the relation between the speed of the propeller and the power it consumes. This is a good enough estimate to be used in many cases. For both of the systems having CPP propellers the RoPax and the Bunker Tanker this was used.
The Dredger on the other hand has FPP propeller and the two operation profiles resulting in different load on the propeller. On one hand free running with empty holds and the other in dredging condition, loaded with sand and silt, dragging the draghead along the bottom.
Propeller torque curves were provided, those needed to be converted to power curves. The pdf files with the torque curves showing torque in kNm versus rpm were imported in AutoCad to measure few torque values. The figures were scaled such that one unit length is equal to one kNm, by this the length of the vertical measuring lines represent the torque value for the respective propeller speed. The torque values were then converted to power values. The list of calculated power versus propeller speed was written in a Nauticus type of text file which can be imported as a propeller curve.

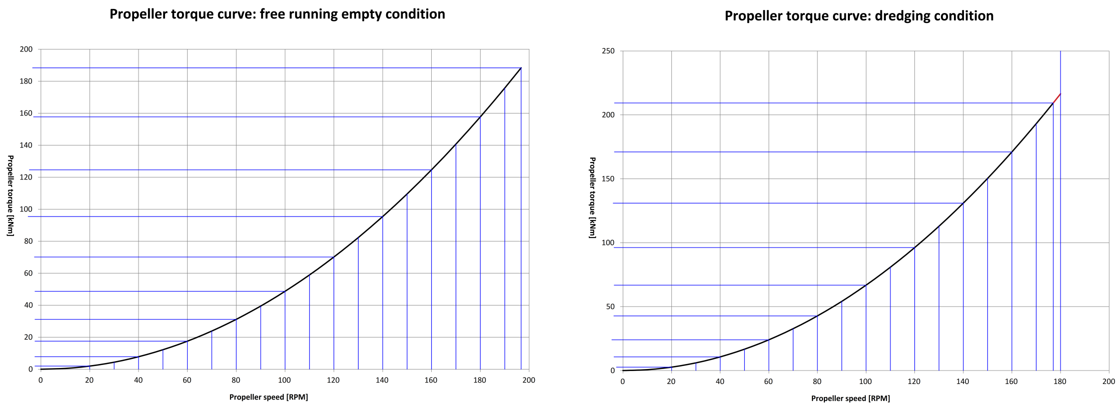

(a) Free running condition **(b)** Dredging condition

Figure 3.9: The propeller torque curves for the two conditions after measurements in AutoCad.

The conversion of propeller torque in kilo-Newton-meters kNm to power in kilo-

Watts kW was done using:

$$P_p = Q_p \cdot 2 \cdot \pi \cdot \frac{n_p}{60} \tag{3.4}$$

Table 3.9: *Notation for propeller torque and power for the propeller curve conversion.*

Q_p	:	Propeller torque $[kNm]$
n	:	Propeller speed $[rpm]$
P_p	:	Propeller needed power $[kW]$

In appendix C.5.3 the reader can find table C.1 listing the torque and power values as well as Nauticus standard format text files for the propeller power curves.

3.3 The improved diameter approach

The method to design a shaft line using DNV-CG-0038 document integrated with Nauticus machinery TVC and Alignment, is "in theory" the whole methodology approach of the thesis project. A guide to the method itself and the case study are reflected in this section here.

3.3.1 The method

Defining an improved step-by-step solution method for the minimum diameter of the propulsion shaft line was the plan. By integrating computational power, empirical methods, and equation approved by the classification society, the improved method was established. Though the aim was to push the rules and regulations to their boundary and try to defy the classification societies, the final calculation route that was come up with should all stay within regulations and rules (has not been tested by a class expert when this is written).
The procedure consists of different steps and there is no argument that this improved method takes a lot longer time to perform compared with the current approach, the ICAS 68.4 formula . Since this method approach is specifically outlined for Berg Propulsion, a conventional user will experience trouble following the step-by-step approach because Berg Propulsion has its own preliminary shaft system software (called ProjCalc). It provides (preliminary) design parameters, both for shaft components, engine, and propeller. Meaning this project calculation approach for the minimum shaft diameter relies on some of the output parameters from ProjCalc. Of course, conventional users can follow this approach, but one has to have the input to do so.
note! in this section writer refer to the procedure as an explanation to a user in a third person. Though the solution method was the same for them.
A user starts by having a preliminary design of a shaft and uses the improved method recommended by DNV, defined in the document DNVGL-CG-0038, previously talked about section 2.4.2.2. The method defines the shaft in respect of fatigue. To perform this method one must have the preliminary design data, such

as what kind of a component, bore of the shaft, surface finish, and other parameters of the design. The user must also have torsional vibration data of the whole propulsion system (TVC), simply the application factor (KA). The data can either be gathered from a TVC report or more conservatively estimated with tables and statements from DNV. In addition, if the vessel has ICE classification the estimated application factor for ice crash vibration must be calculated (section 2.4.2.1). Defining the application factor is not as easy as saying it, the user must have knowledge and access to a TVC software (such as DNV Nauticus Machinery TVC, talked about in previous section 3.2.2). Now to continue with the DNV improved method (DNVGL-CG-0038) the user must also have the rotating bending moment. A simple and conservative way is to define the bending moment as 40% of the nominal torque on the shaft [10] [11]. A more precise bending moment can be acquired using alignment software (such as DNV Nauticus Machinery Alignment, talked about in previous section 3.2.1). The same goes for that procedure, knowledge, and skills of how to set up lateral alignment cases in such software. The user then computes the safety factor for high cycle fatigue (HCF) and low- (LCF). Each safety must be within the defined minimum safety of the method, defined by DNV, 1.25 for LCF and 1.60 for HCF. With that begin said, the user can decrease the diameter (or alter component dimensions, e.g. increase the radius of a flange, switch component) until the desired safety is reached. In this project, the diameter was decreased until either one of the LCF or HCF minimum safety was reached.

At this point in the process, the user has either a shaft design based of a TVC report or using preliminary application factors. The next measure the user must take is to check the propulsion shaft for its minimum shaft diameter based on yield load from the propeller failure load. That is the check if the propeller shaft is stronger than the blades of the propeller because you want the shaft to survive the maximum load of the propeller blades before they break off. According to class, this is only required when the hip has an ice-class [12]. But at Berg Propulsion, they do this for every shaft line, since grounding the propeller can happen to any vessel, ice-classed or not. The user can then take its shaft line design that has been defined by the steps here previously, and check it with the propeller failure load, method mentioned in section 2.4.2.1. It can be that the aft-most propeller shaft must be increased from the previous study to fulfill this criteria. At this stage in the progress the shaft is designed in respect of fatigue limit, it fulfills the yield of one load crash of the propeller, if the user used TVC simulation then shaft is also designed within the natural frequency limit and classification torsional vibration regulations. The last step is to use alignment software to check for lateral vibration frequency, because the previous assessments have not taken into consideration the lateral displacement and its supports (bearings).

If all these design applications are met, the vessel shaft-line should be smaller, lighter, and thus cheaper than the previous conservative method.

3.3.2 Case study

This method for improved shaft diameter is considered to be used when designing a shaft, but it can also be applied to previously designed shaft lines. Either improve the design or to compare how much could have been saved. Hence the task was to look into few old/finished Berg Propulsion orders and see how over-designed the shaft lines are, and how much material could have been saved using this new approach.

Three orders were looked into. For the sake of confidential information of these shaft lines, the vessel name, owner, or other specific information will not be published.
The three study cases were:
-RoPax ferry, 12600 KW (each engine) dual prop vessel, 1B ICE-class.
-Dredger vessel, 4000KW, no ICE-class
-Bunker tanker, 2500KW, 1C ICE-class

Each vessel's shaft line was investigated, and the conclusion was to select few different locations of each shaft line and place that under investigation. To keep the diversity up, various components were selected. Based on the length and complexity of the shaft, two locations were selected on the Bunker and Dredger and three on the RoPax shaft line.

Table 3.10: *Each study location label of the shaft lines*

Vessel	Shaft part no	Component
Bunker tanker	A1 (Prop)	Flange
Bunker tanker	A2 (Interm)	Plain shaft
Dredger vessel	B1 (Prop)	Shirnk fit
Dredger vessel	B2 (Interm)	Flange
RoPax SB	C1 (Prop)	Flange
RoPax SB	C2 (Interm)	Shrink fit
RoPax SB	C3 (Interm)	Flange

See each shaft location in figure 3.10. Where each location is marked with a shaft part no. consistent with labelling in table 3.10.

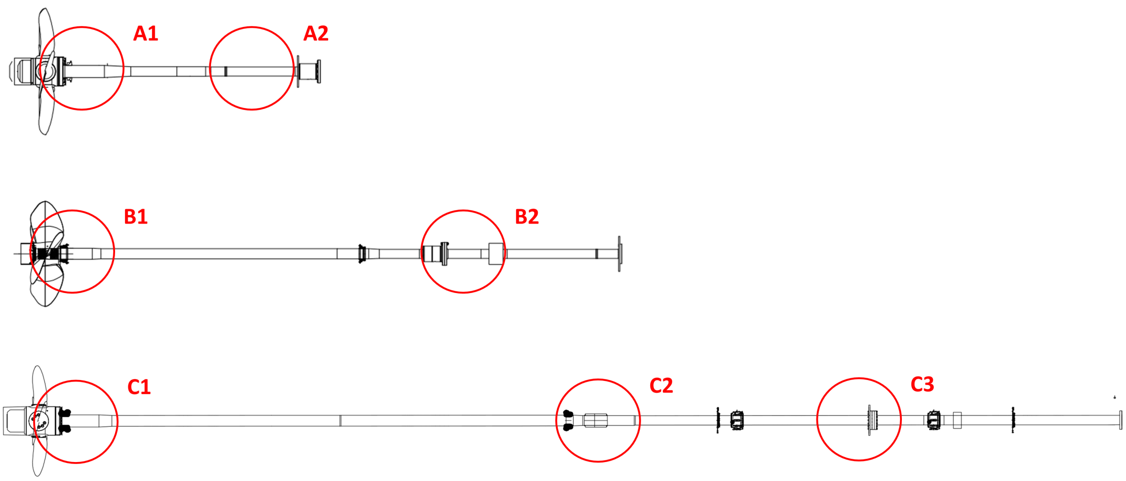

Figure 3.10: *The study cases on the three-shaft lines under investigation. Note, those three shaft lines are not in 1:1 ratio of each other.*

By using the procedure, here previously mentioned in section 3.3.1 each part location is calculated again with that approach. Few variables were applied to each approach in the investigation, resulting in a few different outputs for each re-calculated shaft location. Based on estimated and simulated torsional vibrations (KA factor) and same set for rotating bending moment(Mb).
Approaches used:
-Bending moment equals 40% of nominal torque and KA estimated from class.
-Bending moment simulated from alignment software, and KA estimated from class.
-Bending moment =40% of nominal torque and KA simulated from TVC software.
-Bending moment simulated from alignment software, and KA simulated from TVC software.

Using these input variables (two for each input parameter), four different outputs were provided. A comparison from each approach could then be investigated to monitor how much it affects the final result. In addition for the propeller shaft, there the minimum shaft diameter must fulfill the ice-class criteria required by the classification. This ice requirement is mentioned in section 2.4.2.1 based of DNVGL-RU-SHIP Pt.6 Ch.6 12.5.2. This additional application is based on that the propeller shaft is stronger and could withstand a failure load on the propeller-blades. This requirement was also calculated and applied to the propeller shaft locations (meaning that now five different output criteria are for each investigation)
The final conclusion of a minimum allowed shaft diameter was defined by the critical diameter of these five approaches.
The "new" shaft diameters were simulated in shaft alignment software to investigate if the current smaller shaft line would fulfill the whirling/alignment requirement by classification.
The finalised approved diameters could then be compared with the previously designed parameters defined by Berg Propulsion in the orders.

3.3.3 Additional input values

The methodology in the previous section requires many other input parameters and values than has been mentioned.

3.3.3.1 Dimensions of each component

Each different shaft component result in a different stress concentration. In consideration of each component, the investigation did only have the shaft diameter as a variable, and the dimension of each component was fixed from the initial design. Meaning, for example, though the shaft diameter from the initial design had decreased by some percentage the radius of a flange component stayed the same.

3.3.3.2 Surface roughness of shaft

In the method the R_y, which is the surface roughness, the maximum height of the profile. Also the surface roughness R_a, arithmetical mean deviation of the profile, should normally not exceed $1.6\mu m$. R_y can not be less than $1\mu m$ and can also be estimated as six times R_a. In this study, the estimated critical surface is used. That is $R_a = 1.6\mu m$ and $R_y = 6R_a = 9.6\mu m$.

3.3.3.3 Propeller and ice-applications

Previously talked about in section 2.3.2.3. Where the torque excitation from ice crash can be calculated with empirical formulas. The main input values that are needed to compute the formulas are the Propeller and hub diameter, Pitch ratio at radius 0.7 at bollard condition (which can be acquired from Bergs ProjCalc software), and the mass moment of inertia of all members of the shaft up to the part under investigation ratio against the mass moment of inertia of complete propulsion system. (Note! Alteration of the shaft diameter by a few percentages does not have a large impact on this ratio. meaning that the ratio was considered the same for shaft calculations with variable diameter)
The rules regarding the shaft to withstand the failure of the propeller, mentioned in section 2.4.2.1. The main input parameters needed to compute this minimum propeller diameter are the chord length at a relative radius where the investigation is taking place and max blade thickness at that particular location(which is provided by ProjCals, Berg Propulsion software).

3.3.3.4 Material

The standard shaft material chosen by Berg is '28mn6 steel'. It limits the IACS formula having the ultimate tensile-strength:600MPa and its yield-strength:350MPa. The same goes with the propeller material having it as a standard choice, using the failure stress 0.6*yield-strength+0.4*tensile-strength of the bronze blade material, 395MPa.

3.3.4 Calculator guide

This whole calculation method is vast and spans many rule and guideline documents from DNV, not to mention the significance of performing the TVC and alignment simulations. It can be difficult to grasp the steps taken here in this thesis investigation and in which order to follow them. An interactive script was made (based in excel) where the user is lead through each step of the process. It can be said that the calculation can be divided into three platforms, the main instruction script, a DNV-CG-0038 document calculator, and a TVC/alignment software of choice.
Though these scripts were made in favor of other users to manage, the writers eventually used these scripts to perform the investigation, because of it´s practicality.
Images and screenshots from one of the Excel scripts can be seen in figure 3.11, and with larger and more images in appendix A.3 for the DNV-CG-0038 document calculator and appendix A.2 for the the main instruction script. A flow chart of the DNV-CG-0038 document can be seen in appendix A.1.

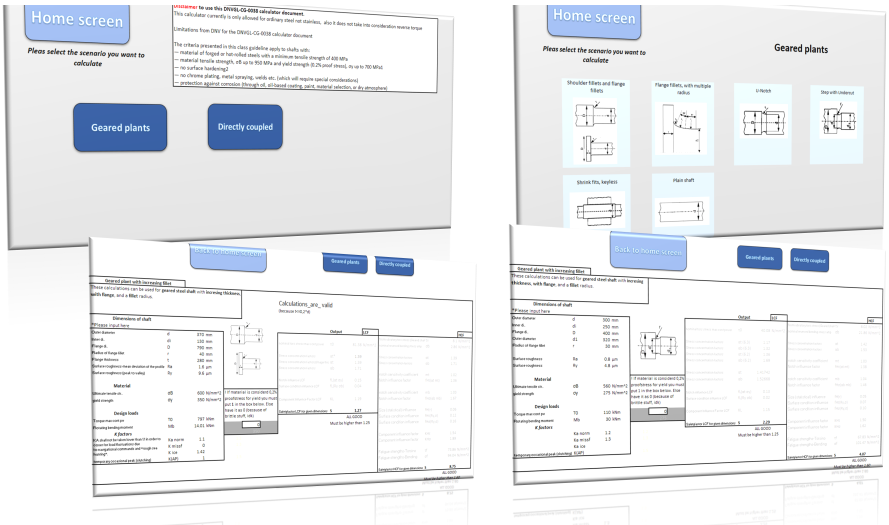

Figure 3.11: *Few screenshots from DNVGL-CG-0038 document calculator.*

4

Results

In this chapter, the results from the procedures previously talked in the report are revealed. The investigation on the IACS formula (IACS M68.4) is developed with a mimic formula, trying to simulate equivalent output. Both formulas are presented with the same input to study if they provide the same result, which could be used to argue the validity of the mimic formula.
The main investigation, developing the improved shaft diameter method, using TVC, and alignment simulations on the case study shaft lines. With a physical comparison on the initial- and improved shaft lines to see how much weight can be saved.
The case studies TVC behaviour is investigated for incremental dimensional changes.

4.1 IACS M68 compared with the mimic-formula

Many different approaches were done to mimic the IACS M68.4 formula, and one stood out comparing to the others. Establishing a formula solving for the diameter of a circular hollow shaft based on torsion, and defining the maximum allowed stress, based on finite-life fatigue endurance limit stress obtained from Dang Van failure criterion. The IACS M68.4 formula (the one that Berg uses for their min shaft diameter) can be seen in equation 4.1

$$d_{min} = F * k \sqrt[3]{\frac{p}{n_0} * \frac{1}{1 - \frac{d_i^4}{d_0^4}} * \frac{560}{\sigma_B + 160}} \tag{4.1}$$

The solved (and simplified) Mimic formula can be seen in equation 4.2

$$d_{min} = \sqrt[3]{\frac{p}{n_0} * \frac{1}{1 - \frac{d_i^4}{d_0^4}} * \frac{442.13}{\sigma_B}} \tag{4.2}$$

The finalised simplified edition of the mimic formula is defined like so (see equation 4.2). But if one would change the stress-concentration factor (SFC) this version of the formula is then not valid. Because the fatigue endurance and the effect of the SCF are "deep" within the 442.13 number, A full step-by-step deduction of the formula can be found in appendix B section B.2.

Comparing the equations can be a little tricky since they both require many variables. A comparison was done on a finished Berg order for a RoPax ferry (see designed data on table 3.1, on page 36) for a simple comparison. For this specific load case setup, the minimum required diameter based on variable power can be seen in figure 4.1.

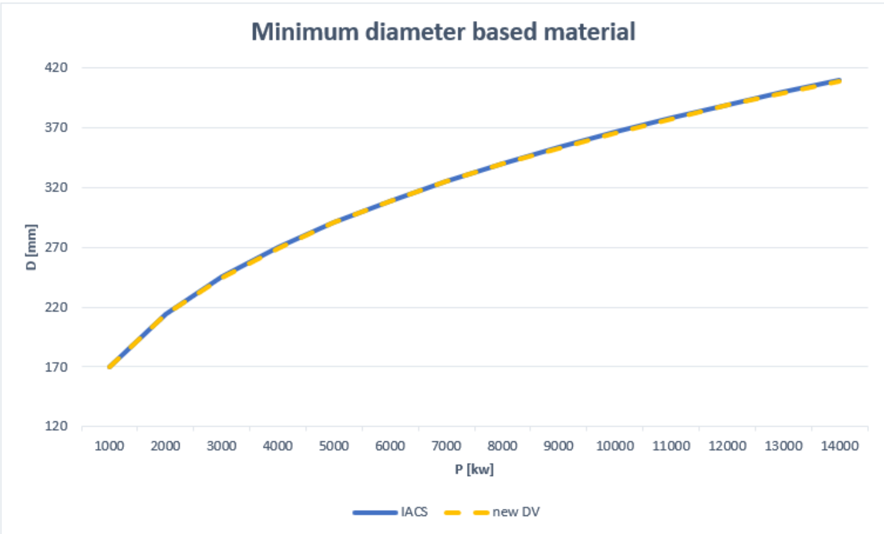

Figure 4.1: *Comparison of the IACS M68.4 formula and the writer's mimic formula of that one. The mimic formula is labeled 'New DV' (new Dang Van). With all design parameters the same and having input power the variable.*

The results were surprisingly similar for the writers. The mimic equation and the IACS one had been compared with random input variables for comparison over the developed time, but when this RoPax comparison was done it was not expected to get so similar result.
Another comparison was done on the two equations. Where different input variables had a randomly generated value.
- Inner diameter = 0
- Power = random generated variable from 800-10,000 KW
- Cycles (RPM) = random generated variable from 50-200 rpm
- Material ultimate tensile strength = random generated variable from 300-600 Mpa

(Each range was solely selected based on the writers' awareness of the expected size of the input values). Each equation received the same sequence of random inputs 100 times. The response graph for the output can be seen in figure 4.2.

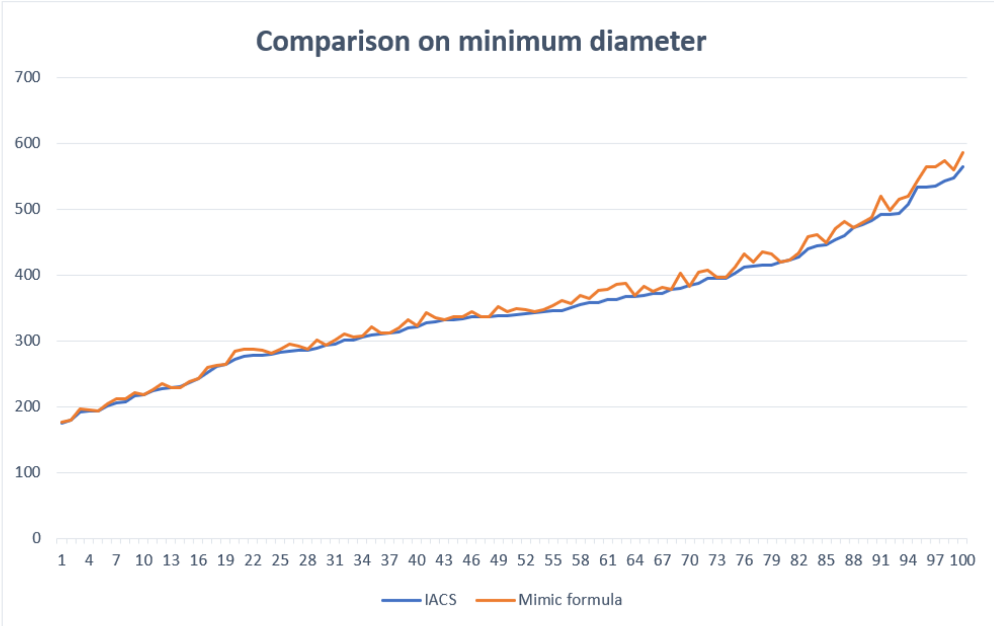

Figure 4.2: *Minimum diameter for IACS M68.4 and writers mimic formula, using random generated input data. Data values (input and output) can be found in appendix C section C.1*

From the graph (figure 4.2) it can be seen how some sequence of input values result in very similar minimum allowed diameter result, while others have a margin between them. The average margin between them is about 8.4mm. It can also be seen that the mimic formula is more conservative since the minimum allowed diameter is in most cases higher than the IACS M68.4 formula defines. The random generated input data values, and each calculated output for the equations can be found in appendix C section C.1.

4.2 Optimized dimensioning of propulsion shafting

Following the procedure defined in the Methods chapter, the shaft lines in the case study were assessed.

4.2.1 Comparison on finished Berg orders

The seven shaft line locations (see image 3.10 on page 54) were put under the scope. Every input parameter was gathered, some could be acquired from dimensions from a technical drawing, some from ProjCal, and others from Nauticus (TVC and alignment). A comparison was done to six different approaches to the diameter.
Approaches used:
-DNVGL CG0038 document method based on, bending moment equals 40% of nominal torque and KA estimated from class.

-DNVGL CG0038 document method based on, bending moment simulated from alignment software, and KA estimated from class.
-DNVGL CG0038 document method based on, bending moment =40% of nominal torque and KA simulated from TVC software.
-DNVGL CG0038 document method based on, bending moment simulated from alignment software, and KA simulated from TVC software.
-Minium allowed propeller shaft diameter, based on propeller failure load.
-The IACS M68.4 formula.
-And of course compared with the initial diameter.

The results for each approach can be seen in image 4.3, where one can see a comparison of each method in a column chart. The initial diameter and finalised diameter for each shaft location are labeled with blue and red icon tags. Where the final diameter lines up with the largest (most critical) diameter, excluding the IACS formula column.
Each approach is labeled with an abbreviation of the method descriptions which was listed here up in this section. The definition of each abbreviation can be seen on table 4.1, and should be used if one is not sure what each approach (column) represents

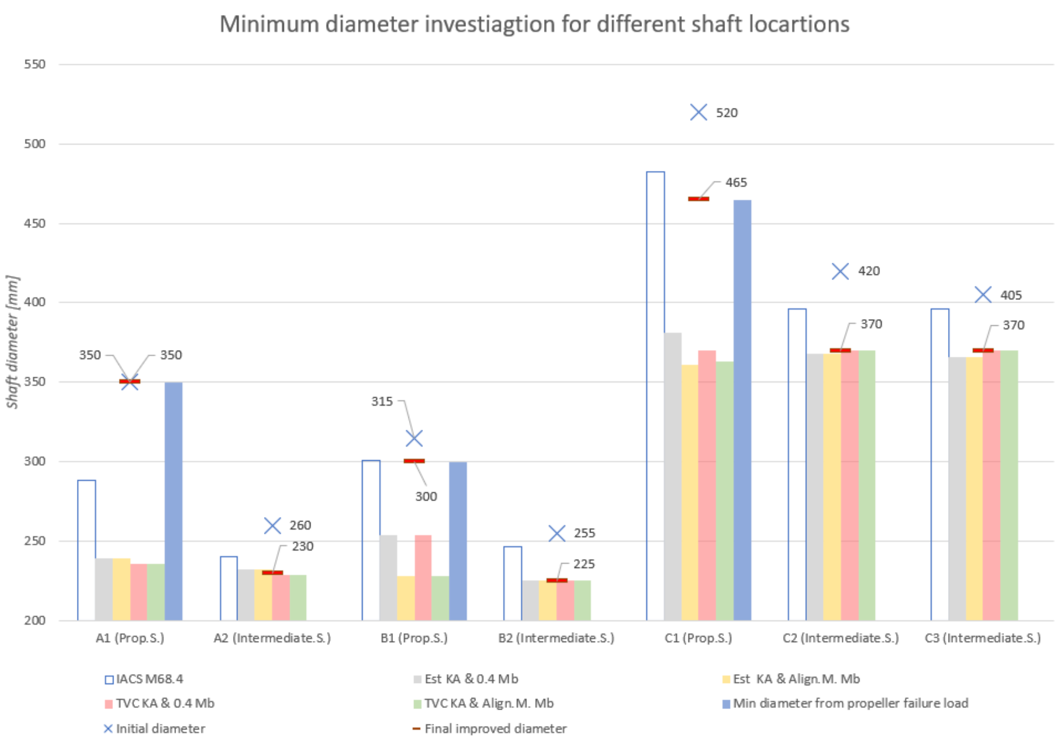

Figure 4.3: *Minimum allowed diameter from each approach, for all case study shaft locations, for comparison. Blue cross marks the final design from BERG, red bar the final design in this thesis investigation(our improved method).*

The results show by using this method for calculating the shaft diameter the min-

Table 4.1: *Description of abbreviations used in figure 4.3*

Approach labels	Description
Est KA	*Using estimated application factor(KA) values.*
0.4 Mb	*Estimating the bending moment (Mb) to be 40% off the torque.*
TVC KA	*Simulating the torsional vibration of the system to more precisely estimate KA.*
Align.M. Mb	*Simulating the lateral alignment of the shaft to more precisely estimate the bending Mb.*
Prop.S.	*Propeller-shaft*
Intermediate.S.	*Intermediate-shaft*

imum diameter can be smaller than the IACS formula states. In every case, the previous diameter (from the old orders) could be decreased, except for A1.
When the shaft location is the aftmost part of the propeller-shaft the design criteria 'minimum diameter from propeller failure load' applies, and each time it passes all of the other four DNV CG 0038 methods. Meaning that the minimum diameter limit that this study is trying to reach with the comprehensive calculations methods (using DNV CG 0038, TVC, and Alignment) is outmatched when this additional criterion is added for that shaft location. (The blade failure load, based on DNVGL-RU-SHIP Pt.6 Ch.6 12.5.2 [12]). That is why the minimum diameter and the blue column for A1, B1, and C1 on figure4.3

The other four approaches yield a similar result for some (graph, figure 4.3). The main reason that some approaches (column) have the exact same result is that each method could share the same critical input parameter. Let's set up an example case, it does not matter for a certain design if one estimates the rotating bending moment (40% of torque) or acquires it from alignment because for this hypothetical situation the torsional dynamic shock from ice crash (KA_ice) defines the minimum diameter. Or if another hypothetical scenario is looked at, the KAP (which is always inputted as 1.4) is the most critical input parameter of this hypothetical example, it outmatches the other application factors and the effect of the rotating bending moment is lesser than the KAP. This means in this case it does not matter how one acquires the application factors or the rotating bending moment. Because of this effect, the results for the shafts (in figure 4.3) do show few diameter outputs as the same.

4.2.1.1 The Tanker shaft

The investigation for the Tanker shaft line showed that using the improved method yields the same minimum diameter for the aftmost propeller shaft, location A1. The plain shaft in location A2 can be decreased from 260mm to 230mm.*All current*

and initial parameters for the Tanker shaft line can be seen in figure 4.4, the yellow highlighted volume represents material that could be cut off.
Larger scale of figure 4.4 can be found in appendix A.4

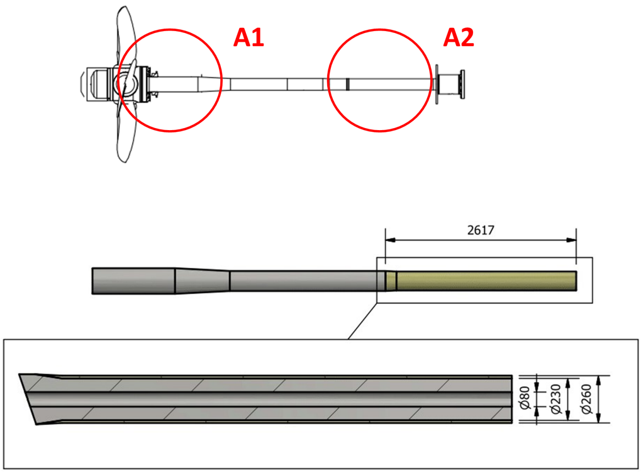

Figure 4.4: *Dimensions for the Berg design of the shaft and the currently improved dimensions. The material that can be removed/also represent the initial design is highlighted yellow on the shafts on the image.*

4.2.1.2 The Dredger shaft

The investigation of the Dredger shaft line was done on two locations. Based on the current improved method both of these shaft locations can be decreased from the Berg order design. Where the aftmost propeller diameter, B1, could be changed from 315mm to 300mm. Note, for the sake of total volume change the tapered parts and especially on this shaft where the propeller attachment is a tapered cone-thread, the outer diameter was just linearly decreased. The other location, the connector flange between both shafts, B2, can be decreased from 255 to 225mm. *All current and initial parameters for the Dredger shaft line can be seen in figure 4.5, the yellow highlighted volume represents material that could be cut off.*
Larger scale of figure 4.5 can be found in appendix A.4

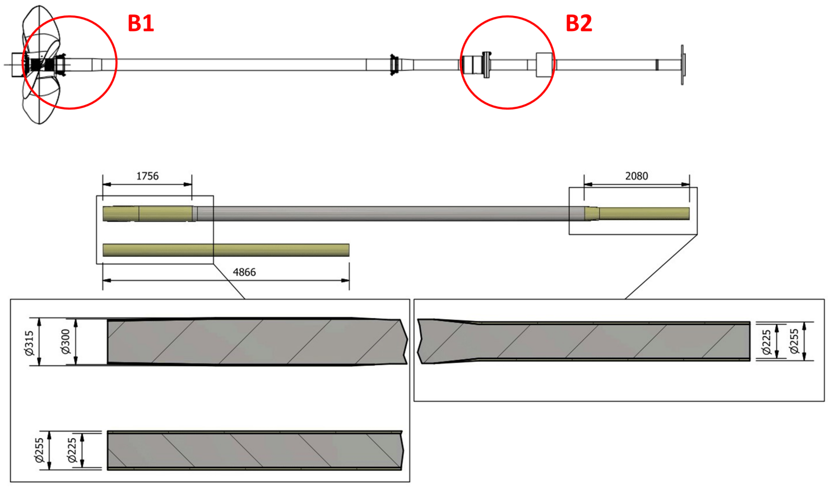

Figure 4.5: *Dimensions for the Berg design of the shaft and the currently improved dimensions. The material that can be removed/also represent the initial design is highlighted yellow on the shafts on the image.*

4.2.1.3 The RoPax ferry shaft

Based on each location the shaft could be decreased based on the result (in figure 4.3). C1 could be decreased from 520mm to 465mm. C2 and C3 had a slightly different diameter in the initial design, they resulted in the same diameter in the current result. C2 from 420mm to 370mm and C3 405mm to 370mm.*All current and initial parameters for the RoPax ferry shaft line can be seen in figure 4.6, the yellow highlighted volume represents material that could be cut off.*
Larger scale of figure 4.6 can be found in appendix A.4

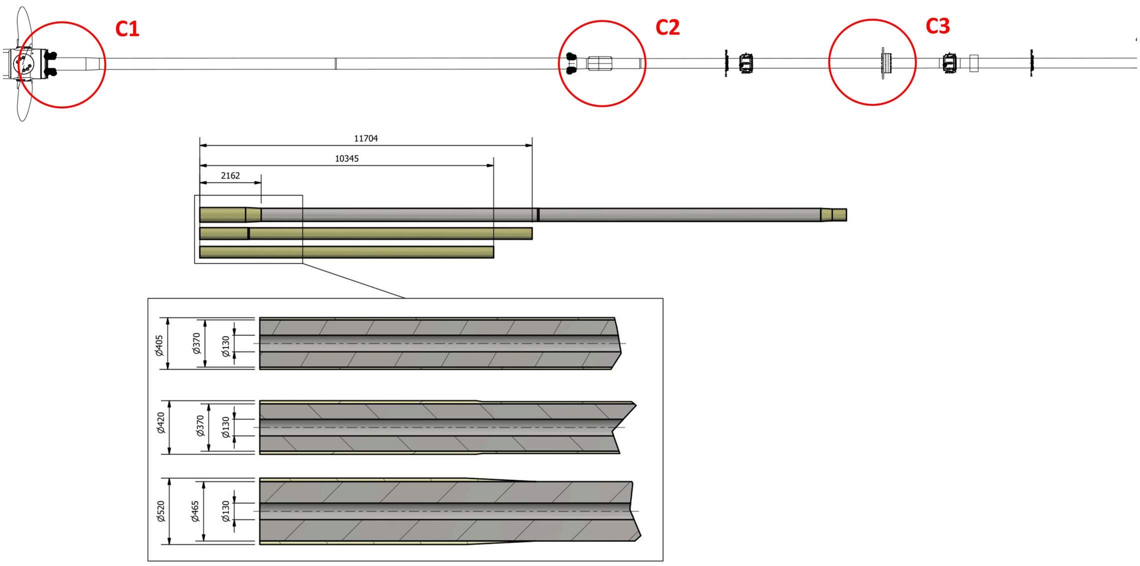

Figure 4.6: *Dimensions for the Berg design of the shaft and the currently improved dimensions. The material that can be removed/also represent the initial design is highlighted yellow on the shafts on the image.*

4.2.2 Weight reduction of raw material

The total steel weight of the shafts that can be removed resulted from the current method and the final design in the three Berg order was calculated, and can be seen in table 4.2.

Table 4.2: *Steel weight reduction on each shaft line*

	Before[kg]	**After[kg]**	**Difference [kg]**	
Tanker	3118	2889	229	7,35%
Dredger	7805	7112	693	8,88%
Ropax	47972	43379	4592	9,57%

The total weight reduction is largely different from each shaft line, seeing that the RoPax shaft line weight reduction is more than ten times larger than the Tanker. The overall volume of each shaft line has to be considered. When the weight optimization is compared in relation to the proportion of initial volume, it can be seen that each shaft line can reduce weight by a similar margin, 7.4-9.6% (see table 4.2) Just for an interesting visual comparison, a rendering of the volumetric size comparison of each mass of steel that can be decreased from each shaft line was done, see image 4.7.

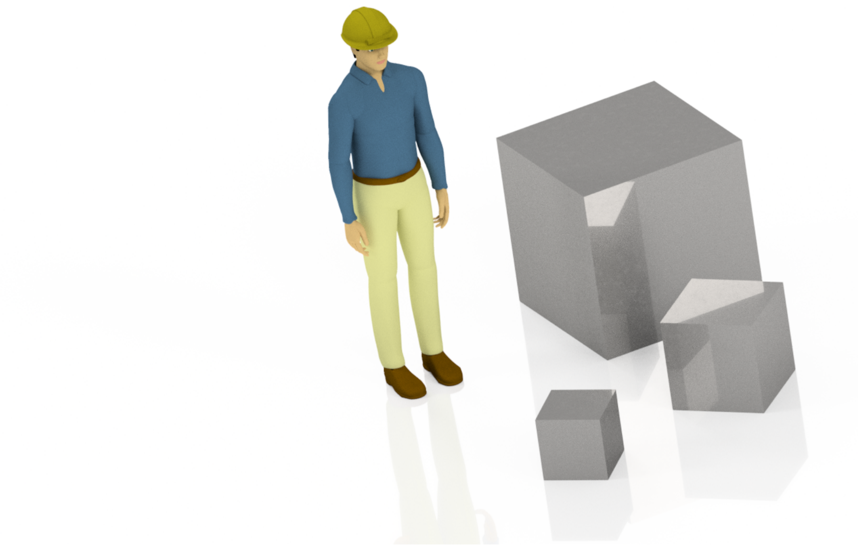

Figure 4.7: *Visual comparison of the weight/volume of raw steel that could be saved from the three orders*

4.2.2.1 Sensitivity-DNV CG 0038 calculations

By performing manual inputs into the calculations the writers developed an awareness of which input parameters are important, and who have a minor effect on the output result.

From the input parameters, a user needs to operate (calculate) the DNV CG 0038 calculator (section 3.3.4) some have more influence than others.
The inner bore diameter of the shaft in Bergs case is defined by the hub size, regarding the hydraulic equipment. If one would like to optimize the weight of the shaft the inner bore can be increased, since the outermost part of the shaft is the body that reacts most in torsion and bending (talked about in section 2.2) [5]. It can be seen in the graph in figure 4.8. where the inner bore was increased in the ratio of the outer diameter. The inner bore effect does not influence the result much until the inner bore is about 60 to 70% of the outer bore (IACS M68 document states if the inner bore is less than 40% of the diameter, the inner diameter can be disregarded [21])

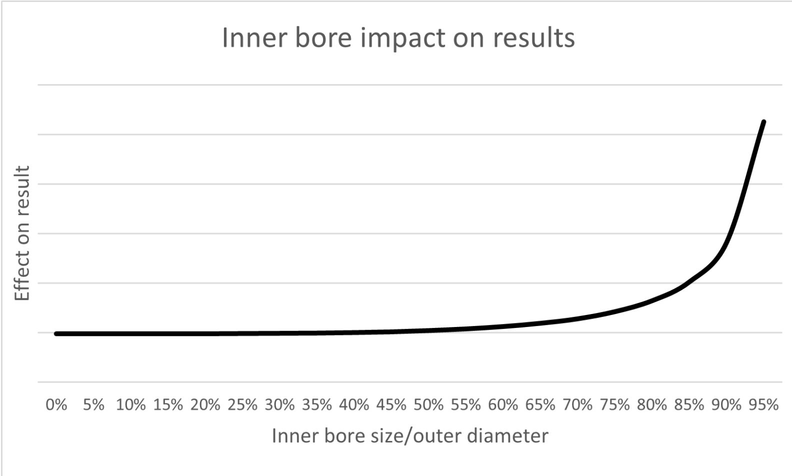

Figure 4.8: *Unitless graph showing the effect of the inner diameter bore in relation to the outer diameter on resulted safety of a shaft design*

The effect from the surface finish is included in the DVN CG 0038 document, but with inspection, the size value of the surface finish does not affect much the fatigue life of the shaft. It states in DNV that Ra (Surface roughness-mean deviation of the profile) should not be more than 1.6 μm, and Ry (Surface roughness, peak to valley) can be estimated $Ry \approx 6Ra$ [12]. So with that relation, running a vector up to Ra=1.6 it can be seen that for every component the output of the calculations does not shift much(based on DNV CG 0038 [10]).
Crucial parameters are the outer diameter, material, the KA (application) factors, and the reaction loads (bending and torsion). But as noticed in the diameter result in the sections here above (see section 4.2.1 and graph in figure 4.3), it can be seen how the result vary little from how the KA (application) factor or the bending moment is acquired. With a grain of salt, the sensitivity of the result is small depending on how the user defines these two inputs.

4.2.3 Shaft alignment - whirling analysis

This section will summarise findings from the Shaft Alignment analysis, the results focused on are the shaft vertical deflections, bearing slope and lubrication pressure. Another important thing is the shaft rotational speed where the shaft has natural frequencies. The program gives the revolutions per minutes and plots the mode shapes for the whirling vibration modes, only the first 3 modes are printed out. The program calculates much more, there can be set a limit to how high frequencies the program computes. The default setting is quite high and the program usually gave first 10 to 20 of the natural frequencies and mode shapes.

Each case study shaft line is compared with the initial (approved) alignment reaction result to the optimised diameter shaft line alignment reaction result. Each diameter modification can be seen, for the RoPax ferry in section 4.2.1.3, for the Bunker tanker in section 4.2.1.1, and Dredger vessel in 4.2.1.2

4.2.3.1 Ro-Pax

The RoPax had few changes done on the shaft line, as it can be seen in section 4.2.1.3. The behaviour of the deflection does not change much for the naked eye, reflecting from the graphs, see deflection graphs in figures 4.9a and 4.9b. But pressures and slopes do change. Small increments on the vertical offset of the bearings were changed to meet regulations on the slopes. (All the bearing reaction, before and after shafts optimisations can be seen in appendix C.3). The main noticeable reaction after the adjustment was the stern tube slope in 0-pitch condition, where it was a little bit over 3mm/m which is the standard for full pitch operation [11]
The behaviour of whirling does shift from locations on the shaft, as well as the critical speed (natural frequency of the system) of each vibrating mode shifts down in rotations, see graphs in figures 4.10a and 4.10b.

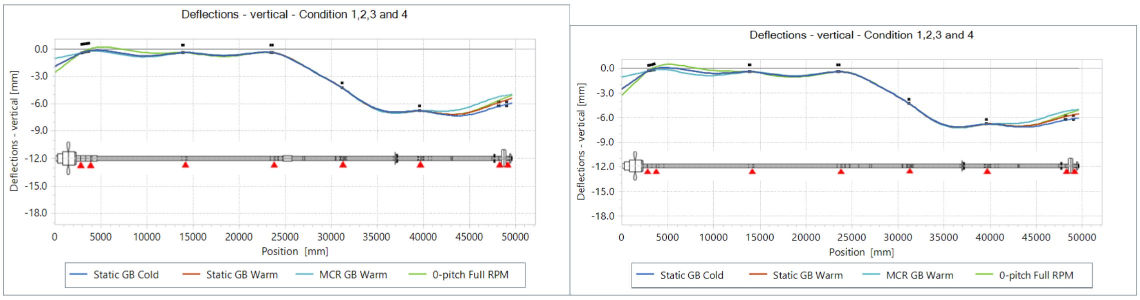

(a) Deflection original

(b) Deflection decreased diameter

Figure 4.9: *Shaft deflection for all operating condition, side by side comparison for the RoPax vessel.*

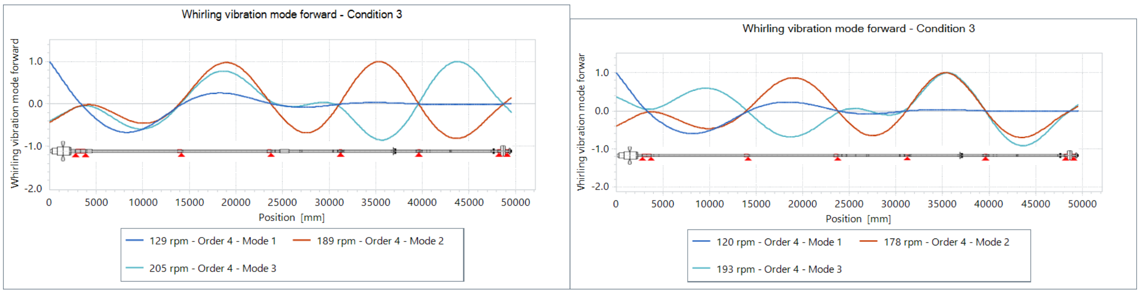

(a) Whirling modes original

(b) Whirling modes decreased diameter

Figure 4.10: *Whirling modes in forwarding condition, side by side comparison for the RoPax vessel.*

All graphs in larger scale and bearing reactions can bee seen in appendix C.3.

4.2.3.2 Bunker tanker

For the Bunker tanker, the propeller shaft is could not be decreased from the previous design due to propeller blade failure load criteria. Thus the result from alignment software for both design was almost the same. Both in deflection, reaction on bearings and in whirling, see deflection graphs for the Tanker in figures 4.11a and 4.11b. The only noticeable difference in whirling is seeing a shift in critical speed of few rpm´s for a different mode, see whirling graphs in figure 4.12a and 4.12b.

Because of this "uninteresting" result, it was decided to ignore the propeller blade failure load for the tanker vessel, just to see how much the alignment could be pushed. See that investigation in section 4.2.3.5.

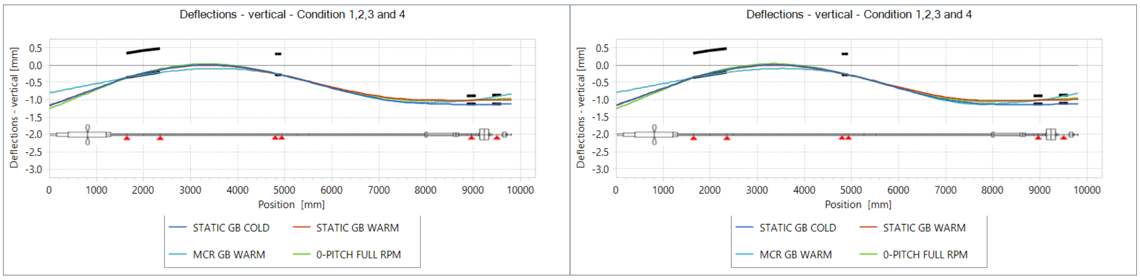

(a) Deflection original **(b)** Deflection decreased diameter

Figure 4.11: *Shaft deflection for all operating condition, side by side comparison for the Bunker tanker.*

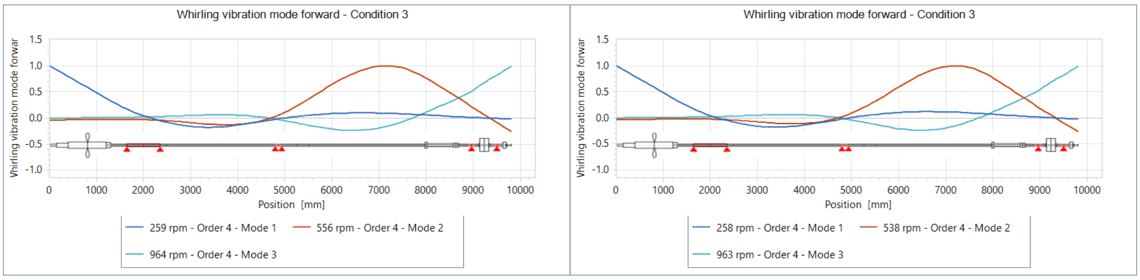

(a) Whirling modes original **(b)** Whirling modes decreased diameter

Figure 4.12: *Whirling modes in forwarding condition, side by side comparison for the Bunker tanker vessel.*

All graphs in larger scale and bearing reactions can bee seen in appendix C.3.

4.2.3.3 Dredger

Since the propeller shaft was not much changed (from 315 to 300mm) the result from alignment was quite similar to the initial one (similar as for the Tanker vessel). The slope and pressure of the stern tube bearing did not change a lot and is within the regulations, see the deflection of the shaft line in figures, 4.13a and 4.13b. The Dredger is a difficult shaft since the first whirling mode critical speed is close to the operating speed. In this case, the MCR is 197rpm and the initial shaft design first mode critical speed is 108rpm, but for the optimised shaft the critical speed has shifted down to 103rpm, see whirling result in graphs in figures 4.14a and 4.14b .

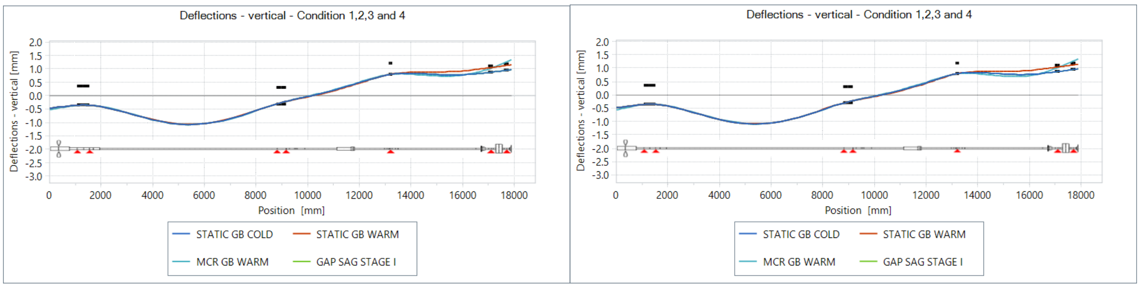

(a) Deflection original **(b)** Deflection decreased diameter

Figure 4.13: *Shaft deflection for all operating condition, side by side comparison for the Dredger vessel.*

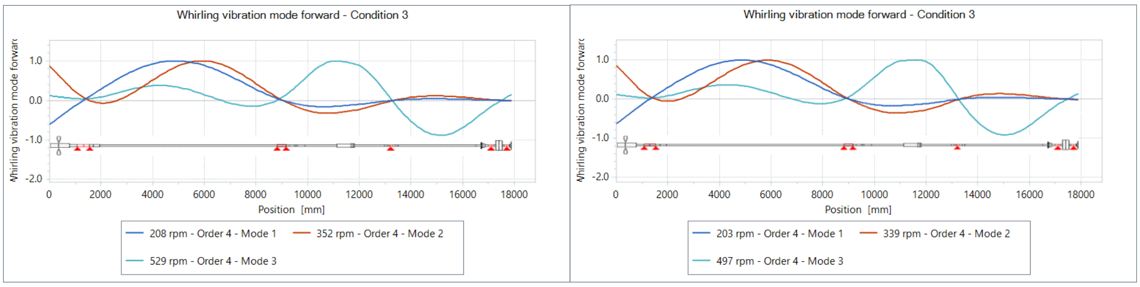

(a) Whirling modes original **(b)** Whirling modes decreased diameter

Figure 4.14: *Whirling modes in forwarding condition, side by side comparison for the Dredger vessel.*

All graphs in larger scale and bearing reactions can bee seen in appendix C.3.

4.2.3.4 Result for the case study

Each case study was simulated in Nauticus Alignment software to check if the new design (new diameters) would be approved in terms of lateral vibrations (has been talked about in the previous sections). Though diameters were not altered much, the critical RPM of the shaft line can be shifted to a more severe region.

There were two benchmarks that the writers looked at to assess if whirling criteria are approved. That is, based on class requirements, and based on the fact that the initial designs of the BERG orders (design before it was changed) are approved by the class, some having some exception approvement from the class.

Note. definition of success was mainly in respect of the shaft whirling. Other measures were roughly taken into consideration: Stern tube slope not more than 0.3mm/m, bearing pressure not less than 1bar and with an eye on other rules and regulations (mentioned in 2.4.3). Meaning some bearings could be slightly miss adjusted (which is just a result of lack of knowledge from writers using alignment software), which was not the main study and could be solved with extent knowledge *in alignment software to adjust everything correctly. In addition, the shaft line was correctly aligned before the diameters were decreased. The writers only modified the shaft diameter, stern tube bearing effective length, and small increments in vertical offset of bearings, in alignment software from the initial design.*

Results from alignment whirling investigation can be seen in table 4.3.

Table 4.3: *Critical speed RPM of the shaft line, before diameters, were decreased and after optimisation.*

	Inital design-Freq mode[rpm]		**Optimised design-Freq mode[rpm]**	
Vessel	**1st critical mode**	**2nd -**	**1st critical mode**	**2nd -**
Bunker	259	556	258	538
Dredger	208	352	203	339
RoPax	129	189	120	178

For comparison, Bunker tanker vessel has its MCR at 142 rpm, Dredger at 197 rpm, and RoPax at 151 rpm. Beginning with the Bunker, it can be seen that the critical speed does not change much after applying some changes to the shaft diameters. Therefore the lateral vibrations on the bunker shift is not an issue after diameters have been optimised. The Dredger is a difficult case. Both knowing some information from BERG that the initial design of that shaft line is not within an approved range(± 20% of MCR [11]), but the rotordynamics engineers at BERG did get an exception from the class, with some conditions of serious precision when building in the shipyard. Now resulting in even more critical natural frequency with a margin of 6 rpm from the MCR(previous 11 rpm), it is difficult to say if that will be approved. The RoPax can also not fulfil the critical speed demand. The initial design is within the 20%. The same circumstances is for the RoPax as for the Dredger, that is BERG got a special approvement from class. Having that in mind and comparing the critical speed after optimisation, it can be seen that the critical speed has shifted away from the MCR resulting in a more reliable shaft against whirling(initial design, mode one is 14.6% from MCR, in the optimised diameter design mode 2 178rpm is 17.8% from MCR).

4.2.3.5 Alignment Tanker without ICE-class

Having in mind that the optimised diameter is dependant on the four different approaches using the DNV-CG-0038 documents and the additional propeller blade failure (meant for ICE class). To see how much the whirling could be pushed, it was decided to ignore the ICE-class criterion on the Bunker tanker propeller shaft, and see how small the propeller shaft can be until the alignment rules will not approve. With manual trial and errors, the smallest diameter that could be reached was 300mm. See alignment result graphs in figures 4.15a and 4.15b. The whirling happens aft of the aft-most stern tube bearing so additional bearings could not be added. The limiting factor was reaching the maximum allowed slope in stern tube bearing, and the foremost stern bearing had already gone below the pressure limit. All output data from the alignment can be seen appendix C.3.

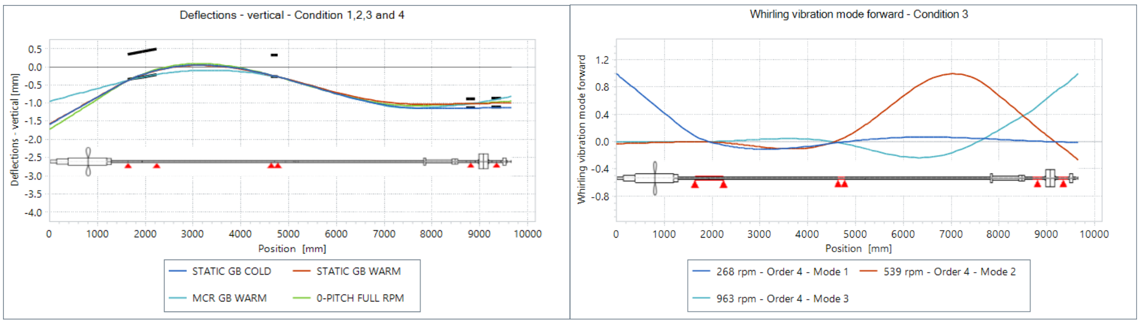

(a) Deflection Tanker without ICE-class **(b)** Whirling modes Tanker without ice

Figure 4.15: *Reaction for Tanker shaft line when The propeller failure ICE criteria is not considered*

4.2.4 Torsional vibration calculation

Calculation results are compared in the form of plots, usually having engine or propeller speed on the horizontal axis and different types of physical response on the vertical axis. Most of the calculations are done in frequency domain, the program simulates excitation's and responses in the system for a range of revolution speed. With this natural frequencies and harmonics are established.

4.2.4.1 Ro-Pax

The Ro-Pax reference shaftline represents the most complicated system of the three systems analysed in this project work, see simplified arrangement schema. What makes the system more complicated is first and foremost the fact that it has a 4 stroke diesel engine delivering the propulsion power. Compered to the electric motors used for the Tanker and Dredger shaft lines the diesel engine requires much more inputs and is comprised of many different modeling components. The electric motor is in essence just one inertia node with a definition of power and MCR speed, on top of that one stiffness element and one inertia node represent the stiffness and inertia of the output shaft.
Another important thing is that the shaftline has a reduction gear with PTO, *power-take-off*, where an shaft generator is connected. There are clutches for both the generator output and propulsion shaft output, resulting in many possible operation profiles for the shafting system.

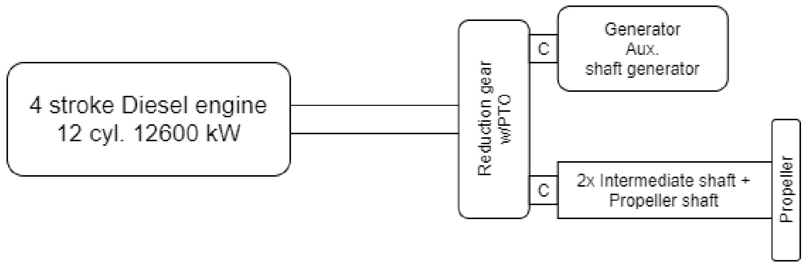

Figure 4.16: *Simple schema representing the RoPax shaftline arrangement. Connections marked with C represent clutches.*

The RoPax shaft line was the first system to be modeled which took a lot of research to get running without errors. But after all the check for natural frequencies showed too low values to be regarded correct. The results could be compared to a benchmark report done by industry experts, analysed in similar type of software. It was understood that most likely there was a mistake somewhere in the definition of an inertia or stiffness, possibly damping. Damping how ever normally does not influence the natural frequency of the system much. "In case of natural vibrations there is no excitation, ($M_E = 0$). Furthermore the influence of damping is considered to be negligible" [28]. The natural frequencies are calculated as free vibrations, the effect of the damping can be seen on figure 2.9. Damping dissipates high amplitudes but does not shift the frequency of the harmonics of any considerable amount.
Below are printouts from the Nauticus TVC tool showing natural frequencies of the first 3 vibration modes, for two separate models of the RoPax. This check is a good indication of correctly defined model.

```
NATURAL FREQUENCIES AND MODE SHAPES

Mode number                              1             2             3

Natural frequency (rad/s)             0.34         19.32         31.97
Natural frequency (vibs/min)          3.27        184.48        305.29
Natural frequency (Hz)                0.05          3.07          5.09

NATURAL FREQUENCIES AND MODE SHAPES

Mode number                              1             2             3

Natural frequency (rad/s)             0.22         20.91         44.62
Natural frequency (vibs/min)          2.12        199.72        426.10
Natural frequency (Hz)                0.04          3.33          7.10
```

Looking at the frequency values given as $\frac{vibs}{min}$, *vibrations per minutes*, the first natural frequency is 3.27 and 2.12 $\frac{vibs}{min}$ respectively. This is a very low frequency, the rotational speed of the shaft at MCR is 150.8 rpm for comparison. This indicated to authors that most likely a shaft stiffness somewhere in the system was defined with an error of 10^6. Having an effect on the system just as on of the steel shafts where replaced with a rubber one. The reason for this suspicious is because the same kind of error had occurred while building the shaft alignment model. The effect there was whirling deflections of about a meter instead of millimeters. The reason for such type of an error was found being that specifications for stiffness are often given as

$\frac{MN*m}{rad}$, *mega newton meters per radian*, while the setting in Nauticus was in $\frac{N*m}{rad}$ and needed therefor multiplication by 10^6. The trick with computer simulations like those is that the packages just deliver the numbers however out of reality they can be, of course in both of those cases the shaft would fail immediately. After building the model from scratch two times, going through all inputs multiple times and studying the function behind different elements in a quest for understanding what part could cause such a large error in the frequency of the system.
Finally it was found as suspected that stiffness for the input shaft for the reduction gear had been defined as 108.63 $\frac{N*m}{rad}$ resulting in value inside Nauticus as 1.086E+002 N*m/rad instead of the correct one being 1.086+008 N*m/rad.
The main cause of error was by this eliminated but in the process another mistake was discovered, the damping of the engine crankshaft damper had been defined twice. Both as absolute damping in inertia node one, representing the outside portion of the engine damper, and in the damper stiffness element also as relative damping. The damper stiffness being shaft element no. 1. All input data can be found in appendix C.
Below frequency check shows values of mode number 1 and 3 within 0.2% and mode number 2 within 3%.

NATURAL FREQUENCIES AND MODE SHAPES

Mode number	1	2	3
Natural frequency (rad/s)	16.80	23.47	50.73
Natural frequency (vibs/min)	160.40	224.15	484.46
Natural frequency (Hz)	2.67	3.74	8.07

While the RoPax model still had errors the study proceeded with the two electric driven shaft lines, the Tanker and Dredger. It was believed that part of the problem could be related to the definition of the diesel engine. For this reason the main part of the study was proceeded on those two models.

The results presented here for the RoPax shaft focus mainly on representing vibration behaviour related to the diesel engine in comparison with the electric motor. The comparison is between the engine running normal and misfiring. The TVC calculation for a diesel engine in a misfiring condition is an important and required step, here cylinder no. 12 is compressing but there is no fuel and therefore no power stroke. The operation mode is both clutches engaged, such that both propulsion shaft and shaft generator is spinning. The propeller is at full pitch and the engine on full power, how ever the generator is spinning passive. The propeller is consuming all the engine power.

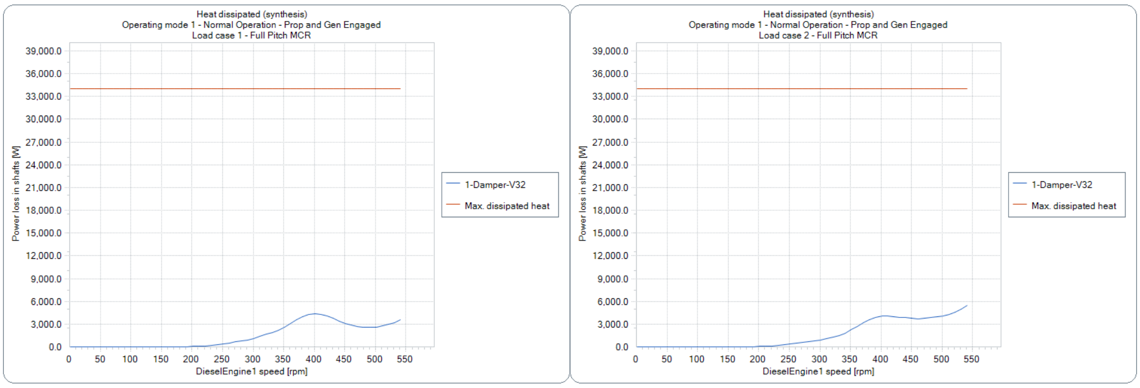

(a) Normal **(b)** Misfire

Figure 4.17: *Heat dissipation from the engine damper, indicating the work done by the damper.*

The engine damper is of a steel spring design, which has two circular steel sections with steel springs in between, voids between the springs are filled with oil. This type of vibration damper can be specifically tuned for each application [19]. The exact type of the spring is not known, interested reader can find information about this type of dampers from company called Geislinger. According to figure 4.17 there is just slightly elevated heat build up in the damper, well within limits. Figure 4.18 shows the alternating torque experienced by the damper.

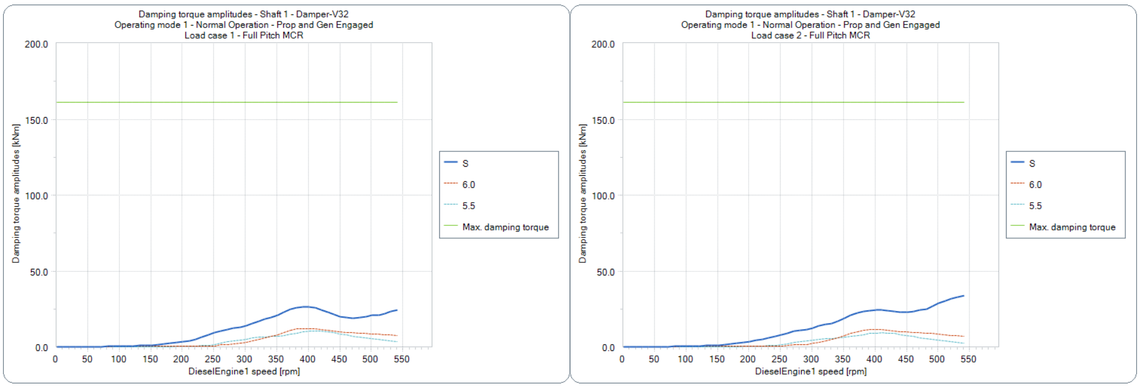

(a) Normal **(b)** Misfire

Figure 4.18: *Engine damper alternating torque, the thick blue line shows synthesis of vibratory torque amplitudes measured at the damper element. The thinner red and cyan represent the most prominent excitation modes.*

Between the engine and the gearbox it is normal to have a flexible coupling, this is in large part an elastic vibration damper, but can also accommodate for some misalignment.

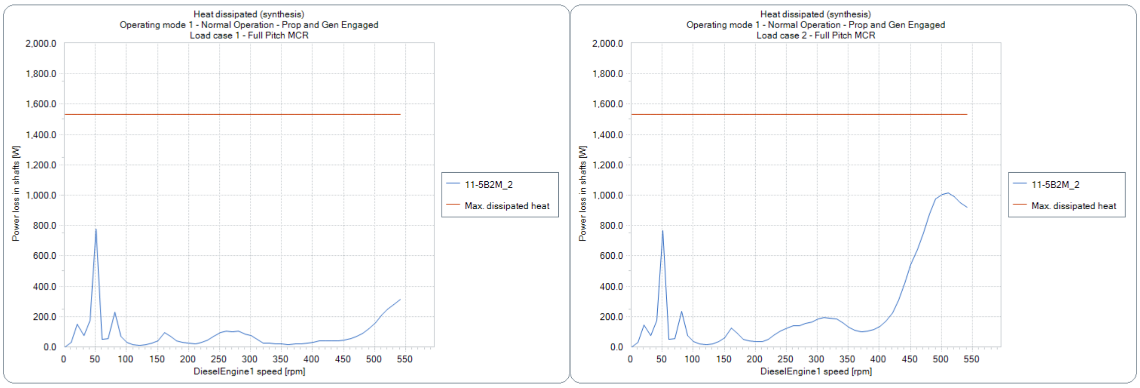

(a) Normal **(b)** Misfire

Figure 4.19: *Main flexible coupling heat dissipation.*

By investigating figure 4.19b it becomes clear what effects it has to run the engine under misfiring condition. Uneven forces will certainly affect the engine itself but what can happen before is failure of the flexible coupling. The heat builds up in the rubber elements, causing the coupling to loose stiffness, elevating the risk of failure.

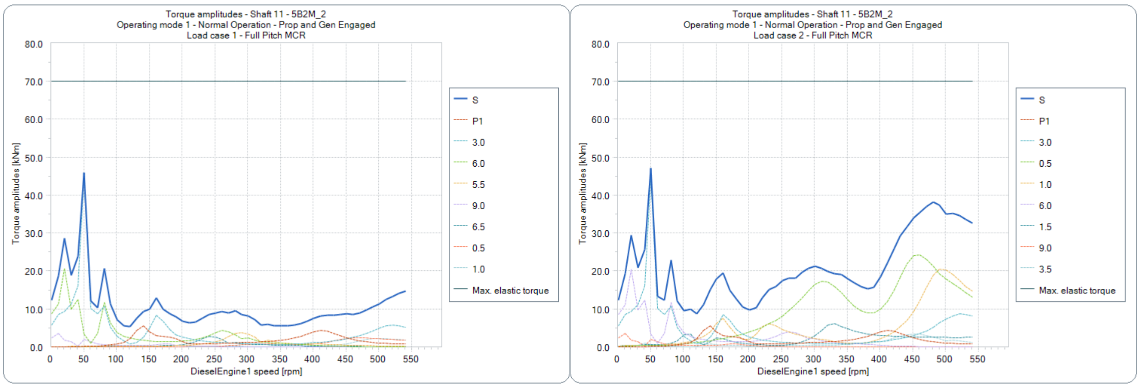

(a) Normal **(b)** Misfire

Figure 4.20: *Main flexible coupling alternating torque.*

When studying the responses for the coupling in figures 4.19 and 4.20 it is important to realize the operating range of the propulsion engine, the MCR speed is 514 rpm, the clutch in speed is between 60% and 70% of the maximum speed. This means the engine and shaft will never operate on lower speed than about 300 rpm [8]. Looking at the high alternating torque to the left, the shaft will never dwell at this speed, it is however worth noting the higher torque amplitudes at operating speed for the misfiring condition.
Worth noting also is the number of excitation modes contributing to the total synthesis, the thick blue line. The order plotted are just the most prominent. This shows the effect of the reciprocating engine, when studying the Tanker and Dredger shaft lines, propelled by electric motors. Usually the only excitation's seen is P1 and P2, the first and second propeller orders.

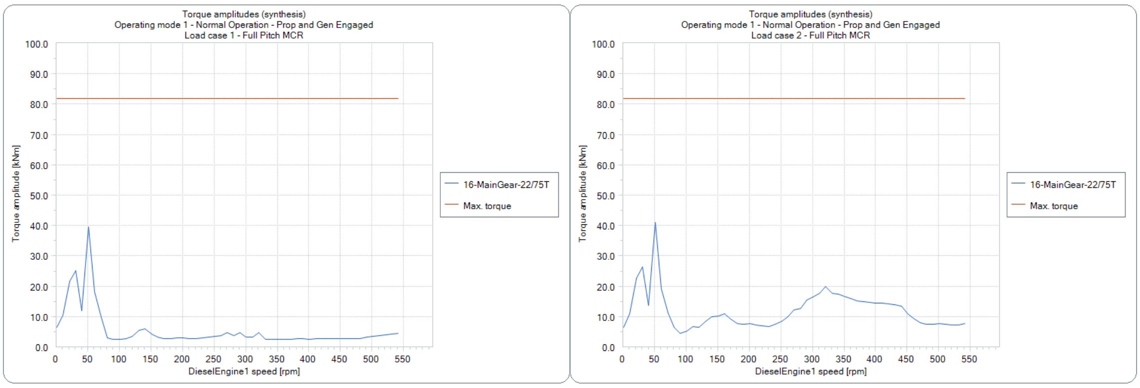

(a) Normal **(b)** Misfire

Figure 4.21: *Main gear alternating torque.*

Alternating torque over gears can cause gear hammering, in figure 4.21 the alternating torque amplitudes for the main reduction gear are presented. As before the rotational speed below 300 rpm are not of real interest. A clear increase can be seen in alternating torque for the misfiring condition compared to the normal condition, however the torque amplitudes are still small and well below limits of 81.9 kN*m. Final calculation for the RoPax shaft line is torsional stress amplitude synthesis. In figure 4.22 the torsional stress amplitudes are compared to alternating stress limits in regards to fatigue failure of the propeller shaft. It can be seen that alternating torsional stresses are of no concern for either the normal nor the misfiring engine.

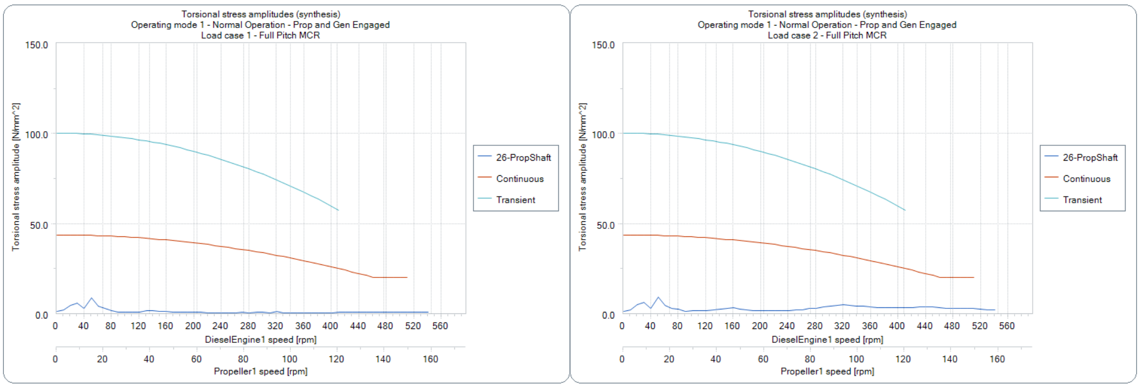

(a) Normal **(b)** Misfire

Figure 4.22: *Propeller shaft torsional stress amplitudes for normal running engine and misfiring engine.*

In figures 4.22a and 4.22b the cyan colored line at the top represents a transient fatigue stress limit. The stress is not allowed to get higher than the transient limit. The red colored line in the middle is the continuous running fatigue stress limit, stresses during normal operation are not allowed to be higher than the continuous limit. The zone between the continuous and transient represent stress level that should be avoided, the shaft should not dwell on this speed. Speeds having harmonic spikes causing shaft stresses to rise above the continuous limit should be regarded as barred speed ranges and ship operators must be aware of those speeds. See discussion about IACS M68 in chapter 2.4.1. The simulation results indicate that flexible couplings and gearbox should be checked carefully for alternating torque but the propulsion shafting is not affected much.

4.2.4.2 Bunker tanker

The reference shaftline for the Tanker type of a vessel is much shorter, has fewer components and results in a considerably less complicated model than the RoPax, especially for the TVC analysis. It has similar setup as for 2 stroke shaft but using two electric motors through a reduction gearbox instead of a diesel engine. Hence skipping the trouble some vibration behaviour of the 2 stroke engine. The operating condition considered in this investigation is *2 Motor Mode - Normal Operation*. The torsional vibration response is calculated in frequency domain from zero to MCR speed.

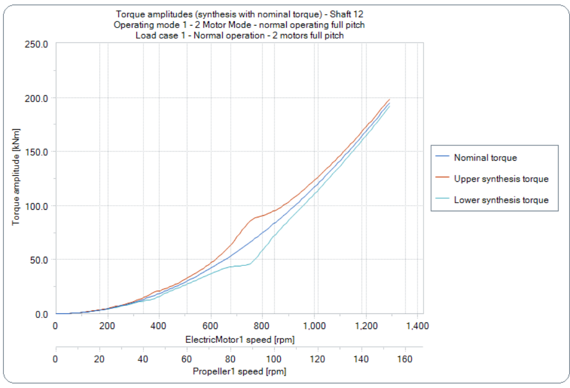

(a) Original diameter

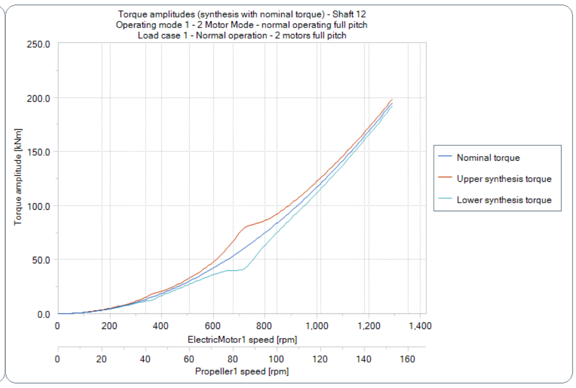

(b) Decreased 10 mm

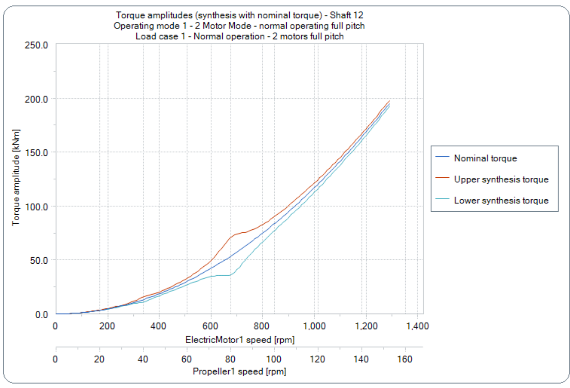

(c) Decreased 20 mm

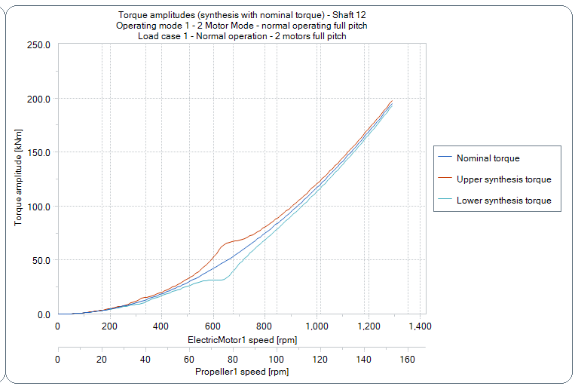

(d) Decreased 30 mm

Figure 4.23: *Propeller shaft nominal torque and upper and lower torque synthesis, where the upper and lower synthesis diverge from the nominal indicates fluctuating shaft torque. Comparison of original diameter to -10mm, -20mm and -30mm decrease.*

Figure 4.23 demonstrates that alternating torque is not a problem in the Tanker's propeller shaft, further it demonstrates that with decreased diameter the response frequency moves to lower speeds and the stress amplitudes become smaller.

Figure 4.24 compares the propeller shaft torsional stress amplitudes, for the different diameters. The curve at top is the transient curve, next below is the continuous line according to IACS M68.5, see equations 2.37 and 2.38. The fat blue line is the torsional stress amplitude synthesis, P1 and P2 represent the first and second propeller excitation.

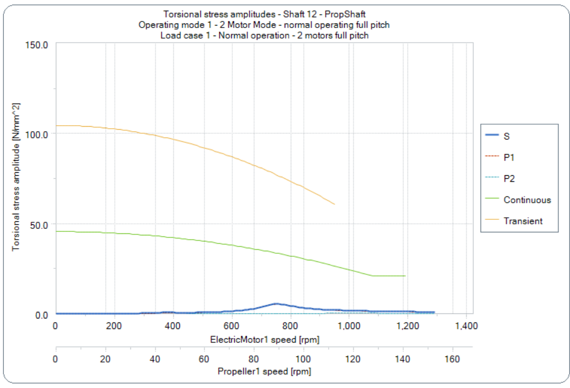

(a) Original diameter

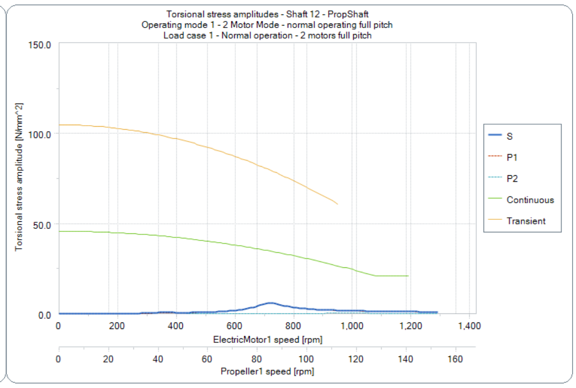

(b) Decreased 10 mm

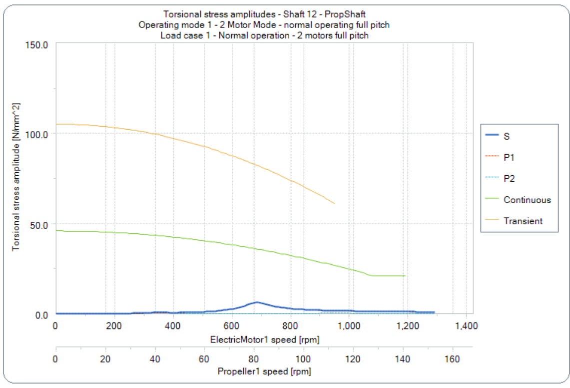

(c) Decreased 20 mm

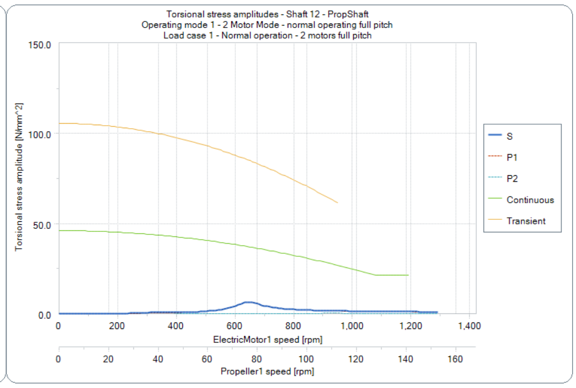

(d) Decreased 30 mm

Figure 4.24: *Propeller shaft torsional stress amplitudes, comparison of original diameter to -10mm, -20mm and -30mm decrease. IACS M68 torsional stress limits plotted also, as can be seen the stress levels are well below the limits.*

"Deflection is not affected by strength, but rather by stiffness as represented by the modulus of elasticity, which is essentially constant for all steels. For that reason rigidity cannot be contolled by material decisions, but only by geometric decisions" [5, p. 348].
From the behaviour of the shaft with decreased diameter it is suggested that the stiffness of the shaft influences mostly the torsional frequencies but not the actual strength of the shaft. Figure 4.24 shows no increase in stresses, but the harmonics occur at lower speeds. It was also noted that the natural frequencie of the whole system got lower.

Figure 4.25 compares the vibratory torque amplitudes in the flexible coupling for motor 1. The horizontal line at the top indicates the maximum elastic torque, 4.1 kNm. The limit is a manufacturers specification, from a torsional vibratory report authors had access to at BERG Propulsion.

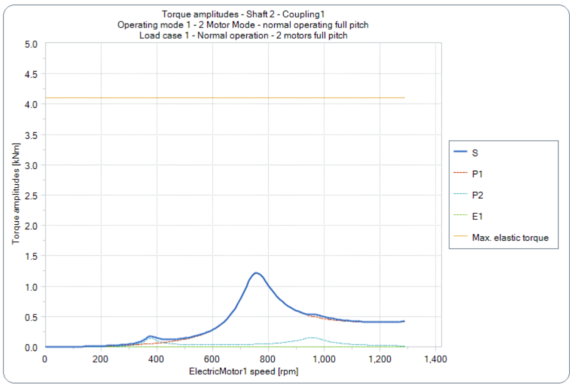

(a) Original diameter

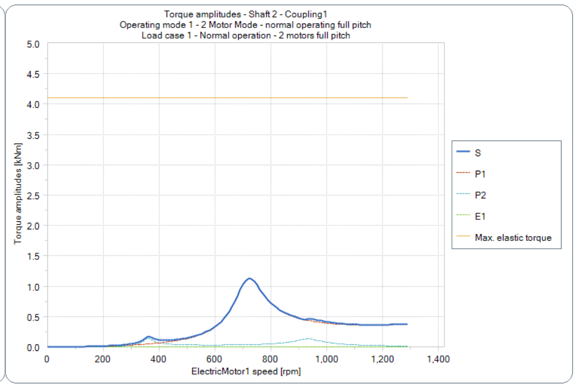

(b) Decreased 10 mm

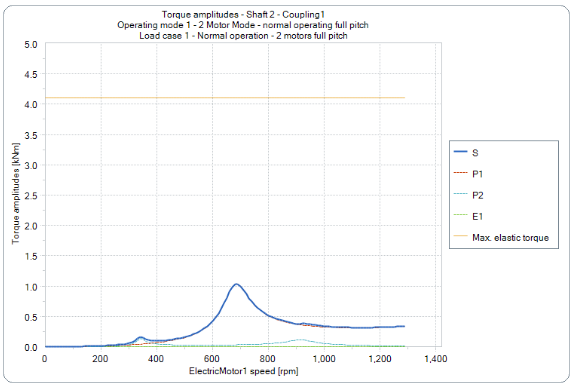

(c) Decreased 20 mm

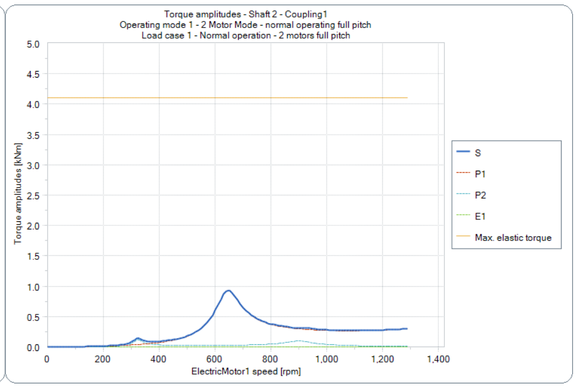

(d) Decreased 30 mm

Figure 4.25: *Vibratory torque amplitudes in motor coupling, comparison of original diameter to -10mm, -20mm and -30mm decrease. Limits for vibratory torque is set at 4.1 kNm.*

Figure 4.26 compares the heat dissipated, representing power loss in the flexible coupling for motor 1. The horizontal line at the top indicates the maximum heat dissipation of 0.480 kW. The limit is a manufacturers specification, from a torsional vibratory report authors had access to at BERG Propulsion. The heat builds in the coupling when the rubber elements flex under vibratory torque. The flexible coupling thus dampens the torsional vibrations but if the load becomes to much and the rubber element start to heat up, the rubber loses stiffness, gets softer and eventually can not support the torque and could fail. This is why for combustion engines it is important to investigate the load on the coupling under misfire condition. Misfiring is obviously not relevant for electric motors. This is the real cause of worry, not a power loss of 0.48 kW when transmitting 1250 kW.

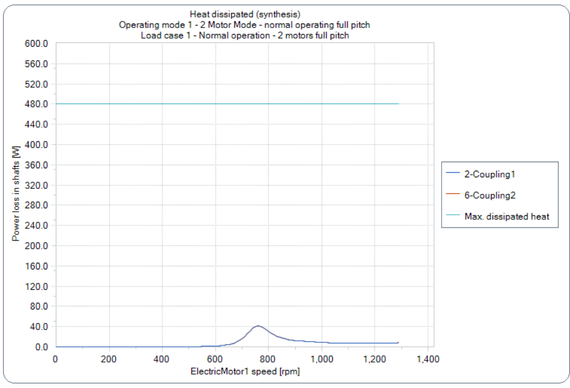

(a) Original diameter

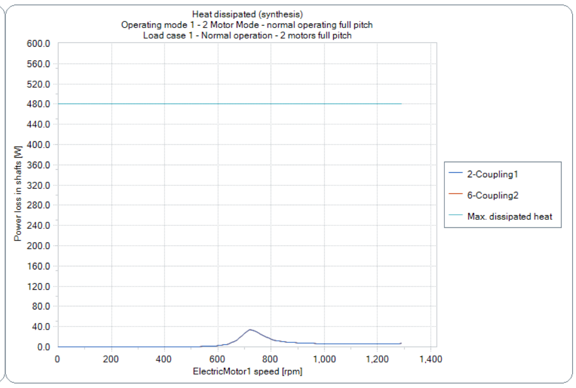

(b) Decreased 10 mm

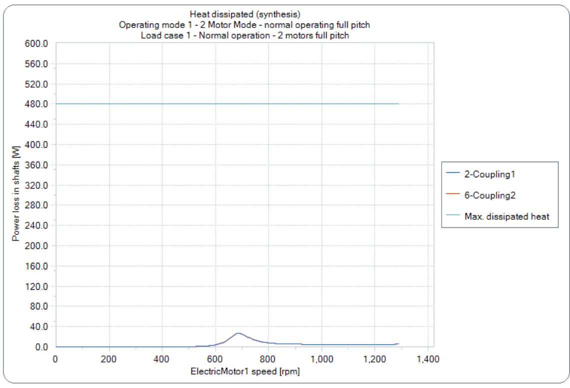

(c) Decreased 20 mm

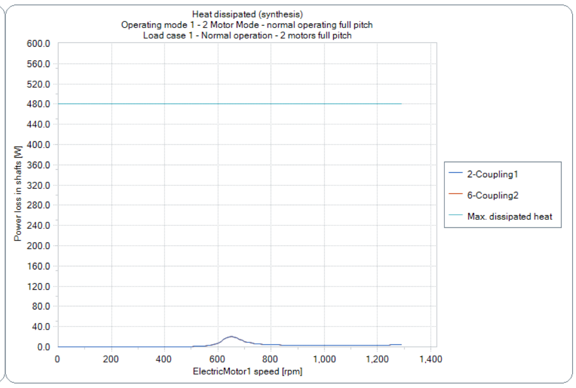

(d) Decreased 30 mm

Figure 4.26: *Heat dissipated in motor coupling, comparison of original diameter to -10mm, -20mm and -30mm decrease. Limits for heat dissipation or power loss is set at 0.480 kW.*

The results indicate that torsional vibrations are not so much a problem of strenght, rather a design challenge on a system level. The main thing is to know where harmonics occur and then the system can be modified in a way such that the shafting is not operating at bad speeds. Example from DNV class guidelines suggest for a 2 stroke system with vibration problems to decrease the diameter of the shaft to move the vibration excitation to lower speeds away from the operating speed [10, p. 65]. This result is also supporting why the natural frequency of the RoPax shaftline was so low, because the stiffness value defined for a mistake represented a input shaft having diameter of about 13mm instead of 310 mm. The above study has demonstrated the effects of decreased diameter of the shafting, which mostly affects the stiffness of the propulsion system. The shaft does not have high inertia compared to the propeller, in this case the propeller shaft has inertia of about 40 kgm^2 compared to the propeller's 4000 kgm^2 with the added entrained water. In appendix C.4 a comparison of how different propeller inertia affects the flexible coupling loads can be seen.

4.2.4.3 Dredger

The Dredger is a twin screw vessel with fixed pitch shrouded propellers. For the analysis only on of the shafting is considered, the starboard and portside are identical. Two running conditions are considered, free running and dredging.
This is due to the fact that the vessel has fixed pitch propellers and the propeller curves, hence the power curve are different between the operation profiles.

4.2.4.3.1 Free running empty condition The free running condition would be when the dredger is sailing with empty dredging material cargo holds.

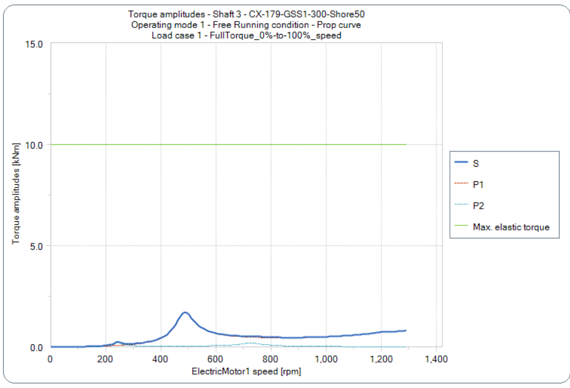

(a) Original diameter

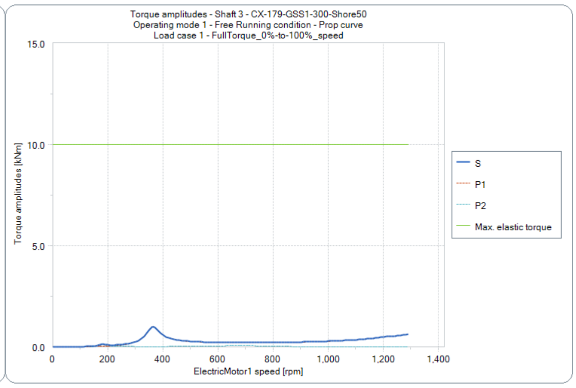

(b) Decreased

Figure 4.27: *Vibratory torque amplitudes in motor coupling, limits for vibratory torque is set at 10 kNm.*

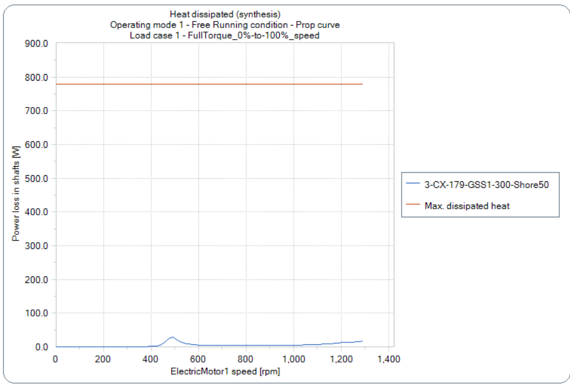

(a) Original diameter

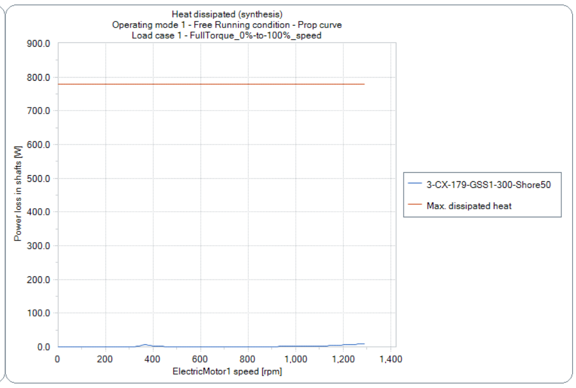

(b) Decreased

Figure 4.28: *Heat dissipated in motor coupling, limits for heat dissipation or power loss is set at 0.780 kW.*

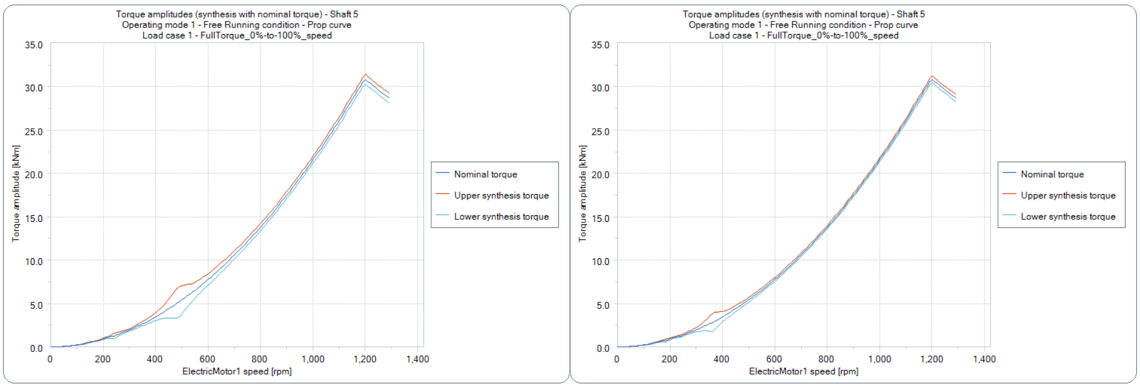

(a) Original diameter **(b)** Decreased

Figure 4.29: *Nominal torque in main gear with upper and lower torque synthesis. The alternating torque demonstrated by the upper and lower synthesis are showed to be small for the whole speed range.*

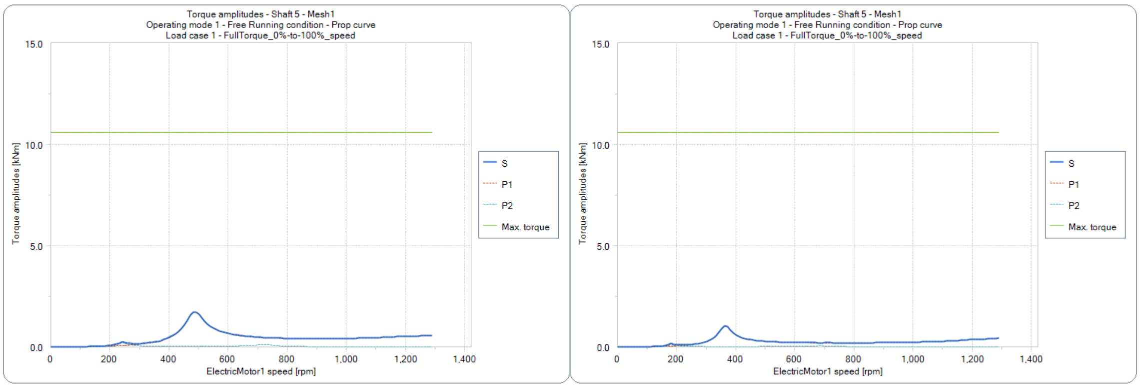

(a) Original diameter **(b)** Decreased

Figure 4.30: *Torque amplitudes in the main gear meshing. Excessive alternating torque in the messing indicates gear hammering, this would result in high forces on the gears and shorter life. The results show torque well within limits.*

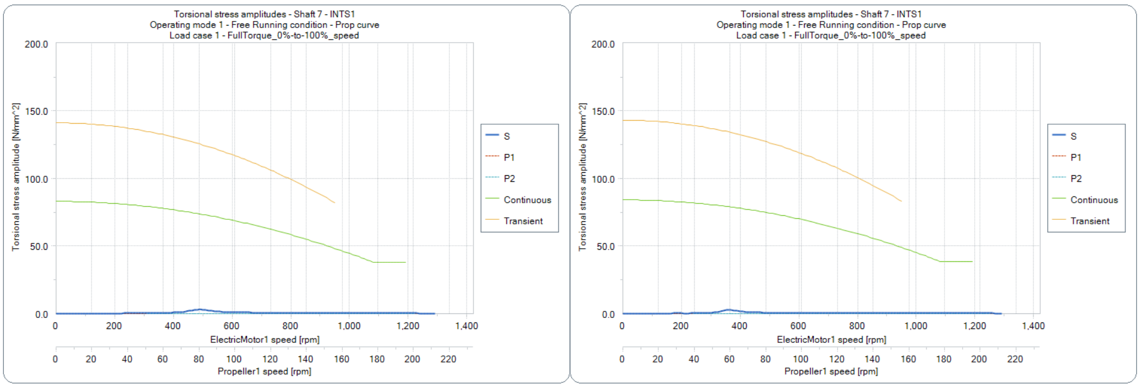

(a) Original diameter **(b)** Decreased

Figure 4.31: *Intermediate shaft torsional stress amplitudes, IACS M68 torsional stress limits plotted also, as can be seen the stress levels are well below the limits.*

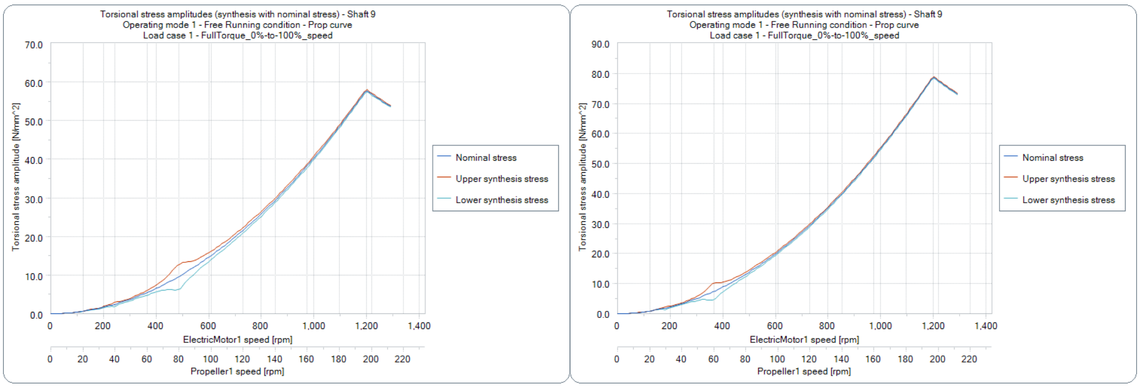

(a) Original diameter **(b)** Decreased

Figure 4.32: *Propeller shaft nominal torsional stress with upper and lower alternating stress synthesis.*

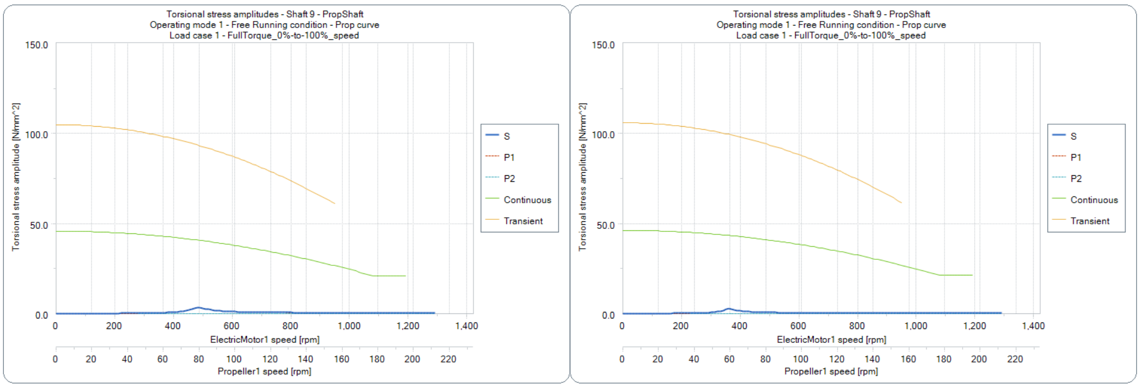

(a) Original diameter

(b) Decreased

Figure 4.33: *Propeller shaft torsional stress amplitudes, IACS M68 torsional stress limits plotted also, as can be seen the stress levels are well below the limits.*

4.2.4.3.2 Dredging condition Dredging condition is when the dredger has sand and mud in the cargo hold and has the dredging head and pumping pipe down. Dragging the dredging digger head along the bottom. More of a bollard pull condition.

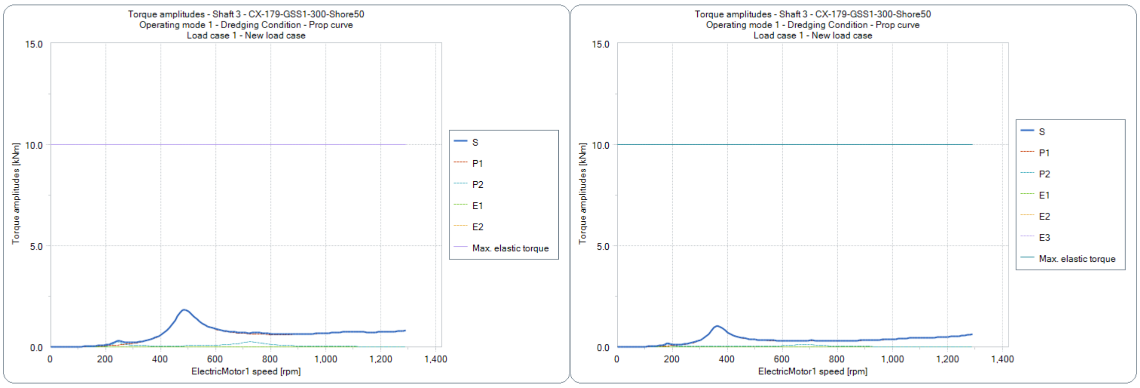

(a) Original diameter

(b) Decreased

Figure 4.34: *Vibratory torque amplitudes in motor coupling, limits for vibratory torque is set at 10 kNm.*

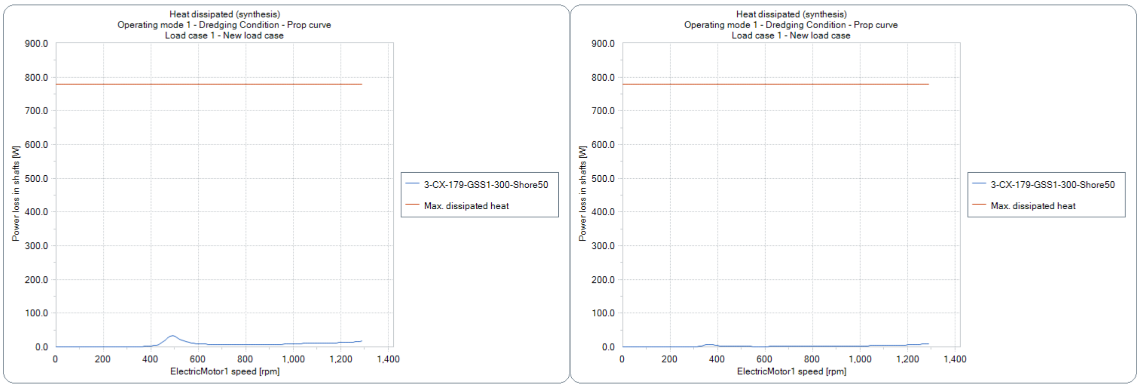

(a) Original diameter

(b) Decreased

Figure 4.35: *Heat dissipated in motor coupling, limits for heat dissipation or power loss is set at 0.780 kW.*

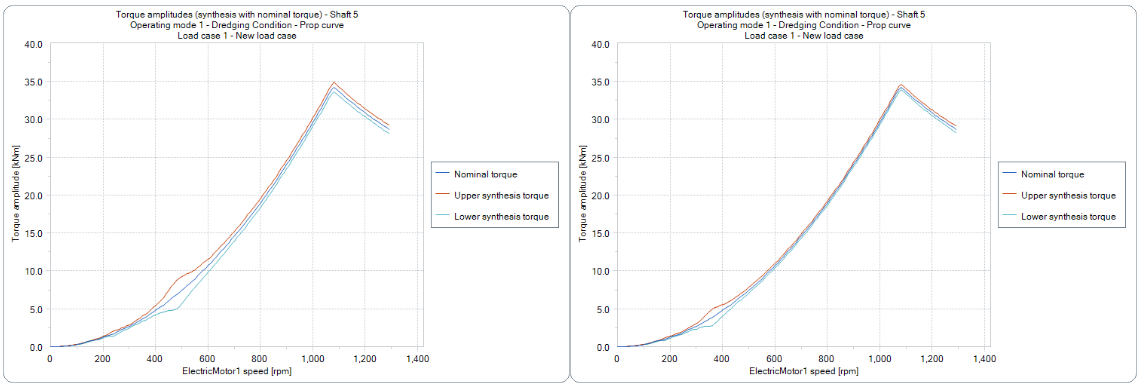

(a) Original diameter

(b) Decreased

Figure 4.36: *Nominal torque in main gear with upper and lower torque synthesis. The alternating torque demonstrated by the upper and lower synthesis are showed to be small for the whole speed range.*

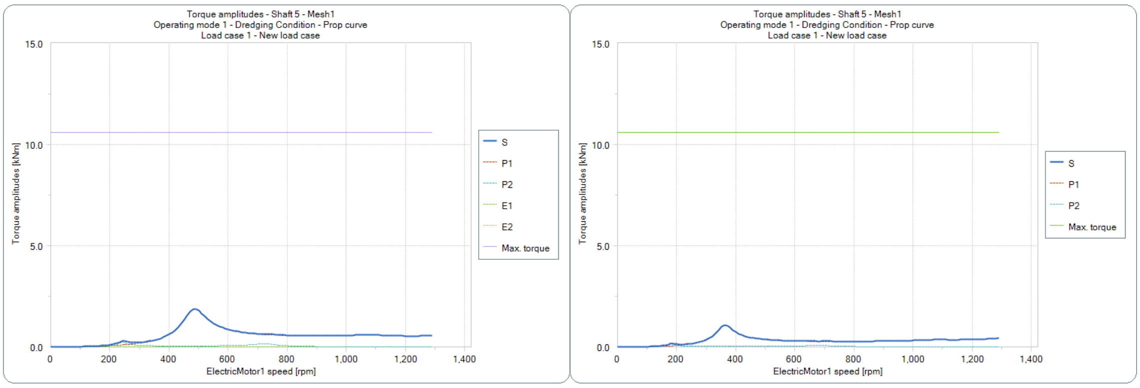

(a) Original diameter **(b)** Decreased

Figure 4.37: *Torque amplitudes in the main gear meshing. Excessive alternating torque in the messing indicates gear hammering, this would result in high forces on the gears and shorter life. The results show torque well within limits.*

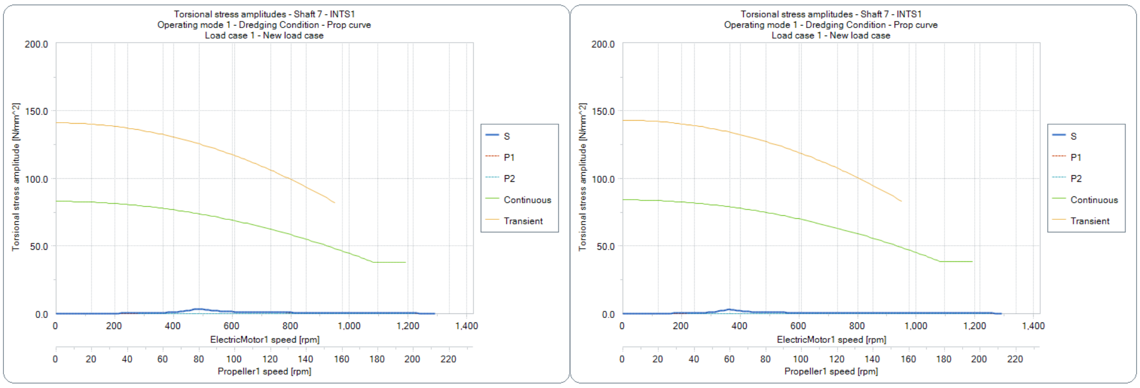

(a) Original diameter **(b)** Decreased

Figure 4.38: *Intermediate shaft torsional stress amplitudes, IACS M68 torsional stress limits plotted also, as can be seen the stress levels are well below the limits.*

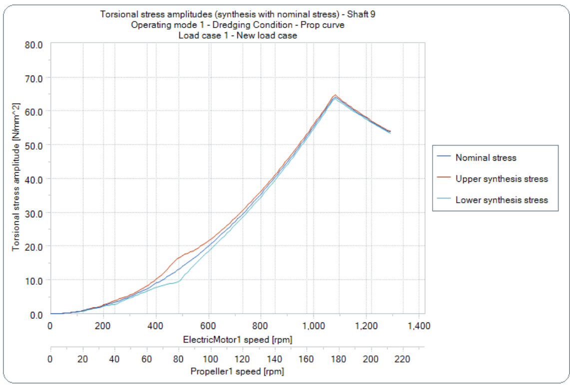

(a) Original diameter

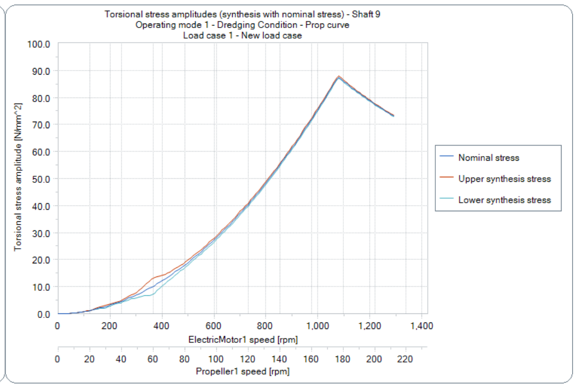

(b) Decreased

Figure 4.39: *Propeller shaft nominal torsional stresses plotted with upper and lower alternating stress synthesis.*

This shows the scale of the alternating torsional stresses in comparison to the nominal torque. The alternating stresses appear at low speed, but are mild. This could be something to have in mind if the vessel had diesel engine coupled to the propeller because this speed range could be the idling speed of the engine. Also because this vessel has fixed pitch propeller it would be worse to dwell on this speed. With CP propeller one usually would rev quickly through any bad speed ranges with low pitch. Since the dredger uses electric motor there is no idling speed, but it could be advisable to limit sailing time on this speed. Overall though the stress amplitudes are very low and well under recommended limits therefor this would not be considered a reason for any actions. There are almost no alternating stresses at operating speeds.

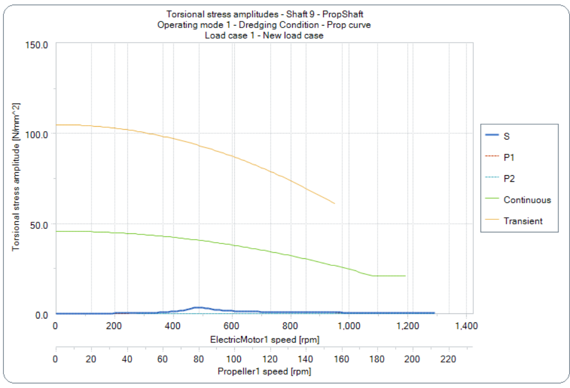

(a) Original diameter

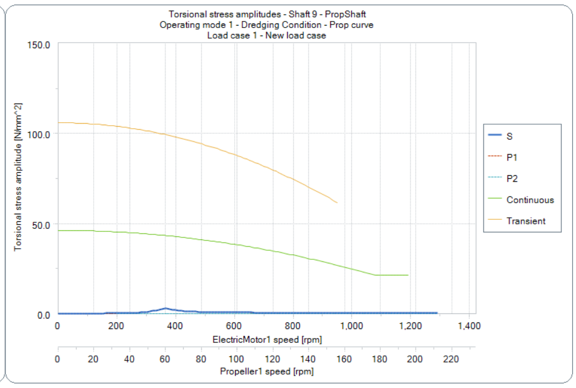

(b) Decreased

Figure 4.40: *Propeller shaft torsional stress amplitudes, IACS M68 torsional stress limits plotted also, as can be seen the stress levels are well below the limits.*

5
Future work

When work commenced for this project, the literature study suggested the torsional vibration behaviour of the shafting would be the critical case to study. During briefing meetings and discussions with propulsion experts at Berg Propulsion this was also suggested to be the limiting factor, especially in the case of the IACS M68 unified requirements. It was however pointed out by Berg Propulsion rotor dynamics experts that in majority of cases the shaft line solutions included medium or high speed engines connected to a reduction gear. For a geared plants the torsional vibrations are realized in the flexible couplings and can affect the gear with gear hammering. Since flexible couplings can be ordered with specific damping stiffness behavior, the systems can most often be tuned in accordance to torsional vibration calculation results.

5.1 More thorough alignment investigation

During the process of this work the shaft alignment analysis was found to be a more limiting factor for the dimensioning of the shafts. For torsional vibrations decreasing the diameter of the shafting caused no problem, except when considering ice loads. However considering the bearing loads and whirling in alignment analysis the first whirling frequency was just above the operating speed of the shaft for two cases. Thus making even a small decrease in diameter problematic. Since this first mode of vibration was related to the overhang bending load of the propeller weight it is not an easy fix to just add an extra intermediate bearing to tune the vibration mode, as could have been the case for whirling in intermediate shafts. As an extra challenge the bearing slope in the aft stern tube bearing reaches classification limits and lubrication becomes a challenge. All above suggest further detailed study for the shaft alignment as a limiting factor in the dimensioning of a propeller shaft.

5.2 Propeller failure load criteria

The project was to go around the IACS M68.4 formula and push the classification rules to the limit, which in theory was done with a typical shaft. But applying the propeller failure load criterion (section 2.4.2.1 and method in 3.3.1) on top of the improved method results that the comprehensive approach that had been done is in vain, it is useless. Because the propeller failure load criteria will always result in a larger diameter than going through all the hassle of defining the diameter based on

DNV CG 0038 document (the improved method [10]). The chain is never stronger than the weakest link.
So there has to be more investigation done on this propeller failure load. The classification method that was followed in this study is simply more conservative than the DNV CG 0038 document.

5.3 More precise investigation of the case study

For a higher certainty an investigation on more parts and sections of the case study (the three shafts). In this thesis study, only two or three locations were examined and taken through the analysis steps. Though the most critical ones were chosen to rule out allowed diameter in the shaft sections around it, it can be that the next component next to the investigated section has a more critical design. Or the opposite, that a further investigation would result in a smaller shaft at some sections and lead to a more complicated optimal design.
If the whole shaft is designed in respect of this improved method this minor uncertainty will not apply.
With regards to the TVC study in Nauticus Machinery further study of the misfiring condition of a 4 stroke diesel engine would be beneficial to support further claims of torsional vibrations not to be a prominent problem in propulsion shafting using geared medium and high speed propulsion engines.
Shaft fatigue study using a multi-physics FEM software setting up load cycle history according to Section 5 in DNV guidelines, document DNVGL-CG-0038 would be a good starting point.

6

Conclusion

This report presents a generalized methodology for determining the diameter of low speed marine propulsion shafts, which aims to reduce weight in relation to current designs. With limited information, a shaft line needs to be dimensioned which is fit for purpose, fulfils class requirements as well as showing good vibrational behaviour. It is believed to be possible to step away from current methods and provide slimmer and more power-dense shaft lines. The writers evaluate an improved method to define the minimum shaft diameter.

The path and the goal to proceed from the initial method, using the IACS formula to an improved method is what defined the thesis work. Early on, the writers moved into two directions from the research of the initial background theory. One where the writers tried to improve and boldly trying to find a way around it. That lead to the determination of the "mimic formula". Which is an emulated mimic formula of the IACS formula, made for further understanding of the IACS M68 formula. The other path from the initial research was to come up with a new definition of a method to define the minimum shaft diameter. The "improved method" is mainly defined by three definitions, The DNV improved method (DNV CG-0038), and using computer software to define the shaft alignment (lateral vibrations) and TVC (torsional vibrations). Old finished Berg Propulsion orders were acquired to test the effect of the newly defined approach (case study investigation), to compare and see how much could have been saved in shaft material. In addition, an extra TVC investigation was performed on the case study shaft lines to analyse the vibrational behaviour of the shaft lines with incremental diametric changes. Finally, when the new shaft diameter approach was achieved, showing promising results, the approach was defined in a step by step guide for a user to utilise. See in figure 6.1, a flow-cart of the work from the initial formula to the final method.

The results of the TVC simulation analysis suggest that for the simulated shaft lines the dimensions are on the safer side and quite reservative.

Though the *mimic formula* of the IACS M68.4 formula looks right and are good results in the study, it does not in fact change anything in the whole investigation of the improved method. It just gave the writers an inside into the current formula that BERG uses today(or at the time this was written). This separate study was done in request from the company. There are great possibilities that the writers approach of the formula is not like the approach that IACS experts did when they formulated theirs, but it is a trial of an approach to that rule.

The same goes with the investigation on the stress concentration factor of the IACS formula. It was a separate investigation done on the IACS M68.4 to try to understand it better.

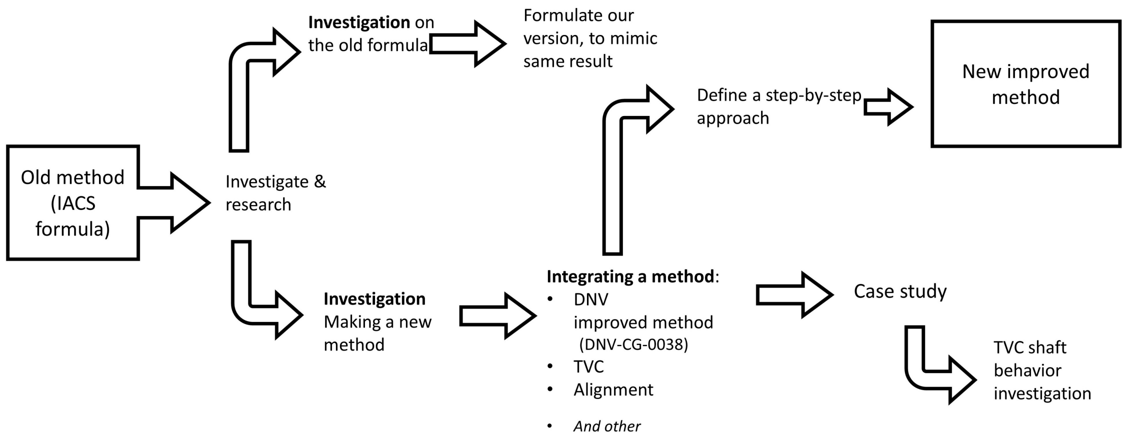

Figure 6.1: *Flow chart of the thesis process*

The improved method approach, which is mainly defined by the DNV CG-0038 document follows four different routes (as has been explained in the report, depending on est KA and bending moment). Though the three different vessels can not define a theory confirmation of a conclusion, it does though indicate that all of the four approaches do result in a similar outcome. It seems regarding the thesis result that the most conservative approach is to define the bending as 40% of the shaft torque and KA based on estimations (can be applied in the future use of the method).
If Berg Propulsion decides to integrate this method into their regular procedure and every time save around 8% in material weight, it is questionable how much is actually saved in material cost, due to the fact that whole axles are bought and cut down. Meaning, that one shaft piece that has different diameters and slopes is always dependant on the largest diameter of that piece as the initial bought raw steel axle. Answering the research question, how much room is there for weight/design optimisation. The simple answer is a weight optimization around 8%. But as said, it can not be equal in material cost saving.

The current method, using the IACS m68.4 formula is quick and simple, especially compared with the writers improved method. If Berg Propulsion decided to integrate it into their routine default procedure of designing a shaft line, the most probable solution would be to use (as stated here previously in conclusion) use estimated KA and bending moment (Mb). Since the method requires input values for the shaft component, the procedure could be as it is today, defining the shaft and other values using the ICAS formula, to support and acquire the input values to perform the "new improved method". Followed by TVC and alignment simulations, as it is already done today.

For the case study optimised dimensions, and the approval in terms of alignment and whirling. Since the classification expert has not looked over the data (at the time) it is not know for certain if all three shaft lines will be approved. To begin with, the Tanker vessel will most surely be approved, since it has gotten approval before, and the improved shaft has little to no whirling changes from the initial result. The RoPax result looks better than the initial one, for critical whirling. But for the initial (approved) one the critical speed is 14.6% from the MCR in mode shape 1, and for the improved shaft, the critical speed is 17.9% from MCR in mode 2, see the whirling graphs in appendix C.3. The first mode shape appears behind the propeller and the second mode shape between the bearings on the shaft, which is a problem. The regulations say the critical speed must be more than 20% from the MCR, but if it is within that and the whirling happens on the area aft of the stern tube (at propeller), the classification society does consider how much the propeller dampens the vibrations, and thus give exceptions for that. This statement is solely based on experience from BERG expert. Based on this statement the improved RoPax critical speed 17.9% from MCR can result in a problem because that is within the 20% and is not at the propeller, thus it must be considered that it will not get approval from the class. But with more experience using the alignment software, better adjustments and possibly moving and adding some bearing could solve this. The dredger is a difficult one to predict if the class will approve it, hence it must be consider and have in mind that it will not be approved.

*In general, the **improved method** will most surely be approved by class since all of the calculations and computation manoeuvres are all based on classification rules. Nothing is really defying or challenging the regulations, everything is in fact provided within different classification documents and softwares.*

References

[1] ABS (2019). *ABS Guidence notes on - Propulsion shafting alignment* (September 2019). American Bureau of Shipping, New York.

[2] Adnan, M. (2019). Retrieved 2021-03-15 from <https://www.researchgate.net/publication/333747137_A_Design_Approach_Against_Predictable_Fatigue_Failure_of_Airplane_Hydraulic_Pump_Shaft_in_Combined_Rotating_Bending_and_Torsional_Loading_Problem_Statement>

[3] The International Association of Classification Societies – IACS (2020). *Classification societies – what, why and how?*. Westminster, London, United Kingdom

[4] Batrak, Y. (2017). *Torsional vibration calculation issues with propulsion systems.* ShaftDesigner, c/o Machine Support B.V.

[5] Budynas, R. G., Nisbett, J. K. (2008). *Shigley's Mechanical Engineering Design* (8. ed.). McGraw-Hill.

[6] Caterpillar Inc. (2013, July 1). *CATERPILLAR TO ACQUIRE BERG PROPULSION, SIGNIFICANTLY EXPANDING CUSTOMER OPTIONS FOR ADVANCED MARINE POWER SOLUTIONS* Retrieved 2021-05-06 from https://www.caterpillar.com/en/news/corporate-press-releases/h/caterpillar-to-acquire-berg-propulsion-significantly-expanding-customer-options-for-advanced-marine-power-solutions.html

[7] Caterpillar Inc. (2013, September 1). *CATERPILLAR UNVEILS CAT® MARINE PROPULSION SYSTEMS, SUCCESSFULLY COMPLETES ACQUISITION OF JOHAN WALTER BERG AB* Retrieved 2021-05-06 from <https://www.cat.com/en_ZA/news/engine-press-releases/caterpillar-unveilscatsup174supmarinepropulsionsystemssuccessful.html>

[8] Caterpillar (2008). *MaK - VM43C Propulsion* (Issue September 2008). Caterpillar Motoren GmbH & Co. KG, Kiel.

[9] Department of Shipping and Marine Technology (2014) *Reliability Analysis of Marine Structuress SJO750* Division of Marine Design, CHALMERS UNIVERSITY OF TECHNOLOGY, Göteborg, Sweden 2014

[10] DNV-GL (2019). *Class Guidelines DNVGL-CG-0038, Calculation of shafts in marine applications* (Edition July 2019). DNV GL AS.

[11] DNV-GL (2018). *Rules for classification: DNVGL-RU-SHIP Pt.4,Systems and components* (Edition January 2018). DNV GL AS.

[12] DNV-GL (2020). *Rules for classification: DNVGL-RU-SHIP Pt.6,Additional class notations Chapter 6 Cold climate* (Edition July 2020). DNV GL AS.

[13] DNV-GL (2020). *User manual - Nauticus Torsional Vibration* (Version 14.3.0 - November 2020). DNV GL - Digital Solutions.

[14] DNV-GL (2020). *Rules for classification: DNVGL-RU-SHIP-Pt4Ch2 - Rotating machinery, general* (Edition July 2020). DNV GL AS.

[15] DNV-GL Digital Solutions (2018). *Nauticus Machinery - For marine propulsion design and analysis.* DNV GL - Digital Solutions.

[16] Dokkum, K. V, et.al (2016). *Ship Knowledge - Ship dsign, construction and operation* (9. ed). Dokmar Maritime Publishers B.V.

[17] Dowling, N. E. (2013)*Mechanical Behavior of Materials - Engineering Methods for Deformation, Fracture, and Fatigue* (4th ed). Pearson Education. Courier Westford, USA.

[18] EKBERG, A. (2018), *Multiaxial Fatigue Edition 5.3*, Department of Applied Mechanics, CHALMERS UNIVERSITY OF TECHNOLOGY Gothenburg, Sweden, 2018

[19] Geislinger GmbH (2021). *Geislinger damper - Tuned, torsional vibration damper.* Retrieved 2021-05-28 from <https://www.geislinger.com/en/products/product/damper>

[20] Gustaver, M. (2020) A Chalmers University of Technology Master's thesis template for LaTeX. Unpublished.

[21] IACS (2015). *UR M68 Dimensions of propulsion shafts and their permissible torsional vibration stresses - Rev.2 Apr 2015.* IACS - the International Association of Classification Societies and International Association of Classification Societies Limited.

[22] Inman, D. J. (2001). *Engineering vibration* (2. ed.). Prentice Hall.

[23] Korean Register (2020), *Rules for the Classification of Steel Ships Part 5 Machinery Installations*, 2020

[24] MAN Energy Solutions (2021). *A powerful portfolio: MAN B&W two-stroke propulsion engines.* Retrieved 2021-03-09 from <https://www.man-es.com/marine/products/two-stroke-engines>

[25] Murawski, L., & Charchalis, A. (2014). Simplified method of torsional vibration calculation of marine power transmission system. *Marine structures*, 39:335-349. ISSN 0951-8339, https://doi.org/10.1016/j.marstruc.2014.10.004.

[26] Polski Rejestr Statków (2021), *RULES FOR THE CLASSIFICATION AND CONSTRUCTION OF SEA-GOING SHIPS PART VI MACHINERY INSTALLATIONS AND REFRIGERATING PLANTS*, Gdansk 2021

[27] Russian Maritime Register of Shipping (2020), *FOR THE CLASSIFICATION AND CONSTRUCTION OF SEA-GOING SHIPS PART VII MACHINERY INSTALLATIONS*, Saint-Petersburg 2020

[28] Senjanović, I., Hadžić, N., Murawski, L., Vladimir, N., Alujević, N., & Cho, D.S. (2019). Analytical procedures for torsional vibration analysis of ship power transmission system. *Engineering Structures*, 178:227-244. ISSN 0141-0296, https://doi.org/10.1016/j.engstruct.2018.10.035.

[29] Sjöström, P.H. (2020, June 12). Berg Propulsion är tillbaka: Caterpillar Propulsion AB blir åter svenskägt och återfår namnet Berg Propulsion AB. *Sjöfartstidningen.* Retrieved 2021-05-06 from <https://www.sjofartstidningen.se/caterpillar-propulsion-far-ny-agare/>

[30] Sold by Cat, Berg Propulsion Returns to its Original Name. (2020, June 9). *THE MARITIME EXECUTIVE*. Retrieved 2021-05-06 from <https://www.maritime-executive.com/article/sold-by-cat-berg-propulsion-returns-to-its-original-name>

[31] Vulić, N., Dobrota, Đ., & Komar, I. (2016). Damping and excitation in the torsional vibrations calculation of ship propulsion systems. In Conference Proceedings, *Contemporary Issues in Economy & Technology* (CIET 2016), June 16th-18th 2016 (pp. S-165 - S-174). University of Split, University Department of Professional Studies. Split, Croatia.

[32] Wärtsilä (2021). *Wärtsilä Encyclopedia of marine technology*. Retrived on 2021-05-08 from <https://www.wartsila.com/encyclopedia/term/sterntube>

[33] Wärtsilä (2021). *Wärtsilä Encyclopedia of marine technology*. Retrived on 2021-05-08 from <https://www.wartsila.com/encyclopedia/term/propeller-shaft-tail-shaft>

[34] Wärtsilä (2021). *Wärtsilä Encyclopedia of marine technology*. Retrieved on 2021-05-08 from <https://www.wartsila.com/encyclopedia/term/intermediate-shafting>

[35] Winterthur Gas & Diesel Ltd (2021). *WinGD Company Overview* Retrieved 2021-03-09 from <https://www.wingd.com/en/about-wingd/wingd-company-overview/>

[36] Winterthur Gas & Diesel Ltd (2021). *World Record 12X92DF*. Retrieved 2021-03-09 from <https://www.wingd.com/en/engines/world-record-12x92df-en/>

A

Appendix-Screenshots

A.1 DNVGL-CG-0038 flowchart

See next full page.

Flow chart for Low cycle fatigue

Extra equations

$$\tau_0 = \frac{T_0 10^6}{W_t} = \frac{16\, d\, T_0\, 10^6}{\pi(d^4 - d_i^4)}$$

$$\tau_v = (K_{Anorm.} - 1)\tau_0$$

Can be used **ONLY** for gear plant

For direct coupled, use highest τv for the rpm range(see left graph at bottom). To do that

$$\tau_n = (\frac{n}{n_0})^2 * \tau_0$$

$$\tau_{max} = \tau_n + \tau_v$$

$$\lambda = \frac{n}{n_0}$$

Is it directly coupled or geard?

Direct coupled

$$\tau_{max} = (\tau + \tau_v)_{max}$$

Or $\tau max = \tau 0 \cdot K_{Aice}$ if that is greater

Geard

$$\tau_{max} = \tau_0 K_A$$

KA is the factor for different scenarios, ice, missfire and so on. Also check „extra equation in left corner“

Component Influence Factor (follow both paths, right and left)

$$K_L = 1 + f_L(\alpha_t, \sigma_y) + f_L(R_y, \sigma_B)$$

$f_L(R_y, \sigma_B)$

Ordinary steel or is it stainless- in salt water?

Ordinary

$$f_L(R_y, \sigma_B) = 10^{-4}(\sigma_B - 200)\log R_y$$

Stainless

$$f_L(R_y, \sigma_B) = 0.14 \log R_y$$

$f_L(\alpha_t, \sigma_y)$

To find out what αt to use look at tables on the right.

$$f_L(\alpha_t, \sigma_y) = (\alpha_t - 1)\frac{\sigma_y}{900}$$

Now for the given parameters the safety can be checked with given formula. Note! If yield is gotten from 0.2% proofstress, σy = 0.7 σb

$$\tau_{max} \le \frac{\sigma_y}{2SK_L}$$

Allowed stress factors can be seen in a table on flow chart „Flow chart direct coupled plant, high cycle fatigue”

If the shaft is also under reverse torque

Is it directly coupled or geard?

Coupled

$$\Delta\tau \approx (\tau + \tau_v)$$

$$\tau_{max} \approx (\tau + \tau_v) \text{ , and } \tau_{max\,reversed} = (\tau + \tau_v) \text{ ,}$$

$$\text{Then} \quad \Delta\tau = \tau_{max} + \tau_{max\,reversed} \text{ ,}$$

$$\text{equals} \quad \Delta\tau \approx 2 * (\tau + \tau_v)$$

Geard

$$\Delta\tau = \tau_0 \Delta K_A$$

To find out what αt to use look at tables on the right.

Other than that . The safety can be calculated with this formula, with selected parameters

$$\alpha_t \Delta\tau \le \frac{2\sigma}{S\sqrt{3}}$$

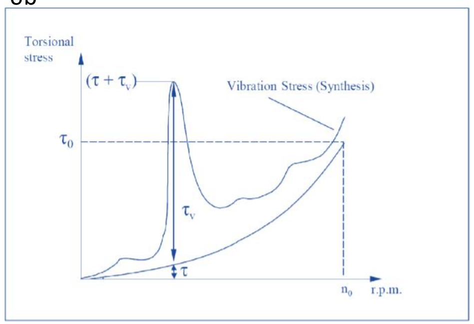

Typical torsion stress in shaft in direct couple plant

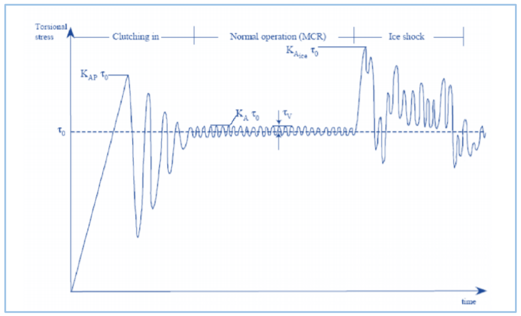

Typical geard shaft torsional stress amplitude with the relation to Ka

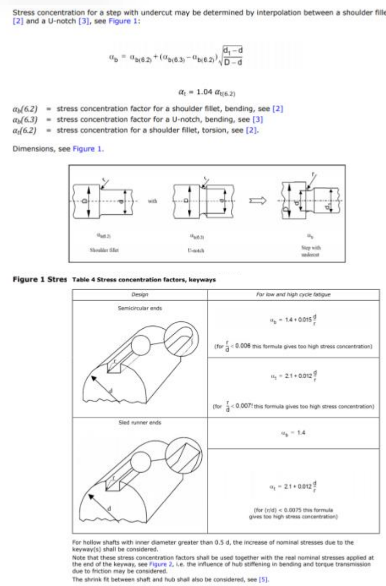

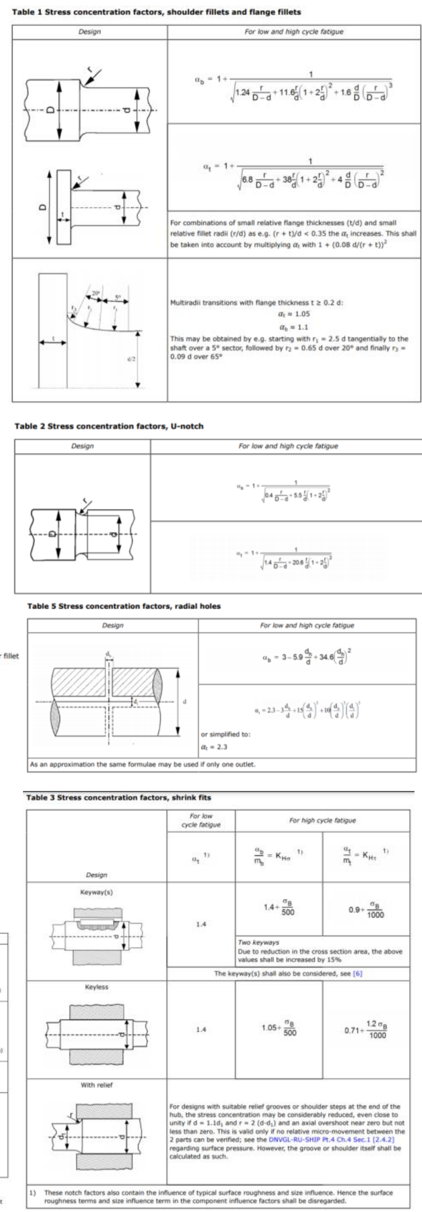

Flow chart for geard plant, high cycle fatigue

Safety is given with this formula. Follow all three paths for each variable(use τ max instructions from(Flow chart for Low cycle fatigue)

$$\left(\frac{\tau_v}{\tau_f}\right)^2 + \left(\frac{\sigma_b}{\sigma_f}\right)^2 \leq \frac{1}{S^2}$$

τv

For ice class: As long as the natural frequency of the "propeller versus engine"-mode is much lower than the propeller blade passing frequency (ratio < 50%): 0.5 τ_0 (K_{Aice} − 1), otherwise: $\tau_0\,(K_{Aice} - 1)$

$$\tau_v = (K_{Anorm.} - 1)\tau_0$$

Nominal vibratory torsional stress for continuous operation. This formula, unless a higher value applies below the full speed range (~90% to 100% engine speed).

σb

$$\sigma_b = \frac{32 * d * M_b * 10^6}{\pi(d^4 - d_i^4)}$$

Note. Mb is the rotating bending moment and is the moment created by alignment. The value can be zero (resulting in σb=0) I believe that it can be acquired from alignment software.

If the component under inspection is a shrink-fit (no notch) go to the right, else continue down.

Shrink fit (no notch)

KHτ and KHσ formulas have to be gotten from the table on the left (not the blue one).

If stainless steel

If stainless steel

Torsion: $K_{H\tau} = \boxed{f_{H\tau}(\alpha_t, m_t)} + \boxed{f_H(r)} + \boxed{f_{H\tau}(R_y, \sigma_B)}$

Bending: $K_{H\sigma} = \boxed{f_{H\sigma}(\alpha_b, m_b)} + \boxed{f_H(r)} + \boxed{f_{H\sigma}(R_y, \sigma_B)}$

r = notch radius, use r described for different component from tables on the left or shaft radius whichever is smaller. If r >100, 100 shall be used.

$$f_H(r) = 0.01\sqrt{r}$$

αt and αb can be found for different components in tables on the left. If the component is just a plain shaft, mt and mb = 1.

$$f_{H\tau}(\alpha_t, m_t) = \frac{\alpha_t}{m_t} \qquad m_t = 1 + \left(\frac{60}{\sigma_y} - 0.05\right)\sqrt{\frac{1}{r}}$$

$$f_{H\sigma}(\alpha_b, m_b) = \frac{\alpha_b}{m_b} \qquad m_b = 1 + \left(\frac{60}{\sigma_y} - 0.05\right)\sqrt{\frac{2}{r}}$$

For ordinary steels:

Torsion: $f_{H\tau}(R_y, \sigma_B) = 3 \cdot 10^{-4}(\sigma_B - 200)\log R_y$

Bending: $f_{H\sigma}(R_y, \sigma_B) = 4 \cdot 10^{-4}(\sigma_B - 200)\log R_y$

For stainless steel exposed to sea water:

Torsion and Bending: $f_{H\tau}(R_y, \sigma_B) = f_{H\sigma}(R_y, \sigma_B) = 0.35\log R_y$

τ is typically used as τ0.. Probably because that is the highest torsion experieced on nominal rpm for HCF yield strength or 0.2% proof stress limited to 0.7 σB.

$$\tau_f = \frac{0.24\,\sigma_y + 42 - 0.15\,\tau}{K_{H\tau}}$$

$$\sigma_f = \frac{0.4\,\sigma_y + 70 - 0.4\,\tau}{K_{H\sigma}}$$

At this stage, all variables ar known to calculate the safety for the given parrameters and set-up.

$$\left(\frac{\tau_v}{\tau_f}\right)^2 + \left(\frac{\sigma_b}{\sigma_f}\right)^2 \leq \frac{1}{S^2}$$

Material	Cycles[1]	
	$\approx 10^6$	10^9 to 10^{10}
Stainless steel I[2] (in sea water)	$\tau_f = \frac{105}{K_{H\tau}}$	$\tau_f = \frac{90}{K_{H\tau}}$
	$\sigma_f = \frac{165}{K_{H\sigma}}$	$\sigma_f = \frac{140}{K_{H\sigma}}$
Stainless steel II[2] and III[2] (in sea water)	$\tau_f = \frac{118}{K_{H\tau}}$	$\tau_f = \frac{97}{K_{H\tau}}$
	$\sigma_f = \frac{184}{K_{H\sigma}}$	$\sigma_f = \frac{150}{K_{H\sigma}}$

1) The number of cycles refers to those accumulated in the full load range. 10^9 is a suitable estimate for e.g. pleasure craft. 10^9 to 10^{10} should be used for ferries, etc.
2) Stainless steel I = austenitic steels with 16 to 18% Cr, 10 to 14% Ni and > 2% Mo with σ_B = 490 to 600 MPa and σ_y > 0.45 σ_B.
Stainless steel II = martensitic steels with 15 to 17% Cr, 4 to 6% Ni and > 1% Mo with σ_B = 850 to 1000 MPa and σ_y > 0.75 σ_B.
Stainless steel III – ferritic-austenitic (duplex) steels with 25 to 27% Cr, 4 to 7% Ni and 1 to 2% Mo with σ_B = 600 to 750 MPa and σ_y > 0.65 σ_B.
For other kinds of stainless steel, special consideration applies to fatigue values and pitting resistance, see DNVGL-RU-SHIP Pt.4 Ch.4 Sec.1 [2.2.4]

Allowed stress factors can be seen in a table on flow chart „Flow chart direct coupled plant, high cycle fatigue"

Table 4 Stress concentration factors, keyways

Design	For low and high cycle fatigue
Semicircular ends 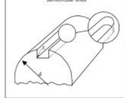	$\alpha_b = 1.4 + 0.015\frac{d}{r}$ (for $\frac{r}{d}$ < 0.006 this formula gives too high stress concentration)
	$\alpha_t = 2.1 + 0.012\frac{d}{r}$ (for $\frac{r}{d}$ < 0.007! this formula gives too high stress concentration)
Sled runner ends 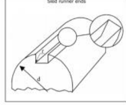	$\alpha_b = 1.4$
	$\alpha_t = 2.1 + 0.012\frac{d}{r}$ (for (r/d) < 0.0075 this formula gives too high stress concentration)

For hollow shafts with inner diameter greater than 0.5 d, the increase of nominal stresses due to the keyway(s) shall be considered.
Note that these stress concentration factors shall be used together with the real nominal stresses applied at the end of the keyway, see Figure 2, i.e. the influence of hub stiffening in bending and torque transmission due to friction may be considered.
The shrink fit between shaft and hub shall also be considered, see [5].

Table 1 Stress concentration factors, shoulder fillets and flange fillets

Design	For low and high cycle fatigue
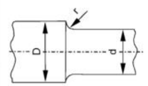	$\alpha_b = 1 + \frac{1}{\sqrt{1.24\frac{r}{D-d} + 11.6\frac{r}{d}\left(1+2\frac{r}{d}\right)^2 + 1.6\frac{d}{D}\left(\frac{r}{D-d}\right)^3}}$
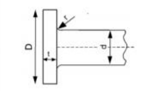	$\alpha_t = 1 + \frac{1}{\sqrt{6.8\frac{r}{D-d} + 38\frac{r}{d}\left(1+2\frac{r}{d}\right)^2 + 4\frac{d}{D}\left(\frac{r}{D-d}\right)^2}}$
	For combinations of small relative flange thicknesses (t/d) and small relative fillet radii (r/d) as e.g. (r + t)/d < 0.35 the α_t increases. This shall be taken into account by multiplying α_t with 1 + (0.08 d/(r + t))^2
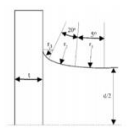	Multiradii transitions with flange thickness t ≥ 0.2 d: $\alpha_t \approx 1.05$, $\alpha_b \approx 1.1$. This may be obtained by e.g. starting with r_1 = 2.5 d tangentially to the shaft over a 5° sector, followed by r_2 = 0.65 d over 20° and finally r_3 = 0.09 d over 65°

Table 2 Stress concentration factors, U-notch

Design	For low and high cycle fatigue
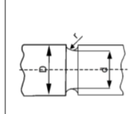	$\alpha_b = 1 + \frac{1}{\sqrt{0.4\frac{r}{D-d} + 5.5\frac{r}{d}\left(1+2\frac{r}{d}\right)^2}}$
	$\alpha_t = 1 + \frac{1}{\sqrt{1.4\frac{r}{D-d} + 20.6\frac{r}{d}\left(1+2\frac{r}{d}\right)^2}}$

Table 5 Stress concentration factors, radial holes

Design	For low and high cycle fatigue
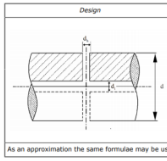	$\alpha_b = 3 - 5.9\frac{d_h}{d} + 34.6\left(\frac{d_h}{d}\right)^2$
	$\alpha_t = 2.3 - 3\frac{d_h}{d} + 15\left(\frac{d_h}{d}\right)^2 + 10\left(\frac{d_h}{d}\right)^2\left(\frac{d_i}{d}\right)^2$ or simplified to: α_t = 2.3
As an approximation the same formulae may be used if only one outlet.	

Table 3 Stress concentration factors, shrink fits

Design	For low cycle fatigue	For high cycle fatigue	
	α_t [1]	$\frac{\alpha_b}{m_b} = K_{H\sigma}$ [1]	$\frac{\alpha_t}{m_t} = K_{H\tau}$ [1]
Keyway(s) 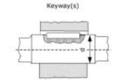	1.4	$1.4 + \frac{\sigma_B}{500}$	$0.9 + \frac{\sigma_B}{1000}$
		Two keyways Due to reduction in the cross section area, the above values shall be increased by 15%	
	The keyway(s) shall also be considered, see [6]		
Keyless 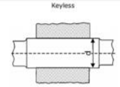	1.4	$1.05 + \frac{\sigma_B}{500}$	$0.71 + \frac{1.2\,\sigma_B}{1000}$
With relief 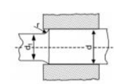	For designs with suitable relief grooves or shoulder steps at the end of the hub, the stress concentration may be considerably reduced, even close to unity if d = 1.1d_1 and r = 2 (d-d_1) and an axial overshoot near zero but not less than zero. This is valid only if no relative micro-movement between the 2 parts can be verified; see the DNVGL-RU-SHIP Pt.4 Ch.4 Sec.1 [2.4.2] regarding surface pressure. However, the groove or shoulder itself shall be calculated as such.		

1) These notch factors also contain the influence of typical surface roughness and size influence. Hence the surface roughness terms and size influence term in the component influence factors shall be disregarded.

Flow chart direct coupled plant, high cycle fatigue

Similar procedure to geared. But the major difference is that the ´τv´ Nominal vibratory torsional stress amplitude can not be calculated, thus the safety calculation goes the other direction. For a specific parameter setup and a certain safety factor the allowed vibratory stress can be calculated, called τvHC *Permissible high cycle torsional vibration stress amplitude.* For the rpm range.
(I guess in software, like Nauticus machinery, the vibrational behavior of the system can be plotted (blue graph) through the rpm range (0 to Shaft rotational speed at maximum continuous power, r.p.m (n0))

$$\left(\frac{\tau_v}{\tau_f}\right)^2 + \left(\frac{\sigma_b}{\sigma_f}\right)^2 \leq \frac{1}{S^2}$$

Use highest τv for the rpm range (n)
(Just the same as in LCF)

$$\tau_n = \left(\frac{n}{n_0}\right)^2 * \tau_0$$

$$\tau_{max} = \tau_n + \tau_v$$

Same steps to calculate KHτ and KHσ, as in „Flow chart for geard plant, high cycle fatigue“

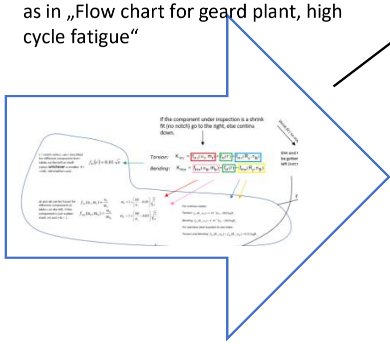

To analyze how the τvHC Permissible high cycle torsional vibration stress amplitude, is through the rpm range, we have to look at τv as a function.

$$\lambda = \frac{n}{n_0}$$

$$\tau_f(n) = \frac{0.24 * \sigma_y + 42 - 0.15 * \tau_0 * \lambda^2(n)}{K_{H\tau}}$$

$$\sigma_f(n) = \frac{0.4 * \sigma_y + 70 - 0.4 * \tau_0 * \lambda^2(n)}{K_{H\sigma}}$$

For the given parameters and safety the limit for continuous operation can be calculated (orange graph) to the Torsional vibration calculations (blue graph). The barred speed range section above the permissible torsional vibration.

$$\tau_v(n) = \tau_{vHC}(n) = \sqrt{\left(\frac{1}{S^2} - \frac{\sigma_b^2}{\left(\frac{0.4 * \sigma_y + 70 - 0.4 * \tau_0 * \left(\frac{n}{n_0}\right)^2}{K_{H\sigma}}\right)^2}\right) * \left(\frac{0.24 * \sigma_y + 42 - 0.15 * \tau_0 * \left(\frac{n}{n_0}\right)^2}{K_{H\tau}}\right)^2}$$

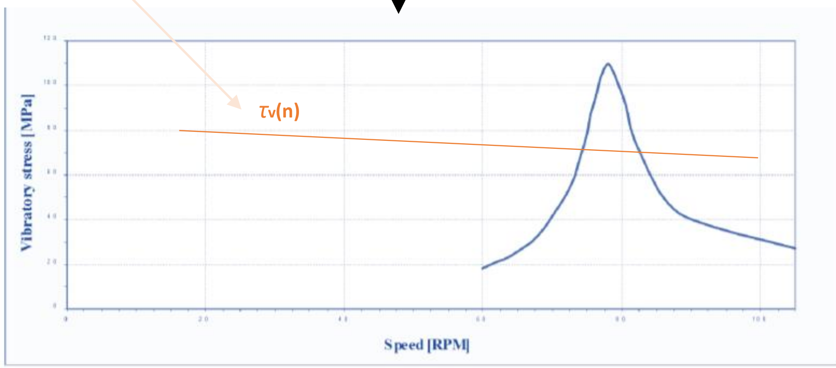

Torsional vibration stress from analysis of the shaft (blue) compared with the permissable torsional stress (orange) in respect of the parameters and specific safety for HCF. Continous opperation can not be above the permissable stress (orange). So the rpm width were the torsional vibration passes the permissable stress is the e barred speed range

Table 6 Shaft safety factors

Criteria	*Safety factor, S*
Low cycle ($N_C < 10^4$ stress cycles)	1.25
High cycle ($N_C >> 3{\cdot}10^6$ stress cycles)	1.6
Transient vibration when passing through a barred speed range: ($10^4 < N_C < 3{\cdot}10^6$ stress cycles)	Linear interpolation (logτ-logN diagram) between the low cycle, peak stresses criterion with S = 1.25 and the high cycle criterion with S = 1.5. For propeller shafts in way of and aft of the aft stern tube bearing, the bending influence is covered by an increase of S by 0.05.

A.2 Main instruction manual script

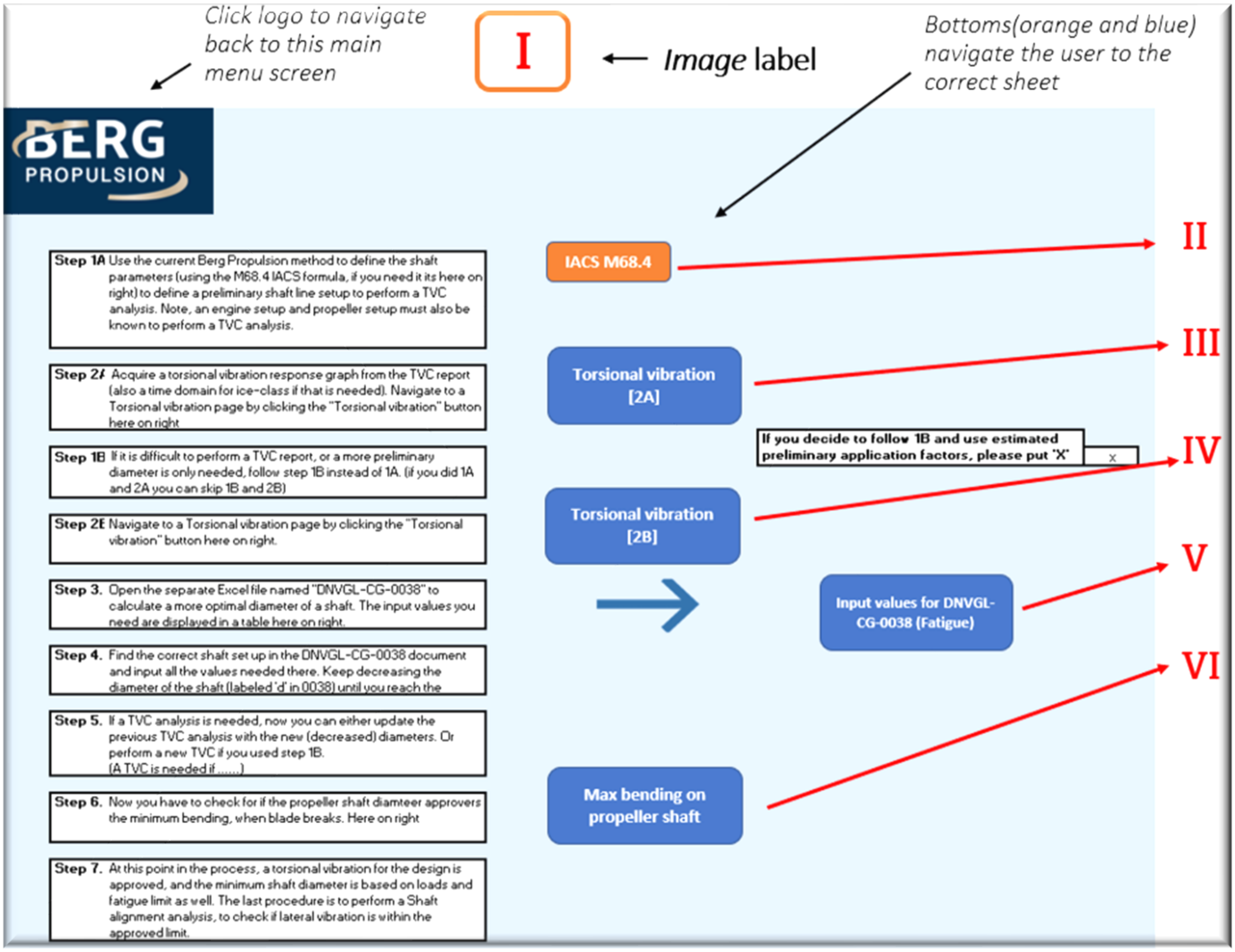

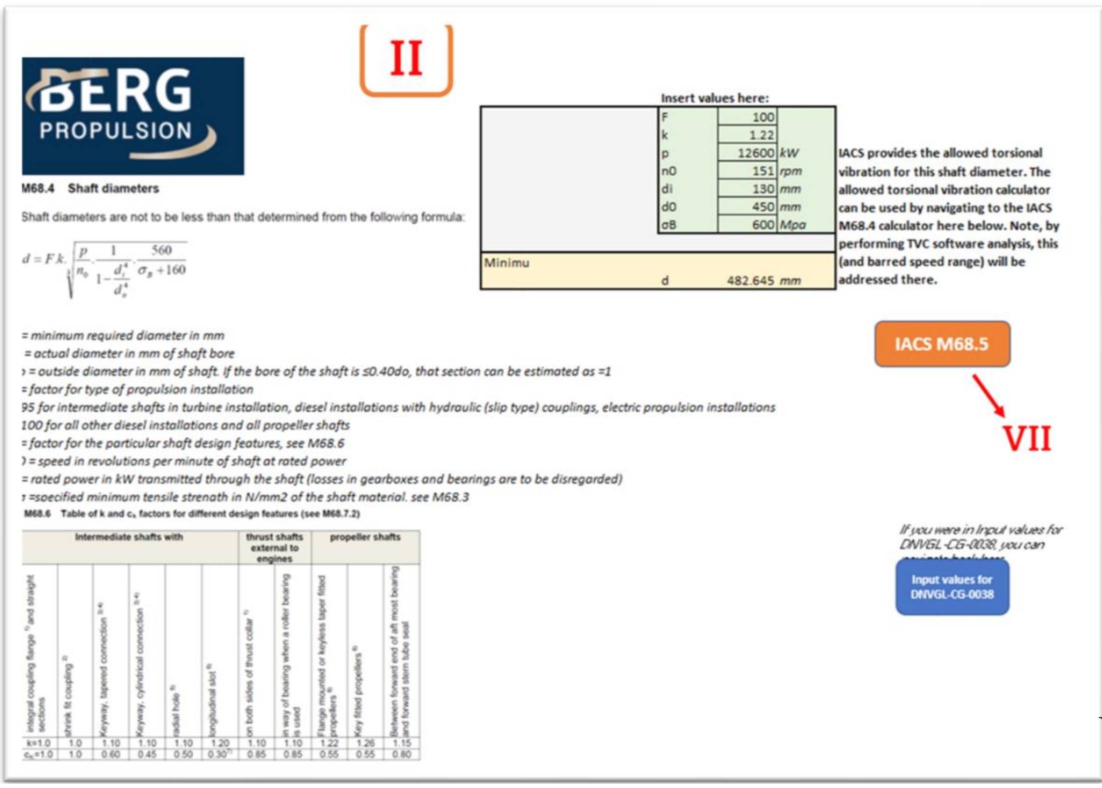

IV

BERG PROPULSION

Here you define more preliminary/conservative values for the application factors. Before you begin please mark the box here above. Please select the appropriate KA value from the table here on the left, and place the selected value in the box below.

An estimated value from DNV is said to be not less than 1.4. so KAP = 1.4 (or not more than 1.5)

Navigate to KA_ice sheet by clicking the button here on right. If no Iceclass. Leave Kaice = 1

System type KA	KA
Turbines and electric drives	1.1
Diesel engine drive system with fluid clutch between engine and gears	1.1
Diesel engine systems with highly flexible coupling between engine and gears	1.3
Diesel engine system with no flexible coupling between engine and gears	1.5
Generator drives	1.5

Table 2.2: *DNV definition for estimated application factor for different system setup*

Application factor	
KA norm	1.3
KAP	1.4
KAice	1.92

KA_ice calculator

VIII

15.5.3 Torsional design loads

15.5.3.1 Design ice torque on propeller Q_{max} for open propellers

Q_{max} is the maximum torque on a propeller during the service life of the ship resulting from ice/propeller interaction.

$$Q_{\max} = 10.9 \cdot \left(1 - \frac{d}{D}\right) \cdot \left(\frac{P_{0.7}}{D}\right)^{0.16} \cdot (n \cdot D)^{0.17} \cdot D^3 \text{ [kNm]}$$

when $D \leq D_{limit}$

VIII

BERG PROPULSION

These calculations are based on DNVGL-RU-SHIP Pt.6 Ch.6. Part 15.5.3 To estimate the application factor KA_ice, before or without performing TVC report. **This sheet is for open propellers.**

Fill in the input values, then proceed further down and fill in the correct values based on the three tables.

Note! Ie/It is the mass moment of inertia ratio between the propulsion side and engine side. This value can be calculated if the user has the data, using Mathcad - 6568MMOI.pdf.

Input value P_D = Pitch ratio at radius 0.7 at bollard condition, can be acquired from ProjCalc.

Is the propeller ducted or not? Please insert 'X' in the correct box:

Open:	
Ducted:	x

Please insert values here. Note D and d are the diameters of the propeller and hub:

Propeller	D	3.6	m
Hub	d	0.9	m
	P	2500	KW
	n	142	rpm
	P_D	1.24	
mass moment of inertia ratio	Ie/It	0.34	

k1_du_op	7.7
k2_du_op	14.6
D_lim	2.16
n_n	142
Qe_max	168.121
Qmax	455.9
Qpeak	323.137
KA_ice	1.92204

Move back to

Torsional vibration [2B]

Propeller type	*Rotational speed n*
CP propellers	n_n
FP propellers driven by turbine or electric motor	n_n
FP propellers driven by diesel engine	$0.85\ n_n$

Insert 1 or 0.85 in box here on right, accordingly to table on right 1

Table 19 Thickness of the design maximum ice block H_{ice} entering the propeller.

Ice class	Ice(1A*)	Ice(1A)	Ice(1B)	Ice(1C)
H_{ice}	1.75 m	1.5 m	1.2 m	1.0 m

Inster value of Hice from table on left Hice 1.2 m

Table 27 Default values for prime mover maximum torque Q_{emax}

Propeller type	Q_{emax}
Propellers driven by electric motor	Q_{motor}^{*}
CP propellers not driven by electric motor	Q_n
FP propellers driven by turbine	Q_n
FP propellers driven by diesel engine	$0.75\ Q_n$
$^{*}Q_{motor}$ is the electric motor peak torque.	

Insert 1 or 0.75 in box here on right, accordingly to table on right 1

V

BERG PROPULSION

Table 1.1

n	142	rpm
P	2500	kW
T0	168.12	kNm

Table 1.2

T0	168.12	kNm
Mb	67.24857	kNm

Here you get the provided input data for the DNVGL-CG-0038 calculator.

If you need to convert RPM and Power to Torque (T0), I recommend using the converter here in table 1.1.

If you do not have the rotating bending moment (which can be acquired from alignment), DNV provides a simple solution. Where the bending moment (Mb) can be estimated as 0.4*T0. Note in most cases the bending moment is neglectable in front of the forward stern bearing. Use table 1.2 if you want to do that.

Use this input data for the DNVGL-CG-0038 calculator

Surface roughness-mean	Ra	1.6	µm
Surface roughness (peak	Ry	9.6	µm
Torque max cont pw	T0	168	kNm
Rotating bending moment	Mb	67	kNm
	Ka norm	1.30	
	K missf	0	
	K ice	1.92	
	K(AP)	1.4	
	d0		mm
	di	90	mm

you decide if you want to us

The surface roughness is needed. If you do not know the surface roughness, DNV defines Ra to be, Ra< 1.6µm (Surface roughness-mean deviation of the profile) and Ry<1 µm (Surface roughness, peak to valley). According to DNV Ry~6Ra.

The diameter is not crucial to know since you are gonna define it in the DNVGL-CG-0038 calculator document, but it's good to know the approximate diameter of where to start the calculations, iterations. You can use IACS m68.4 to calculate the diameter to start with.

IACS M68.4

VI

BERG PROPULSION

After calculating the minimum shaft in respect of fatigue, the propeller shaft must fulfill the bending load befor the propeller breaks a blade. Either due to hitting ice or from grounding. DNVGL-RU-SHIP Pt.6 Ch.6 12.5.2

Here you calculate the minimum propeller shaft diameter, at the aft part and mid way. Most of the input values you have used here previusly. The new ones can be acquired from ProjCalc.

Insert values in green box

Blade failure load Fex

		Input*		
		d0	440	*mm*
		di	130	*mm*
Get from Proj calc	*Propeller diameter*	D	4.8	*m*
	Relative radius where to look at stress	r_R	0.35	*m*
	Chord length at r/R	c	1.017	
	Max thickness at r/R	t	0.166	
	Yield strength	Sigma_B	600	*N/mm^2*
	Ultimate strength	Simga_y	350	*N/mm^2*
		sigma_ref	395	

Sigma_ref	395	*Mpa*
r	0.84	
Fex	1537.45	*kNm*
D_aft	**443.2**	*mm*
D_mid	**351.7**	*mm*

A.3 DNVGL-CG-0038 document calculator

The user navigates to correct location (sheet) by clicking the blue buttons on each page.

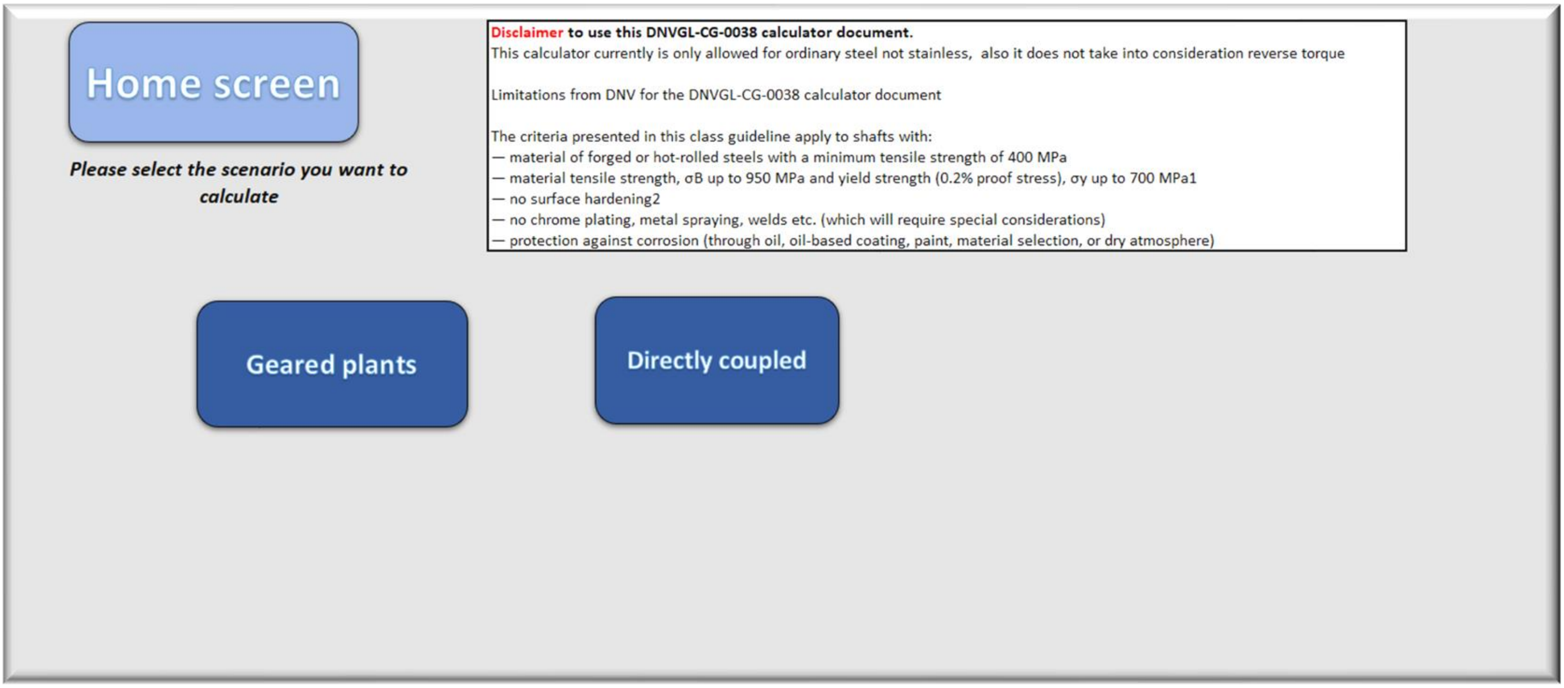

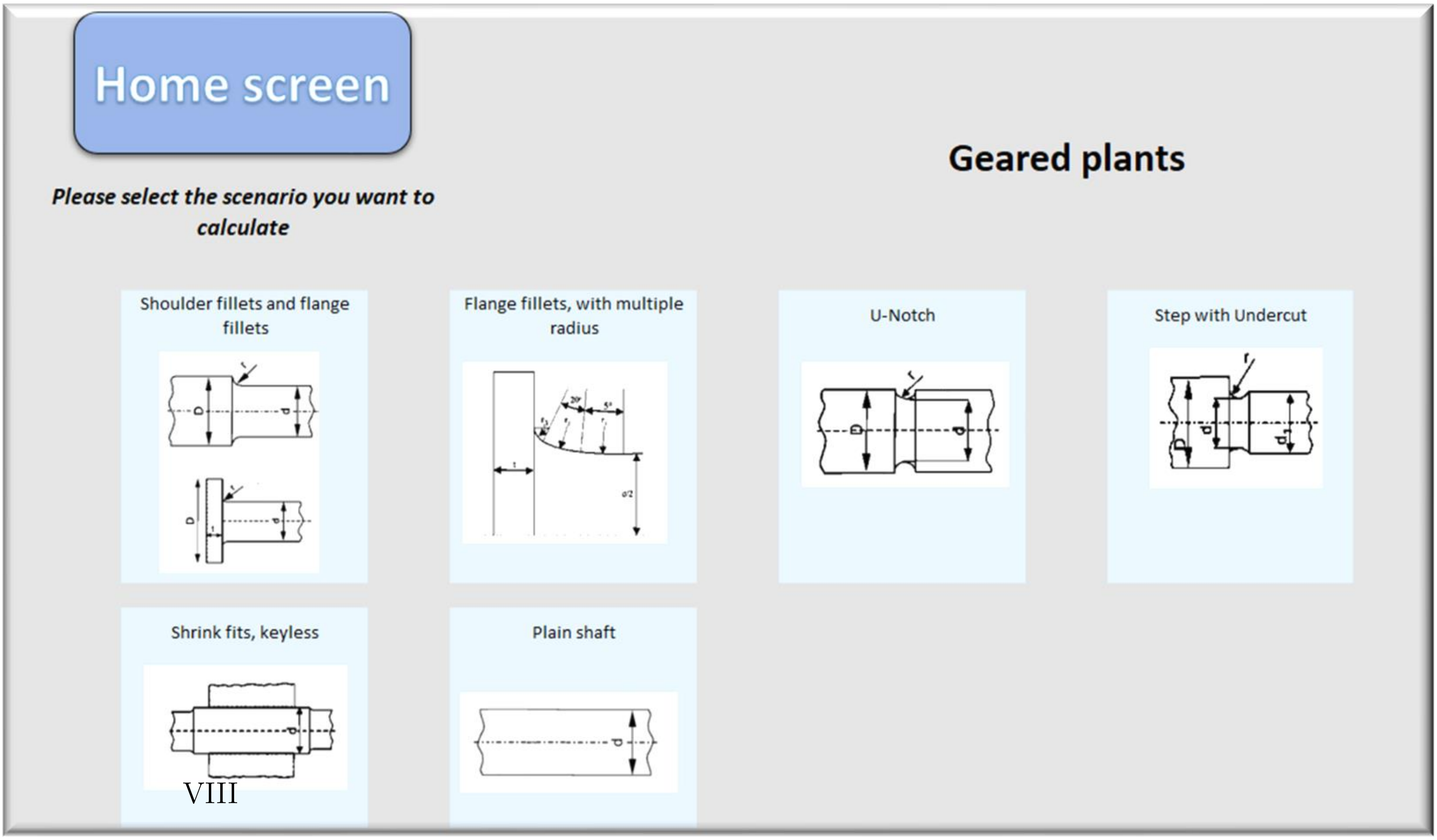

Geared – Step with undercut (with some input values)

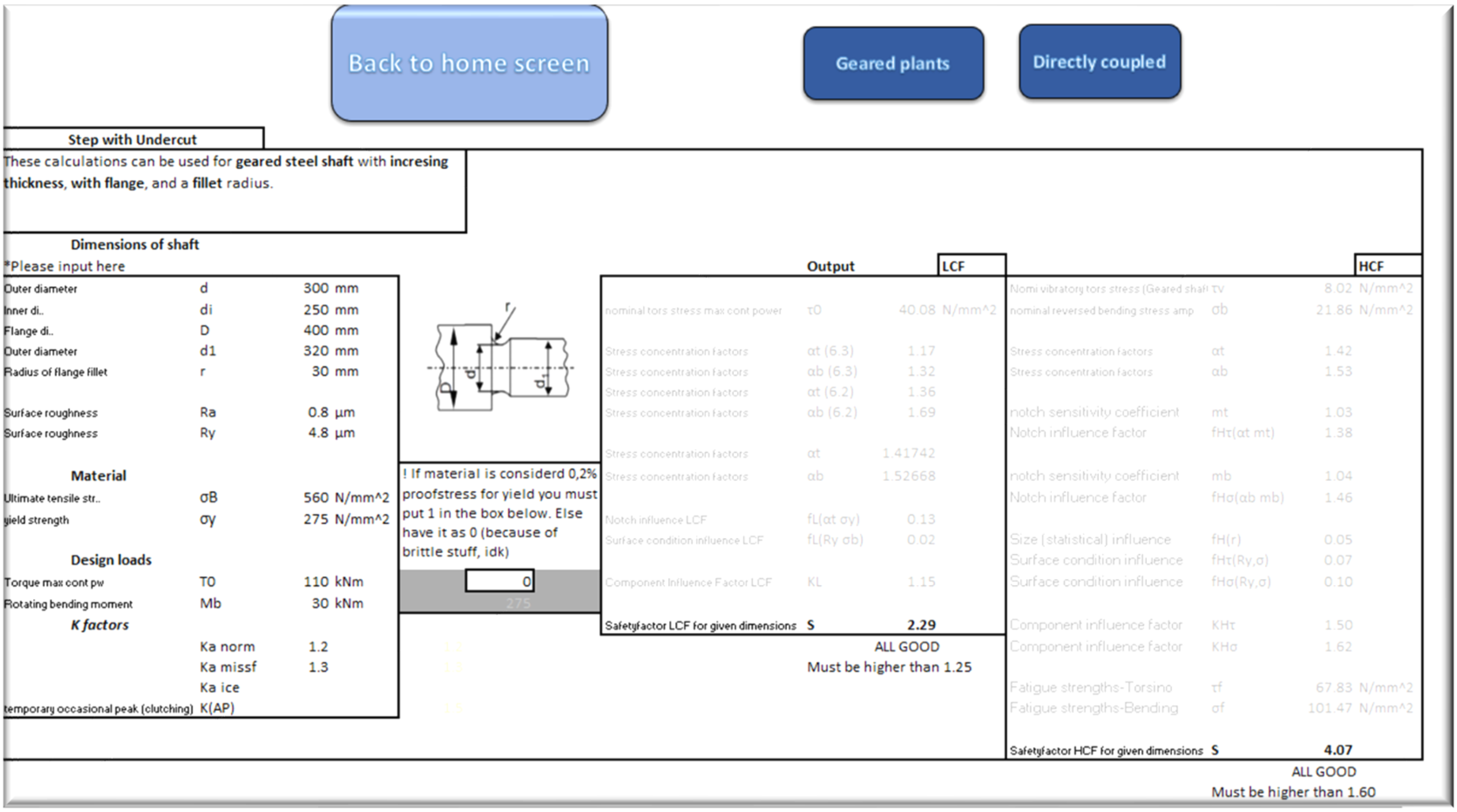

Geared - flange/fillet component (with some input values)

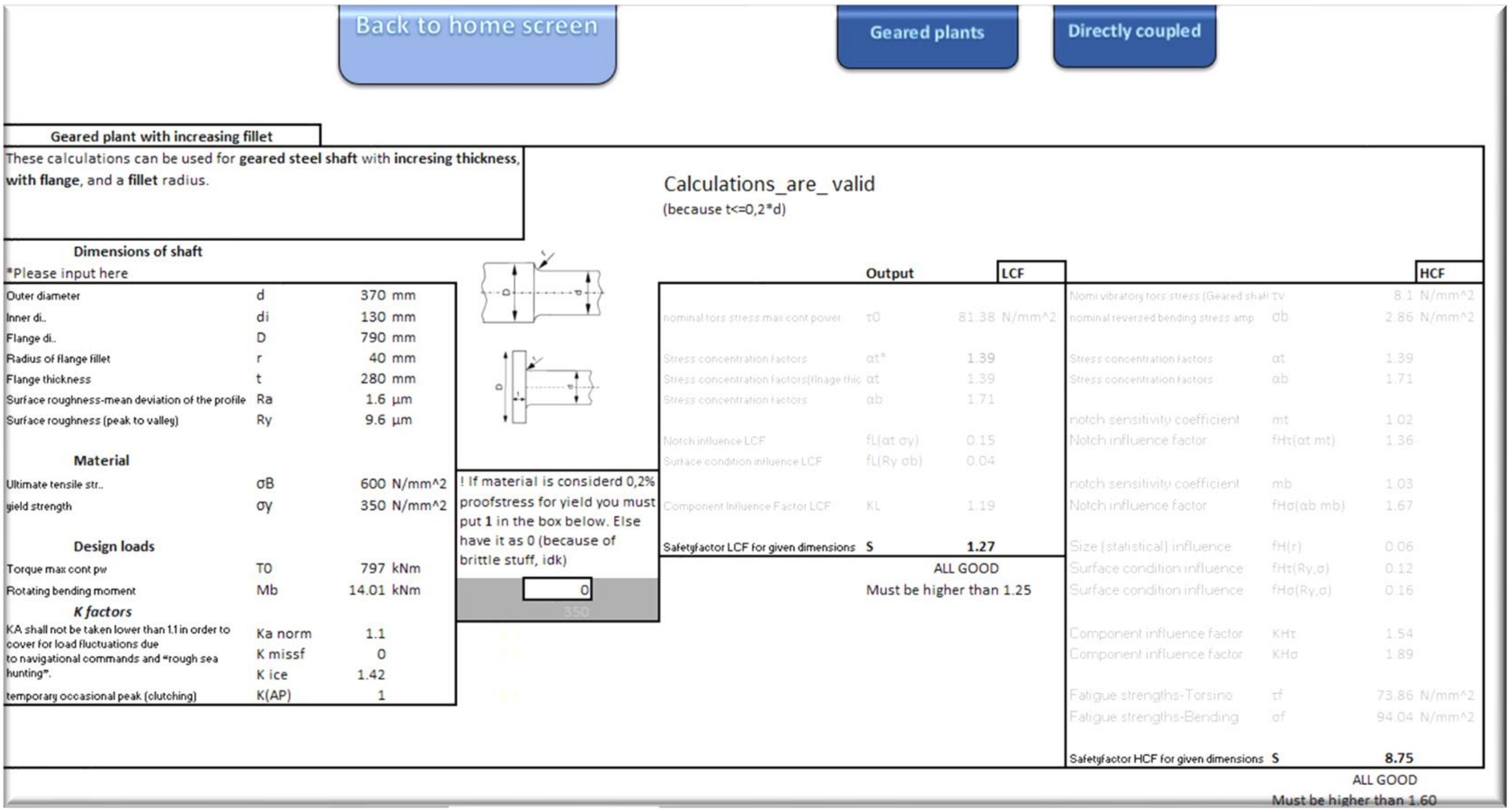

A.4 Shaft lines (without components) dimensions

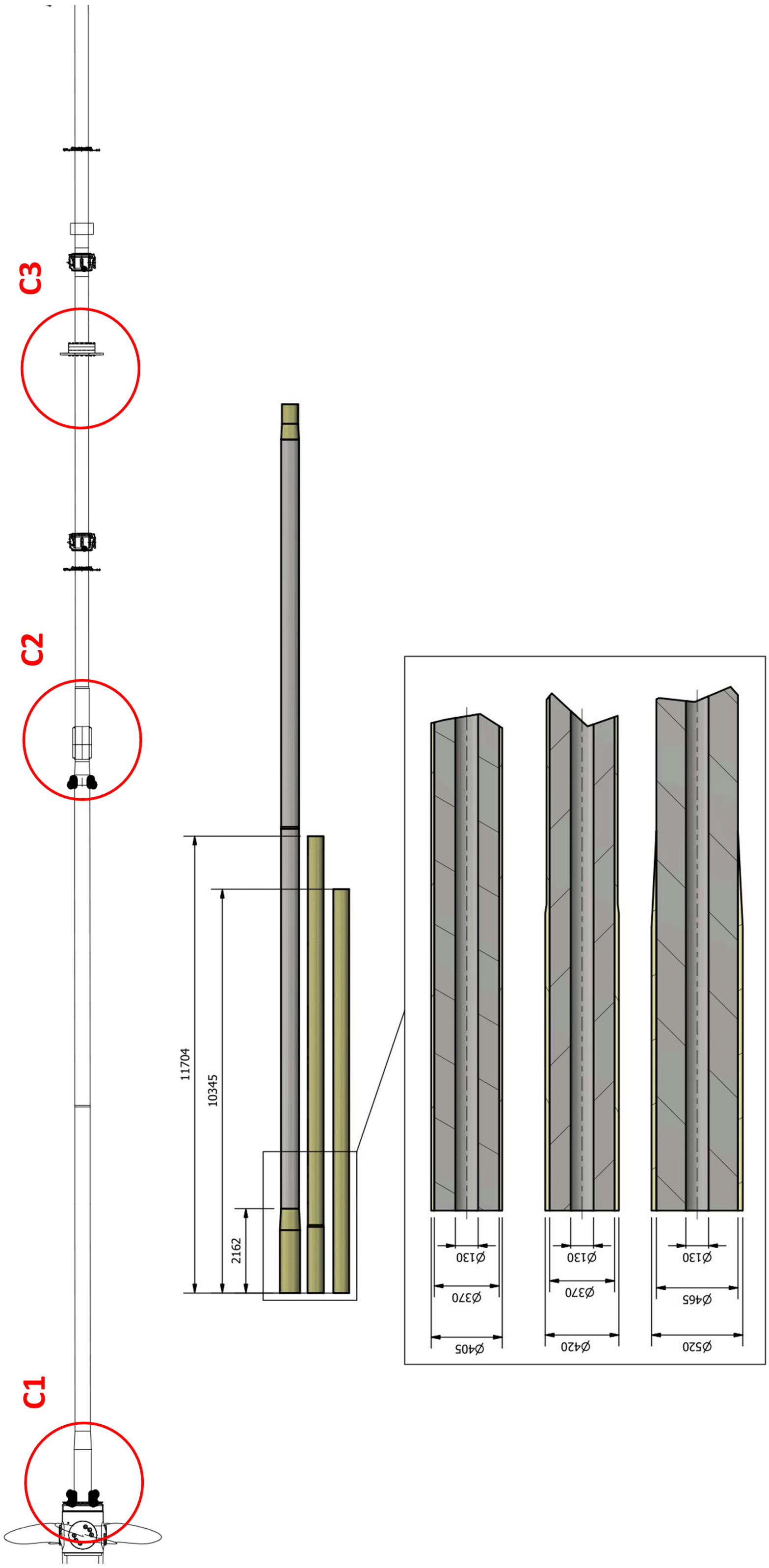

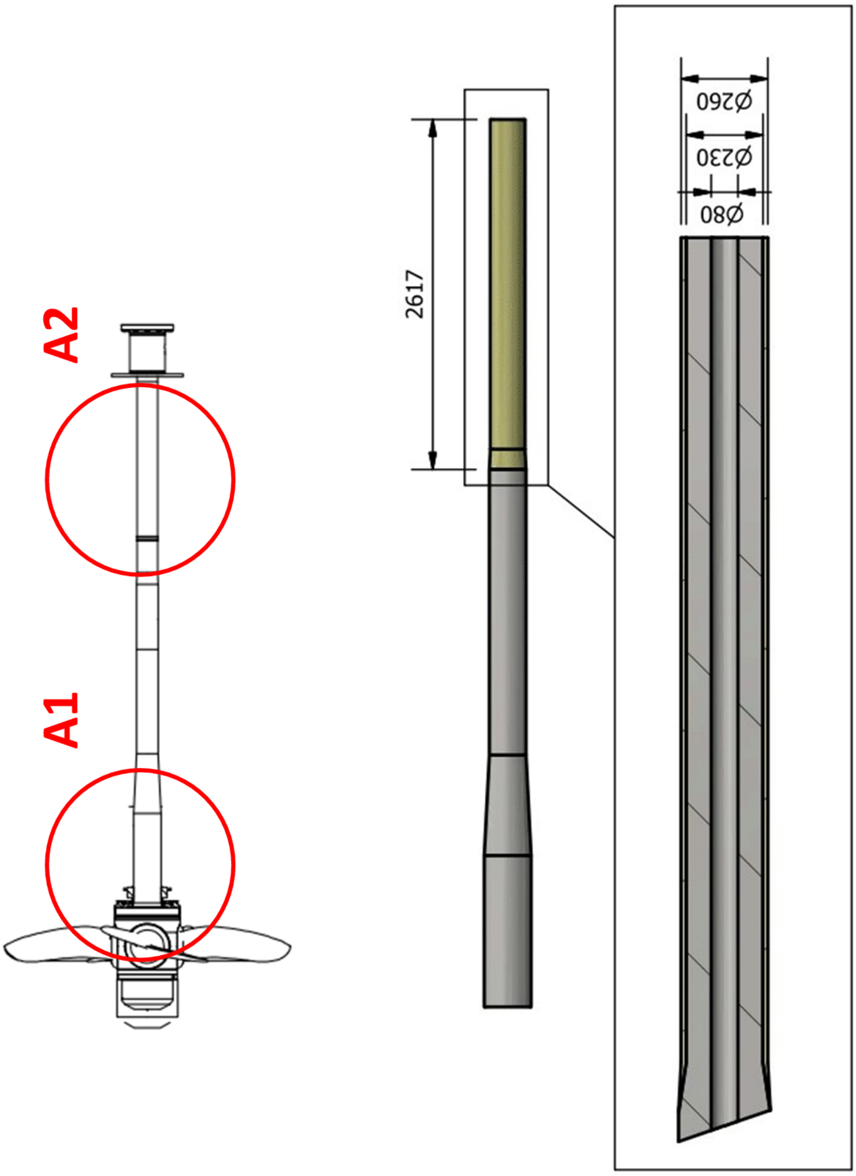
A2
A1
2617
Ø260
Ø230
Ø80

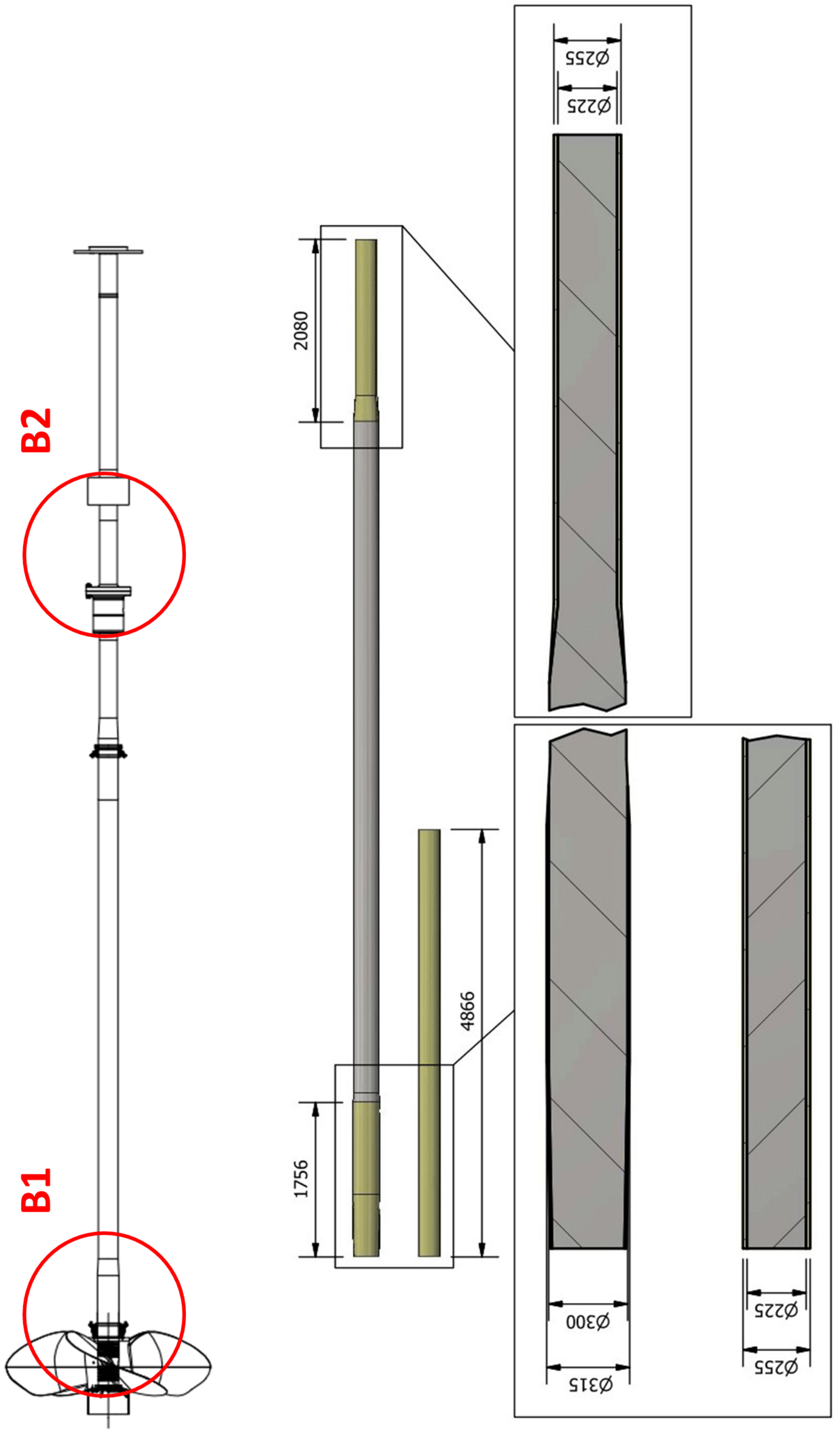
B2
B1
2080
1756
4866
Ø255
Ø225
Ø300
Ø315
Ø225
Ø255

B

Appendix step-by-step deduction

B.1 Torsional-static step-by-step deduction making mimic formula

τ: Shear stress (from torsion)
D: External diameter
d: Internal diameter
J: Polar moment of inertia
T: Torque
P: Power
n: rpm

Begin with equation for torsional shear stress from torque.

$$\tau = \frac{T \cdot r}{J} \longrightarrow \frac{T \cdot D}{2 \cdot J} \tag{B.1}$$

Polar moment of inertia for hollow cylinder.

$$J = \pi/32 \cdot (D^4 - d^4)$$

$$T = \frac{60}{2\pi} \cdot P/n$$

Merge:

$$\tau = \frac{60 \cdot P \cdot D \cdot 32}{2 \cdot \pi \cdot n \cdot 2 \cdot \pi \cdot (D^4 - d^4)} \longrightarrow \frac{1}{\tau} = \frac{\pi^2 \cdot n}{D \cdot 480 \cdot P} \cdot (D^4 - d^4)$$
$$\longrightarrow \frac{1}{\tau} = \frac{D^4 \cdot \pi^2 \cdot n}{D \cdot 480 \cdot P} - \frac{d^4 \cdot \pi^2 \cdot n}{D \cdot 480 \cdot P} \longrightarrow \frac{480 \cdot P}{\tau \cdot D^3 \cdot \pi^2 \cdot n} = \left(1 - \frac{d^4}{D^4}\right)$$
$$\longrightarrow \frac{\tau \cdot D^3 \cdot \pi^2 \cdot n}{480 \cdot P} = \frac{1}{1 - \frac{d^4}{D^4}} \longrightarrow D^3 = \frac{P}{n} \cdot \frac{1}{1 - \frac{d^4}{D^4}} \cdot \frac{480}{\tau * \pi^2}$$

$$D = \sqrt[3]{\frac{P}{n} \cdot \frac{1}{1 - \frac{d^4}{D^4}} \cdot \frac{480}{\tau * \pi^2}} \tag{B.2}$$

B.2 Mimic formula- step-by-step deduction with fatigue limit criteria applied

D: External diameter
d: Internal diameter
P: Power
n: rpm
σ_B or S_{ut}: Ultimate tensile strength
σ_e or Se: Endurance limit ($\sigma_{edv} : withDangVancriterion$
K_a: surface reduction factor (will use machined surface)
K_f: stress concentration factor
k_c: Load factor
σ_{fl}: Fluctuating loading
σ_{flp}: Pulsation loading.

We shall begin by defining the reduced fatigue limit for a typical rotating shaft.

All reduction factors are based on Shigleys [5].

Se' = 0.5*σ_B
$K_a = 4.51 \cdot \sigma_B^- 0.265$
$k_c = 0.59$
$K_f = 1.45$

$$Se = Se' \cdot k_a \cdot k_c / K_f = 0.166 \cdot \sigma_B MPa$$

Now applying the Dang Van criterion.

$$\sigma fl = 0.166 \cdot \sigma_B \quad \sigma_{flP} = \sigma_{fl} * 0.8$$

$$\sigma_{edv} = \frac{\sigma_{fl}}{2} + C_{dv} * \frac{\sigma_{fl}}{3} = 0.5$$

$$\sigma_{edv} = \frac{\sigma_1 - \sigma_3}{2} + C_{dv} \frac{\sigma_1 + \sigma_2 + \sigma_3}{3}$$

$$\sigma_{edv} = \frac{\sigma_{fl}}{2} + C_{dv} * \frac{\sigma_{fl}}{3} = 0.111 \sigma_B$$

Insert the newly defined Dang Van reduced endurance limit into the statical statical torsion mimic equation.

$$D = \sqrt[3]{\frac{P}{n} \cdot \frac{1}{1 - \frac{d^4}{D^4}} \cdot \frac{442.13}{\sigma_B}} \tag{B.3}$$

B.3 KA_{ice} Estimate ice hit torque on shaft

If the propeller is in duct:
k1 = 7.7 and k2 = 14.6

If the propeller is open:
k1 = 10.9 and k2 = 20.7

D: Propeller diameter
d: Hub diameter
P: Power
n: cycle speed [rpm] (n_n: rotational speed bollard condition, see table)
I_e/I_t : The mass moment of inertia ratio between the propulsion side and engine side,
$P_{0.7}/D$: the pitch ratio at radius 0.7
Q: Torque

Define H_{ice}:

Table 19 Thickness of the design maximum ice block H_{ice} entering the propeller.

Ice class	Ice(1A*)	Ice(1A)	Ice(1B)	Ice(1C)
H_{ice}	1.75 m	1.5 m	1.2 m	1.0 m

n_n taken from table(of not known):

Propeller type	*Rotational speed n*
CP propellers	n_n
FP propellers driven by turbine or electric motor	n_n
FP propellers driven by diesel engine	0.85 n_n

If $D < 1.8 * H_{ice}$

$$Q_{max} = k1 * (1 - d/D) * (P_{0.7}/D)^{0.16} * (n_n * D)^{0.17} * D^3 \tag{B.4}$$

If $D > 1.8 * H_{ice}$

$$Q_{max} = k1 * (1 - d/D) * (P_{0.7}/D)^{0.16} * (n_n * D)^{0.17} * D^{1.9} * H_{ice} \tag{B.5}$$

Qe_{max} taken from table:

Table 27 Default values for prime mover maximum torque Q_{emax}

Propeller type	Q_{emax}
Propellers driven by electric motor	$Q_{motor}{}^{*}$
CP propellers not driven by electric motor	Q_n
FP propellers driven by turbine	Q_n
FP propellers driven by diesel engine	0.75 Q_n
$^{*}Q_{motor}$ is the electric motor peak torque.	

$$Q_{peak} = Qe_{max} + Q_{max} * I_e/I_t \tag{B.6}$$

Now everything is known to calculate the application factor KA_{ice}:

$$KA_{ice} = Q_{peak}/Q_0 \tag{B.7}$$

Based on DNVGL-RU-SHIP Pt.6 Ch.6 15.5.3 [12]

B.4 Failure load of propeller

$$d = 160 \sqrt[3]{\frac{F_{ex} * D}{\sigma y_s haft * 1(\frac{di^4}{d^4})}} \tag{B.8}$$

D: The Propeller diameter.
F_{ex}: Blade Failure Load.

Where:

$$F_{ex} = \frac{300 \cdot c \cdot t^2 \cdot \sigma ref}{0.8 \cdot D \cdot 2 \cdot r} \tag{B.9}$$

σref:
c: Chord length at r/R.
t: Max blade thickness at r/R.

Where:

$$r = \frac{D * r\_R}{2} \tag{B.10}$$

r_R= relative radius of the stress scope.

Based on DNVGL-RU-SHIP Pt.6 Ch.6 12.5.2 [12]

C
Appendix- Data

C.1 Mimic formula compared with IACS M68.4

	50-800	800-10000	50-200	300-600		
#	D	P	n	σB	IACS	Mimic
1	345	9715	74	320	535.0396	564.3666
2	221	5744	110	345	386.8769	404.7702
3	402	8332	134	337	412.2481	432.3935
4	737	3192	149	363	284.1325	295.7088
5	127	1066	126	496	193.2963	195.5131
6	444	2947	133	355	288.8261	301.2828
7	775	8389	195	459	338.8891	345.0075
8	113	7096	140	458	358.1198	364.654
9	599	2788	173	405	251.8423	259.3014
10	65	7822	56	494	492.6971	498.5115
11	406	1011	103	588	194.4166	194.1123
12	749	3477	51	425	402.614	412.6889
13	288	7247	189	555	310.8323	311.656
14	557	8879	51	380	565.1921	585.5235
15	793	6490	65	578	423.1435	423.0017
16	275	3854	64	389	394.5625	407.8198
17	503	7809	92	379	445.1116	461.2437
18	574	1425	190	433	192.0429	196.5164
19	342	3215	103	337	327.6361	343.6467
20	624	4909	108	303	380.2408	403.5678
21	140	9895	153	566	368.1221	368.5617
22	50	4118	150	404	300.9548	309.9409
23	618	3116	113	443	294.7564	301.0089
24	384	4343	71	508	371.519	375.0566
25	213	6244	181	518	305.4318	307.8642
26	279	2069	62	446	313.5894	320.0508
27	186	7057	52	316	542.4994	573.039
28	581	3275	64	588	337.1107	336.5831
29	357	2040	127	519	236.6182	238.4665
30	346	6168	71	465	426.9706	434.1955
31	523	4236	198	511	261.3678	263.7328
32	237	4610	181	471	282.7442	287.2156
33	266	1424	184	589	179.5282	179.2255
34	713	9538	122	547	395.6295	397.1102
35	550	3650	71	590	337.3291	336.7196
36	547	3313	172	591	243.0788	242.6104
37	668	4398	189	548	264.0276	264.9793
38	773	9734	75	316	534.4869	564.5754
39	166	3961	141	370	309.6226	321.6145
40	172	3824	61	332	414.7665	435.7368
41	139	8571	176	379	369.8617	383.2665

42	89	6177	127	585	331.8959	331.4975
43	271	3153	172	349	272.2003	284.4446
44	257	5781	147	457	329.2528	335.3236
45	469	7391	81	385	454.2935	470.0313
46	450	1049	125	383	205.3137	212.5347
47	612	1137	117	449	207.5145	211.6656
48	210	7768	57	517	483.0713	486.9924
49	66	1888	198	486	202.1921	204.8524
50	485	3808	152	443	285.4793	291.5351
51	717	4290	148	537	285.5729	287.0437
52	239	3340	107	371	320.4931	332.8157
53	56	5118	67	596	383.911	382.9429
54	790	3106	64	470	350.7166	356.3271
55	269	7950	100	363	439.8972	457.8197
56	633	1321	192	551	175.6467	176.2075
57	346	4706	110	491	332.6254	336.7184
58	618	2464	179	577	218.6936	218.6477
59	678	5702	73	549	395.1379	396.5077
60	273	1943	182	429	216.5167	221.7459
61	413	1450	109	501	224.2037	226.5908
62	197	9273	92	315	491.6344	519.4952
63	548	8294	192	494	333.1893	337.1213
64	374	7731	173	442	346.4126	353.8317
65	510	7601	111	373	415.9133	431.672
66	150	9926	56	442	548.3518	560.0957
67	438	2170	109	365	276.9198	288.0411
68	448	7420	136	432	372.3149	381.067
69	56	7973	73	350	493.1423	515.1708
70	536	1864	91	376	277.6361	287.9253
71	163	4561	147	471	301.9723	306.7479
72	371	7028	165	320	367.6474	387.7992
73	324	4996	126	323	358.2319	377.4772
74	605	9595	121	468	413.5195	420.2866
75	284	4434	132	585	293.3714	293.0193
76	477	7996	194	427	340.0481	348.4084
77	780	1269	114	371	227.2742	236.0126
78	546	8977	65	432	507.4128	519.3406
79	74	3746	92	439	336.3931	343.8054
80	414	5179	118	460	340.9731	347.064
81	468	3270	117	552	280.1281	280.9842
82	293	1483	95	564	229.4153	229.7491
83	266	5210	109	499	343.7462	347.5184
84	767	7709	87	349	460.2386	480.9413
85	772	4835	133	366	338.2588	351.7457
86	298	3546	161	414	278.0117	285.6572

87	540	9926	102	574		420.2961	420.3667
88	394	3458	90	357		346.5453	361.2815
89	592	9817	58	465		533.2771	542.3008
90	646	6164	141	355		362.2498	377.8731
91	796	4737	111	372		355.4831	369.0513
92	630	9319	66	589		472.6183	471.8214
93	56	9875	73	537		477.225	479.6829
94	520	9763	137	575		378.6644	378.6802
95	659	2476	150	598		230.1757	229.541
96	749	8717	79	536		446.1076	448.4692
97	529	7990	195	589		312.9004	312.3728
98	569	7899	200	302		363.1026	385.5251
99	302	3564	71	537		342.9348	344.7011
100	381	6594	159	540		321.327	322.8447

C.2 Shaft diameter investigation input and output

Vessel	Shaft part no	P_D	I/It	ICE CLASS	*Shaft/Component* di	r	D	t	*Propeller* D	d	t	c	r_d
Bunker tanker	A1 (Prop)	1.24	0.34	1B	90	50	800		3.6	0.91	0.134	0.734	0.35
Bunker tanker	A2 (Interm)	1.24	0.34	1B	90				3.6	0.91	0.134	0.734	
Dredger vessel	B1 (Prop)	1.48		No	0				3	0.6	0.117	0.754	0.25
Dredger vessel	B2 (Interm)	1.48		No	0	40	660	119	3	0.6	0.117	0.754	
RoPax SB	C1 (Prop)	1.27	0.33	1C	130	75	1180		4.8	1.18	0.166	1.017	0.35
RoPax SB	C2 (Interm)	1.27	0.31	1C	130				4.8	1.18	0.166	1.017	
RoPax SB	C3 (Interm)	1.27	0.31	1C	130	40	790	280	4.8	1.18	0.166	1.017	

Vessel	Shaft part no	omponen	n [rpm]	Power [kW]	T0 (KNm)	EST KA	Mb (from alignment) [kNm]	KA/KAP/ Kice (TVC)
Bunker tanker	A1 (Prop.S.)	Flange	142	2500	168	1.3/1.4/1.92	47.40	1.1/1.85
Bunker tanker	A2 (Intermediate.S.)	Plain shaf	142	2500	168	1.3/1.4/1.92	8.60	1.04/1.85
Dredger vessel	B1 (Prop.S.)	Seal (Shirr	197	4000	194	1.3/1.4/0	30.90	1.03/0
Dredger vessel	B2 (Intermediate.S.)	Flange	197	4000	194	1.3/1.4/0	14.10	1.03/0
RoPax SB	C1 (Prop.S.)	Flange	151	12600	797	1.3/1.4/1.4	213.40	1.02/1.42
RoPax SB	C2 (Intermediate.S.)	Shrink fit	151	12600	797	1.3/1.4/1.38	27.1	1.04/1.4
RoPax SB	C3 (Intermediate.S.)	Flange	151	12600	797	1.3/1.4/1.38	-38.50	1.04/ 1.4

Vessel	Shaft part no	*Calculated output [mm]* Initial diameter	IACS M68.4	Est KA & 0.4 Mb	Est KA & Align.M. Mb	TVC KA & 0.4 Mb	TVC KA & Align.M. Mb	Min diameter from propeller failure load	Final improved diameter	Differeance
Bunker tanker	A1 (Prop.S.)	350	288.5	239	239	236	236	350	350	0
Bunker tanker	A2 (Intermediate.S.)	260	240.1	232	232	229	229		230	30
Dredger vessel	B1 (Prop.S.)	315	300.6	254	228	254	228	300	300	15
Dredger vessel	B2 (Intermediate.S.)	255	246.4	225	225	225	225		225	30
RoPax SB	C1 (Prop.S.)	520	482.2	381	361	370	363	465	465	55
RoPax SB	C2 (Intermediate.S.)	420	396	368	368	370	370		370	50
RoPax SB	C3 (Intermediate.S.)	405	396	366	366	370	370		370	35

C.3 Case study result data from Nauticus Alignment

On left-Dredger initial shaft design (BERG order design)

On right- Derdger improved diameter

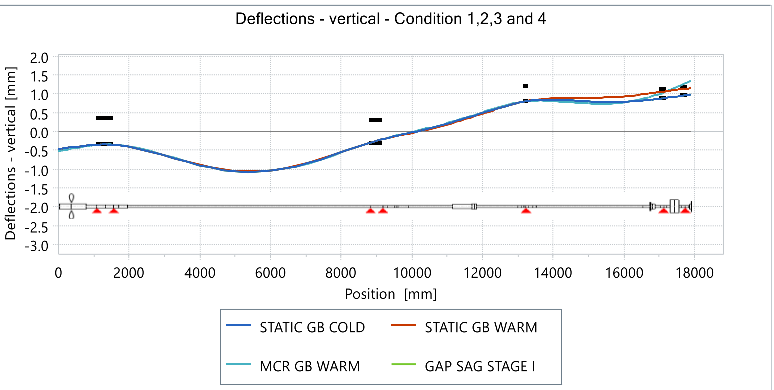

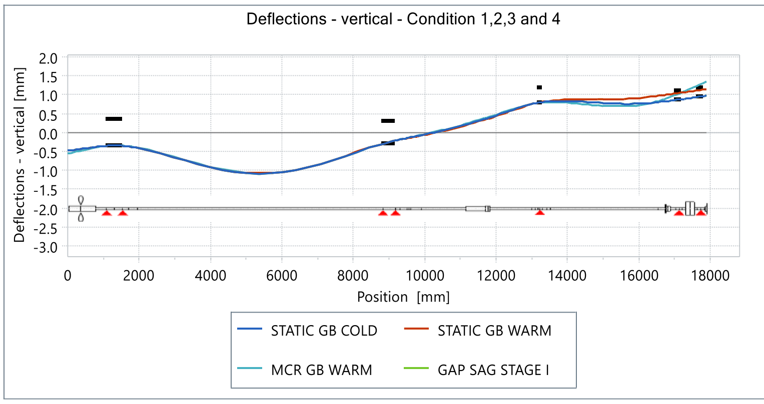

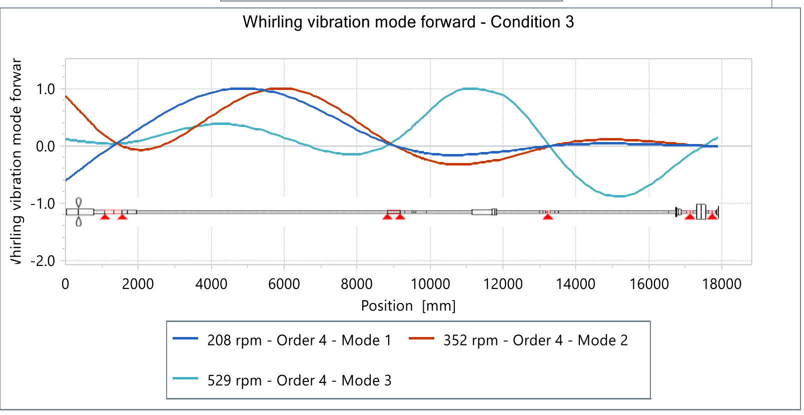

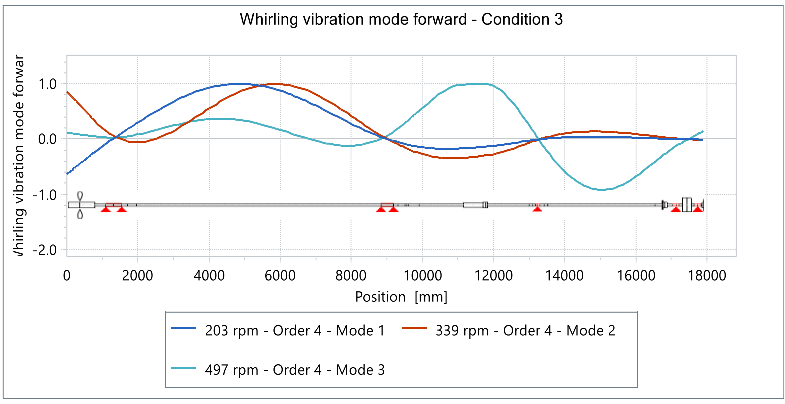

All available results | Bearing reactions in vertical | 3 - MCR GB WARM

Deflection: Showing the deformation of the shaft
Slope: Showing the relative nominal slope between shaft and unloaded bearing

	Position [mm]	Load [kN]	Pressure [bar]	Offset [mm]	Deflection [mm]	Slope [mrad]
ASTB - Part 1	1055	46	6.18	0.000	-0.359	
ASTB - Part 2	1530	6	0.86	0.000	-0.351	
Nominal		53	3.52			0.02
FSTB - Part 1	8795	25	4.99	0.000	-0.305	
FSTB - Part 2	9145	0	0.00	0.000	-0.214	
Nominal		25	2.50			0.26
INTB	13195	28	7.95	1.000	0.791	0.11
AGBB	17090	138	29.08	1.175	1.018	0.32
FGBB	17700	-7	-1.37	1.250	1.260	0.42
TOTAL		238				

Slope: Showing the relative nominal slope between shaft and unloaded bearing

	Position [mm]	Load [kN]	Pressure [bar]	Offset [mm]	Deflection [mm]	Slope [mrad]
Bearing6 - Part 1	1055	48	7.14	0.000	-0.360	
Bearing6 - Part 2	1505	4	0.53	0.000	-0.351	
Nominal		52	3.84			0.02
FSTB - Part 1	8795	26	5.21	0.000	-0.305	
FSTB - Part 2	9145	0	0.00	0.000	-0.218	
Nominal		26	2.60			0.25
INTB	13195	23	7.28	1.000	0.792	0.13
AGBB	17090	143	30.18	1.175	1.014	0.34
FGBB	17700	-11	-2.40	1.250	1.265	0.43
TOTAL		233				

On left-RoPax initial shaft design (BERG order design)

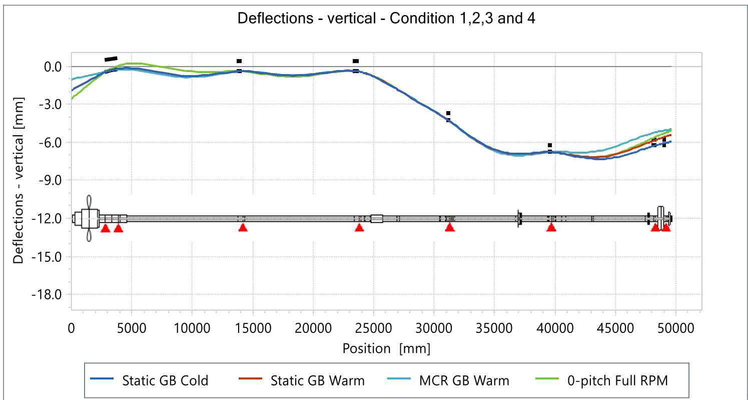

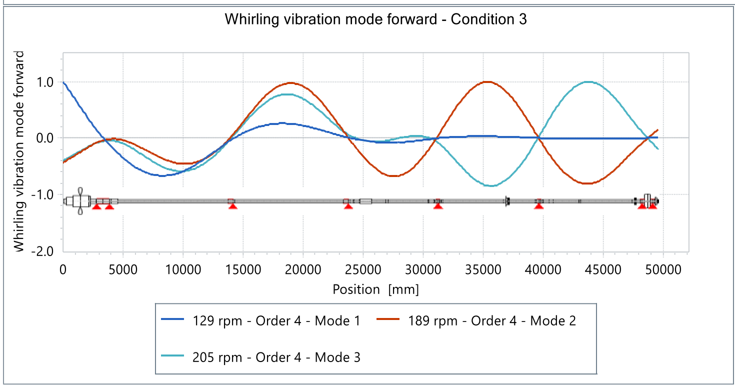

All available results — Bearing reactions in vertical — 3 - MCR GB Warm

```
Offset:     Showing the influence of initial offset, thermal expansion,hull deflection
            and vertical offset correction
Deflection: Showing the deformation of the shaft
Slope:      Showing the relative nominal slope between shaft and unloaded bearing
```

	Position [mm]	Load [kN]	Pressure [bar]	Offset [mm]	Deflection [mm]	Slope [mrad]
ASTB - Part 1	2728	77	2.79	0.000	-0.465	
ASTB - Part 2	3792	163	5.87	0.213	-0.270	
Nominal		240	4.33			0.02
MSTB	14078	95	5.18	0.000	-0.419	0.06
FSTB	23703	106	5.91	0.000	-0.421	0.11
INTB1	31165	66	4.93	-4.000	-4.272	0.68
INTB2	39566	83	6.23	-6.500	-6.776	0.06
AGBB	48170	-324	-21.25	-5.575	-5.255	0.27
FGBB	49040	-492	-32.34	-5.575	-5.089	0.13
TOTAL		-225				

All available results — Bearing reactions in vertical — 4 - 0-pitch Full RPM

```
Description of columns:

Offset:     Showing the influence of initial offset, thermal expansion,hull deflection
            and vertical offset correction
Deflection: Showing the deformation of the shaft
Slope:      Showing the relative nominal slope between shaft and unloaded bearing
```

	Position [mm]	Load [kN]	Pressure [bar]	Offset [mm]	Deflection [mm]	Slope [mrad]
ASTB - Part 1	2728	246	8.87	0.000	-0.499	
ASTB - Part 2	3792	0	0.00	0.213	-0.005	
Nominal		246	4.43			0.26
MSTB	14078	88	4.78	0.000	-0.418	0.03
FSTB	23703	109	6.07	0.000	-0.422	0.09
INTB1	31165	63	4.73	-4.000	-4.271	0.66
INTB2	39566	89	6.69	-6.500	-6.779	0.02
AGBB	48170	13	0.87	-5.575	-5.642	0.42
FGBB	49040	-86	-5.66	-5.575	-5.300	0.38
TOTAL		523				

On right- RoPax improved diameter

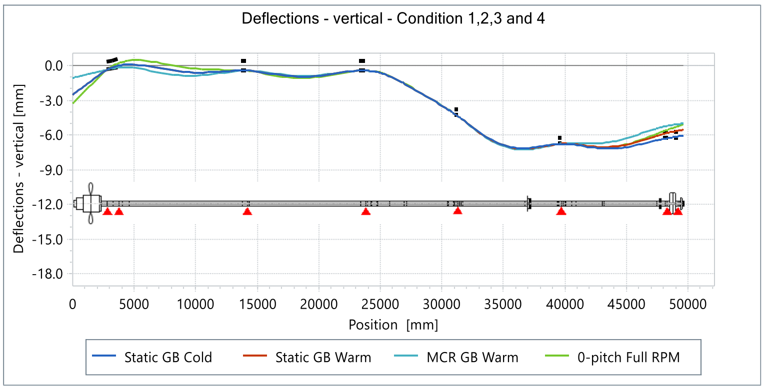

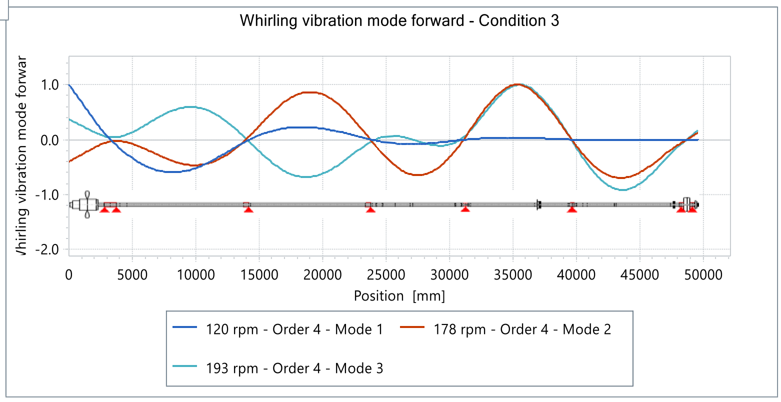

All available results — Bearing reactions in vertical — 3 - MCR GB Warm

```
--------------------------------------------------------------------------------
Description of columns:

Offset:     Showing the influence of initial offset, thermal expansion,hull deflection
            and vertical offset correction
Deflection: Showing the deformation of the shaft
Slope:      Showing the relative nominal slope between shaft and unloaded bearing
```

	Position [mm]	Load [kN]	Pressure [bar]	Offset [mm]	Deflection [mm]	Slope [mrad]
Bearing7 - Part 1	2728	63	2.92	0.000	-0.363	
Bearing7 - Part 2	3658	169	7.82	0.223	-0.161	
Nominal		233	5.37			0.02
MSTB	14078	100	5.44	0.000	-0.420	0.04
FSTB	23703	88	4.90	0.000	-0.418	0.00
INTB1	31165	53	4.35	-4.000	-4.267	0.77
INTB2	39566	75	5.62	-6.500	-6.773	0.14
AGBB	48170	-342	-22.46	-5.575	-5.245	0.25
FGBB	49040	-481	-31.59	-5.575	-5.095	0.12

```
Offset:     Showing the influence of initial offset, thermal expansion,hull deflection
            and vertical offset correction
Deflection: Showing the deformation of the shaft
Slope:      Showing the relative nominal slope between shaft and unloaded bearing
```

	Position [mm]	Load [kN]	Pressure [bar]	Offset [mm]	Deflection [mm]	Slope [mrad]
Bearing7 - Part 1	2728	240	11.08	0.000	-0.398	
Bearing7 - Part 2	3658	0	0.00	0.223	0.188	
Nominal		240	5.54			0.39
MSTB	14078	90	4.91	0.000	-0.418	0.08
FSTB	23703	91	5.09	0.000	-0.418	0.04
INTB1	31165	51	4.16	-4.000	-4.267	0.76
INTB2	39566	80	5.95	-6.500	-6.776	0.07
AGBB	48170	6	0.41	-5.575	-5.606	0.38
FGBB	49040	-85	-5.58	-5.575	-5.298	0.34
TOTAL		474				

On left-Bunker tanker initial shaft design (BERG order design) **On right- Bunker tanker improved dia**

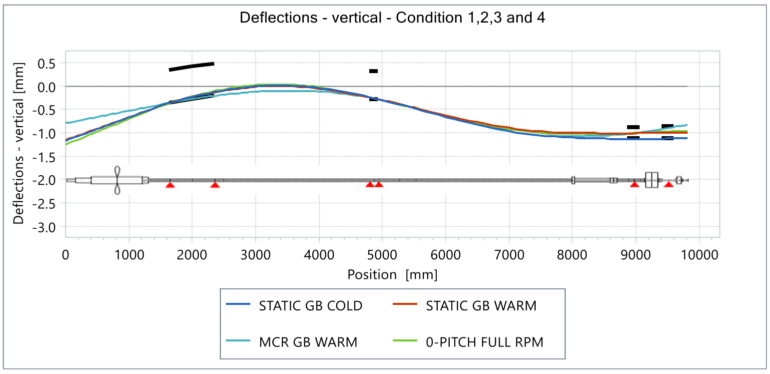

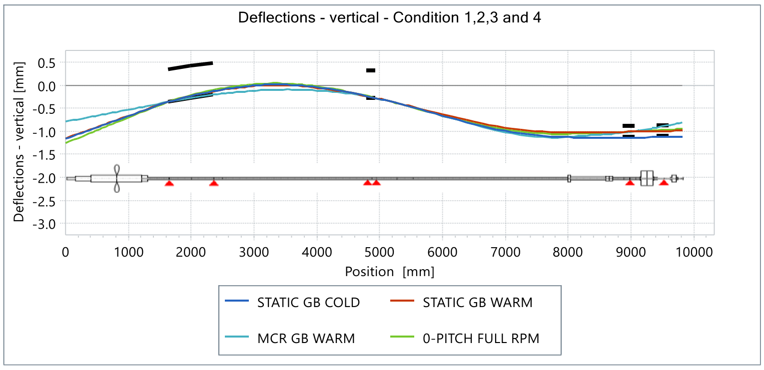

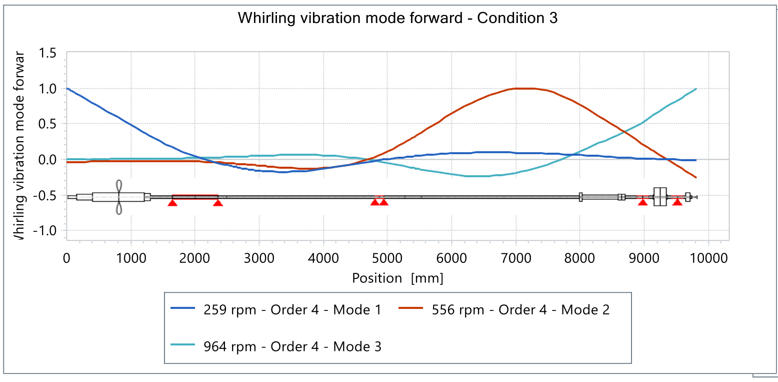

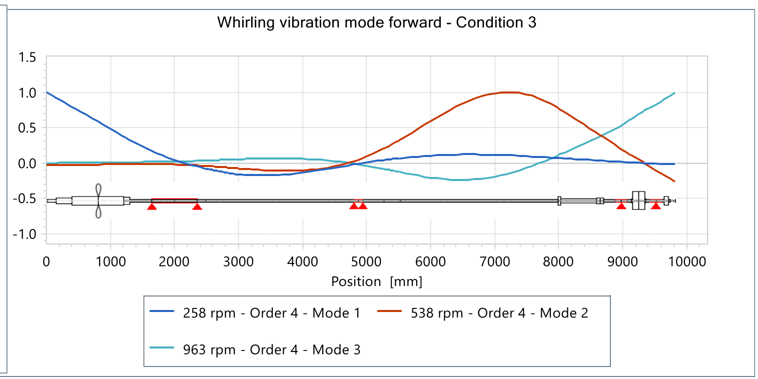

All available results | Bearing reactions in vertical | 3 - MCR GB WARM

Deflection: Showing the deformation of the shaft
Slope: Showing the relative nominal slope between shaft and unloaded bearing

	Position [mm]	Load [kN]	Pressure [bar]	Offset [mm]	Deflection [mm]	Slope [mrad]
ASTB - Part 1	1630	55	4.38	0.000	-0.361	
ASTB - Part 2	2340	10	0.77	0.142	-0.210	
Nominal		64	2.58			0.01
FSTB - Part 1	4787	0	0.00	0.028	-0.241	
FSTB - Part 2	4925	18	9.51	0.028	-0.276	
Nominal		18	4.75			0.25
AGBB	8963	98	20.52	-0.875	-1.011	0.13
FGBB	9503	19	4.45	-0.865	-0.900	0.23
TOTAL		198				

All available results | Bearing reactions in vertical | 3 - MCR GB WARM

Offset: Showing the influence of initial offset, thermal expansion, hull deflection and vertical offset correction
Deflection: Showing the deformation of the shaft
Slope: Showing the relative nominal slope between shaft and unloaded bearing

	Position [mm]	Load [kN]	Pressure [bar]	Offset [mm]	Deflection [mm]	Slope [mrad]
ASTB - Part 1	1630	54	4.37	0.000	-0.361	
ASTB - Part 2	2340	10	0.80	0.142	-0.210	
Nominal		64	2.58			0.01
FSTB - Part 1	4787	0	0.00	0.028	-0.241	
FSTB - Part 2	4925	16	8.42	0.028	-0.275	
Nominal		16	4.21			0.25
AGBB	8963	102	21.38	-0.875	-1.015	0.16
FGBB	9503	14	3.39	-0.865	-0.892	0.25
TOTAL		196				

All available results | Bearing reactions in vertical | 4 - 0-PITCH FULL RPM

and vertical offset correction
Deflection: Showing the deformation of the shaft
Slope: Showing the relative nominal slope between shaft and unloaded bearing

	Position [mm]	Load [kN]	Pressure [bar]	Offset [mm]	Deflection [mm]	Slope [mrad]
ASTB - Part 1	1630	74	5.93	0.000	-0.365	
ASTB - Part 2	2340	0	0.00	0.142	-0.108	
Nominal		74	2.96			0.16
FSTB - Part 1	4787	0	0.00	0.028	-0.228	
FSTB - Part 2	4925	5	2.37	0.028	-0.273	
Nominal		5	1.19			0.32
AGBB	8963	44	9.31	-0.875	-1.007	0.04
FGBB	9503	23	5.51	-0.865	-0.975	0.07
TOTAL		146				

All available results | Bearing reactions in vertical | 4 - 0-PITCH FULL RPM

Offset: Showing the influence of initial offset, thermal expansion, hull deflection and vertical offset correction
Deflection: Showing the deformation of the shaft
Slope: Showing the relative nominal slope between shaft and unloaded bearing

	Position [mm]	Load [kN]	Pressure [bar]	Offset [mm]	Deflection [mm]	Slope [mrad]
ASTB - Part 1	1630	74	5.92	0.000	-0.365	
ASTB - Part 2	2340	0	0.00	0.142	-0.107	
Nominal		74	2.96			0.16
FSTB - Part 1	4787	0	0.00	0.028	-0.227	
FSTB - Part 2	4925	3	1.57	0.028	-0.272	
Nominal		3	0.79			0.33
AGBB	8963	46	9.77	-0.875	-1.009	0.06
FGBB	9503	20	4.83	-0.865	-0.969	0.08
TOTAL		143				

Bunker tanker without propeller blade failure load criteria (no ICE)- Aftmost shaft from 350 to 300mm

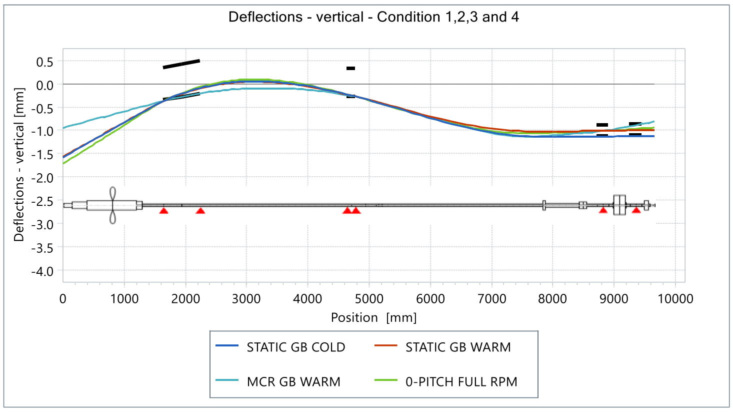

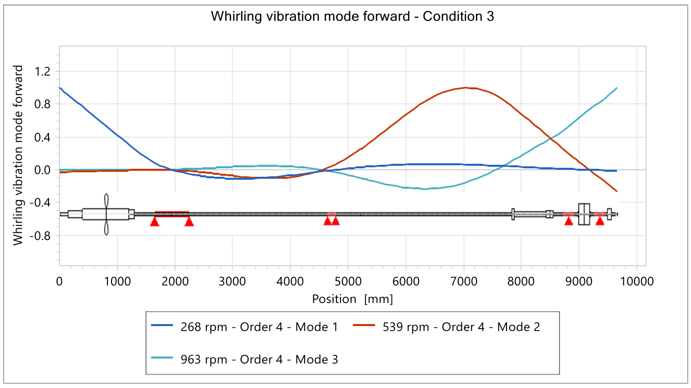

All available results · Bearing reactions in vertical · 3 - MCR GB WARM

Deflection: Showing the deformation of the shaft
Slope: Showing the relative nominal slope between shaft and unloaded bearing

	Position [mm]	Load [kN]	Pressure [bar]	Offset [mm]	Deflection [mm]	Slope [mrad]
Bearing5 - Part 1	1630	54	5.97	0.000	-0.372	
Bearing5 - Part 2	2230	7	0.78	0.142	-0.211	
Nominal		61	3.38			0.03
FSTB - Part 1	4627	0	0.00	0.038	-0.241	
FSTB - Part 2	4765	16	8.44	0.028	-0.275	
Nominal		16	4.22			0.18
AGBB	8803	102	21.39	-0.875	-1.015	0.16
FGBB	9343	14	3.38	-0.865	-0.892	0.25
TOTAL		193				

All available results · Bearing reactions in vertical · 4 - 0-PITCH FULL RPM

and vertical offset correction
Deflection: Showing the deformation of the shaft
Slope: Showing the relative nominal slope between shaft and unloaded bearing

	Position [mm]	Load [kN]	Pressure [bar]	Offset [mm]	Deflection [mm]	Slope [mrad]
Bearing5 - Part 1	1630	72	7.97	0.000	-0.379	
Bearing5 - Part 2	2230	0	0.00	0.142	-0.070	
Nominal		72	3.99			0.28
FSTB - Part 1	4627	0	0.00	0.038	-0.221	
FSTB - Part 2	4765	1	0.55	0.028	-0.270	
Nominal		1	0.28			0.28
AGBB	8803	47	9.99	-0.875	-1.010	0.06
FGBB	9343	19	4.65	-0.865	-0.968	0.09

C.4 Case study - Effects of propeller inertia change on flexible coupling alternating torque.

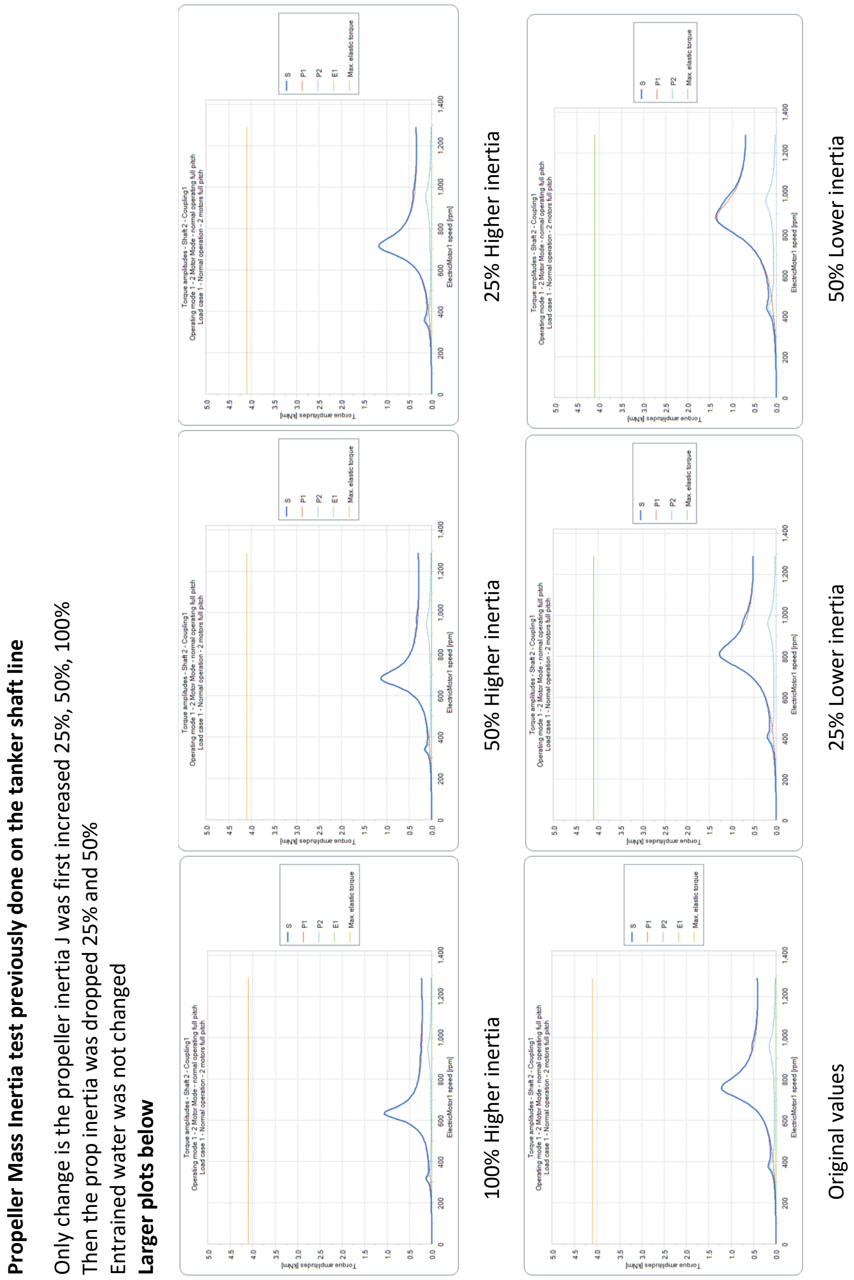

100% Higher inertia

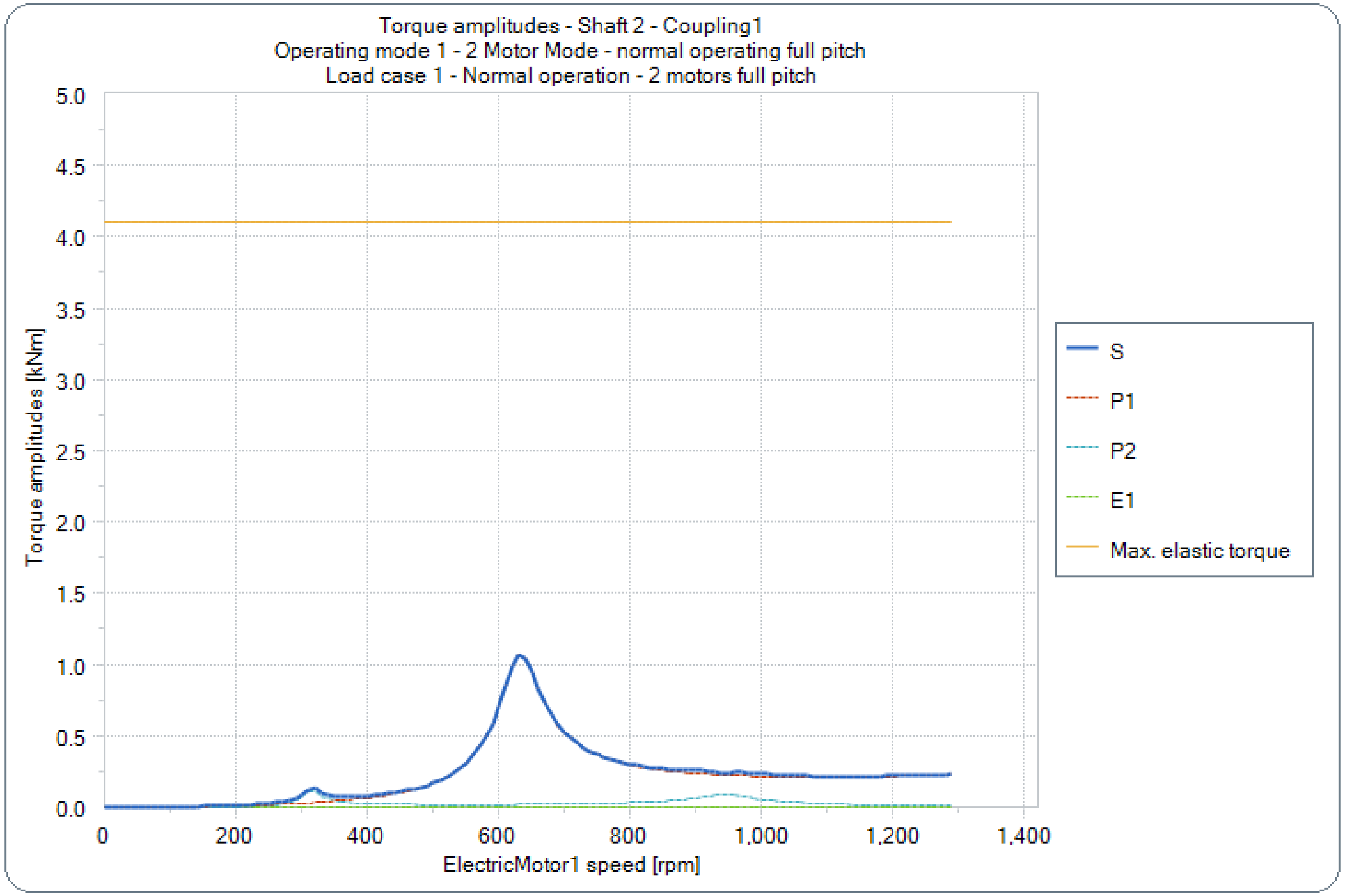

50% Higher inertia

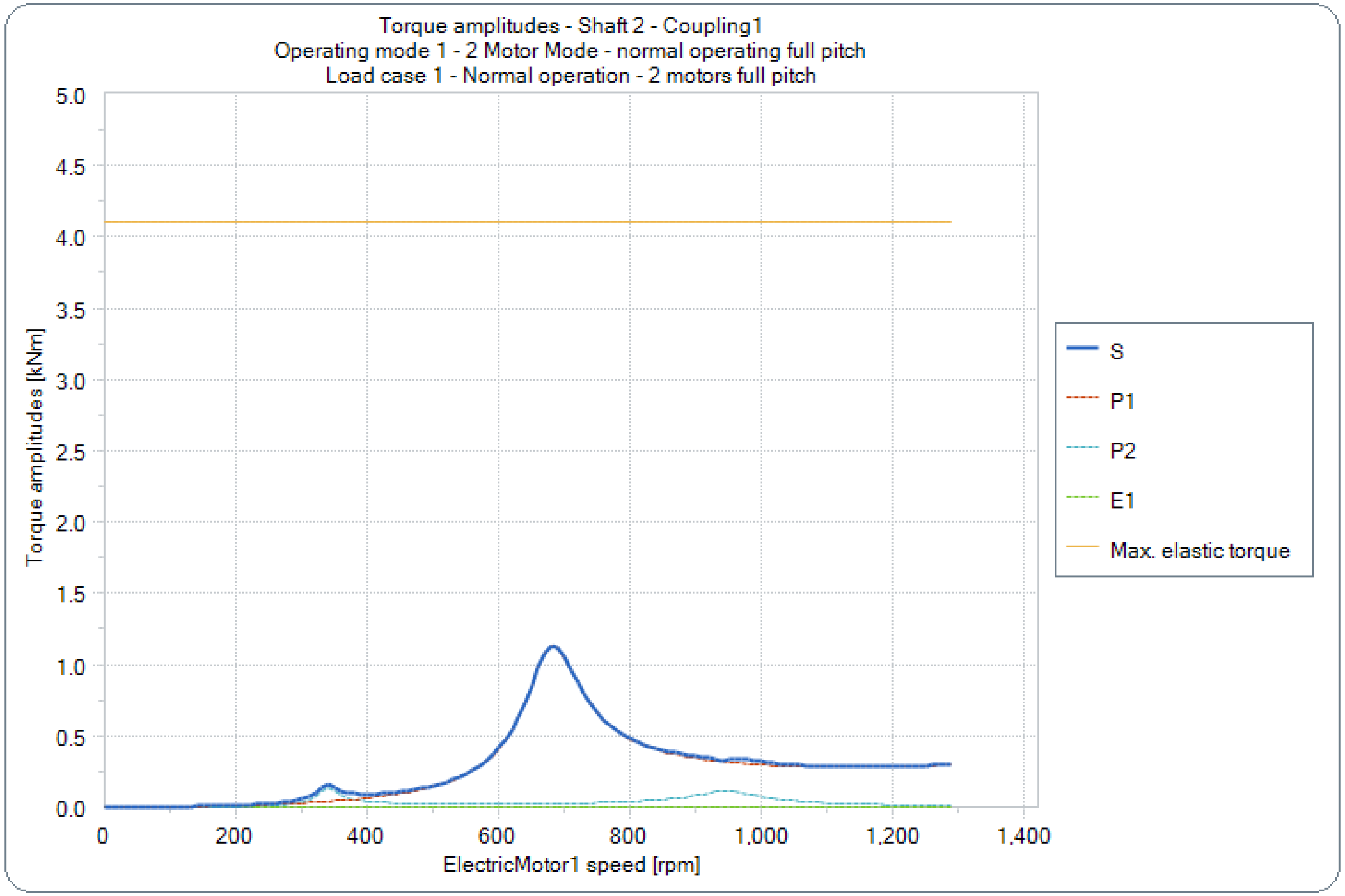

25% Higher inerta

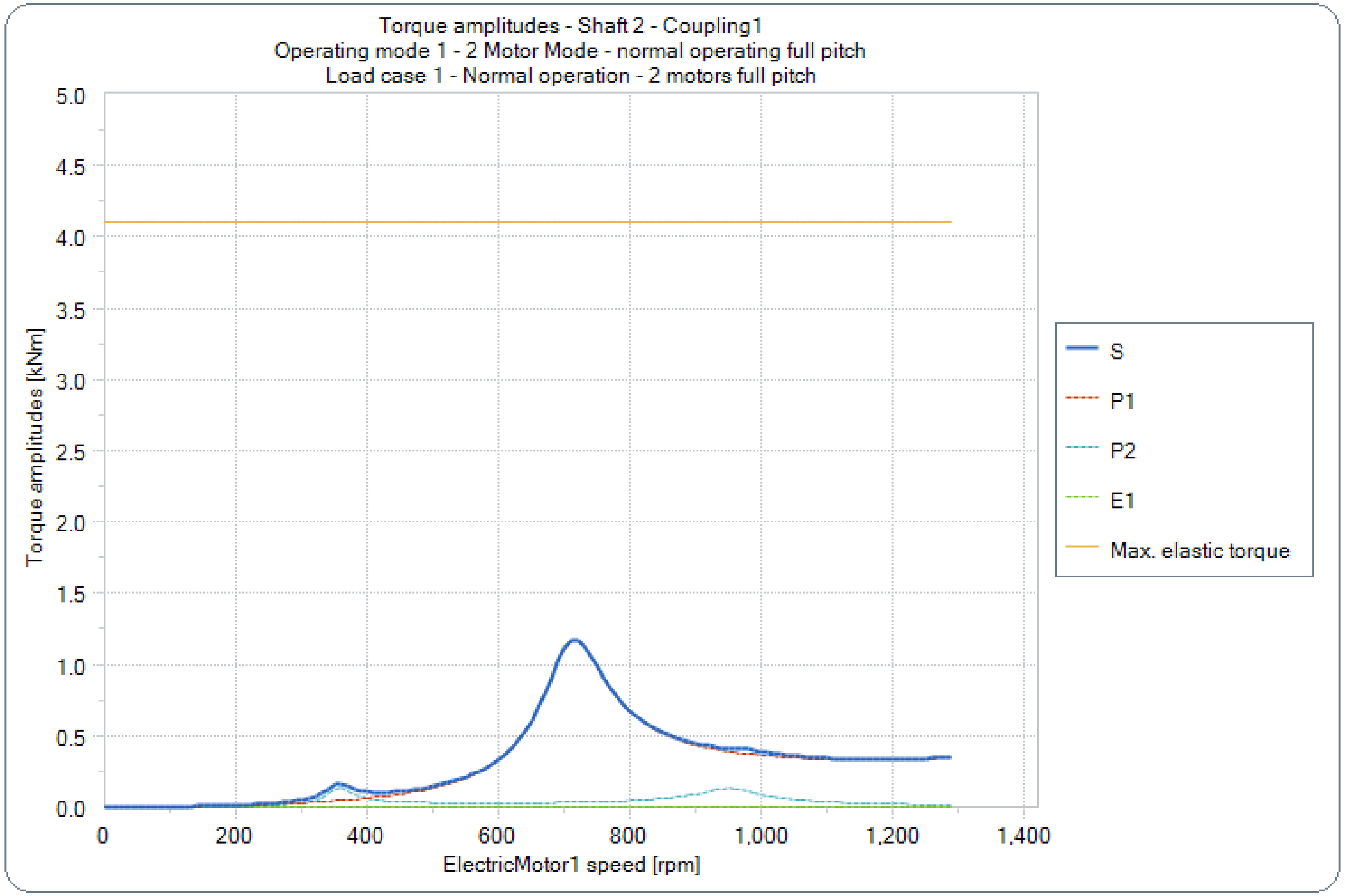

Original values

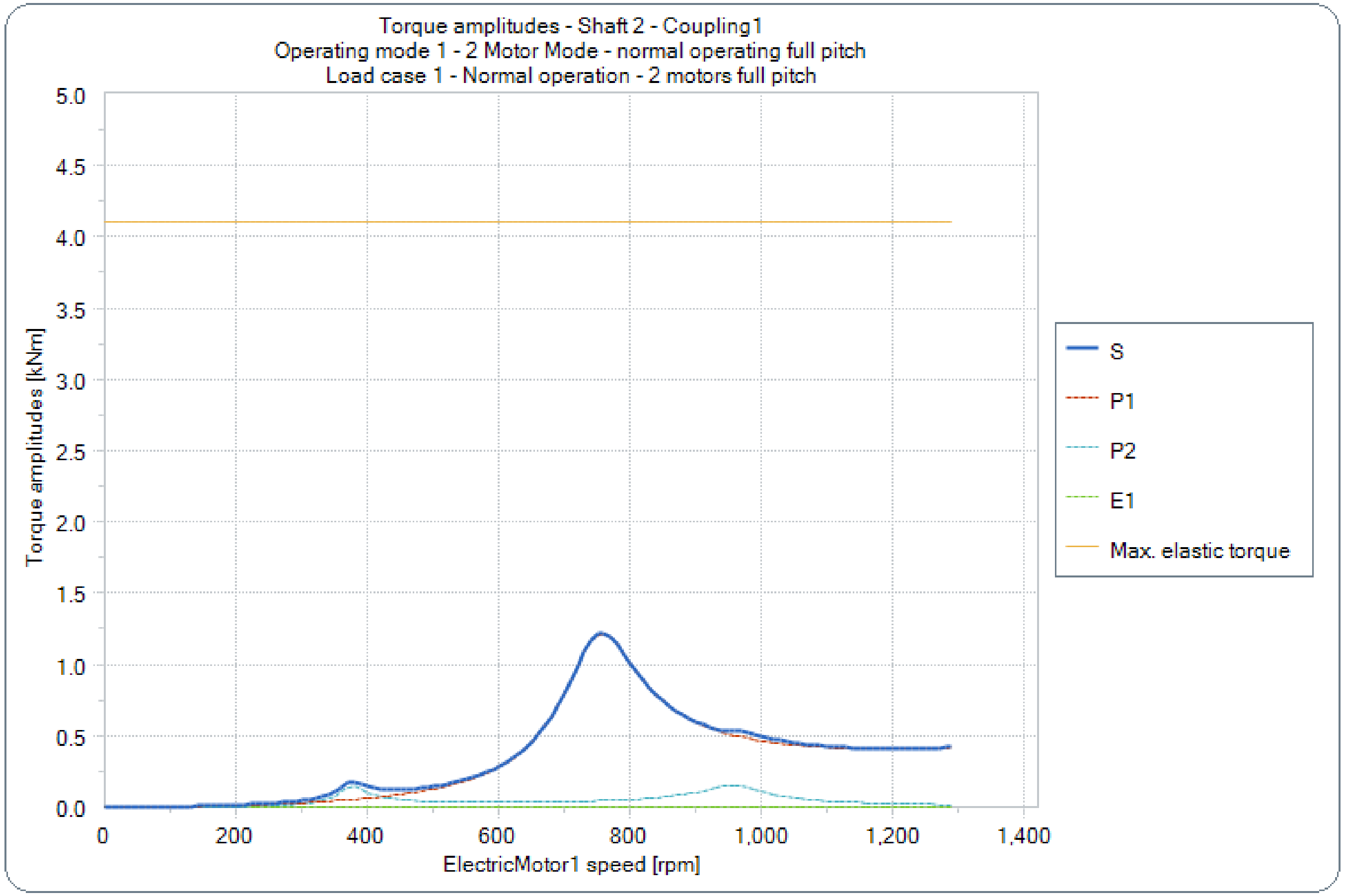

25% Lower inertia

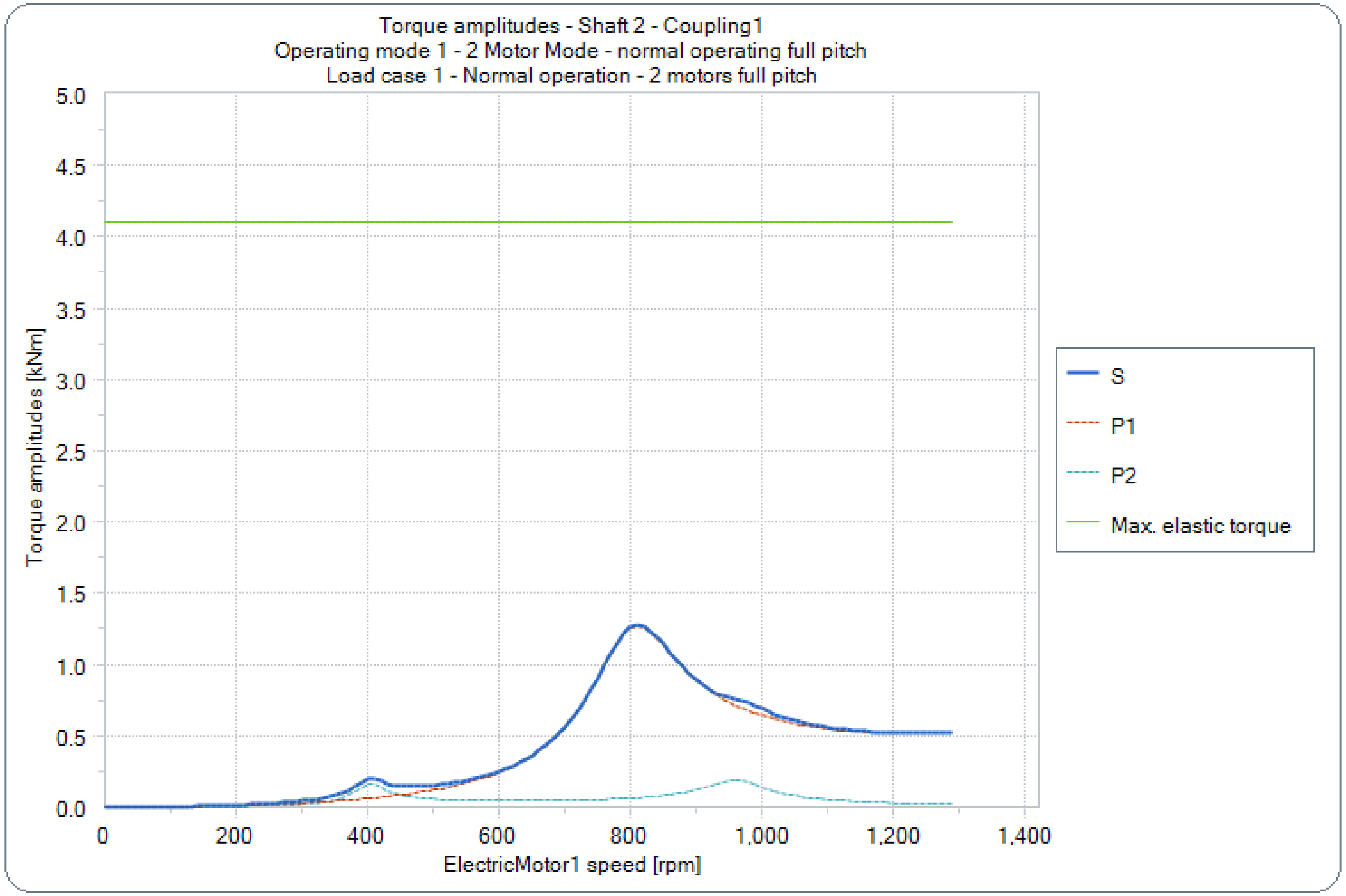

50% Lower inertia

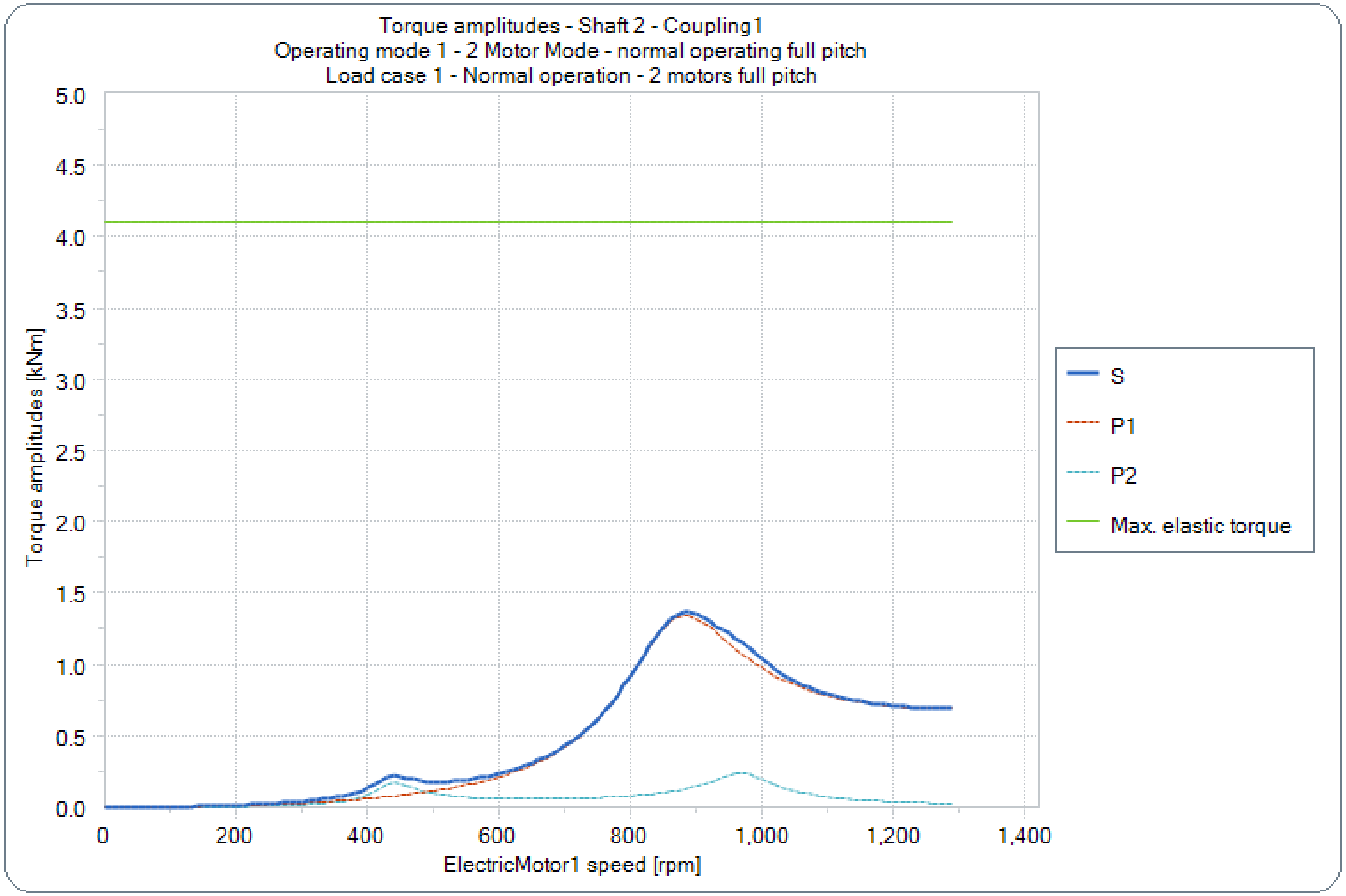

C.5 Input data for Nauticus Machinery Analysis

C.5.1 Shaft Alignment model inputs

C.5.2 Torsional Vibration Calculation model inputs

RoPax

DATA FOR MASSES AND DAMPERS

Mass No	DESCRIPTION	RPM RATIO [-]	MASS MOMENT OF INERTIA [kg*m^2]	DAMPING see note [N*s*m/rad]	FIRING ANGLE A [deg]	FIRING ANGLE B [deg]	TYPE
1	OPDamper	1.000	3.7700E+002	0.000E+000			Lump mass
2	IPDamper	1.000	1.2150E+002	0.000E+000			Lump mass
3	Cyl-A6B6	1.000	5.3670E+002	5.400E+002	0	50	Cylinder
4	Cyl-A5B5	1.000	5.3670E+002	5.400E+002	120	170	Cylinder
5	Cyl-A4B4	1.000	5.3670E+002	5.400E+002	600	650	Cylinder
6	Cyl-A3B3	1.000	5.3670E+002	5.400E+002	240	290	Cylinder
7	Cyl-A2B2	1.000	5.3670E+002	5.400E+002	480	530	Cylinder
8	Cyl-A1B1	1.000	5.3670E+002	5.400E+002	360	410	Cylinder
9	Flywheel	1.000	1.8360E+003	0.000E+000			Lump mass
10	PPCoup	1.000	1.4800E+002	0.000E+000			Lump mass
11	MPCoup	1.000	2.2800E+002	0.000E+000			Lump mass
12	SPCoup	1.000	3.9000E+002	0.000E+000			Lump mass
13	PTOWheel-J5-T95	1.000	9.4730E+001	0.000E+000			Lump mass
14	ClutchOP-J4	1.000	1.2636E+002	0.000E+000			Lump mass
15	ClutchIP-J3	1.000	7.6850E+001	0.000E+000			Lump mass
16	Pinion-J2-T22	1.000	4.3680E+001	0.000E+000			Lump mass
17	Gear-J1-T75	0.293	2.2622E+003	0.000E+000			Lump mass
18	GBFlange	0.293	1.3352E+002	0.000E+000			Lump mass
19	INT2frw	0.293	1.3352E+002	0.000E+000			Lump mass
20	INT2aft	0.293	1.3352E+002	0.000E+000			Lump mass
21	SpacerRing	0.293	3.0000E+001	0.000E+000			Lump mass
22	BrakeDisc	0.293	1.1992E+002	0.000E+000			Lump mass
23	INT1frw	0.293	1.3669E+002	0.000E+000			Lump mass
24	INT1aft	0.293	1.3669E+002	0.000E+000			Lump mass
25	OKCX	0.293	4.7800E+001	0.000E+000			Lump mass
26	PropShaft-frw	0.293	4.1140E+002	0.000E+000			Lump mass
27	PropShaft-aft	0.293	4.1140E+002	0.000E+000			Lump mass
28	Propeller1	0.293	1.9150E+004	0.000E+000			Propeller
29	HubCap	0.293	1.7300E+002	0.000E+000			Lump mass
30	PTOPinion	3.519	2.9800E+000	0.000E+000			Lump mass
31	PTOClutchIn	3.519	1.8000E+000	0.000E+000			Lump mass
32	PTOClutchOut	3.519	1.5200E+000	0.000E+000			Lump mass
33	PTOCoupPP	3.519	3.7000E+000	0.000E+000			Lump mass
34	PTOCoupMP	3.519	4.7000E+000	0.000E+000			Lump mass
35	PTOCoupMP1	3.519	4.7000E+000	0.000E+000			Lump mass
36	PTOCoupSP	3.519	1.0400E+001	0.000E+000			Lump mass
37	Generator1	3.519	5.5000E+001	0.000E+000			Generator

Note: Negative sign on mass damping means dynamic magnifier

DATA FOR SHAFT ELEMENTS

SHAFT No	NODES		RPM RATIO [-]	TORSIONAL STIFFNESS [N*m/rad]	DAMPING see note [N*s*m/rad]	DIAMETER OUTER [mm]	INNER [mm]	TYPE
1	1	2	1.000	1.350E+007	3.200E+004	0.0	0.0	DamperStiffness
2	2	3	1.000	3.106E+008	-180.0	380.0	0.0	Shaft
3	3	4	1.000	2.012E+008	2.012E+004	380.0	0.0	Crankthrow
4	4	5	1.000	2.012E+008	2.012E+004	380.0	0.0	Crankthrow
5	5	6	1.000	2.012E+008	2.012E+004	380.0	0.0	Crankthrow
6	6	7	1.000	2.012E+008	2.012E+004	380.0	0.0	Crankthrow

7	7	8	1.000	2.012E+008	2.012E+004	380.0	0.0	Crankthrow
8	8	9	1.000	2.551E+008	-180.0	0.0	0.0	Shaft
9	9	10	1.000	1.000E+012	-180.0	0.0	0.0	Shaft
10	10	11	1.000	3.038E+006	-7.1	0.0	0.0	Coupling
11	11	12	1.000	3.038E+006	-7.1	0.0	0.0	Coupling
12	12	13	1.000	1.086E+008	-180.0	310.0	0.0	Shaft
13	13	14	1.000	2.495E+009	-180.0	855.0	0.0	Shaft
14	14	15	1.000	1.000E+012	0.000E+000	0.0	0.0	Shaft
15	15	16	1.000	1.200E+008	-180.0	295.0	0.0	Shaft
16	16	17	1.000	1.000E+012	-100.0	0.0	0.0	Mesh
17	17	18	0.293	4.126E+008	-180.0	450.0	0.0	Shaft
18	18	19	0.293	1.000E+012	0.000E+000	0.0	0.0	Shaft
19	19	20	0.293	1.990E+007	-180.0	405.0	0.0	Shaft
20	20	21	0.293	1.000E+012	0.000E+000	0.0	0.0	Shaft
21	21	22	0.293	1.000E+012	0.000E+000	0.0	0.0	Shaft
22	22	23	0.293	1.000E+012	0.000E+000	0.0	0.0	Shaft
23	23	24	0.293	1.790E+007	-180.0	405.0	0.0	Shaft
24	24	25	0.293	1.000E+012	0.000E+000	0.0	0.0	Shaft
25	25	26	0.293	1.000E+012	0.000E+000	0.0	0.0	Shaft
26	26	27	0.293	1.600E+007	-180.0	420.0	0.0	Shaft
27	27	28	0.293	1.000E+012	0.000E+000	0.0	0.0	Shaft
28	28	29	0.293	1.000E+012	0.000E+000	0.0	0.0	Shaft
29	30	31	3.519	9.680E+006	-180.0	140.0	0.0	Shaft
30	13	30	3.519	1.000E+012	-100.0	0.0	0.0	Mesh
31	31	32	3.519	7.508E+007	0.000E+000	210.0	0.0	Shaft
32	32	33	3.519	4.110E+006	-180.0	130.0	0.0	Shaft
33	33	34	3.519	1.350E+005	-6.1	0.0	0.0	Coupling
34	34	35	3.519	1.350E+005	-6.1	0.0	0.0	Coupling
35	35	36	3.519	1.350E+005	-6.1	0.0	0.0	Coupling
36	36	37	3.519	1.406E+007	-180.0	160.0	0.0	Shaft

Note: Negative sign on shaft damping means dynamic magnifier

ENGINE DATA

Index:	#2
Manufacturer:	MaK
Type:	12VM43C
Crank throw:	
Mass numbers:	3,4,5,6,7,8
RPM (@MCR):	514.0 rpm
Total power (@MCR):	12600.0 kW
Firing order:	A1-B1-A2-B2-A4-B4-A6-B6-A5-B5-A3-B3
Firing interval:	Uneven
Firing type:	Consecutive
Number of strokes:	4
Firing angle between banks:	50.00 deg
Cylinder diameter:	430.0 mm
Length of stroke:	610.0 mm
Connecting rod ratio:	0.236
Compression ratio:	16.8
Reciprocating mass (per cylinder):	467.4 kg
Number of cylinders:	12
Angle ignition:	-5.0 deg
Angle end of combustion:	55.0 deg
Angle exhaust starts:	150.0 deg
Angle inlet starts:	0.0 deg
Angle Inlet/exhaust close:	0.0 deg
Compression Ratio:	16.8
Thermal efficiency:	0.47
Compression exponent:	1.39
Expansion exponent:	1.33
Form Factor:	1.00
Pressure charge air:	3.40 bar
Pressure compression:	175 bar
Max cylinder pressure at MCR:	210 bar
Temperature charge air:	45 DegC

```
DAMPER DATA

Damper type:                     Steel

Node numbers:                    1-2
Inertia outer member:            377.00000 kg*m^2
Inertia inner member:            121.50000 kg*m^2
Dynamic magnifier:               0.000
Damping coefficient:             32000.000 N*s*m/rad
Torsional stiffness:             1.350E+007 N*m/rad


GEAR DATA

Manufacturer:                    RENK
Type:                            RSHL-1120

Mesh index:                      16
Node numbers:                    16-17
RPM ratio:                       1.000
Ratio reference:                 Ingoing


GEAR DATA

Manufacturer:
Type:

Mesh index:                      30
Node numbers:                    13-30
RPM ratio:                       3.519
Ratio reference:                 Outgoing


PROPELLER DATA

Index:                           #28
Manufacturer:
Type:

Ice class notation:              ICE-1C

MCR Power:                       12600.0 kW
MCR Speed:                       150.8 rpm
Bollard Speed:                   150.8 rpm
Ducted propeller:                No
Pitch type:                      Controllable pitch
Number of propeller blades:      4
Damping method:                  Frahm (Frahm number 2.9)

Boss diameter:                   965.0 mm
Blade diameter:                  4800.0 mm
Pitch ratio:                     1.000
Expanded area ratio (Ae/Ao):     0.000

Inertia, in air (@MCR):                             1.327E+004 kg*m^2
Inertia, entrained water (@MCR):                    5.880E+003 kg*m^2
Inertia, entrained water 0 Pitch (@MCR):            9.700E+002 kg*m^2

Propeller excitation in % of shaft torque (Nm):     6.0%
Propeller excitation (*2) in % of shaft torque (Nm):   1.5%
```

Bunker tanker - Original diameter

```
DATA FOR MASSES AND DAMPERS

Mass  DESCRIPTION      RPM      MASS MOMENT      DAMPING          FIRING    TYPE
No                     RATIO    OF INERTIA       see note         ANGLE
```

```
                       [-]      [kg*m^2]         [N*s*m/rad]      [deg]
---------------------------------------------------------------------------------------
1     ElectricMotor1   1.000    8.5000E+001      0.000E+000                 Electric motor
2     ShaftEnd         1.000    1.5000E-001      0.000E+000                 Lump mass
3     CouplingPrimary1 1.000    2.6500E+000      0.000E+000                 Lump mass
4     CouplingSecondar 1.000    4.2200E+000      0.000E+000                 Lump mass
5     ElectricMotor2   1.000    8.5000E+001      0.000E+000                 Electric motor
6     ShaftEnd         1.000    1.5000E-001      0.000E+000                 Lump mass
7     CouplingPrimary2 1.000    2.6500E+000      0.000E+000                 Lump mass
8     CouplingSecondar 1.000    4.2200E+000      0.000E+000                 Lump mass
9     InputGear        1.000    2.1900E+000      0.000E+000                 Lump mass
10    OutputGear       0.118    1.7610E+003      0.000E+000                 Lump mass
11    OMC-Coupling     0.118    2.1730E+001      0.000E+000                 Lump mass
12    BreakDisk+HalfSh 0.118    4.0000E+001      0.000E+000                 Lump mass
13    HalfPropShaft    0.118    1.9925E+001      0.000E+000                 Lump mass
14    Propeller1       0.118    3.9938E+003      0.000E+000                 Propeller

Note: Negative sign on mass damping means dynamic magnifier

DATA FOR SHAFT ELEMENTS

SHAFT NODES        RPM     TORSIONAL        DAMPING           DIAMETER      TYPE
No                 RATIO   STIFFNESS        see note        OUTER   INNER
                   [-]     [N*m/rad]        [N*s*m/rad]     [mm]    [mm]
---------------------------------------------------------------------------------------
1     1     2      1.000   1.000E+012       0.000E+000      0.0     0.0     Shaft
2     3     4      1.000   9.676E+004       -7.0            0.0     0.0     Coupling
3     2     3      1.000   5.460E+006       -180.0          140.0   0.0     Shaft
4     5     6      1.000   1.000E+012       0.000E+000      0.0     0.0     Shaft
5     6     7      1.000   5.460E+006       -180.0          140.0   0.0     Shaft
6     7     8      1.000   9.676E+004       -7.0            0.0     0.0     Coupling
7     9     10     1.000   1.000E+012       -100.0          0.0     0.0     Mesh
8     4     9      1.000   1.594E+007       -180.0          150.0   0.0     Shaft
9     8     9      1.000   1.613E+007       -180.0          150.0   0.0     Shaft
10    10    11     0.118   6.575E+007       -180.0          0.0     0.0     Shaft
11    11    12     0.118   1.000E+012       0.000E+000      0.0     0.0     Shaft
12    12    13     0.118   6.800E+006       -180.0          268.0   90.0    Shaft
13    13    14     0.118   1.000E+012       0.000E+000      0.0     0.0     Shaft

Note: Negative sign on shaft damping means dynamic magnifier
```

Input data for system components: propulsion motor/engine, reduction gear, flexible couplings and propeller.
This information is given for the original system and not repeated. Changes are not done on those components, just the shafts.

```
ELECTRIC MOTOR DATA

Manufacturer:                      Siemens 1NA1504
Type:                              A5E46380263A
Node number:                       1
RPM (@MCR):                        1200.0 rpm
Power (@ MCR):                     1250.0 kW

ELECTRIC MOTOR DATA

Manufacturer:                      Siemens 1NA1504
Type:                              A5E46380263A
Node number:                       5
RPM (@MCR):                        1200.0 rpm
Power (@ MCR):                     1250.0 kW

GEAR DATA

Manufacturer:                      RENK B747507
```

```
Type:                           RSV-1060HR i=8.45
Mesh index:                     7
Node numbers:                   9-10
RPM ratio:                      1.000
Ratio reference:                Ingoing

ELASTIC COUPLING DATA

Manufacturer:
Type:                           CX-72-GFS1-300-60-0637
Stiffness index:                2
Node number:                    3-4
Stiffness type:                 Linear
Nominal coupling torque:        0.000 kN*m
Norminal torsional stiffness:   9.676E+004 N*m/rad

ELASTIC COUPLING DATA

Manufacturer:
Type:                           CX-72-GFS1-300-60-0637
Stiffness index:                6
Node number:                    7-8
Stiffness type:                 Linear
Nominal coupling torque:        0.000 kN*m
Norminal torsional stiffness:   9.676E+004 N*m/rad

PROPELLER DATA

Index:                          #14
Manufacturer:
Type:
Ice class notation:             ICE-1B
MCR Power:                      2500.0 kW
MCR Speed:                      142.0 rpm
Bollard Speed:                  142.0 rpm
Ducted propeller:               No
Pitch type:                     Controllable pitch
Number of propeller blades:     4
Damping method:                 Archer (Archer number 27.0)
Boss diameter:                  760.0 mm
Blade diameter:                 3600.0 mm
Pitch ratio:                    1.000
Expanded area ratio (Ae/Ao):    0.000

Inertia, in air (@MCR):                             2.647E+003 kg*m^2
Inertia, entrained water (@MCR):                    1.347E+003 kg*m^2
Inertia, entrained water 0 Pitch (@MCR):            3.367E+002 kg*m^2

Propeller excitation in % of shaft torque (Nm):     6.0%
Propeller excitation (*2) in % of shaft torque (Nm):   2.0%
```

Bunker tanker - Diameter decreased by 10 mm

DATA FOR MASSES AND DAMPERS

Mass No	DESCRIPTION	RPM RATIO [-]	MASS MOMENT OF INERTIA [kg*m^2]	DAMPING see note [N*s*m/rad]	FIRING ANGLE [deg]	TYPE
1	ElectricMotor1	1.000	8.5000E+001	0.000E+000		Electric motor
2	ShaftEnd	1.000	1.5000E-001	0.000E+000		Lump mass
3	CouplingPrimary1	1.000	2.6500E+000	0.000E+000		Lump mass
4	CouplingSecondar	1.000	4.2200E+000	0.000E+000		Lump mass
5	ElectricMotor2	1.000	8.5000E+001	0.000E+000		Electric motor
6	ShaftEnd	1.000	1.5000E-001	0.000E+000		Lump mass
7	CouplingPrimary2	1.000	2.6500E+000	0.000E+000		Lump mass
8	CouplingSecondar	1.000	4.2200E+000	0.000E+000		Lump mass

9	InputGear	1.000	2.1900E+000	0.000E+000		Lump mass
10	OutputGear	0.118	1.7610E+003	0.000E+000		Lump mass
11	OMC-Coupling	0.118	2.0110E+001	0.000E+000		Lump mass
12	BreakDisk+HalfSh	0.118	3.7460E+001	0.000E+000		Lump mass
13	HalfPropShaft	0.118	1.7350E+001	0.000E+000		Lump mass
14	Propeller1	0.118	3.9938E+003	0.000E+000		Propeller

Note: Negative sign on mass damping means dynamic magnifier

DATA FOR SHAFT ELEMENTS

SHAFT No	NODES		RPM RATIO [-]	TORSIONAL STIFFNESS [N*m/rad]	DAMPING see note [N*s*m/rad]	DIAMETER OUTER [mm]	INNER [mm]	TYPE
1	1	2	1.000	1.000E+012	0.000E+000	0.0	0.0	Shaft
2	3	4	1.000	9.676E+004	-7.0	0.0	0.0	Coupling
3	2	3	1.000	5.460E+006	-180.0	140.0	0.0	Shaft
4	5	6	1.000	1.000E+012	0.000E+000	0.0	0.0	Shaft
5	6	7	1.000	5.460E+006	-180.0	140.0	0.0	Shaft
6	7	8	1.000	9.676E+004	-7.0	0.0	0.0	Coupling
7	9	10	1.000	1.000E+012	-100.0	0.0	0.0	Mesh
8	4	9	1.000	1.594E+007	-180.0	150.0	0.0	Shaft
9	8	9	1.000	1.613E+007	-180.0	150.0	0.0	Shaft
10	10	11	0.118	6.575E+007	-180.0	0.0	0.0	Shaft
11	11	12	0.118	1.000E+012	0.000E+000	0.0	0.0	Shaft
12	12	13	0.118	5.860E+006	-180.0	258.0	90.0	Shaft
13	13	14	0.118	1.000E+012	0.000E+000	0.0	0.0	Shaft

Note: Negative sign on shaft damping means dynamic magnifier

Bunker tanker - Diameter decreased by 20 mm

DATA FOR MASSES AND DAMPERS

Mass No	DESCRIPTION	RPM RATIO [-]	MASS MOMENT OF INERTIA [kg*m^2]	DAMPING see note [N*s*m/rad]	FIRING ANGLE [deg]	TYPE
1	ElectricMotor1	1.000	8.5000E+001	0.000E+000		Electric motor
2	ShaftEnd	1.000	1.5000E-001	0.000E+000		Lump mass
3	CouplingPrimary1	1.000	2.6500E+000	0.000E+000		Lump mass
4	CouplingSecondar	1.000	4.2200E+000	0.000E+000		Lump mass
5	ElectricMotor2	1.000	8.5000E+001	0.000E+000		Electric motor
6	ShaftEnd	1.000	1.5000E-001	0.000E+000		Lump mass
7	CouplingPrimary2	1.000	2.6500E+000	0.000E+000		Lump mass
8	CouplingSecondar	1.000	4.2200E+000	0.000E+000		Lump mass
9	InputGear	1.000	2.1900E+000	0.000E+000		Lump mass
10	OutputGear	0.118	1.7610E+003	0.000E+000		Lump mass
11	OMC-Coupling	0.118	2.1730E+001	0.000E+000		Lump mass
12	BreakDisk+HalfSh	0.118	3.5115E+001	0.000E+000		Lump mass
13	HalfPropShaft	0.118	1.5035E+001	0.000E+000		Lump mass
14	Propeller1	0.118	3.9938E+003	0.000E+000		Propeller

Note: Negative sign on mass damping means dynamic magnifier

DATA FOR SHAFT ELEMENTS

SHAFT No	NODES		RPM RATIO [-]	TORSIONAL STIFFNESS [N*m/rad]	DAMPING see note [N*s*m/rad]	DIAMETER OUTER [mm]	INNER [mm]	TYPE
1	1	2	1.000	1.000E+012	0.000E+000	0.0	0.0	Shaft
2	3	4	1.000	9.676E+004	-7.0	0.0	0.0	Coupling
3	2	3	1.000	5.460E+006	-180.0	140.0	0.0	Shaft
4	5	6	1.000	1.000E+012	0.000E+000	0.0	0.0	Shaft

5	6	7	1.000	5.460E+006	-180.0	140.0	0.0	Shaft
6	7	8	1.000	9.676E+004	-7.0	0.0	0.0	Coupling
7	9	10	1.000	1.000E+012	-100.0	0.0	0.0	Mesh
8	4	9	1.000	1.594E+007	-180.0	150.0	0.0	Shaft
9	8	9	1.000	1.613E+007	-180.0	150.0	0.0	Shaft
10	10	11	0.118	6.575E+007	-180.0	0.0	0.0	Shaft
11	11	12	0.118	1.000E+012	0.000E+000	0.0	0.0	Shaft
12	12	13	0.118	5.010E+006	-180.0	248.0	90.0	Shaft
13	13	14	0.118	1.000E+012	0.000E+000	0.0	0.0	Shaft

Note: Negative sign on shaft damping means dynamic magnifier

Bunker tanker - Diameter decreased by 30 mm

DATA FOR MASSES AND DAMPERS

Mass No	DESCRIPTION	RPM RATIO [-]	MASS MOMENT OF INERTIA [kg*m^2]	DAMPING see note [N*s*m/rad]	FIRING ANGLE [deg]	TYPE
1	ElectricMotor1	1.000	8.5000E+001	0.000E+000		Electric motor
2	ShaftEnd	1.000	1.5000E-001	0.000E+000		Lump mass
3	CouplingPrimary1	1.000	2.6500E+000	0.000E+000		Lump mass
4	CouplingSecondar	1.000	4.2200E+000	0.000E+000		Lump mass
5	ElectricMotor2	1.000	8.5000E+001	0.000E+000		Electric motor
6	ShaftEnd	1.000	1.5000E-001	0.000E+000		Lump mass
7	CouplingPrimary2	1.000	2.6500E+000	0.000E+000		Lump mass
8	CouplingSecondar	1.000	4.2200E+000	0.000E+000		Lump mass
9	InputGear	1.000	2.1900E+000	0.000E+000		Lump mass
10	OutputGear	0.118	1.7610E+003	0.000E+000		Lump mass
11	OMC-Coupling	0.118	2.1730E+001	0.000E+000		Lump mass
12	BreakDisk+HalfSh	0.118	3.3040E+001	0.000E+000		Lump mass
13	HalfPropShaft	0.118	1.2960E+001	0.000E+000		Lump mass
14	Propeller1	0.118	3.9938E+003	0.000E+000		Propeller

Note: Negative sign on mass damping means dynamic magnifier

DATA FOR SHAFT ELEMENTS

SHAFT No	NODES		RPM RATIO [-]	TORSIONAL STIFFNESS [N*m/rad]	DAMPING see note [N*s*m/rad]	DIAMETER OUTER [mm]	INNER [mm]	TYPE
1	1	2	1.000	1.000E+012	0.000E+000	0.0	0.0	Shaft
2	3	4	1.000	9.676E+004	-7.0	0.0	0.0	Coupling
3	2	3	1.000	5.460E+006	-180.0	140.0	0.0	Shaft
4	5	6	1.000	1.000E+012	0.000E+000	0.0	0.0	Shaft
5	6	7	1.000	5.460E+006	-180.0	140.0	0.0	Shaft
6	7	8	1.000	9.676E+004	-7.0	0.0	0.0	Coupling
7	9	10	1.000	1.000E+012	-100.0	0.0	0.0	Mesh
8	4	9	1.000	1.594E+007	-180.0	150.0	0.0	Shaft
9	8	9	1.000	1.613E+007	-180.0	150.0	0.0	Shaft
10	10	11	0.118	6.575E+007	-180.0	0.0	0.0	Shaft
11	11	12	0.118	1.000E+012	0.000E+000	0.0	0.0	Shaft
12	12	13	0.118	4.260E+006	-180.0	238.0	90.0	Shaft
13	13	14	0.118	1.000E+012	0.000E+000	0.0	0.0	Shaft

Note: Negative sign on shaft damping means dynamic magnifier

Dredger - Original diameter

DATA FOR MASSES AND DAMPERS

Mass No	DESCRIPTION	RPM RATIO	MASS MOMENT OF INERTIA	DAMPING see note	FIRING ANGLE	TYPE

		[-]	[kg*m^2]	[N*s*m/rad]	[deg]	
1	MotorRotor	1.000	1.7490E+002	0.000E+000		Electric motor
2	MotorOutput	1.000	8.5000E+000	0.000E+000		Lump mass
3	CoupSP	1.000	1.6950E+001	0.000E+000		Lump mass
4	CoupPP-B	1.000	8.9400E+000	0.000E+000		Lump mass
5	GB-Pinion-20T	1.000	2.9700E+000	0.000E+000		Lump mass
6	GB-Wheel-122T	0.164	8.2596E+002	0.000E+000		Lump mass
7	BreakDisc	0.164	2.7630E+001	0.000E+000		Lump mass
8	INTSFlange	0.164	1.4705E+001	0.000E+000		Lump mass
9	OMC	0.164	5.0740E+001	0.000E+000		Lump mass
10	PropFlange	0.164	2.9010E+001	0.000E+000		Lump mass
11	Propeller1	0.164	2.4000E+003	0.000E+000		Propeller

Note: Negative sign on mass damping means dynamic magnifier

DATA FOR SHAFT ELEMENTS

SHAFT No	NODES		RPM RATIO [-]	TORSIONAL STIFFNESS [N*m/rad]	DAMPING see note [N*s*m/rad]	DIAMETER OUTER [mm]	INNER [mm]	TYPE
1	1	2	1.000	9.270E+006	-180.0	180.0	0.0	Shaft
2	2	3	1.000	1.000E+012	0.000E+000	0.0	0.0	Shaft
3	3	4	1.000	2.465E+005	-7.1	0.0	0.0	Coupling
4	4	5	1.000	2.613E+007	-180.0	200.0	0.0	Shaft
5	5	6	1.000	1.000E+012	-100.0	0.0	0.0	Mesh
6	6	7	0.164	6.694E+007	-180.0	249.0	0.0	Shaft
7	7	8	0.164	6.640E+006	-180.0	260.0	0.0	Shaft
8	8	9	0.164	1.000E+012	0.000E+000	0.0	0.0	Shaft
9	9	10	0.164	4.740E+006	-180.0	255.0	0.0	Shaft
10	10	11	0.164	1.000E+012	0.000E+000	0.0	0.0	Shaft

Note: Negative sign on shaft damping means dynamic magnifier

ELECTRIC MOTOR DATA

Manufacturer: AMI
Type: 560L6L BSFTMS

Node number: 1
RPM (@MCR): 1200.0 rpm
Power (@ MCR): 4000.0 kW

GEAR DATA

Manufacturer: RENK
Type: RSV-900 HR Ratio 20/122

Mesh index: 5
Node numbers: 5-6
RPM ratio: 1.000
Ratio reference: Ingoing

ELASTIC COUPLING DATA

Manufacturer: CENTA
Type: CX-179-GSS1-50Sh

Stiffness index: 3
Node number: 3-4
Stiffness type: Linear
Nominal coupling torque: 0.000 kN*m
Norminal torsional stiffness: 2.465E+005 N*m/rad

PROPELLER DATA

Index:	#11
Manufacturer:	BERG Propulsion
Type:	MPP 950 Fixed
Ice class notation:	No ice class
MCR Power:	4000.0 kW
MCR Speed:	197.0 rpm
Ducted propeller:	Yes
Pitch type:	Fixed pitch
Number of propeller blades:	4
Damping method:	Archer (Archer number 27.0)
Boss diameter:	0.0 mm
Blade diameter:	0.0 mm
Pitch ratio:	1.000
Expanded area ratio (Ae/Ao):	0.000
Inertia, in air (@MCR):	1.360E+003 kg*m^2
Inertia, entrained water (@MCR):	1.040E+003 kg*m^2
Propeller excitation in % of shaft torque (Nm):	6.0%
Propeller excitation (*2) in % of shaft torque (Nm):	2.0%

Dredger - Diameter decreased, 230mm propshaft and 225mm intermediate

DATA FOR MASSES AND DAMPERS

Mass No	DESCRIPTION	RPM RATIO [-]	MASS MOMENT OF INERTIA [kg*m^2]	DAMPING see note [N*s*m/rad]	FIRING ANGLE [deg]	TYPE
1	MotorRotor	1.000	1.7490E+002	0.000E+000		Electric motor
2	MotorOutput	1.000	8.5000E+000	0.000E+000		Lump mass
3	CoupSP	1.000	1.6950E+001	0.000E+000		Lump mass
4	CoupPP-B	1.000	8.9400E+000	0.000E+000		Lump mass
5	GB-Pinion-20T	1.000	2.9700E+000	0.000E+000		Lump mass
6	GB-Wheel-122T	0.164	8.2596E+002	0.000E+000		Lump mass
7	BreakDisc+HalfINT	0.164	3.8845E+001	0.000E+000		Lump mass
8	INTSFlange	0.164	1.1225E+001	0.000E+000		Lump mass
9	OMC+HalfProp	0.164	3.3675E+001	0.000E+000		Lump mass
10	PropFlange	0.164	1.1945E+001	0.000E+000		Lump mass
11	Propeller1	0.164	2.4000E+003	0.000E+000		Propeller

Note: Negative sign on mass damping means dynamic magnifier

DATA FOR SHAFT ELEMENTS

SHAFT No	NODES		RPM RATIO [-]	TORSIONAL STIFFNESS [N*m/rad]	DAMPING see note [N*s*m/rad]	DIAMETER OUTER [mm]	DIAMETER INNER [mm]	TYPE
1	1	2	1.000	9.270E+006	-180.0	180.0	0.0	Shaft
2	2	3	1.000	1.000E+012	0.000E+000	0.0	0.0	Shaft
3	3	4	1.000	2.465E+005	-7.1	0.0	0.0	Coupling
4	4	5	1.000	2.613E+007	-180.0	200.0	0.0	Shaft
5	5	6	1.000	1.000E+012	-100.0	0.0	0.0	Mesh
6	6	7	0.164	6.694E+007	-180.0	249.0	0.0	Shaft
7	7	8	0.164	3.920E+006	-180.0	225.0	0.0	Shaft
8	8	9	0.164	1.000E+012	0.000E+000	0.0	0.0	Shaft
9	9	10	0.164	2.040E+006	-180.0	230.0	0.0	Shaft

```
10    10    11    0.164    1.000E+012       0.000E+000       0.0     0.0     Shaft

Note: Negative sign on shaft damping means dynamic magnifier
```

C.5.3 Propeller curves for the dredger

The table below lists the propeller torque and propeller power consumption versus speed, for the two operating conditions.

Free running empty condition			Dredging condition		
Prop Speed [RPM]	Prop Torque [kNm]	Power [kW]	Prop Speed [RPM]	Prop Torque [kNm]	Power [kW]
20	2.0	4.1	20	2.7	5.6
30	4.4	13.8	30	6.0	18.9
40	7.8	32.6	40	10.7	44.8
50	12.2	63.7	50	16.7	87.4
60	17.5	110.0	60	24.0	151.1
70	23.9	174.9	70	32.7	240.0
80	31.2	261.1	80	42.7	358.1
90	39.4	371.8	90	54.1	510.1
100	48.7	509.9	100	66.8	699.8
110	58.9	678.7	110	80.8	931.3
120	70.1	881.1	120	96.2	1209.0
130	82.3	1120.2	130	112.9	1537.2
140	95.4	1399.0	140	131.0	1920.1
150	109.5	1720.6	150	150.3	2361.6
160	124.6	2088.1	160	171.0	2865.6
170	140.7	2504.5	170	193.1	3437.8
180	157.7	2972.9	177	209.3	3879.9
190	175.7	3496.6			
196.7	188.4	3880.0			

Table C.1: *Propeller torque values from given curves and calculated power for given propeller speed.*

Below is a .txt file defining the propeller power curve for the free running condition. This file is loaded in the propeller load definition.

```
// Comments starting with two backslash are allowed and will not
be read
// Blank lines shall also be allowed

//'Speed' and 'Power' columns MUST be included in custom load curve
//'Speed' column should be with 'Speed' word on top, it should be the
first column
//'Power' column should be with 'Power' word on top and this column
should be on right side of 'Speed' column
//'PitchRatio' column CAN be included. If it is, it should be the
third column and with 'PitchRatio' word on top
//'EntrainedWater' column CAN be included. If it is, it should be the
last column and with 'EntrainedWater' word on top
//If Custom load curve contains only the 'Speed' and 'Power' columns,
it means the user has defined the power changes to each speed
//If 'PitchRatio' column is defined, it means power changes according
to PitchRatio.
//'EntrainedWater' column could be added if user wants to define the
Inertia of Entrained Water of Propeller changes to Speed (or
PitchRatio).
//'EntrainedWater' column could be empty in some of the cells but the
other columns should be fully specified at each step
//If 'PitchRatio' column is not defined, no duplicated values are
allowed in the "Speed" column .
//If 'PitchRatio' column is defined, no duplicated values are allowed
in the 'PitchRatio' column.But duplicated values are allowed for
"Speed"
column to simulate like 'constant speed and variable pitch'
condition.

//User can freely define the speed step (or PitchRatio steps)
//The unit of each column is fixed as this example

// Dredger
// Free running empty condition

Speed[Rpm]          Power[KW]
    20              4.1
    30              13.8
    40              32.6
    50              63.7
    60              110.0
    70              174.9
    80              261.1
    90              371.8
    100             509.9
    110             678.7
    120             881.1
    130             1120.2
    140             1399.0
    150             1720.6
    160             2088.1
    170             2504.5
    180             2972.9
    190             3496.62
    196.7           3880.0
```

Below is a .txt file defining the propeller power curve for the dredging condition. This file is loaded in the propeller load definition.

```
// Comments starting with two backslash are allowed and will not be
read
// Blank lines shall also be allowed

//'Speed' and 'Power' columns MUST be included in custom load curve
//'Speed' column should be with 'Speed' word on top, it should be the
first column
//'Power' column should be with 'Power' word on top and this column
should be on right side of 'Speed' column
//'PitchRatio' column CAN be included. If it is, it should be the
third column and with 'PitchRatio' word on top
//'EntrainedWater' column CAN be included. If it is, it should be the
last column and with 'EntrainedWater' word on top
//If Custom load curve contains only the 'Speed' and 'Power' columns,
it means the user has defined the power changes to each speed
//If 'PitchRatio' column is defined, it means power changes according
to PitchRatio.
//'EntrainedWater' column could be added if user wants to define the
Inertia of Entrained Water of Propeller changes to Speed (or
PitchRatio).
//'EntrainedWater' column could be empty in some of the cells but the
other columns should be fully specified at each step
//If 'PitchRatio' column is not defined, no duplicated values are
allowed in the "Speed" column .
//If 'PitchRatio' column is defined, no duplicated values are allowed
in the 'PitchRatio' column.But duplicated values are allowed for
"Speed"
column to simulate like 'constant speed and variable pitch'
condition.


//User can freely define the speed step (or PitchRatio steps)
//The unit of each column is fixed as this example

// Dredger
// Dredging condition

Speed[Rpm]      Power[KW]
    20          5.6
    30          18.9
    40          44.8
    50          87.43
    60          151.1
    70          240.0
    80          358.1
    90          510.1
    100         700.0
    110         931.3
    120         1209.0
    130         1537.2
    140         1920.1
    150         2361.6
    160         2865.6
    170         3437.8
    177         3880.0
```

DEPARTMENT OF SOME SUBJECT OR TECHNOLOGY
CHALMERS UNIVERSITY OF TECHNOLOGY
Gothenburg, Sweden
www.chalmers.se

AVANCEZ
1829

CHALMERS
UNIVERSITY OF TECHNOLOGY